

International Energy Agency  
Programme on  
Energy in Buildings and Communities



# Annex 59: High Temperature Cooling & Low Temperature Heating in Buildings

## **Final Report**

### **IV. Design guide for HTC and LTH systems**

September, 2016

© Copyright Tsinghua University 2016

All property rights, including copyright, are vested in Tsinghua University, Operating Agent for EBC Annex 59, on behalf of the Contracting Parties of the International Energy Agency Implementing Agreement for a Programme of Research and Development on Energy in Buildings and Communities.

In particular, no part of this publication may be reproduced, stored in a retrieval system or transmitted in any form or by any means, electronic, mechanical, photocopying, recording or otherwise, without the prior written permission of Tsinghua University.

Published by Department of Building Science and Technology, Tsinghua University, 100084 Beijing, P.R. China

Disclaimer Notice: This publication has been compiled with reasonable skill and care. However, neither Tsinghua University nor the Contracting Parties of the International Energy Agency Implementing Agreement for a Programme of Research and Development on Energy in Buildings and Communities make any representation as to the adequacy or accuracy of the information contained herein, or as to its suitability for any particular application, and accept no responsibility or liability arising out of the use of this publication. The information contained herein does not supersede the requirements given in any national codes, regulations or standards, and should not be regarded as a substitute for the need to obtain specific professional advice for any particular application.

Participating countries in EBC:

Australia, Austria, Belgium, Canada, P.R. China, Czech Republic, Denmark, Finland, France, Germany, Ireland, Italy, Japan, Republic of Korea, the Netherlands, New Zealand, Norway, Portugal, Singapore, Spain, Sweden, Switzerland, United Kingdom and the United States of America.

Additional copies of this report may be obtained from:

EBC Executive Committee Support Services Unit (ESSU)  
C/o AECOM Ltd  
The Colmore Building  
Colmore Circus Queensway  
Birmingham B4 6AT  
United Kingdom  
Web: [www.iea-ebc.org](http://www.iea-ebc.org)  
Email: [essu@iea-ebc.org](mailto:essu@iea-ebc.org)

## Preface

### The International Energy Agency

The International Energy Agency (IEA) was established in 1974 within the framework of the Organisation for Economic Co-operation and Development (OECD) to implement an international energy programme. A basic aim of the IEA is to foster international co-operation among the 30 IEA participating countries and to increase energy security through energy research, development and demonstration in the fields of technologies for energy efficiency and renewable energy sources.

### The IEA Energy in Buildings and Communities Programme

The IEA co-ordinates international energy research and development (R&D) activities through a comprehensive portfolio of Technology Collaboration Programmes. The mission of the IEA Energy in Buildings and Communities (IEA EBC) Technology Collaboration Programme is to develop and facilitate the integration of technologies and processes for energy efficiency and conservation into healthy, low emission, and sustainable buildings and communities, through innovation and research. (Until March 2013, the IEA EBC Programme was known as the IEA Energy Conservation in Buildings and Community Systems Programme, ECBCS.)

The R&D strategies of the IEA EBC Programme are derived from research drivers, national programmes within IEA countries, and the IEA Future Buildings Forum Think Tank Workshops. These R&D strategies aim to exploit technological opportunities to save energy in the buildings sector, and to remove technical obstacles to market penetration of new energy efficient technologies. The R&D strategies apply to residential, commercial, office buildings and community systems, and will impact the building industry in five areas of focus for R&D activities:

- Integrated planning and building design
- Building energy systems
- Building envelope
- Community scale methods
- Real building energy use

### The Executive Committee

Overall control of the IEA EBC Programme is maintained by an Executive Committee, which not only monitors existing projects, but also identifies new strategic areas in which collaborative efforts may be beneficial. As the Programme is based on a contract with the IEA, the projects are legally established as Annexes to the IEA EBC Implementing Agreement. At the present time, the following projects have been initiated by the IEA EBC Executive Committee, with completed projects identified by (\*) and joint projects with the IEA Solar Heating and Cooling Technology Collaboration Programme by (☼):

Annex 1:	Load Energy Determination of Buildings (*)
Annex 2:	Ekistics and Advanced Community Energy Systems (*)
Annex 3:	Energy Conservation in Residential Buildings (*)
Annex 4:	Glasgow Commercial Building Monitoring (*)
Annex 5:	Air Infiltration and Ventilation Centre
Annex 6:	Energy Systems and Design of Communities (*)
Annex 7:	Local Government Energy Planning (*)
Annex 8:	Inhabitants Behaviour with Regard to Ventilation (*)
Annex 9:	Minimum Ventilation Rates (*)
Annex 10:	Building HVAC System Simulation (*)
Annex 11:	Energy Auditing (*)
Annex 12:	Windows and Fenestration (*)
Annex 13:	Energy Management in Hospitals (*)
Annex 14:	Condensation and Energy (*)

- Annex 15: Energy Efficiency in Schools (\*)
- Annex 16: BEMS 1- User Interfaces and System Integration (\*)
- Annex 17: BEMS 2- Evaluation and Emulation Techniques (\*)
- Annex 18: Demand Controlled Ventilation Systems (\*)
- Annex 19: Low Slope Roof Systems (\*)
- Annex 20: Air Flow Patterns within Buildings (\*)
- Annex 21: Thermal Modelling (\*)
- Annex 22: Energy Efficient Communities (\*)
- Annex 23: Multi Zone Air Flow Modelling (COMIS) (\*)
- Annex 24: Heat, Air and Moisture Transfer in Envelopes (\*)
- Annex 25: Real time HVAC Simulation (\*)
- Annex 26: Energy Efficient Ventilation of Large Enclosures (\*)
- Annex 27: Evaluation and Demonstration of Domestic Ventilation Systems (\*)
- Annex 28: Low Energy Cooling Systems (\*)
- Annex 29: ☀ Daylight in Buildings (\*)
- Annex 30: Bringing Simulation to Application (\*)
- Annex 31: Energy-Related Environmental Impact of Buildings (\*)
- Annex 32: Integral Building Envelope Performance Assessment (\*)
- Annex 33: Advanced Local Energy Planning (\*)
- Annex 34: Computer-Aided Evaluation of HVAC System Performance (\*)
- Annex 35: Design of Energy Efficient Hybrid Ventilation (HYBVENT) (\*)
- Annex 36: Retrofitting of Educational Buildings (\*)
- Annex 37: Low Exergy Systems for Heating and Cooling of Buildings (LowEx) (\*)
- Annex 38: ☀ Solar Sustainable Housing (\*)
- Annex 39: High Performance Insulation Systems (\*)
- Annex 40: Building Commissioning to Improve Energy Performance (\*)
- Annex 41: Whole Building Heat, Air and Moisture Response (MOIST-ENG) (\*)
- Annex 42: The Simulation of Building-Integrated Fuel Cell and Other Cogeneration Systems (FC+COGEN-SIM) (\*)
- Annex 43: ☀ Testing and Validation of Building Energy Simulation Tools (\*)
- Annex 44: Integrating Environmentally Responsive Elements in Buildings (\*)
- Annex 45: Energy Efficient Electric Lighting for Buildings (\*)
- Annex 46: Holistic Assessment Tool-kit on Energy Efficient Retrofit Measures for Government Buildings (EnERGo) (\*)
- Annex 47: Cost-Effective Commissioning for Existing and Low Energy Buildings (\*)
- Annex 48: Heat Pumping and Reversible Air Conditioning (\*)
- Annex 49: Low Exergy Systems for High Performance Buildings and Communities (\*)
- Annex 50: Prefabricated Systems for Low Energy Renovation of Residential Buildings (\*)
- Annex 51: Energy Efficient Communities (\*)
- Annex 52: ☀ Towards Net Zero Energy Solar Buildings (\*)
- Annex 53: Total Energy Use in Buildings: Analysis and Evaluation Methods (\*)
- Annex 54: Integration of Micro-Generation and Related Energy Technologies in Buildings (\*)
- Annex 55: Reliability of Energy Efficient Building Retrofitting - Probability Assessment of Performance and Cost (RAP-RETRO) (\*)
- Annex 56: Cost Effective Energy and CO<sub>2</sub> Emissions Optimization in Building Renovation (\*)
- Annex 57: Evaluation of Embodied Energy and CO<sub>2</sub> Equivalent Emissions for Building Construction (\*)
- Annex 58: Reliable Building Energy Performance Characterisation Based on Full Scale Dynamic Measurements (\*)
- Annex 59: High Temperature Cooling and Low Temperature Heating in Buildings (\*)
- Annex 60: New Generation Computational Tools for Building and Community Energy Systems (\*)
- Annex 61: Business and Technical Concepts for Deep Energy Retrofit of Public Buildings (\*)
- Annex 62: Ventilative Cooling (\*)
- Annex 63: Implementation of Energy Strategies in Communities (\*)

- Annex 64: LowEx Communities - Optimised Performance of Energy Supply Systems with Exergy Principles (\*)
- Annex 65: Long-Term Performance of Super-Insulating Materials in Building Components and Systems
- Annex 66: Definition and Simulation of Occupant Behavior in Buildings (\*)
- Annex 67: Energy Flexible Buildings
- Annex 68: Indoor Air Quality Design and Control in Low Energy Residential Buildings
- Annex 69: Strategy and Practice of Adaptive Thermal Comfort in Low Energy Buildings
- Annex 70: Energy Epidemiology: Analysis of Real Building Energy Use at Scale
- Annex 71: Building Energy Performance Assessment Based on In-situ Measurements
- Annex 72: Assessing Life Cycle Related Environmental Impacts Caused by Buildings
- Annex 73: Towards Net Zero Energy Resilient Public Communities
- Annex 74: Competition and Living Lab Platform
- Annex 75: Cost-effective Building Renovation at District Level Combining Energy Efficiency and Renewables
- Annex 76: ☀ Deep Renovation of Historic Buildings Towards Lowest Possible Energy Demand and CO<sub>2</sub> Emissions
- Annex 77: ☀ Integrated Solutions for Daylight and Electric Lighting
- Annex 78: Supplementing Ventilation with Gas-phase Air Cleaning, Implementation and Energy Implications
- Annex 79: Occupant Behaviour-Centric Building Design and Operation
- Annex 80: Resilient Cooling

Working Group - Energy Efficiency in Educational Buildings (\*)

Working Group - Indicators of Energy Efficiency in Cold Climate Buildings (\*)

Working Group - Annex 36 Extension: The Energy Concept Adviser (\*)

Working Group - HVAC Energy Calculation Methodologies for Non-residential Buildings

Working Group - Cities and Communities

Working Group - Building Energy Codes

Working Group - International Building Materials Database

Authors: Cleide APARECIDA SILVA, JCJ Energetics (Belgium)  
Jules HANNAY, JCJ Energetics (Belgium)  
Xiaohua LIU, Tsinghua University (China)  
Jean LEBRUN, JCJ Energetics (Belgium)  
Vincent LEMORT, Université de Liège (Belgium)  
Valentina MONETTI, Politecnico di Torino (Italy)  
Marco PERINO, Politecnico di Torino (Italy)  
Francois RANDAXHE, Université de Liège (Belgium)

Editors: Xiaohua LIU, Tsinghua University (China)  
Francois RANDAXHE, Université de Liège (Belgium)  
Haida TANG, Tsinghua University (China)

Reviewed by:

# Contents

<i>PART 1</i> .....	1
1. Introduction .....	1
2. Impact of Temperature on Primary HVAC System Performance <b>错误! 未定义书签。</b>	
2.1. Gas condensing boiler .....	2
2.2. Air cooled chiller .....	5
2.3. Water cooled chiller .....	7
2.4. Air source heat pump .....	13
2.5. BCHP with internal combustion engine (ICE) .....	14
2.6. District heating network as a primary system .....	17
3. Applications of novel analysis method in HVAC system .....	20
3.1. Application in data centers (with high-density sensible load) .....	20
3.2. Application in office buildings (with both sensible and latent load) .....	29
3.3. Application in large space buildings .....	36
4. Integration of HVAC System in Buildings .....	42
4.1. Reference building model .....	42
4.2. Reference Case HVAC system description .....	55
4.3. Performance assessment of HVAC systems under typical conditions .....	72
4.4. Investigation on the total system performance .....	85
5. Principles for achieving HTC&LTH systems .....	94
5.1. Reducing dissipations of internal processes in the system .....	94
5.2. Principles for reducing dissipations of key processes .....	95
5.3. Balance between consumptions of “sources” and “transportation” .....	97
6. Brief summary of this report .....	100
<i>PART 2</i> .....	103
<b>1 Application in an office building (humid region of China) .....</b>	<b>103</b>
<b>1.1 Description of the THIC System in an office building .....</b>	<b>103</b>
<b>1.2 Performance test of the THIC system .....</b>	<b>108</b>
<b>1.3 Energy consumption of the THIC system .....</b>	<b>115</b>
<b>1.4 Discussions .....</b>	<b>116</b>
<b>1.5 Conclusion .....</b>	<b>118</b>

<b>2</b>	<b>Application in an office building (China)</b> .....	118
2.1	<b>Description of the system</b> .....	118
2.2	<b>Performance in summer</b> .....	120
2.3	<b>Performance in winter</b> .....	123
2.4	<b>Conclusion</b> .....	123
<b>3</b>	<b>Application in a building (Japan)</b> .....	124
3.1	<b>Introduction</b> .....	124
3.2	<b>Composition of the THIC system</b> .....	124
3.3	<b>Demonstration test</b> .....	125
3.4	<b>Conclusion</b> .....	128
<b>4</b>	<b>Application of solar thermal system application (Italy)</b> .....	128
4.1	<b>SYSTEM TYPE</b> .....	128
4.2	<b>BRIEF DESCRIPTION</b> .....	128
4.3	<b>WORKING PRINCIPLE AND STRATEGIES</b> .....	129
4.4	<b>FEATURES AND POTENTIALITIES</b> .....	133
4.5	<b>EXAMPLE (theoretical and/or actual case studies)</b> .....	134
<b>5</b>	<b>Application in a building in Denmark</b> .....	140
5.1	<b>Radiant heating and cooling systems in plus-energy houses</b> .....	140
5.2	<b>A novel system: TABS with diffuse ceiling ventilation</b> .....	154

# **PART 1**

## **1. Introduction**

In designing a building, many HVAC systems options satisfying basic requirements related to its use are available. The design engineer is responsible for considering these systems and recommending a system that will meet the project goals and perform as desired. In addition, regional regulations also have requirements on system performance. In fact, high efficiency requirements are imposed to the HVAC equipment in some strict regional regulations such as the Energy Performance of Buildings Directive (EPBD) in European Union, which requires a minimum efficiency of HVAC equipment in the market. HVAC manufacturers have made major improvements to improve the performance of their systems and meet these criteria. Current technologies in the market have now only a small window of opportunity for improvements still open. As for the nearly zero-energy goal for all newly constructed buildings in Europe after 2020, it seems very likely that the design of future buildings should still rely on today's technologies to meet these targets. The integration of High Temperature Cooling (HTC) and Low Temperature Heating (LTH) may bring a fresh perspective in this context.

The subtask B and C reports have already presented potential solutions on terminal units (Subtask B) and outdoor air handling processes (Subtask C) that use LTH and HTC efficiently, while satisfy these comfort requirements of occupants. Considering the “global energy chain”, this report proposes a broad analysis of the total system from the energy sources/sinks to the indoor environment. The main goals of this report are stated as follows:

- a. To evaluate the benefits of High Temperature Cooling and Low Temperature Heating on performance of *Heat and Cold Generators*.
- b. To evaluate the impacts of High Temperature Cooling and Low Temperature Heating on performance of the *Total System*.
- c. To propose an overview of potential benefits issued from the High Temperature Cooling and Low Temperature Heating HVAC system and to give practical recommendations on design and operation of these systems.

The first section proposes a sensitivity analysis on performance of different heat sources and heat sinks, giving potential benefits of increasing/decreasing the cooling/heating temperature.

In the second section of this report, some applications of this novel analysis method for HVAC systems are presented.

The third section presents different investigation results related to the integration of HVAC systems in buildings and looks at temperature influence on performance of the total system.

## 2. Impact of Temperature on Performance of the Primary HVAC System

Before entering analysis of the total system, this section proposes an overview of potential impact of temperature change on performance of several primary HVAC systems. A detailed analysis of the two primary systems considered was carried out. The temperature impacts on the performance of other types of primary systems are then identified.

### 2.1. Gas condensing boiler

The sensitivity analysis of a gas condensing boiler, based on a simplified boiler model tuned with manufacturer data (Vandenbulcke, 2013) is hereinafter presented

The parameters considered for the boiler sensitivity analysis are stated as follows:

- $T_{w,boiler,su}$ , the supply water temperature of the boiler,
- $T_{w,boiler,ex}$ , the exhaust water temperature of the boiler,
- BHLR, the building heating load ratio defined as the ratio of the actual total building heating load to the nominal building heating load,
- and MFR, the mass flow ratio defined as the ratio of the actual water mass flow rate to the nominal/design mass flow rate in the boiler:

$$MFR = \frac{\dot{M}_{real}}{\dot{M}_{nom}}$$

Some assumptions are made in the analysis:

1. The difference between  $T_{w,boiler,ex}$  and  $T_{w,boiler,su}$  is higher than or equal to 2K.
2.  $T_{w,boiler,su}$  is always higher than or equal to 25°C.
3. The minimal water flow rate is equal to 5% of the maximal value ( $MFR_{min} = 0.05$ ).
4. The maximal water flow rate is evaluated at full load and with a temperature difference of 10K between  $T_{w,boiler,ex}$  and  $T_{w,boiler,su}$ .

The first results presented in Fig. 2-1 and Fig. 2-2 concerning the sensitivity of the condensing boiler efficiency to  $T_{w,boiler,su}$  were obtained at:

- full load: BHLR=1 (Fig. 2-1)
- BHLR=0.3 (Fig. 2-2).

Each curve represents the efficiency of the boiler at a given exhaust water temperature. The load is the same for all curves in a same figure, which means the water flow rate was adjusted at each point.

It can be concluded that, the lower the supply temperature of the boiler, the higher its efficiency (thanks to more latent heat recovered in the fumes). The influence of the exhaust water temperature (usually at the setpoint) is also noticeable, but with a much smaller impact (Fig. 2-3 and Fig. 2-4). At first glance, one could then consider that the optimal conditions would be reached if both the lowest supply and the lowest exhaust temperature are maintained. However, from the perspective of system integration and total system analysis, the sensitivity

of the condensing boiler efficiency to water mass flow rate has also to be taken into account. This sensitivity is presented, at different  $T_{w,boiler,su}$ , under full load in Fig. 2-5 and at 30% of BHLR in Fig. 2-6.

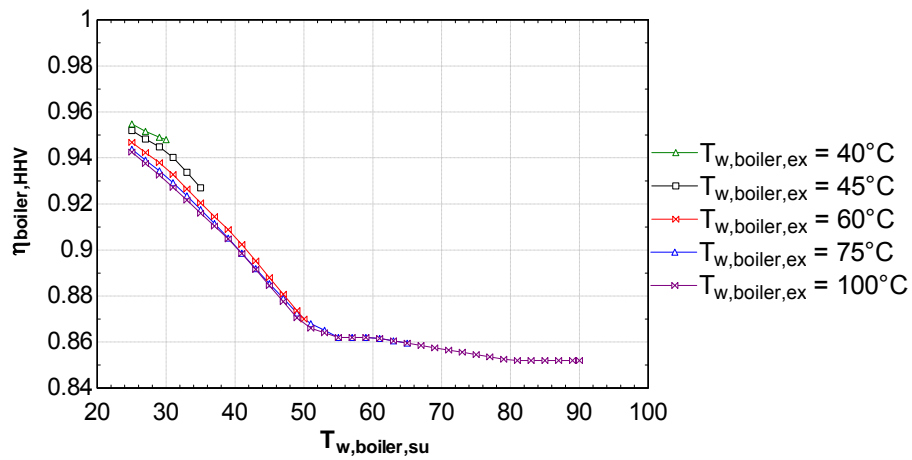


Fig. 2-1 Sensitivity of the gas condensing boiler efficiency to supply water temperature at different exhaust water temperatures at BHLR = 1.

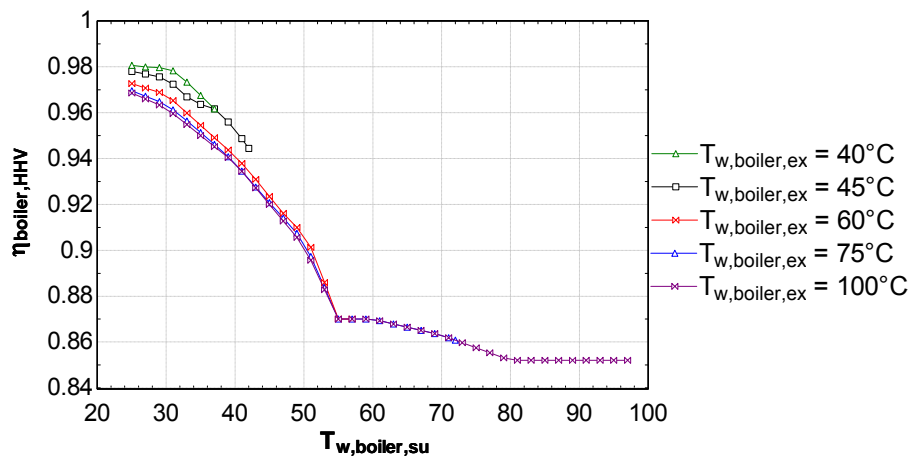


Fig. 2-2 Sensitivity of the gas condensing boiler efficiency to supply water temperature at different exhaust water temperatures at BHLR = 0.3.

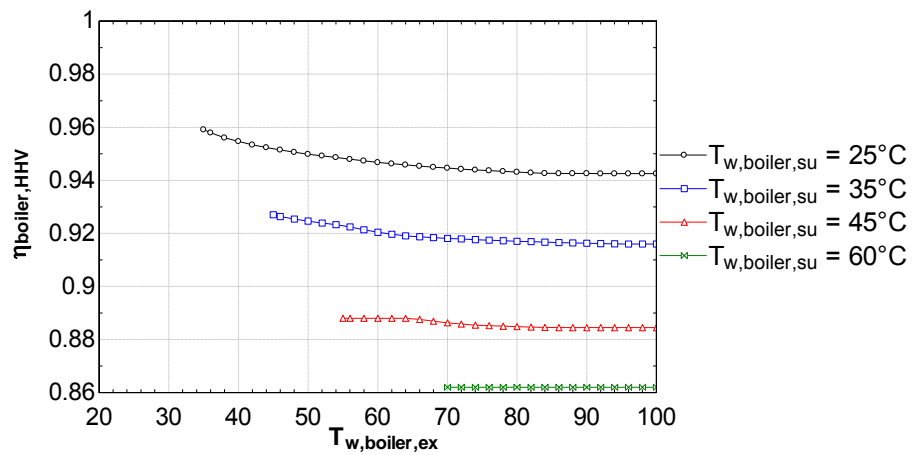


Fig. 2-3 Sensitivity of the gas condensing boiler efficiency to supply water temperature for different exhaust water temperatures at BHLR = 1.

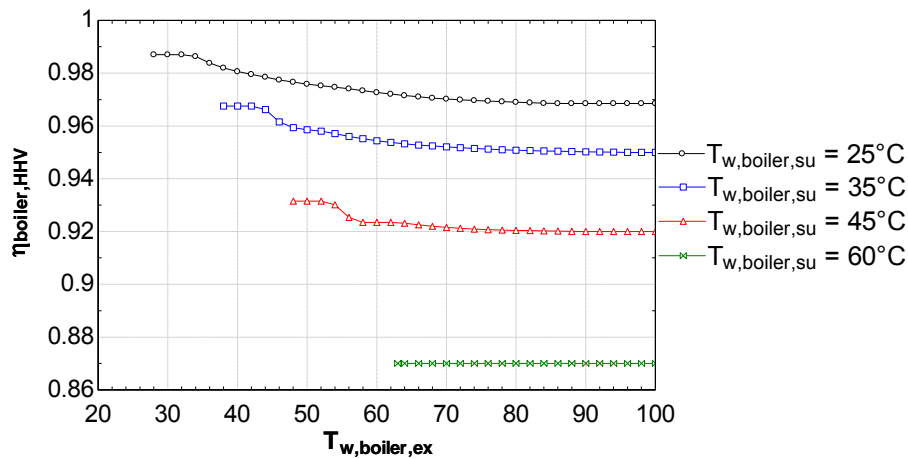


Fig. 2-4 Sensitivity of the gas condensing boiler efficiency to supply water temperature at different exhaust water temperatures at  $BHLR = 0.3$ .

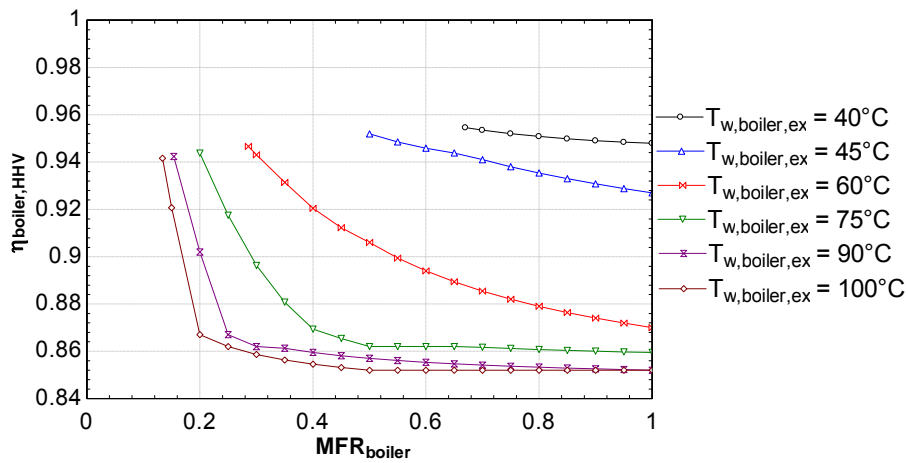


Fig. 2-5 Sensitivity of the gas condensing boiler efficiency to volume flow rate at different exhaust water temperatures at  $BHLR = 1$

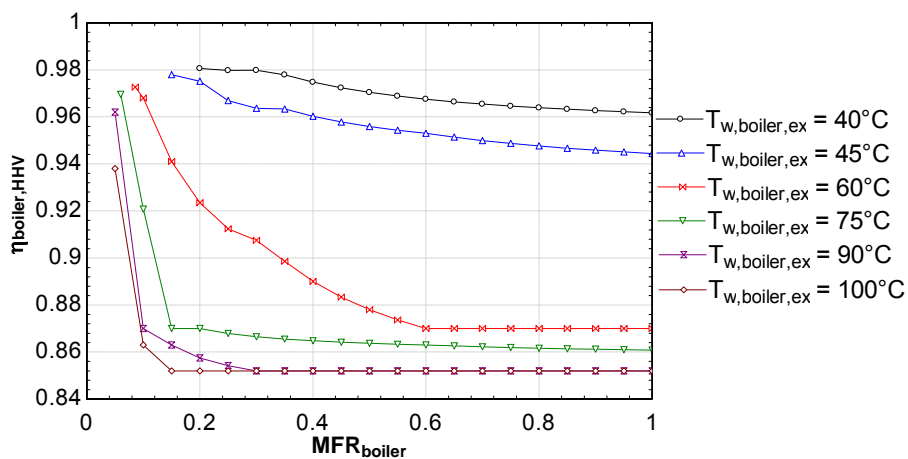


Fig. 2-6 Sensitivity of the gas condensing boiler efficiency to volume flow rate at different exhaust water temperatures at  $BHLR = 0.3$

The influence of the water flow rate on the condensing boiler efficiency is obvious. When the water flow rate in the boiler is properly controlled, high efficiency can be achieved

regardless of the boiler exhaust water temperature. Anticipating a bit on the following, these observations pave the way to system optimization with a compromise between reducing flow rates (and thus the consumption of the auxiliaries), and lowering the water temperature in order to reduce the heat losses in the distribution system and also (slightly) increase the boiler efficiency.

## 2.2. Air cooled chiller

The temperature and flow rate sensitivity analysis presented hereinafter concerns a chiller with screw compressor and air-cooled condenser. The analysis was made based on a semi-empirical model and validated on manufacturer data. Its operating range and the nominal conditions considered for the sensitivity analysis are presented in Table 2-1.

*Table 2-1 Operating range and nominal conditions of the chiller*

	Unit	Minimum	Maximum	Nominal
$T_{w,ev,su}$ —supply water temperature of evaporator	°C	6.8	21	12
$T_{w,ev,ex}$ —exhaust water temperature of evaporator	°C	3.3	15	7
$T_{a,cd,su}$ —supply air temperature of condenser	°C	-10	55	30
$\dot{M}_{w,ev}$ —water flow rate of evaporator	kg/s	5.3	34.1	19.44

The parameters considered for the sensitivity analysis are:

- $T_{a,cd,su}$ , the supply air temperature of condenser
- $T_{w,ev,ex}$ , the exhaust water temperature of evaporator
- BCLR, the building cooling load ratio defined as the ratio of the actual global building cooling load to the nominal/design global building cooling load,
- MFR, the mass flow ratio defined as the ratio of the actual to nominal water mass flow rates.

The assumptions made in the analysis include:

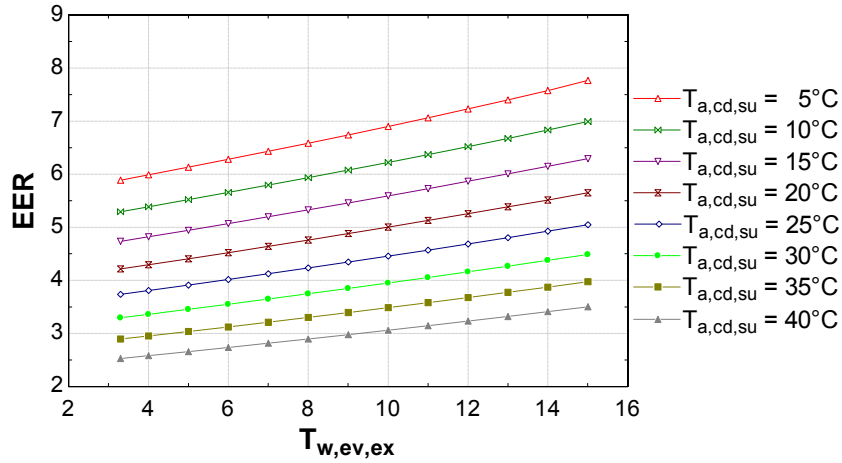
- The chiller only works within the operating range defined in Table 3-1.
- $T_{w,ev,su}$  is always lower than or equal to 21°C.

The sensitivity of the chiller efficiency to  $T_{w,ev,ex}$  at different  $T_{a,cd,su}$  is shown in Fig. 2-7 and Fig. 2-8 under:

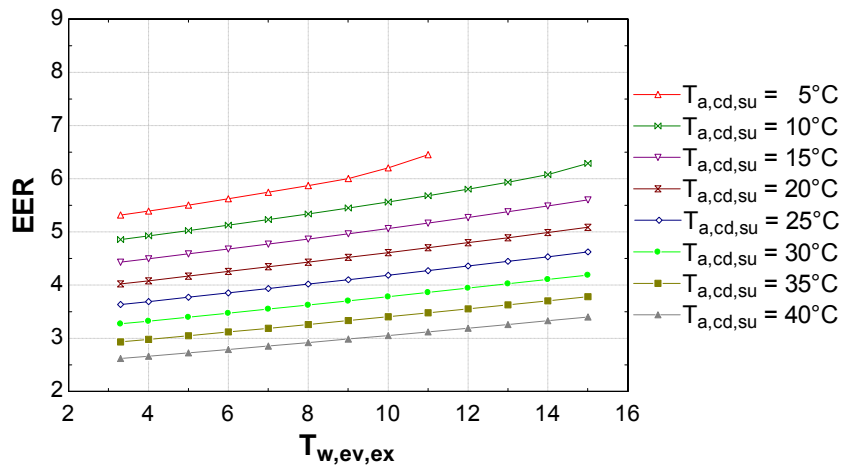
- BCLR = 1 (the nominal load),  $\dot{M}_{w,ev} = \dot{M}_{w,ev,n}$  and  $\Delta T_{w,ev} = 5K$ ,
- BCLR = 0.3,  $\dot{M}_{w,ev} = \dot{M}_{w,ev,n}$  and  $\Delta T_{w,ev} = 5K$ .

The influence of  $T_{w,ev,ex}$  on the chiller efficiency appears to be significant. For an increase of 1K of the  $T_{w,ev,ex}$ , an increase in EER from 2.4% and 2.8% at BCLR = 1 and from 2.0% and 2.2% at BCLR = 0.3 was observed. This means that with, for example, an outside temperature of 25°C, the chiller EER can be increased from 3.85 to 4.36 under BCLR = 1, if rising the  $T_{w,ev,ex}$  from 7°C to 12°C, it would lead to a 13% improvement in efficiency of the system. By comparing the two graphs, one can see that the chiller performances are decreased at part load (at BCLR = 0.3). In terms of the air cooled chiller, the introduction of high

temperature cooling is clearly beneficial. However, this rise of water temperature has also an impact on the sizing of the secondary system, leading to an increase in consumption of auxiliaries (larger flow rate and corresponding pressure drops in the hydraulic system and probably also on the air-side for the AHU's).

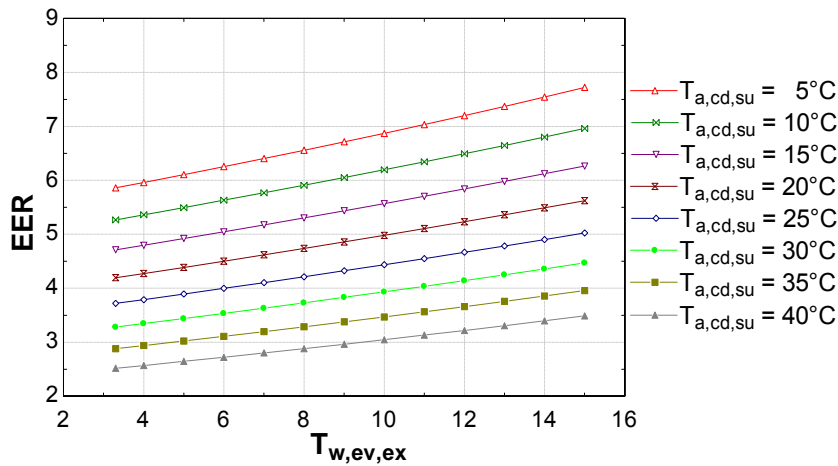


(a)



(b)

Fig. 2-7 Sensitivity of the air-cooled chiller efficiency to exhaust water temperature of evaporator at different supply air temperature of condenser under: (a) BCLR = 1 (at  $\dot{M}_{w,ev} = \dot{M}_{w,ev,n}$  and  $\Delta T_{w,ev} = 5^\circ\text{C}$ ), (b) BCLR = 0.3 (at  $\dot{M}_{w,ev} = \dot{M}_{w,ev,n}$  and  $\Delta T_{w,ev} = 1.5^\circ\text{C}$ )



(a)

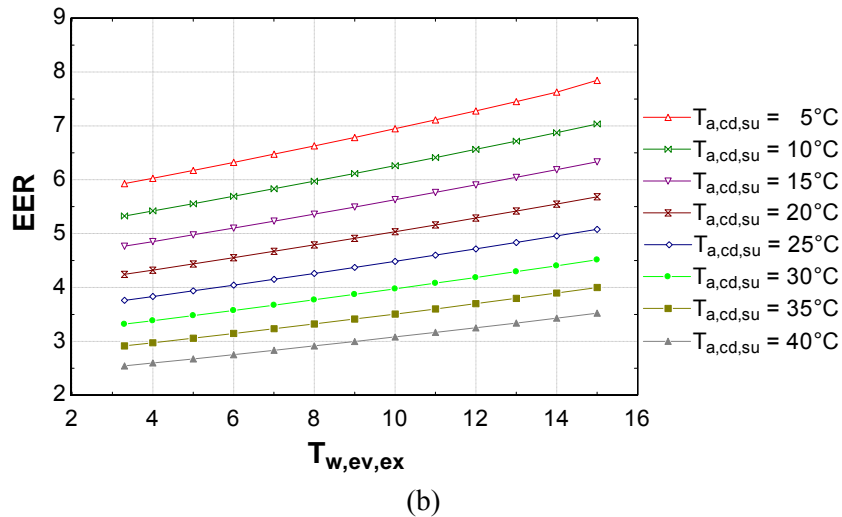


Fig. 2-8 Sensitivity of the air-cooled chiller efficiency to exhaust water temperature of evaporator at different supply air temperature of condenser under: (a)  $BCLR = 1$  (at  $\dot{M}_{w,ev} = 0.5 \cdot \dot{M}_{w,ev,n}$  and  $\Delta T_{w,ev} = 10^\circ\text{C}$ ), (b)  $BCLR = 1$  (at  $\dot{M}_{w,ev} = \dot{M}_{w,ev,max}$  and  $\Delta T_{w,ev} = 1.85^\circ\text{C}$ )

In Fig. 2-8 the sensitivity of the chiller efficiency to evaporator water flow rate, under the same conditions as Fig. 2-7, is presented, but the water flow rate was reduced to 50% of its nominal value. The impact of such reduction of water flow rate (leading to an increase in the difference between water temperatures at supply and exhaust of the evaporator), is lower than that of  $T_{w,ev,ex}$ . An average decrease in EER of 0.65% at  $BCLR=1$  and that of 0.41% at  $BCLR=0.3$  can be observed. It is also worth noting that the chilled water flow rate could be considered as a sensible parameter in the optimization procedure for the cooling system, because its impact on the chiller efficiency is low, but, through direct and indirect influences on the auxiliary consumptions, its impact on the system performance could be high.

### 2.3. Water cooled chiller

This section presents the sensitivity analysis of a cooling plant composed of a water cooled screw chiller coupled to a closed circuit cooling tower. A free-chilling heat exchanger is also included in the system. The schematic of the cooling plant is presented in Fig. 2-9. The influence of the chilled water temperature on the system performance was analyzed based on a detailed simulation model using EES equation solver. Two operating modes were considered in the analysis, as follows:

- Standard operation mode, with the chiller coupled to the cooling tower;
- Free-chilling mode, with the chiller turned off and the free-chilling heat exchanger coupled to the cooling tower.

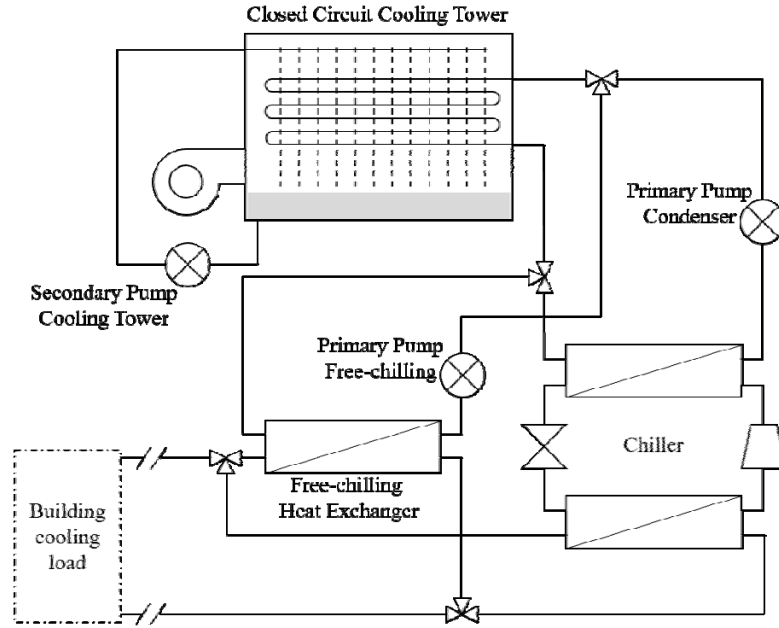


Fig. 2-9 Schematic of the cooling plant.

The control of the two modes is not considered in this section since this analysis was carried out based on steady-state conditions with a fixed chilled water cooling load constant under steady outdoor conditions. Other parameters are considered in the analysis such as the water temperature at set point of the exhaust of the cooling tower, the oversizing of the cooling tower and the type of fan speed control in the cooling tower.

Semi empirical models were used for both the cooling tower (Stabat & Marchio, 2004) and the water cooled chiller (Lemort & Bertagnolio, 2010). The first step consists in sizing the cooling tower together with the other system components. The system's main inputs under nominal condition are summarized in Table 2-2.

The size of the cooling tower capacity depends on the cooling capacity of the evaporator (design cooling load of the building), the chiller energy efficiency ratio (EER) and the cooling tower oversizing factor, stated as follows:

$$\dot{Q}_{ct,n} = \dot{Q}_{ev} \cdot (1 + 1/EER_{chiller}) \cdot f_{ct,oversizing} \quad (2-1)$$

$$\dot{M}_{a,ct,n} = 0.022 * \dot{Q}_{ct,n} \quad (2-2)$$

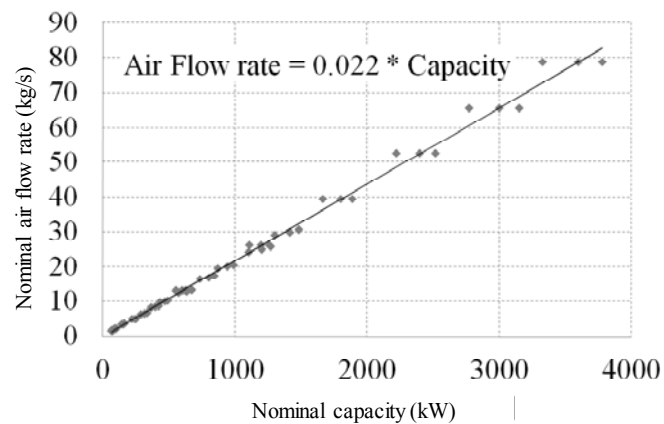
$$\dot{W}_{fan,ct,n} = 0.018 * \dot{Q}_{ct,n} \quad (2-3)$$

$$\dot{W}_{pump,2,ct,n} = 0.002 * \dot{Q}_{ct,n} \quad (2-4)$$

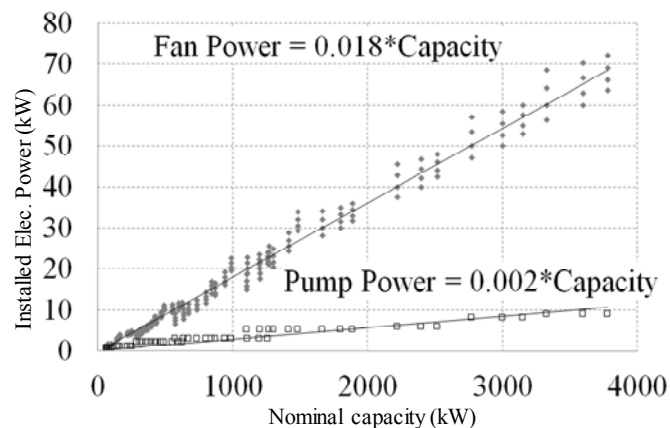
Table 2-2 System sizing data

	Unit	Value
Cooling capacity		
at evaporator/condenser	kW	366.30/445.86
at cooling tower (oversizing factor)	kW	512.42 (1.15)
at free-chilling heat exchanger (oversizing factor)	kW	146.55 (0.40)
Chiller		
EER ( $t_{ev,ex}=7^{\circ}\text{C}$ and $t_{cd,su}=30^{\circ}\text{C}$ )	-	4.62

Condenser nominal water flow rate	kg/s	21.29
Condenser nominal pressure drop(water-side)	kPa	17.50
Condenser pump nominal power	kW	3.10
Free-chilling		
Heat exchanger primary side water flow rate	kg/s	3.50
Heat exchanger primary side pressure drop	kPa	7.35
Free-chilling primary pump nominal power	kW	0.56
Cooling tower		
Supply wet bulb temperature	°C	22.00
Air flow rate	kg/s	11.30
Fan nominal power	kW	9.20
Exhaust water temperature	°C	30.00
Global UA-value	kW/K	41.82
Nominal pressure drop in standard/f-ch. Mode	kPa	62.00/28.49
Secondary cooling tower pump nominal power	kW	1.10



(a)



(b)

Fig. 2-10 Correlation between (a) cooling tower capacity and air flow rate, (b) nominal absorbed power of the centrifugal fans and nominal absorbed power of the secondary pump.

The sizing of the air flow rate in the cooling tower together with the nominal absorbed power of both the centrifugal fans and the secondary pump are then evaluated as a proportion of the cooling capacity (Bertagnolio, Stabat, Soccal, Gendebien, & Andre, 2010) based on manufacturer data as shown in Fig. 2-10(b)

Fig. 2-10

From these inputs, the cooling tower heat transfer global coefficients are evaluated in nominal conditions, giving the global UA-value in nominal condition.

- Standard operation mode

The sensitivity analysis of the system performance to chilled water temperature (set point at evaporator exhaust) can be achieved using the described model. The performance of the system was evaluated through a global performance coefficient as defined in (5).

$$COP_{cooling,plant} = \dot{Q}_{ev} / (\dot{W}_{fan,ct} + \dot{W}_{pump,1,ct} + \dot{W}_{pump,2,ct} + \dot{W}_{chiller}) \quad (2-5)$$

In each simulation, the load at the evaporator (or at the free-chilling heat exchanger) is defined as the building cooling load ratio or BCLR, ratio between the actual cooling load at the evaporator and its nominal load. Fig. 2-11 presents the influence of the cooling tower fan speed control at different cooling load, considering the system as defined in the design phase (Table 2-2). It shows an improvement between one-speed fan and variable-speed with performance increase ranging from 1.3% to 8.1%, especially at lower cooling load.

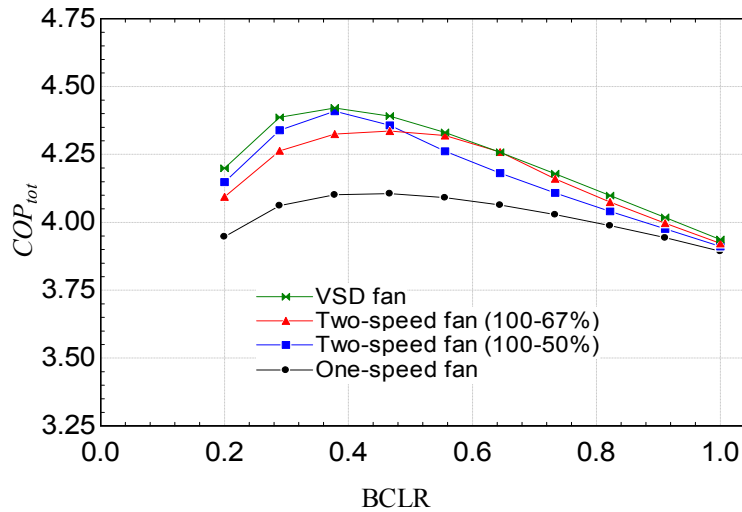


Fig. 2-11 Sensitivity of the cooling plant performance to BCLR of different fan speed control modes

In Fig. 2-12, the influence of the cooling tower oversizing is analyzed considering the VSD fan and the system as designed. It shows, on one side, slight degradation when the cooling tower is oversized, but also, on the other side, severe degradation of the performance of the system at high cooling load when the cooling tower is undersized. This effect is coming from the increase of the water temperature leaving the cooling tower and entering the condenser, which significantly lowers the chiller EER. In Fig. 2-13, the impact of the water temperature leaving the cooling tower is then considered again, based on the system as designed (with VSD?). It shows an optimal temperature of about 28°C almost independent to cooling load.

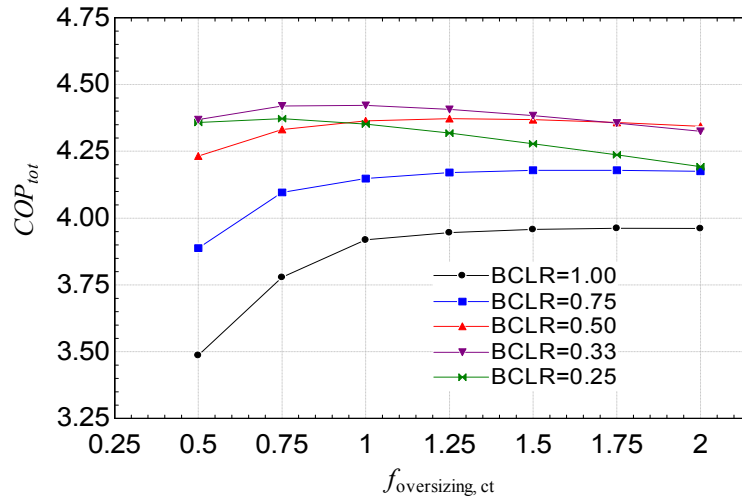


Fig. 2-12 Sensitivity of the cooling plant performance to cooling tower sizing at different BCLR.

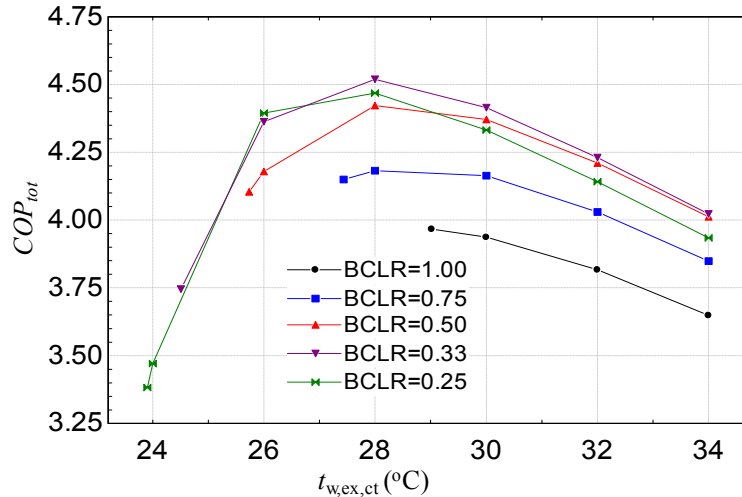


Fig. 2-13 Sensitivity of the performance of the cooling plant at different BCLR.

Some conclusions can be drawn from these three sensitivity analysis. First, the impact of the fan type and of the oversizing of the cooling tower should be taken into account in the sizing of the system. From that, a control law should be established based on climate and the building cooling load associated. Based on the model sized as above, the sensitivity of the performance of the cooling plant to the chilled water temperature can then be predicted. Fig. 2-14 shows that, for wet bulb temperature of 22°C, an increase of 1°C of the chilled water temperature can improve the cooling plant performance by 5.8% in average. This observation shows that importance should be attached to the control of the chilled water at all time.

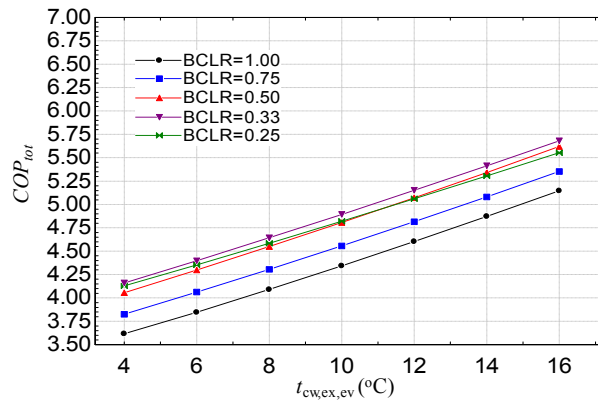


Fig. 2-14 Sensitivity of the performance of the cooling plant to chilled exhaust water temperature at different BCLR's.

● Free-chilling mode

The free-chilling mode can significantly improve system performance under certain outdoor conditions. The sizing of both the free-chilling heat exchanger and its corresponding primary pump (see Fig. 2-9) has a significant impact on the free-chilling potential. In Fig. 2-15, the impact of the sizing is analyzed under 10% of the nominal load (BCLR=0.1) and outdoor conditions of 10°C/50%RH. The sensitivity to sizing is substantial, showing the importance of proper sizing of such system.

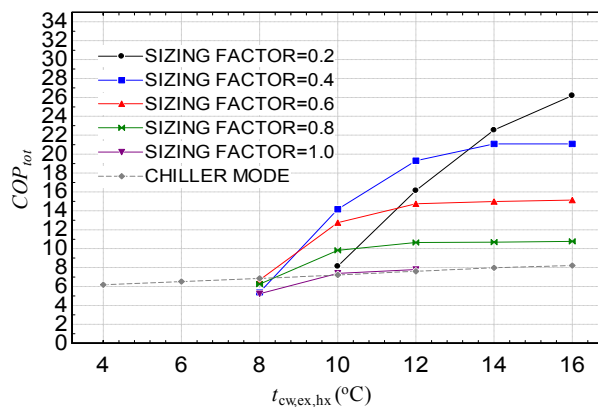


Fig. 2-15 Sensitivity of the cooling plant performance to free-chilling sizing at different chilled water exhaust temperature, at BCLR=0.1 and  $T_{out}=5.5^{\circ}\text{C}/\text{RH}=50\%$ .

Fig. 2-16 presents the sensitivity of the system to chilled water temperature at different cooling load and outdoor conditions of 10°C/50%RH. It shows the potential benefit of the free-chilling when working at higher chilled water temperature and at low cooling load with high COP, under conditions commonly occurring in mild climate. In Fig. 2-17, the available cooling at the free-chilling heat exchanger and the associated COP is given as a function of the outdoor wet bulb temperature at different chilled water temperature.

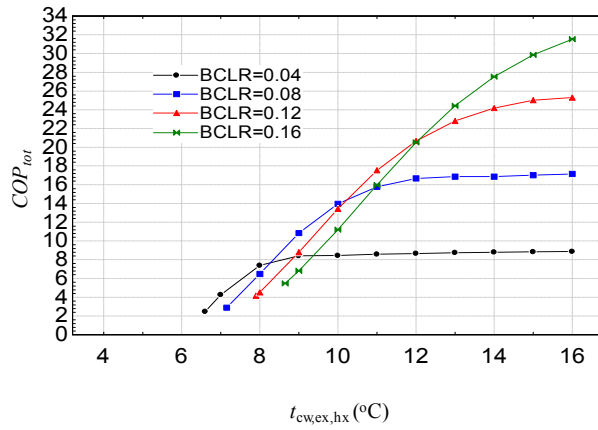


Fig. 2-16 Sensitivity of the cooling plant performance to chilled water temperature leaving the free-chilling heat exchanger at different BCLR.

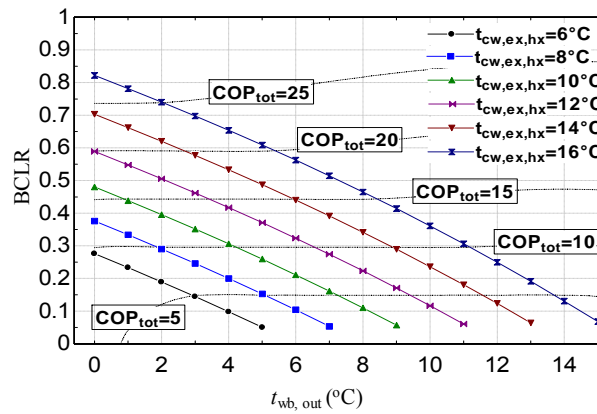
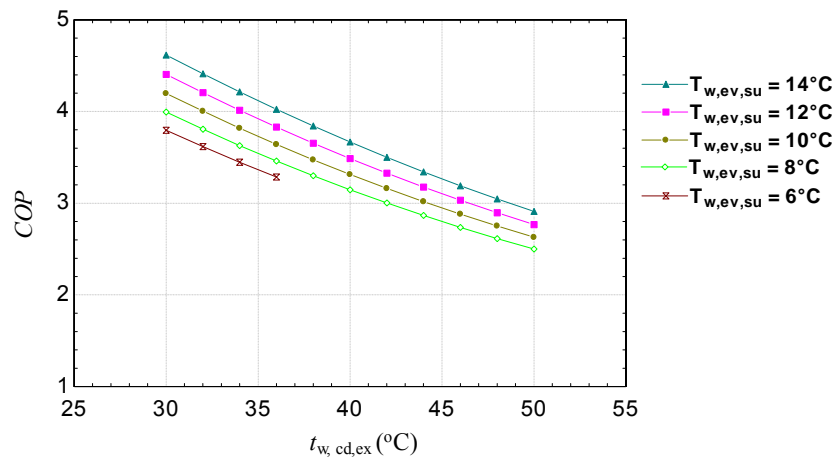


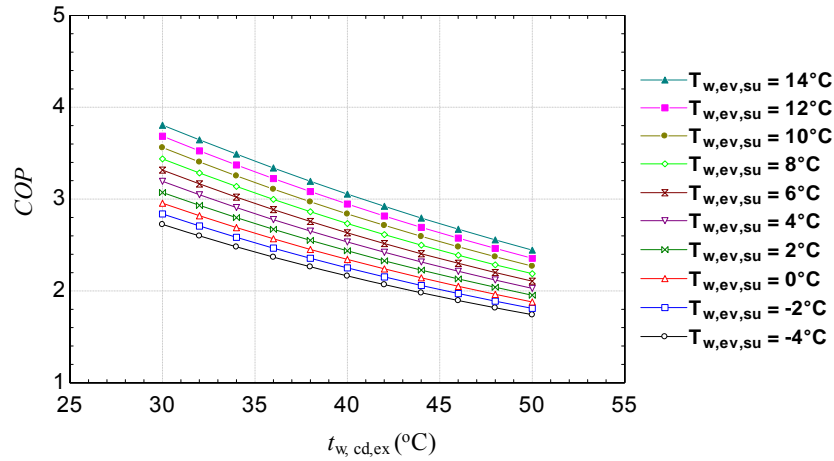
Fig. 2-17 Free-chilling cooling capacity as a function of the outdoor wet bulb temperature at different temperature of chilled water leaving the free-chilling heat exchanger

#### 2.4. Air source heat pump

The methodology for the air cooled and the water cooled chiller was utilized to analyze the sensitivity of air source heat pump. The model considered in the analysis was developed based on manufacturer data for an air source heat pump with a scroll compressor.



(a)



(b)

Fig. 2-18 Sensitivity of the primary system efficiency to exhaust water temperature of condenser under different supply air conditions of evaporator at: (a)  $BHLR = 1$  (for  $\dot{M}_{w,ev} = \dot{M}_{w,ev,n}$  and  $\Delta T_{w,ev} = 5^\circ\text{C}$ ), (b)  $BHLR = 0.3$  (for  $\dot{M}_{w,ev} = \dot{M}_{w,ev,n}$  and  $\Delta T_{w,ev} = 1.5^\circ\text{C}$ )

## 2.5. BCHP with internal combustion engine (ICE)

### 2.5.1. Principle of cogeneration with internal combustion engine (ICE)

The most widespread cogeneration system currently used in buildings is ICE based. This is due to their well-proven technologies and reliability. Moreover, the wide range of powers (from kW to MW) available makes them suitable for a wide range of applications (residential, commercial, industrial) (Knight & Ugursal, 2005).

A cogeneration unit based on ICE produces electricity with an electrical generator driven by engine and heat by recovering the different heat losses. These heat sources include: exhaust gases, engine jacket cooling, lube oil cooling and intercooler of turbocharge. However, usually the unit uses only the two first sources because they account for the most part of the recoverable heat. The Exhaust gases account for 30-50% and the engine jacket cooling for 30% of the energy input (Knight & Ugursal, 2005) (CIBSE CHP Group, 2012).

The cooling of the jacket cannot be directly made by the building heating water because of problems associated with pressure, corrosion, and thermal shock. Therefore, cogeneration unit uses a heat exchanger to transfer the heat from the engine cooling medium (usually glycol-water) to the heating water. This heat exchanger can be mount in series before or after the exhaust gas heat exchanger or in parallel. As the engine cooling water temperature needs to be kept below  $95^\circ\text{C}$ , the cooling heat exchanger is usually placed before the exhaust gas heat exchanger, and this configuration is shown in Fig. 2-19. As the cooling water have a maximum, the return temperature of the heating circuit also has maximum temperature set by the supplier ( $70\text{-}90^\circ\text{C}$ ) (Rosato & Sibilio, 2012).

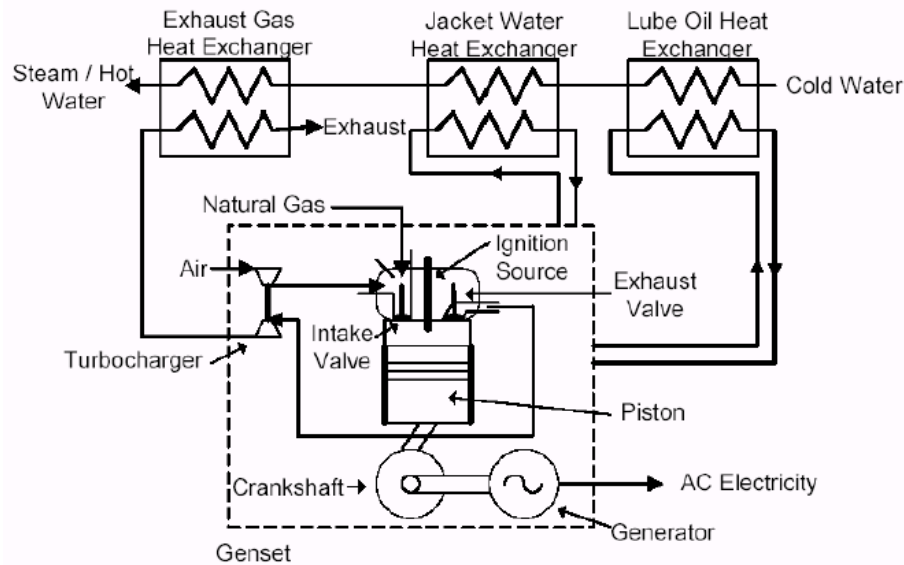


Fig. 2-19 Typical layout of the ICE based CHP (Knight & Ugursal, 2005)

With this configuration, the exhaust gases usually leave the unit at temperature around 90°C. Then in order to improve the thermal efficiency of the CHP unit, a condensation heat exchanger can be added in order to recover the latent heat in the flue gases provided that the return temperature is low enough (dew point of flue gas is around about 45-55°C) (Zhao, Fu, Zhang, Jiang, & Li, 2010).

### 2.5.2. Influence of return water temperature on performance

In order to optimize the performances of the cogeneration unit and the associated heating circuit, the influence of heating water temperature needs to be known. Fig. 2-20 and Fig. 2-21 show the influence of return water temperature on the thermal efficiency of a 5.5kW Senertec (Beausoleil-Morrison, 2007) and a 6kW AISIN SEIKI (Rosato & Sibilio, 2012), experimentally tested in order to evaluate the performance and calibrate the Annex 42 models. These figures show that the return temperature has nearly no influence on thermal efficiency. Consequently, the coefficient relative to the return temperature was set to 0 in the polynomial Annex 42 models. The variation of thermal efficiency of the AISIN SEIKI is due to the variation of the electrical power (the thermal efficiency decreases with the electrical power).

These experimental studies show that return temperature have no influence on the cogeneration unit performance. Nevertheless, as mentioned above, some units have a flue gases condensation heat exchanger (CHE), but this CHE will be effective only if the temperature is below the flue gases dew point and then the return temperature will have an influence. For example, the datasheets of the Cogen Green unit mentioned an increase in thermal power if the return temperature is below 40°C. The Senertec that uses Annex 42 to calibrate the model have a 3 KW condenser, giving a full power if the return temperature is 20°C. This increase in thermal power improves the thermal efficiency by about 10%. X.L. Zhao & al. (Zhao, Fu, Zhang, Jiang, & Li, 2010) also conclude that it is possible to gain a 10% improvement on thermal efficiency with CHE at a low return temperature.

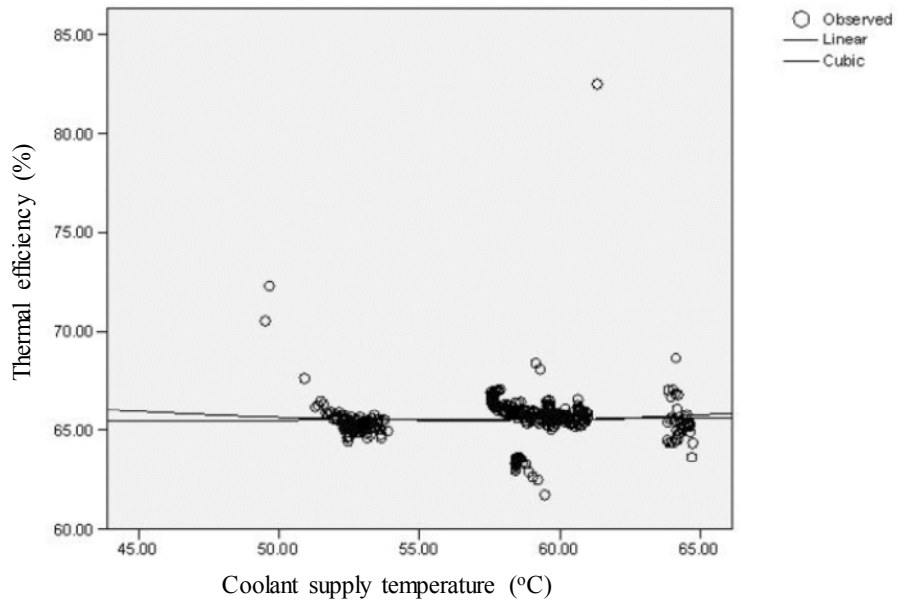


Fig. 2-20 Thermal efficiency Vs return temperature, experimental data from a Senertec of 5.5 kW

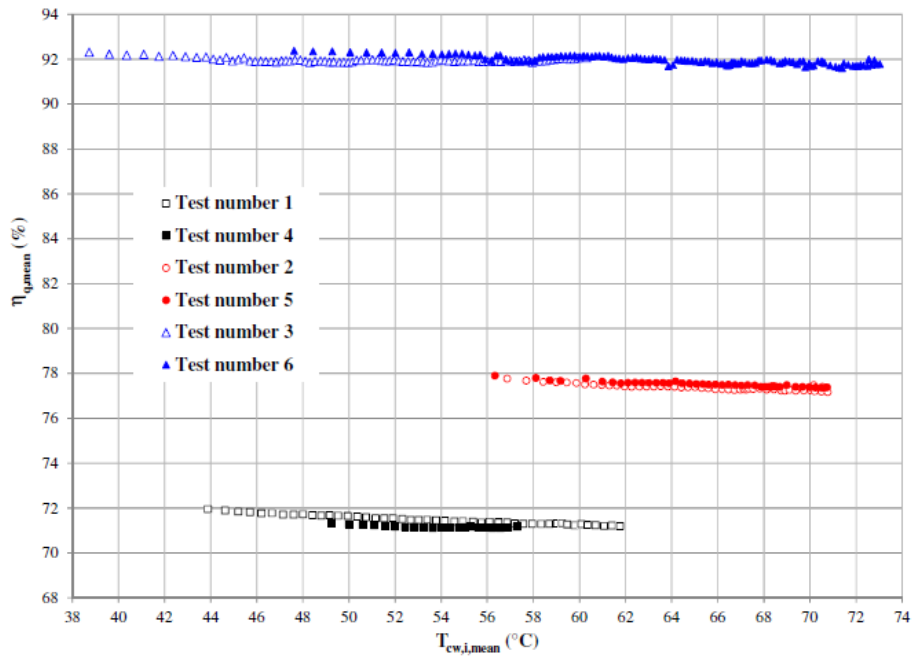


Fig. 2-21 Thermal efficiency Vs return temperature, experimental data from an AISIN SEIKI of 6 kW

## 2.6. District heating network as primary system

### 2.6.1. General information

A district heating network (DHN) has several pipes to connect power plant(s) to consumers (residential buildings, industries, etc.). These pipes can be quite long: from several meters to kilometers for the largest DHN<sup>1</sup>. In these pipes, the working fluid velocity is generally quite reduced (0.5 – 5 m/s) to limit the pressure losses inside the pipes. Therefore, the energy supplied by a power plant could require several minutes to hours to reach the furthest consumers. The working fluid is generally water (< 100°C), hot pressurized water, steam or in some specific applications oils to support higher temperatures (> 200°C). Currently the operating temperature of a residential DHN (4<sup>th</sup> generation) is generally quite reduced (< 80°C) depending of the building heater (conventional heaters, heat pumps or other types) and allows sometimes to make cooling.

The heat supplied to a DHN is worth the total consumption of the consumers majored by the heat losses. The annual heat losses are generally about 10 to 25 percent of the total heat supplied to the DHN depending of insulation and annual load. Indeed, in summertime, when the heat demand is generally reduced, heat losses are quite large compared with the heat transported. And it is the opposite during the winter period.

The heat sources could be very different and combined. Of course conventional boilers using fuels as coal, natural gas, heavy fuel and others could be used. However, with strict laws on emissions and environmental impacts of heating systems, some alternatives have been investigated in recent years:

- Geothermal power, uses energy available in soil;
- Waste heat recovered from industrial applications, allowing a recovery of low temperature heat waste;
- Cogeneration plant, to produce a partial or total power demand of consumers;
- Solar power for inter-seasonal load;

In function of the annual load profile discussed previously, heat plants can combine some of these solutions to reduce costs and environmental impacts. Moreover, they can use heat storage to reduce installed peak load capacity and/or to maximize the use of one of the base load installation. This heat storage can be punctual or seasonal.

Another characteristic of the DHN concerned is the network density that involves profitability. Indeed, if a consumer is too far from the central heating and consumes few heat, it could be not interested, on an economic point of view, in connecting to the network. Here are some profitability levels: 40 MW/km<sup>2</sup> or 4MW/km found in literature.

---

<sup>1</sup> The biggest one is the one in Moscow with overall pipe length of about 10000 kilometres.

## 2.6.2. The operating temperature network

The control of the supplied temperature of a DHN to reduce consumption and therefore the costs is currently a major challenge. Indeed, it also has some influences on the network, directly affecting the annual heat losses: the higher the operating pipe temperature, the larger heat losses. Therefore, operating temperature should be decreased to reduce heat losses while guarantying the comfort in the furthest buildings: a too low temperature can lead to a too low electricity consumption in the last buildings, while there is generally a minimal return temperature to achieve, to ensure correct functioning of the building heaters. Due to these characteristics, the mass flow rate needs be adaptive to satisfy heat demands. However, in the first approximation, the pressure losses in the pipes are related to the mass flow rate by a quadratic law. So, lowering the supplied temperature will reduce heat losses but increase power consumption the electric pump. Therefore, a trade-off is required. Fig. 2-22 presents this influence through an example (the DH network in University of Liege – Belgium).

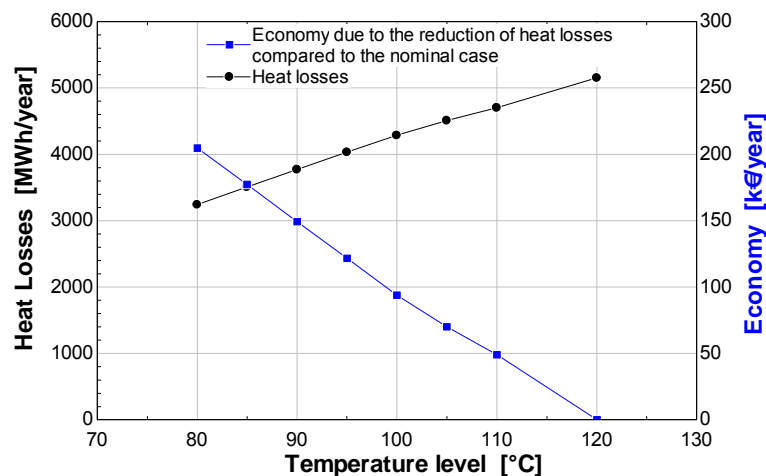
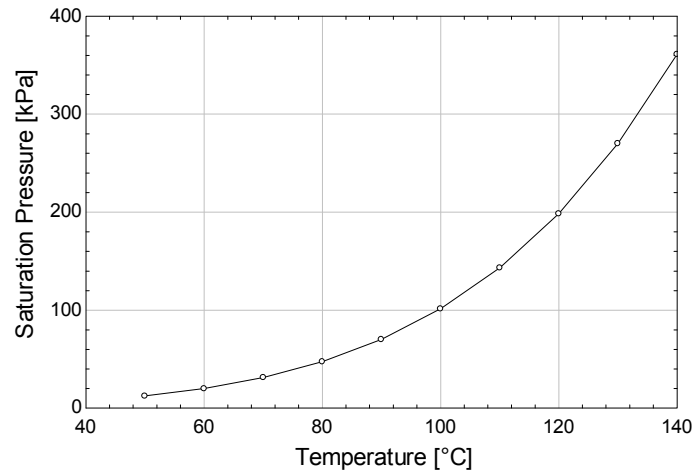


Fig. 2-22 Heat losses and economy as a function of temperature level (in the DH network in University of Liège – Belgium)

Operating temperature can bring a significant influence on the heat sources applications. If the DHN is fed by natural gas boilers, the influence of the temperature level is not that important when the natural gas boiler efficiency varies slightly between 97 and 105 % (based on LHV). Lately, the use of low temperature DHN (when the return water temperature is lower than 50°C) enables the exploitation of latent due to flue gas condensation. However, this type of DHN, so-called the 4th generation DHN, is not widespread used nowadays and most of the DHNs in operation have supply temperature at around 80°C. However, if a cogeneration plant based on a Rankine cycle is used to feed the DHN, lowering the network temperature enables an increase in electricity production. Indeed, the use of back pressure steam turbine allows the production of high temperature steam supplied in a heat exchanger to heat the DHN water by condensing the steam. By setting the temperature of the DHN together with the heat exchanger efficiency, the steam saturation temperature and consequently the level of back pressure can be fixed (Fig. 2-23). The lower the temperature requirement of the

DHN is, the lower the pressure level of the back pressure and the higher the electricity production will be.

In this case, the cogeneration efficiency, defined as the sum of the electrical efficiency and thermal efficiency, is often misleading. Indeed, increasing the level of temperature required by the DHN will increase the back pressure which, in turn, decrease the electrical efficiency. However, the thermal energy not converted into electricity is available as useful thermal energy. As a result, changing the level of water temperature in the DHN slightly affects the cogeneration efficiency.



*Fig. 2-23 Steam saturation pressure in function of temperature.*

To lower operating temperature, the buildings heaters can be changed in the case of a retrofit or designed to use the lowest operating temperature at the design step of a DHN. For example, heat pumps or low temperature heaters can be installed in buildings to limit the required operating temperature.

### 3. Applications of novel analysis method in HVAC system

In the subtask A, temperature differences of the HVAC system are investigated and entransy analysis method is introduced as a novel approach to identify the dissipations. According to the entransy analysis method, typical cases could be chosen to construct a high temperature cooling & low temperature heating system in this section and solutions could be proposed for performance improvement.

#### 3.1. Application in data centers (with high-density sensible load)

##### 3.1.1. Characteristics of the indoor built environment in data centers

Compared with common office building and other civil buildings, data centers show unique characteristics, such as rather high sensible heat load density and 8760 hours continuous air-conditioning requirement. In data centers, most of the sensible heat is coming from servers in different racks, with a load density as high as  $500\sim 3000\text{W/m}^2$ . By contrast, the humidity load in data centers is relatively low and could almost be ignored. Fig. 3-1 shows the schematic of a classical data centers and its cold aisle. Fig. 3-2 provides the energy consumption distribution of different parts in a data center. It could be seen that reducing the air-conditioning system energy consumption is key step to achieving an energy efficient data center.



Fig. 3-1 Schematics of classical data center and cold aisle: (a) Schematic of a data center; and (b) Closed cold aisle.

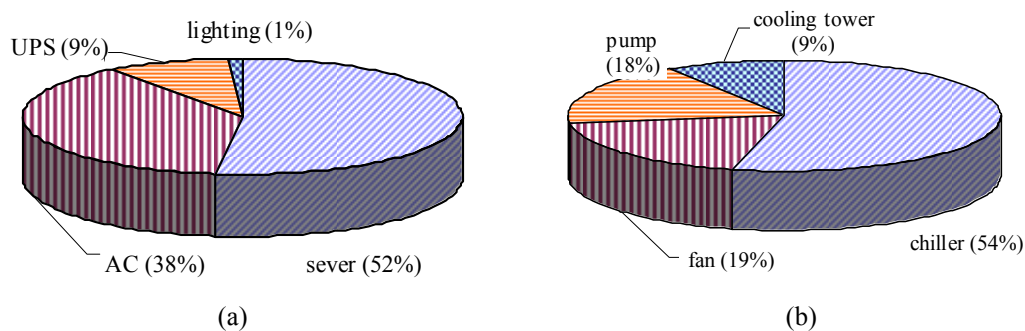


Fig. 3-2 Energy consumption of classical data centers (water-cooling system): (a) the entire data center; (b) air-conditioning system in data center.

The thermal environment maintaining process of data center consists of several steps as shown in Fig. 3-3. This process could be seen as removing sensible heat from indoor to outdoor environment under a certain temperature difference.  $T_{chip}$  is working temperature of data center internal heat source (server chips), and  $T_O$  is the temperature of selected outdoor heat sink. Then the total driven temperature difference of current thermal environment maintaining process is  $\Delta T_d = T_{chip} - T_O$ , showing the total heat transfer driving force of the heat removal process.  $T_O$  could have different values according to variable outdoor heat sinks: if outdoor fresh air is selected as the heat sink,  $T_O$  is the outdoor air dry bulb temperature; if cooling tower is selected as the heat sink,  $T_O$  then becomes outdoor air wet bulb temperature; and if indirect evaporative cooling is chosen,  $T_O$  could be reduced to outdoor air dew point temperature.

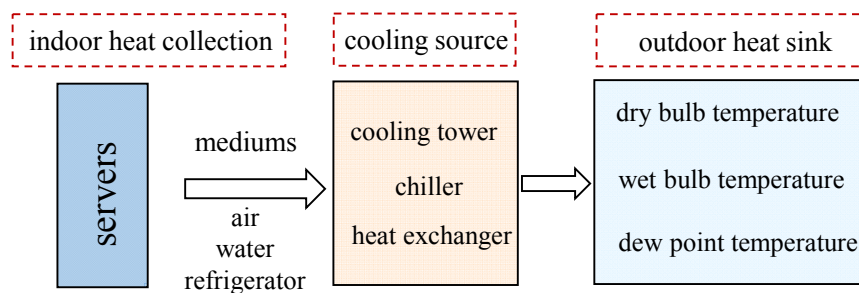


Fig. 3-3 Main processes in data center indoor thermal environment maintaining

To remove a certain amount of heat  $Q$  from indoor to outdoor heat sink, total entransy dissipation is  $\Delta E_{n,dis} = Q \cdot \Delta T_d$ . Fig. 3-4 shows a classical heat removal process from server to outdoor heat sink (natural cooling source) in the  $T$ - $Q$  diagram.

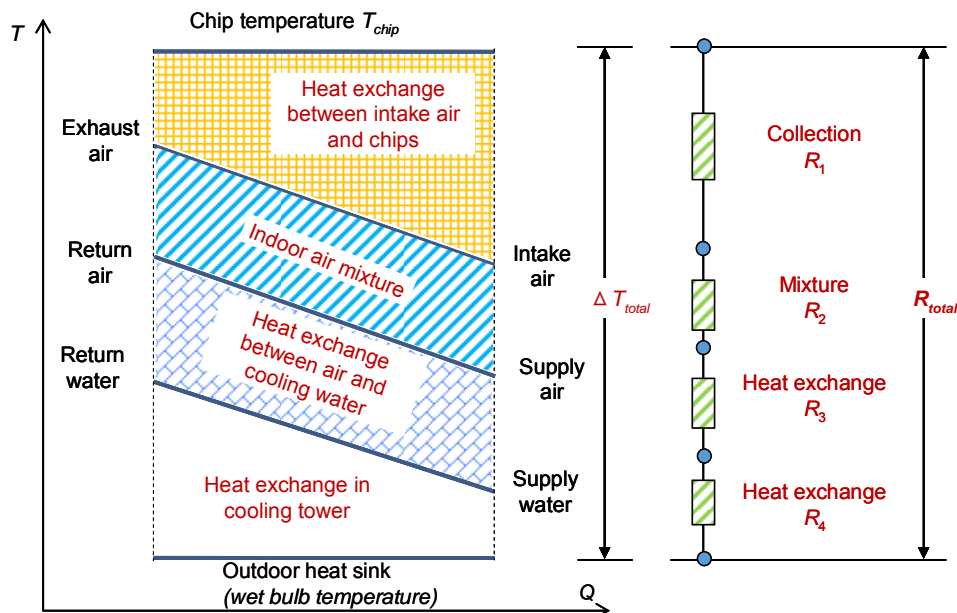


Fig. 3-4  $T$ - $Q$  diagram of a classical heat removal process (adopting outdoor natural cooling source)

As for the heat collection process from server chips to outdoor heat sink, total entransy dissipation and thermal resistance are expressed by Eq. (3-1) and (3-2) respectively:

$$\Delta E_{n,total} = \Delta E_{n,chip-air} + \Delta E_{n,mixture} + \Delta E_{n,air-water} + \Delta E_{n,coolingtower} \quad (3-1)$$

$$R_{total} = \frac{\Delta E_{n,total}}{Q^2} = R_1 + R_2 + R_3 + R_4 \quad (3-2)$$

$R_1, R_2, R_3, R_4$  is heat exchange resistance between chips and supply air, heat resistance of mixture between indoor hot and cold air, heat exchange resistance between air and water in CRAC units, and heat resistance in cooling tower respectively.

Total temperature difference is:

$$\Delta T_{total} = R_{total} \cdot Q = \frac{\Delta E_{n,total}}{Q} \quad (3-3)$$

Thus, reducing dissipation in each part during heat removal process could effectively cut down total temperature difference  $\Delta T_{total}$ . When available driven temperature difference  $T_d \geq \Delta T_{total}$ , outdoor natural cooling source could be adopted directly to achieve the heat removal process. And when temperature of outdoor natural cooling source is too high (namely  $\Delta T_d < \Delta T_{total}$ ), it's hard to remove all indoor cooling load to the outdoor environment, thus mechanical refrigeration must be introduced as the cooling source. Fig. 3-5 shows a classical heat removal process from server to outdoor heat sink (chiller) in a  $T-Q$  diagram. During the process, low temperature intake air is sent into racks to cool the chips, and then the heated exhaust air will mix with return air and be handled by the chilled water which comes from evaporator of the chiller. Indoor sensible heat will be transported to outdoor air by cooling water through coupled mass and heat transfer processes in the cooling tower. Thus, temperature difference offered by the chiller ( $\Delta T_{HP} = T_{evap} - T_{cond}$ ) is:

$$\Delta T_{HP} = \Delta T_{indoor} + \Delta T_{outdoor} - \Delta T_d \quad (3-4)$$

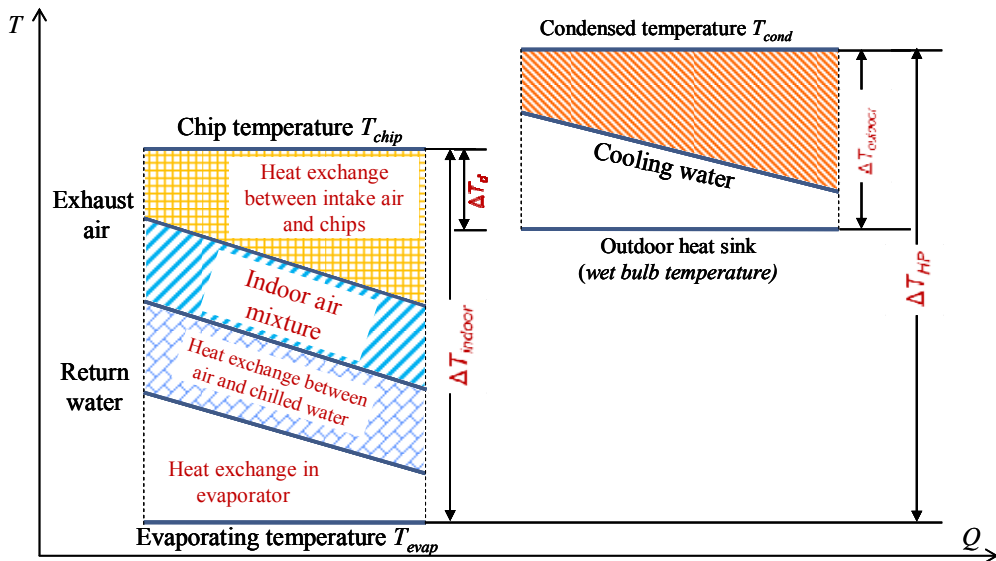


Fig. 3-5  $T-Q$  diagram of a classical heat removal process (adopting chiller)

According to the relationship between available driven temperature difference  $\Delta T_d$  (or available entransy dissipation  $\Delta E_{n,d}$ ) between indoor air and outdoor heat sink, and actual temperature difference  $\Delta T_{total}$  (or total entransy dissipation  $\Delta E_{n,total}$ ) dissipated during heat removal process, indoor thermal environment maintaining process could be classified into two conditions:

- If actual temperature difference  $\Delta T_{total}$  is smaller than available temperature difference  $\Delta T_d$ , it means that current driven force of heat transfer is large enough to overcome all the heat resistance of each part. Thus there is no need of adopting mechanical refrigeration to supply enough driven temperature difference (or driven entransy dissipation). In this condition, heat load is transferred outdoor only through heat collection and transfer process, and no transformation between heat and power is involved.

- If actual temperature difference  $\Delta T_{total}$  is larger than available temperature difference  $\Delta T_d$ , it means that current driven force of heat transfer is not large enough to overcome all the heat resistance. And then additional method should be adopted to enlarge the available driven temperature difference. Generally chillers would be introduced to supply enough temperature difference  $\Delta T_{HP}$  to transfer heat from indoor to outdoor environment. During the process, power is used to help to offer the system with an enough driven temperature difference and finish the heat removal process.

Thus, when outdoor heat sink is fixed, reducing temperature difference consumed (or entransy dissipation) becomes the most essential part in improving indoor thermal environment maintaining process of data centers.

### 3.1.2. Mixing dissipation in removing indoor sensible heat

Indoor heat collection is the most basic part for thermal built environment in data centers. And its main task is to remove servers' waste heat to outdoor heat sink by circulating air or other media. Figs. 2-4 and 2-5 give the most ideal working conditions of indoor heat collection, namely there exists no mixture of cold and hot air. In this condition, intake temperature of racks equals to the supply air temperature of CRAC units, and exhaust temperature of racks then equals to the return air temperature of CRAC units. However, in actual indoor heat collection process, because of the unsatisfactory air distribution and nonuniform heat flux of each rack, short circuits of cold air and backflows of hot air are commonly seen in data centers and entransy dissipation could be adopted as a novel way to describe and analyze indoor heat collection in data centers as shown in Fig. 3-6.

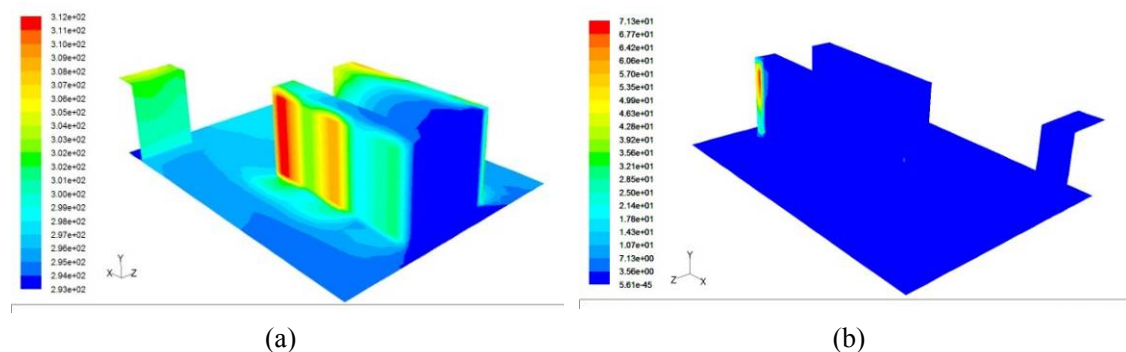


Fig. 3-6 Temperature and entransy dissipation distributions in a data center (CFD results):

(a) temperature distribution; and (b) entransy dissipation distribution.

Taking one rack as an example, Fig. 3-7 explains the indoor heat collection process with mixture between cold and hot air.  $m_c$  is the supply air volume of CRAC units,  $m_s$  is the actual volume of intake air that enters the racks.  $m_b$  and  $m_r$  are the volume of short circuit cold air and backflow hot air respectively.  $T_c$  and  $T_r$  are the temperature of supply and return air of CRAC units.  $T_s$  and  $T_h$  are the temperature of intake and exhaust air of racks respectively.

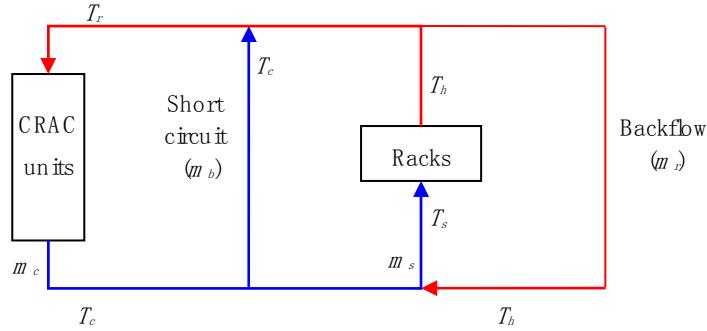


Fig. 3-7 Mixture of cold and hot air in actual heat removal process in data center

- **Backflow of hot air:** backflow of hot air refers to a certain volume of exhaust air ( $T_h$ ) from racks flowing back to the intake side of rack and mixing with the supply air ( $T_c$ ) from CRAC units resulting intake air temperature  $T_s$  to be higher than supply air temperature  $T_c$ .

- **Short circuit of cold air:** short circuit of cold air refers to a certain volume of supply air ( $T_c$ ) from CRAC units bypasses to the exhaust air side and mixes with exhaust air ( $T_h$ ), resulting return air temperature  $T_r$  to be lower than the exhaust air temperature.

Fig. 3-8 shows the actual heat removal process of data centers in a T-Q diagram. During the heat collection process from servers to CRAC units, because of backflow of hot air, intake air of rack is heated from  $T_c$  to  $T_s$ . Due to short circuit of cold air, exhaust air of rack is cooled from  $T_h$  to  $T_r$ . Thus, total entransy dissipation for mixture between hot and cold air could be separated into two parts: entransy dissipation of backflow and entransy dissipation of short circuit, namely  $\Delta E_{n,mix} = \Delta E_{n,mix,r} + \Delta E_{n,mix,b}$ . As a result of the mixing process between hot and cold air, there exists invalid air flow in the data center. It leads to unsatisfactory indoor air distribution and more importantly an evident increase of entransy dissipation. As a result, a higher driving temperature difference (i.e. a lower temperature of cooling source) is needed.

As shown in Fig. 3-8, short circuit between cold air and backflow of hot air results in mixing dissipation (entransy dissipation). Short circuit makes return air temperature evidently decrease (from  $T_h$  to  $T_r$ ), and backflow of hot air makes desired supply air temperature evidently decrease (from  $T_c$  to  $T_s$ ), namely the short circuit between cold air and backflow of hot air affect return air temperature and supply air temperature of CRAC units respectively. According to the entransy dissipation analysis, to avoid mixture between cold and hot air, increasing the supply air temperature is much more important than the return air temperature for engineering practice. Increasing supply air temperature would directly lead to a higher temperature level requirement for cooling source.

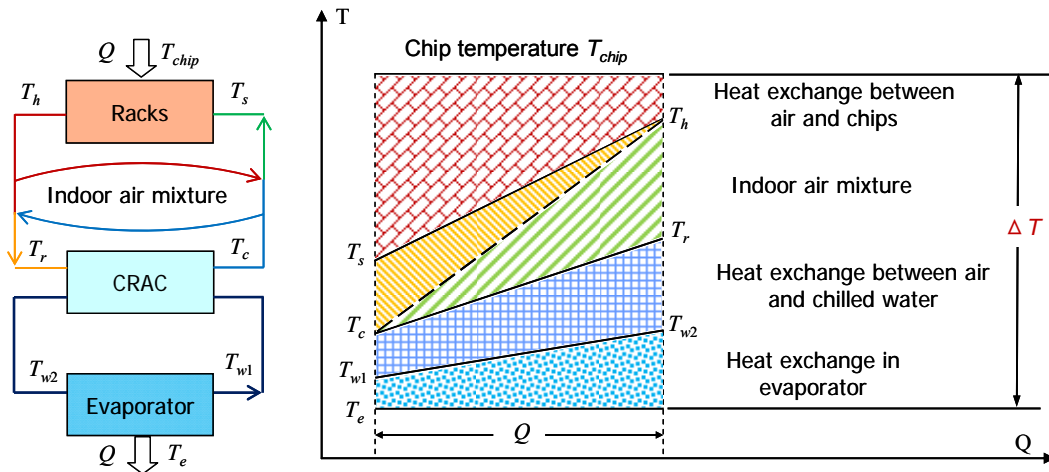


Fig. 3-8 Actual heat removal process in a data center

Thus, both short circuit of cold air and backflow of hot air would bring forward the mixture of cold and hot air and result in evident mixing entransy dissipation, causing both demanded driven temperature difference of heat collection process and total entransy dissipation higher. This kind of mixing process causes stricter requirements for the quality of cooling source and then restricts the utilization of natural cooling source. So to improve indoor heat collection process and to decrease or avoid mixing entransy dissipation is an important solution to improve the indoor thermal environment in data centers.

### 3.1.3. Application in a data center

#### (1) Performance before retrofitting

An operating data center in Beijing is retrofitted using distributed terminals and the combined water loop. To verify the effectiveness of this cooling solution, a measurement based comparison on both thermal and energy performances of the two cooling systems are performed, in condition of similar cooling load and out-door conditions. Before retrofitting, the data center uses non-raised floor or ceiling return layout with cold and hot aisles. The cooling air is delivered to the cold aisle by three CRAC units, with hot air sent back through upper and lateral space.

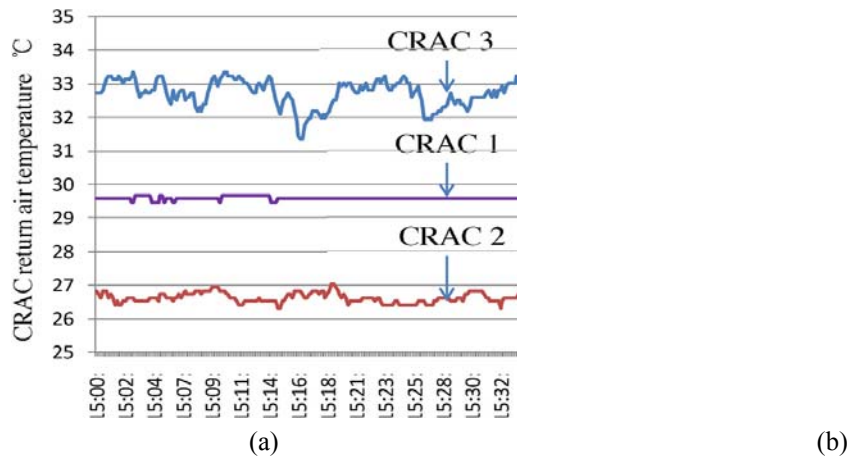


Fig. 3-9 Real-time measurement before retrofitting: (a) return air temperature; and (b) Daily-averaged intake/exhaust air temperature.

Indoor air temperature distribution is measured to evaluate the air flow performance. Real-time measurement of return air temperature for each CRAC unit is illustrated by Fig. 3-9(a), with the measurement error controlled within  $\pm 0.5^{\circ}\text{C}$  and data collected every ten seconds. The maximum return air temperature difference can be  $6^{\circ}\text{C}$ . The non-uniformity of return air temperature can lead to an unfavorable cooling load distribution among the CRAC units. Fig. 3-9(b) shows the daily-averaged intake and exhaust air temperature of all racks. As we can see, the difference between intake air temperature and exhaust air temperature is as large as  $7.5^{\circ}\text{C}$  averagely. The measurement on both the indoor air flow performance and CRAC energy performance shows a practical demand for the retrofitting of cooling system.

## (2) Retrofit: Distributed cooling terminal

An internally cooled rack is proposed as distributed cooling terminal using two-stage heat pipe media heat exchangers illustrated by Fig. 3-13(a). The 1 stage heat pipe is installed at the bottom of the rack to cool the rack intake air from indoor temperature ( $23\text{--}25^{\circ}\text{C}$ ) to server required intake temperature ( $18\text{--}20^{\circ}\text{C}$ ) by supply water ( $10\text{--}12^{\circ}\text{C}$ ). While the second stage heat pipe is installed at the top of the rack to cool the server exhaust air ( $35\text{--}40^{\circ}\text{C}$ ) to indoor temperature ( $23\text{--}25^{\circ}\text{C}$ ) by the output water of 1 stage heat pipe ( $13\text{--}15^{\circ}\text{C}$ ). The output water of outdoor unit 2 (return water,  $22\text{--}24^{\circ}\text{C}$ ) is cooled by the cold source and finally delivers all heat to outdoor environment. Air intake temperature is set by Class A1 Grade recommended by ASHRAE guidelines. In order to fit the server load variation and maintain a uniform intake/exhaust air temperature, the amount of heat exchanged by each unit in the heat pipe loops can be adjusted through fan speed control. Such configuration achieves uniform indoor air temperature distribution and the cold and hot aisle can be replaced by more racks. For indoor humidity control, a few dehumidifiers are arranged at each corner of the room to maintain a recommended rack intake air relative humidity of  $35\text{--}50\%$ .

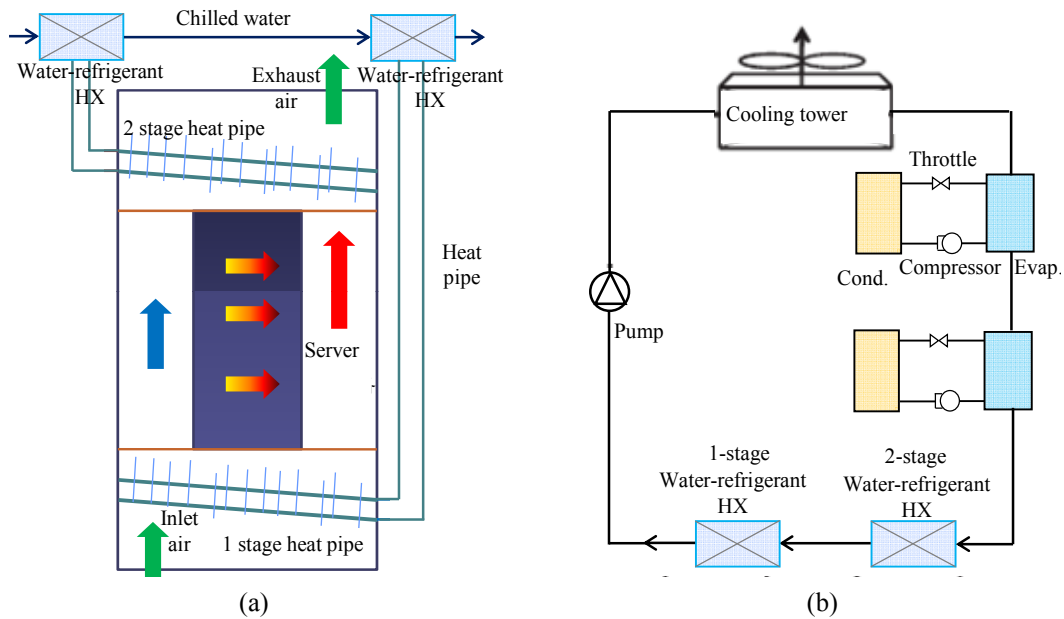


Fig. 3-10 Combined cooling solution using multi-stage heat pipe loops: (a) Schematic of the internally cooled rack; and (b) Schematic of the combined water loop.

To further improve outdoor free cooling potential and energy performance, a combined water loop with multi-cold source is designed to provide large temperature difference between supply and return water ( $\sim 10^{\circ}\text{C}$ ), meeting the requirement of temperature-matched heat transfer. Two chillers and one open cooling tower are connected in series as switchable cold source, which provide cooling water of required temperature. With two heat pipe outdoor units and one pump integrated, the water loop transfers the heat from heat pipe loops to outdoor environment. The multi-cold source enables the water loop to automatically distribute cooling load and choose cold source, according to the availability of waterside free cooling. With fixed supply/return water temperature ( $10\text{--}12^{\circ}\text{C}/22\text{--}24^{\circ}\text{C}$ ), the operating mode of the multi-cold source is decided by the output water temperature of the cooling tower, which is mainly determined by outdoor air wet bulb temperature. When outdoor wet bulb temperature is low enough, all cooling load is undertaken by the cooling tower. When that temperature is not sufficiently low, chillers and the cooling tower co-work to share the cooling load, with chillers started one by one. When that temperature is too high to use the cooling tower, all heat is removed by chillers.

### (3) Performance measurement (after retrofitting)

The combined water loop using distributed cooling terminals proposes a feasible solution for the retrofitting demand. Fig. 3-11 shows the photos of the internally cooled racks filled with operating servers, using specially designed two-stage heat pipe loops. The daily averaged intake and exhaust air temperature of all racks is showed in Fig. 3-12(a), with the measurement error controlled within  $\pm 0.5^{\circ}\text{C}$ . It can be seen that, compared with Fig. 3-9(b), which shows the measurement before retrofitting, the largest temperature difference between the intake and exhaust air is less than  $2.5^{\circ}\text{C}$ , which shows a better indoor cooling. The indoor measurement above shows that compared with the air temperature distribution before retrofitting, the internally cooled racks create a more uniform indoor temperature and

humidity by effectively reducing the cold and hot air mixing. The distributed cooling terminals improve the air flow performance and show a good agreement with the initial design. The daily-averaged temperature distribution of the combined water loop is illustrated by Fig. 3-12(b), with the measurement error controlled within  $\pm 0.5^{\circ}\text{C}$  and data collected every hour. The measurement shows a uniform cooling load allocation for each heat pipe loop, which is in accordance with the air temperature distribution inside the rack.



Fig. 3-11. Internally cooled racks using two-stage heat pipe loops.

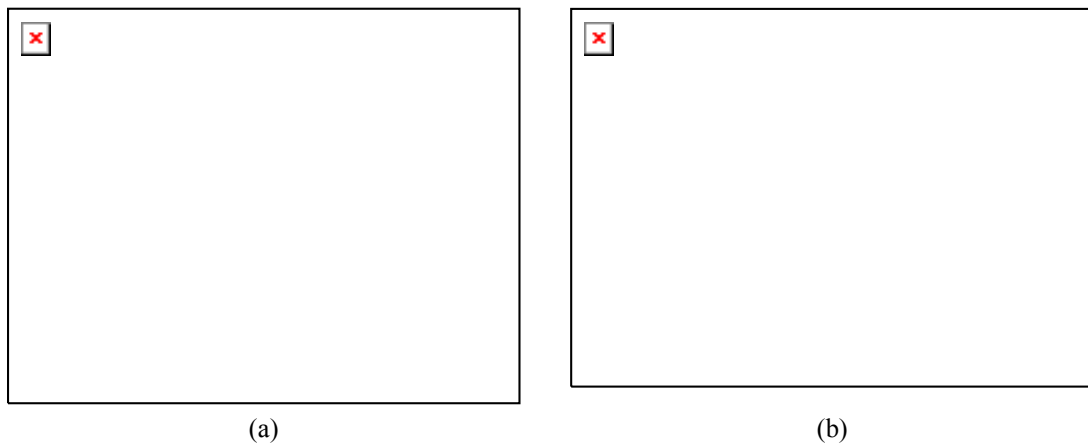


Fig. 3-12 Real-time measurement after retrofitting: (a) Daily-averaged intake/exhaust air temperature; and (b) water temperature.

Before retrofitting, the annual EER (energy efficiency ratio) of the air-conditioning system for this data center is only about 2.6. After retrofitting, annual EER is increased to as high as about 5.0. Compared to former CRAC system, the combined cooling solution effectively reduced the annual cooling energy consumption by about 46%. And total annual energy cost by the entire data center has been reduced by about 13%. The annual average electric consumption of CRAC system before and after retrofitting is 185,000 and 100,000 kWh, respectively. Approximately 46% of the cooling cost is saved per year after retrofitting.

### 3.2. Application in office buildings (with both sensible and latent load)

As indicated by the analysis above, temperature differences in conventional air-conditioning system are mainly caused by limited flow rates, limited transfer ability input and etc. Entransy dissipations are resulted from combined control of indoor temperature and moisture, mixing processes and etc. The main reason for utilizing 7°C chilled water is for air dehumidification, leading to significant dissipation in removing sensible load. To reduce the entransy dissipation due to combined removing indoor sensible load and moisture, approach could be proposed and here will give the performance of the improved air-conditioning system.

#### 3.2.1. Separate treatment of indoor temperature and humidity

Corresponding to reduce entransy dissipation caused by indoor combined control of temperature and humidity to improve the system performance, temperature and humidity independent control (THIC) air-conditioning system is proposed to realize the separate control of indoor temperature and humidity, with a system operating principle shown in Fig. 3-13. In humidity control subsystem, the handled outdoor air assumes the two main tasks of the air-conditioning system, i.e. supplying enough outdoor air to meet the requirements of indoor air quality and dry enough outdoor air to remove the total moisture load in the building to control the indoor humidity. Condensing dehumidification method, liquid desiccant and solid desiccant methods are all applicable for the humidity control subsystem. As for the indoor temperature regulation, another subsystem with a relatively higher temperature cooling source can be utilized to control the indoor temperature. Either water or refrigerant is the recommended fluid medium in the temperature control subsystem from the perspective of reducing the energy use of transportation systems.

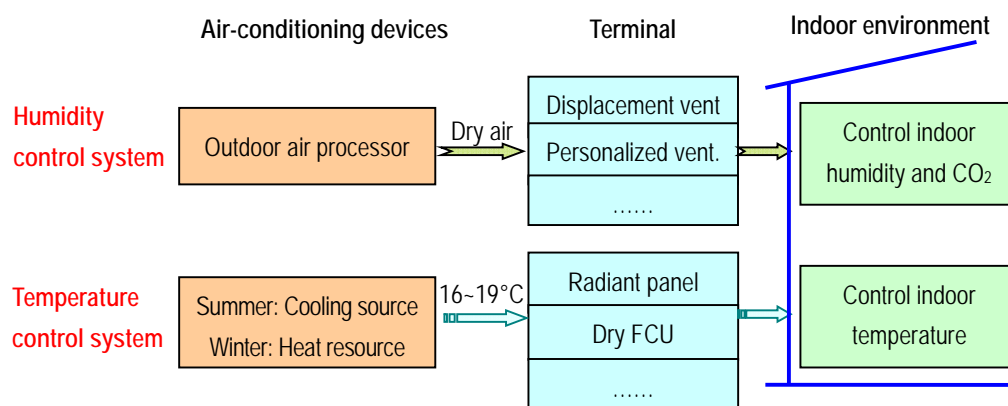
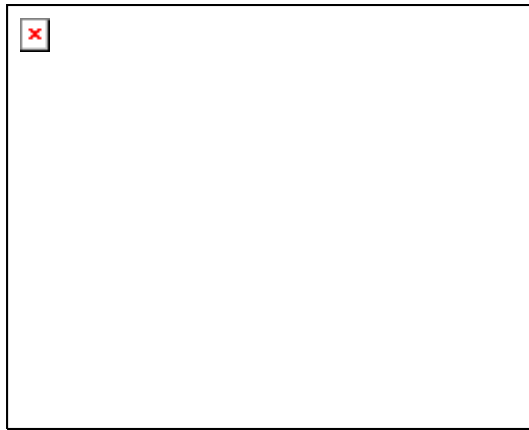
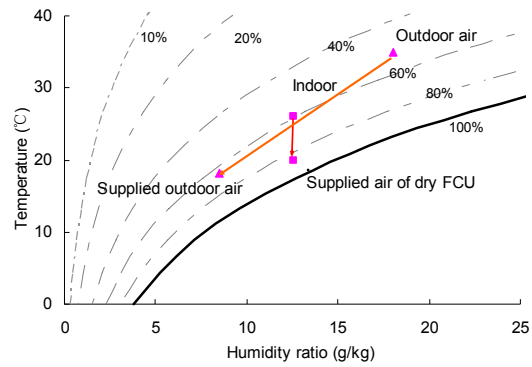


Fig. 3-13 Operating principle of the THIC air-conditioning system.

Fig. 3-14(a) illustrates the operating schematic of a THIC system constructed by desiccant dehumidification method. The heat pump driven liquid desiccant outdoor air processor is adopted for indoor humidity control and dry FCU is for temperature control with the air handling processes shown as Fig. 3-14(b).



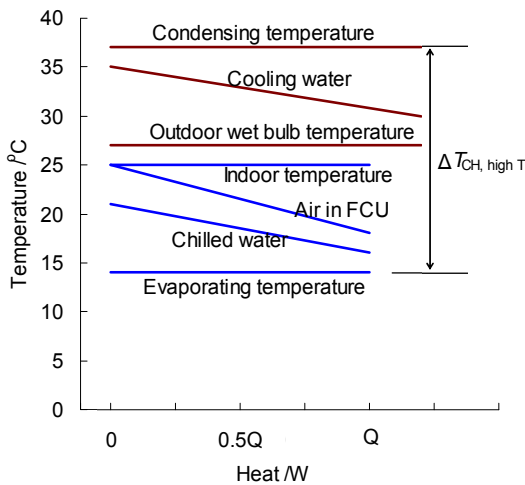
(a)



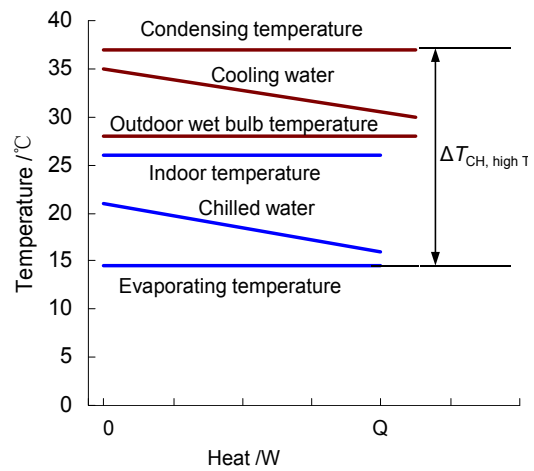
(b)

Fig. 3-14 The THIC air-conditioning system: (a) typical outdoor air system with FCUs; and (b) psychrometric chart of the air handling process.

Taking the dry FCU as an example, Fig. 3-15(a) gives the temperature level of each component in the temperature control subsystem. As indicated by this figure, the required chilled water temperature is much higher than that of the conventional system and evaporating temperature of the chiller can increase a lot. With a similar condensing temperature,  $\Delta T_{CH}$  is only 23K, much lower than the conventional system and  $COP_{CH}$  will be much higher than the conventional system with a similar thermodynamic perfectness  $\eta$ .



(a)



(b)

Fig. 3-15 Temperature differences in a temperature control subsystem of THIC system: (a) dry FCU; and (b) radiant terminal.

To further improve the system performance of the THIC system, radiant panel could be adopted for indoor temperature control. Fig. 3-15(b) shows the temperature level of the temperature control subsystem adopting radiant terminal. Different from the forced convection heat transfer process of dry FCU, cooling capacity is delivered into indoor space through radiation and natural convection heat exchange processes. As there are no fans for forced air circulation, water acts as the media for delivering cooling capacity and energy use for distribution air could be saved.  $COP$  of the entire system is superior to that using dry FCU and averagely 30% higher than conventional system.

### 3.2.2. A case study of an office building in Guangzhou

A typical office building in Guangzhou was used to compare the differences in energy use of various air-conditioning systems. The total area of the 11-floor office building is 66,440 m<sup>2</sup>; each floor consists mostly of offices and meeting rooms and has an area of 6,040 m<sup>2</sup>. A model of this building is built using DeST software shown as Fig. 3-16(a) and the characteristics of building envelopes are set according to the Chinese national standard. The daily schedule of typical office and meeting rooms on workdays in this building is shown in Fig. 3-16(b).

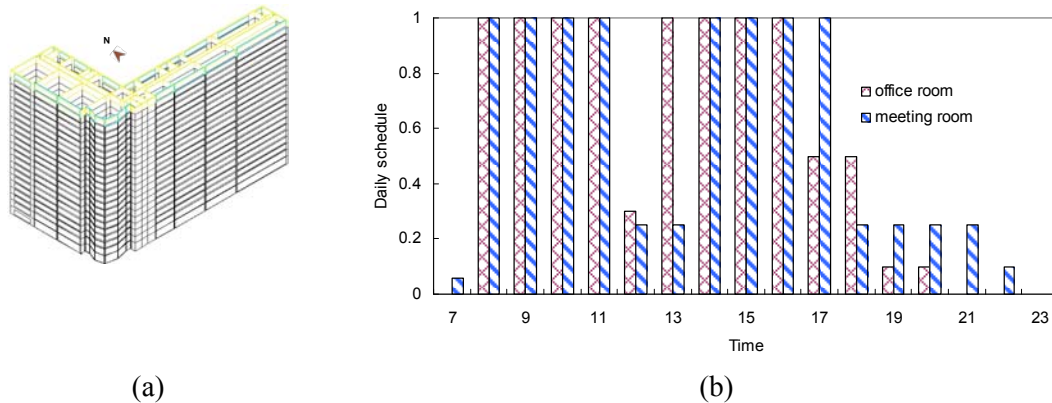
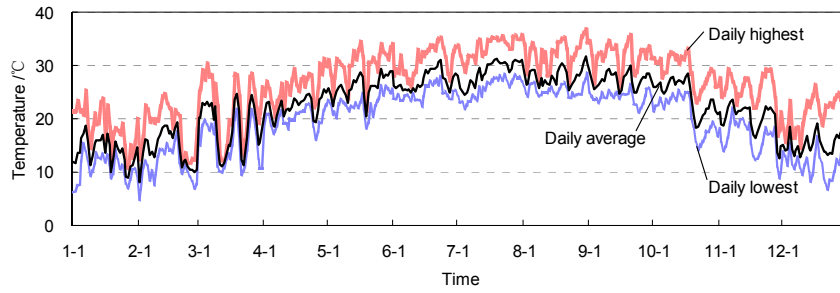
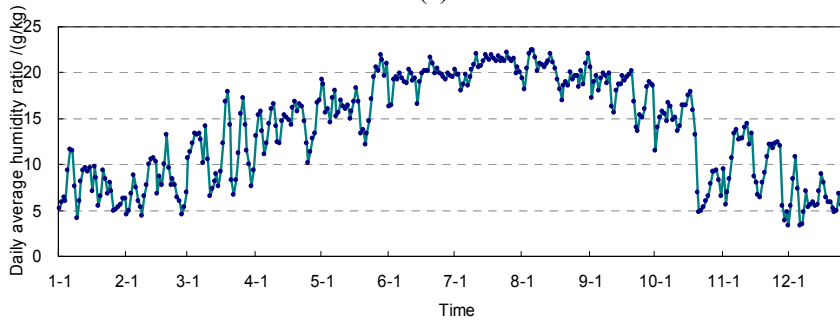


Fig. 3-16 A typical office building in Guangzhou using DeST software: (a) building schematic; and (b) daily schedule.

Guangzhou has a very humid outdoor condition throughout the cooling period, as shown in Fig. 3-17. The hour-by-hour cooling load is shown in Fig. 3-18(a) using DeST software with an indoor condition of 26°C and 60% relative humidity and the air-conditioning period is from May 1 to October 31. In the typical hot and humid outdoor condition, with an outdoor temperature of 36.6°C and a relative humidity of 55%, the total cooling load is 7705 kW. The sensible load from the outdoor air is 786 kW, the sensible load from the indoor building is 4891 kW, the latent load from the outdoor air is 1584 kW, and the latent load from the indoor moisture source is 444 kW. Therefore, the latent load is 26.3% of the total load. Fig. 3-18(b) illustrate the hour-by-hour subentry loads per unit area in a typical week (August 27 to September 2) respectively. As indicated by this figure, the indoor sensible load accounts for most of the building load while the indoor moisture load is the least, usually lower than 10W/m<sup>2</sup>.

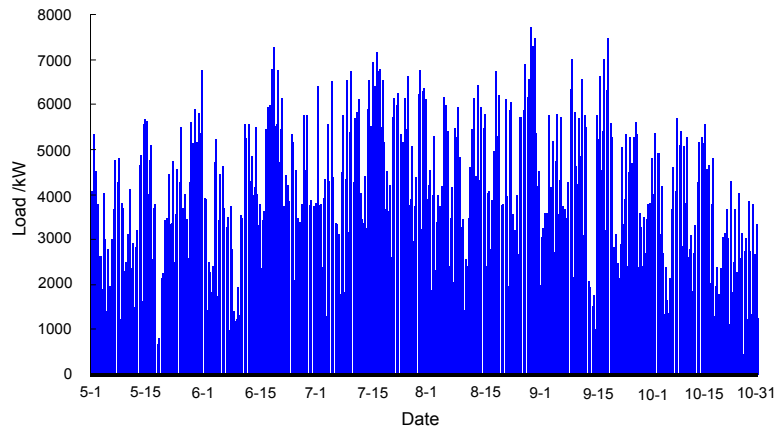


(a)

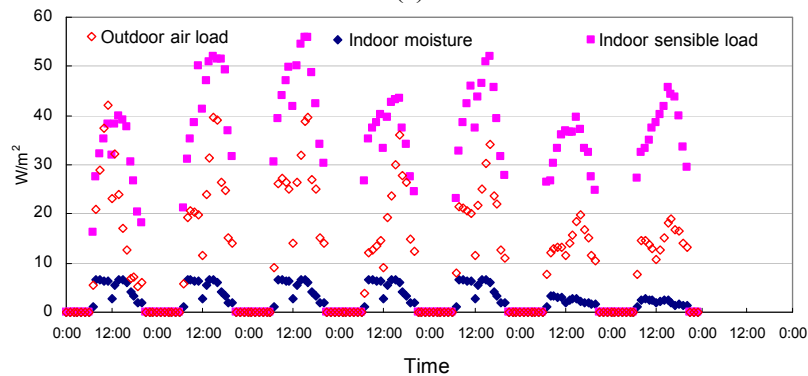


(b)

Fig. 3-17 Annual outdoor condition in Guangzhou: (a) daily highest, average, and lowest temperatures; and (b) daily average humidity ratio.



(a)



(b)

Fig. 3-18 Load characteristics of a typical office building in Guangzhou: (a) hour-by-hour total cooling load; and (b) subentry loads in a typical week.

Four air-conditioning systems were compared: a conventional system (consisting of FCUs and an outdoor air system) and THIC systems I, II and III. In the conventional system, 7°C/12°C chilled water is used to control both the indoor temperature and humidity; no reheating devices are considered. Condensing dehumidification is adopted for humidity control in the THIC system I and Fig. 3-19(a) gives its operating schematic where 7°C/12°C chilled water is used for dehumidification and 16°C/21°C chilled water for indoor temperature control. The air handling process of the THIC system I is illustrated as Fig. 3-19(b) where the outdoor air is dehumidified to a humidity ratio dry enough to extract indoor moisture by the low temperature chilled water. The schematic of the THIC systems II and III is shown in Fig. 3-14; the only difference between these two THIC systems concerns the indoor terminals that remove the sensible load: dried FCUs are adopted in the THIC system II and radiant panels are utilized in the THIC system III. In both THIC system II and III, the heat pump driven outdoor air handler using liquid desiccant is adopted as the dehumidification device, and 16°C/21°C chilled water is used to control the indoor temperature. As condensing dehumidification is adopted in the THIC system I, the temperature of the supplied outdoor air for humidity control is usually lower than 15°C; while in the THIC systems II and III, the temperature of the supplied outdoor air is usually about 18°C~20°C. Based on the models of devices in the DeST software, energy performances of these four systems could be simulated.

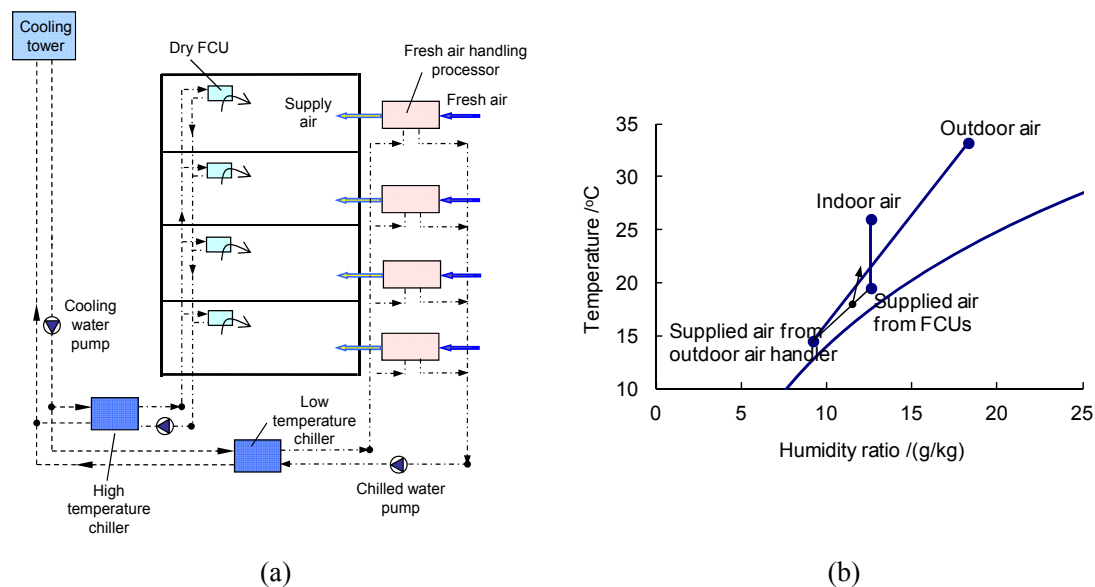


Fig. 3-19 The THIC air-conditioning system with two chillers: (a) typical outdoor air system with FCUs; and (b) psychrometric chart of the air handling process.

The electric consumptions of the three air-conditioning systems in a typical hot and humid outdoor condition are shown in Table 3-1. Because indoor temperature and humidity are separately controlled in the THIC systems, the evaporating temperature of the chiller for temperature control is much higher, leading to lower energy use by the chillers in the THIC systems. The energy use of the FCUs in the THIC system II is greater than that in the conventional system because the transportation coefficient of dried FCUs is much lower than that of conventional wet FCUs. But in the THIC system I the energy use of the FCUs is a bit lower than that in the conventional system because of a lower temperature of supplied

outdoor air and a lower required cooling capacity of FCUs. Practically the total supplied cooling capacity of the dried FCUs is smaller than that of the wet FCUs in the conventional system. The  $COP_{sys}$  of the conventional system, THIC system I, II, and III are 3.5, 4.0, 4.7 and 5.0, respectively, in the typical hot and humid outdoor condition.

Fig. 3-20 shows the annual energy use of the four air-conditioning systems. It shows that the energy use of the THIC systems during the cooling period are lower than that of the conventional system. The total energy consumptions are 36.4kWh/m<sup>2</sup>, 32.7kWh/m<sup>2</sup>, 28.5kWh/m<sup>2</sup>, and 26.4kWh/m<sup>2</sup> for the conventional system, THIC system I, II and III, respectively. The energy consumption of water chillers in THIC system I is lower than that in conventional system as a higher temperature of chilled water is chosen for temperature control. And the seasonal  $COP_{sys}$  are 3.7, 4.1, 4.7 and 5.1 for these four systems respectively.

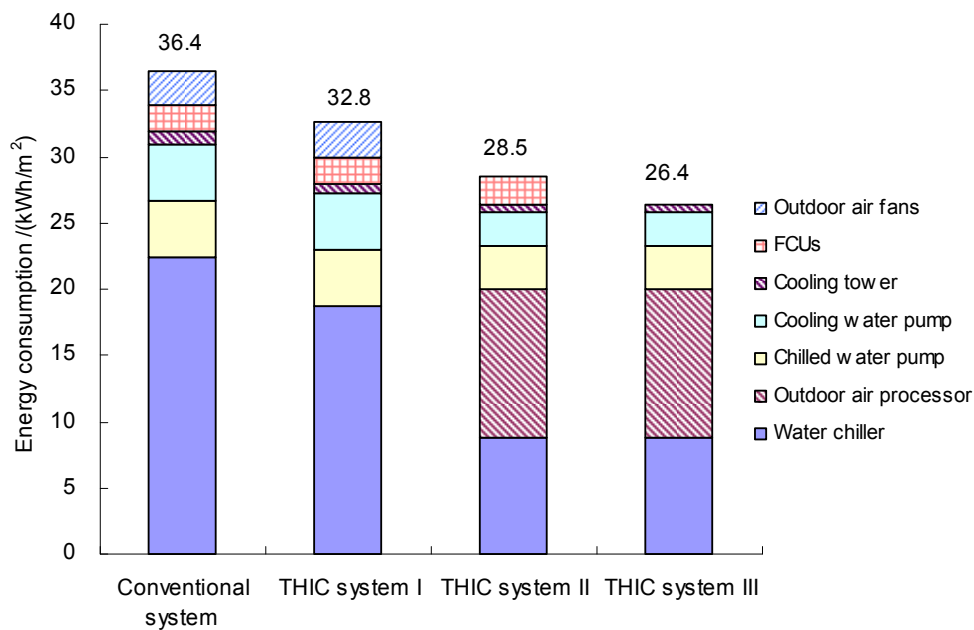


Fig. 3-20 Annual energy use of the four air-conditioning systems in the typical office building in Guangzhou.

Therefore, compared to the conventional system, the energy efficiency improvement of THIC system I is only 11% while of THIC system II and III the energy efficiency improvements are 28% and 38%. It means that the performance improvement of THIC system I shown as Fig. 3-20 is not as significant as that of THIC systems II and III with the heat pump driven liquid desiccant outdoor air processor. But there is still potential for performance improvement of THIC system using condensing dehumidification, for example the 16°C chilled water could be used for precooling the outdoor air before dehumidified by the 7°C chilled water.

Table 3-1 Electric consumption of air-conditioning systems in a typical hot and humid outdoor condition (36.6°C and 55% relative humidity)

		Conventional system	THIC system I	THIC system II	THIC system III
Electric consumption (kW)	Water chillers	1525.3	1285.3	511.4	511.4
	Outdoor air processors using liquid desiccant	-	-	758.3	758.3
	Chilled water pumps	202.5	201.3	135.0	135.0
	Cooling water pumps	212.0	206.5	105.0	105.0
	Cooling towers	65.9	64.2	22.5	22.5
	Fans in outdoor air processors	83.6	87.8	-	-
	FCUs	91.6	89.7	114.4	-
	Entire system	2180.9	1935.0	1646.6	1532.2
System <i>COP</i>	<i>COP<sub>sys</sub></i>	3.5	4.0	4.7	5.0

This section analyzed the energy performances of different air-conditioning systems. The THIC system, which avoids the entransy dissipations of coupled treatment of indoor sensible load and moisture that negatively affect conventional systems, appears to be the good way to significantly improve system performance. Outdoor air is dried and used to remove the total indoor moisture in the humidity subsystem, and chilled water with a relatively higher temperature is utilized to control the indoor temperature. There THIC systems were compared to a conventional system in a typical office building in Guangzhou. Compared to the conventional system, energy efficiency of THIC system I using condensing dehumidification is about 11% higher; the energy efficiency of the THIC system II with dried FCUs and heat pump driven liquid desiccant system is about 28% higher; and energy efficiency improvement of the THIC system III with radiant panels and heat pump driven liquid desiccant system is about 38%.

### 3.3. Application in large space buildings

#### 3.3.1. Characteristics of the indoor built environment in large space buildings

The characteristics of the indoor environment in a large space building can be summarized as follows: (1) a high and large-span structure of space, temperature, and humidity stratification in the vertical direction; (2) intensive solar radiation caused by a large transparent building envelope; (3) high-temperature envelope surfaces caused by solar radiation, heat sources such as heat transfer from the envelope, and equipment and human beings above the ground; (4) the air-conditioning region is less than 2 meters above the floor in order to satisfy the requirement of human comfort.

There are four main heat sources in large space buildings: direct solar radiation through the transparent building envelope, the building envelope, equipment, and human beings. The humidity in large space buildings mainly comes from human beings. Fig. 3-21 shows the typical temperature level of different heat sources in large space buildings. The temperature of the building envelope can reach 40°C for skylights with solar radiation. The temperatures of lights, advertising boxes, and other devices fall into a relatively wide range of 30°C to 50°C. In addition, direct solar radiation can be absorbed by inner surfaces.

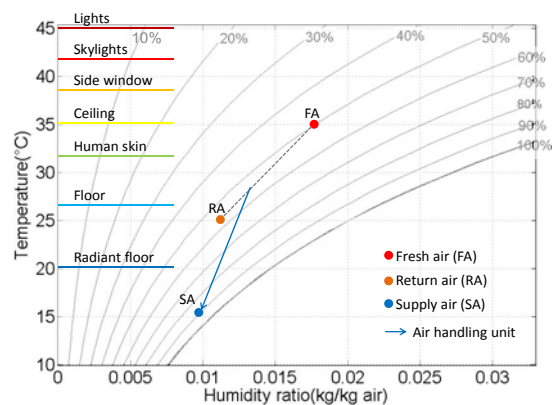


Fig. 3-21 Temperature of heat sources and air handling process in psychrometric chart.

Fig. 3-22(a) shows the schematic diagram of a traditional system in a large space building. The system uses jet ventilation to remove all the heat from the indoor environment, which mixes all the heat into the room air at approximately 26°C. Typical jet supply air outlets in the indoor environment are shown in Fig. 3-22(b). The heat transfer process from the heat sources to the chilled water includes several steps: convective heat transfer from the heat sources to the indoor air; mixing the supply air with the indoor air; mixing the return air with the fresh air, and heat exchange of the air with the chilled water in the air handling unit. The basic heat transfer processes of HVAC systems in large space buildings are convective heat transfer and air mixing, while the basic devices are heat exchangers.

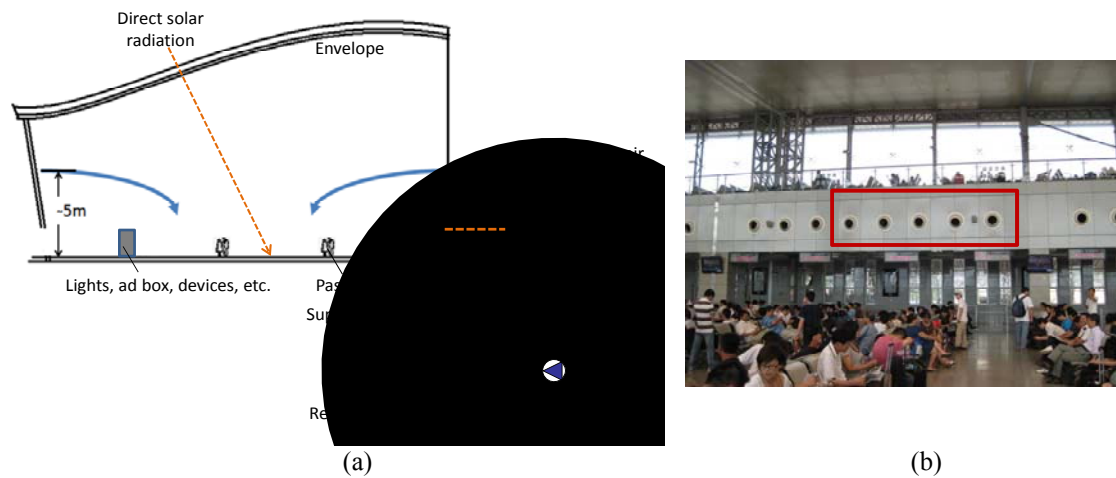


Fig. 3-22 A traditional HVAC system in a large space building: (a) Schematic diagram; and (b) Jet supply air outlets in a large space building.

### 3.3.2. A novel system in a large space building

Fig. 3-23 shows two forms of indoor cooling in large space buildings. Fig. 3-23(a) is the traditional jet ventilation system, which is widely used in airports and railway stations. Low-temperature air is supplied at high speed by outlets at a height of 3-5 meters. In this system, the cooling load from the building envelope and heat sources will mix into the indoor environment and then be removed by low-temperature supply air. This air flow pattern will cause considerable entransy dissipation, which means the high temperature of the building envelope and the heat sources will be wasted in a jet ventilation system. Fig. 3-23(b) shows a new type of indoor cooling system in a large space building. The system is composed of a radiant floor integrated with displacement ventilation, which is based on reducing mixture loss and simplifying the heat transfer process from the heat sources to the chilled water.

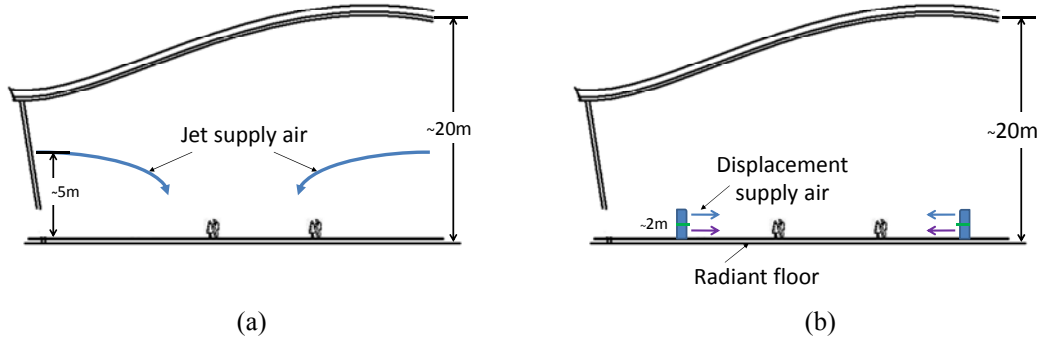


Fig. 3-23 Two indoor cooling systems in a large space building: (a) system I: jet ventilation; and (b) System II: radiant floor and displacement ventilation.

As shown in Fig. 3-24(a), the equivalent thermal resistance of the jet ventilation system consists of three factors:  $R_1$ ,  $R_2$ , and  $R_3$ .  $R_1$  indicates the heat resistance caused by the convective heat transfer from the heat sources to the indoor air, expressed as

$$R_1 = \frac{\sum_{i=1}^n q_{h,i} (T_{h,i} - T_a)}{(\sum_i q_{h,i})^2} \quad (3-5)$$

$R_2$  indicates the heat resistance caused by the mixture between the supply air and the indoor air, expressed by mass flow rate and specific heat of the supply air:

$$R_2 = \frac{\frac{1}{2}(T_a - T_{sa})Q}{Q^2} = \frac{1}{2\dot{m}_a c_{pa}} \quad (3-6)$$

$R_3$  indicates the heat resistance caused by the heat transfer between the supply air and the chilled water, expressed by  $UA$  and flow rate unmatched coefficient  $\xi$ :

$$R_3 = \frac{\frac{1}{2}(T_{sa} + T_{ra} - T_{sw} - T_{rw})Q}{Q^2} = \frac{\xi}{UA} \quad (3-7)$$

The total equivalent thermal resistance from the heat sources to the chilled water is the sum of  $R_1$ ,  $R_2$ , and  $R_3$ :

$$R = R_1 + R_2 + R_3 \quad (3-8)$$

From the expression of  $R_1$ ,  $R_2$ , and  $R_3$ , an increased indoor temperature can decrease  $R_1$ , but the indoor temperature will be limited by the thermal comfort range; increasing the flow rate of the supply air can decrease  $R_2$ , which will cause a higher energy consumption of fans; increasing  $UA$  can decrease  $R_3$ , but this approach involves a greater initial cost. It is clear that in the heat transfer process of the jet ventilation system, decreasing the equivalent thermal resistance has limited benefits.

As shown in Fig. 3-24(b), the equivalent thermal resistance of the radiant floor system consists of two factors:  $R'_1$  and  $R'_2$ .  $R'_1$  indicates the heat resistance caused by the radiant heat transfer among inner surfaces and the floor surface, as well as the convective heat transfer between the indoor air and the floor surface:

$$R'_1 = \frac{\sum_{j=1}^n q_{r,j}(T_{s,j} - T_r) + q_c(T_a - T_r)}{(\sum_{j=1}^n q_{r,j} + q_c)^2} \quad (3-9)$$

$R'_2$  indicates the heat resistance caused by the heat transfer from the floor surface to the chilled water, expressed by

$$R'_2 = \frac{\frac{1}{2}(2T_r - T_{sw} - T_{rw})Q}{Q^2} \quad (3-10)$$

The total equivalent thermal resistance from the heat sources to the chilled water is the sum of  $R'_1$  and  $R'_2$ . Based on entransy theory, any actual heat transfer process with a temperature difference will cause entransy dissipation, so simplifying the heat transfer process from the heat sources to the heat sinks is the most basic way to reduce thermal resistance. In the jet ventilation system, there are three steps from the heat sources to the chilled water: heat sources to indoor air, indoor air to supply air, and supply air to chilled water. In the radiant floor system, there are two steps from the heat sources to the chilled water: heat sources to floor surface, and floor surface to chilled water. As shown in Fig. 3-24, the equivalent thermal resistance of the radiant floor system is lower than that of the jet ventilation system. In other words, the temperature of the chilled water can be higher for the radiant floor cooling system in a large space building.

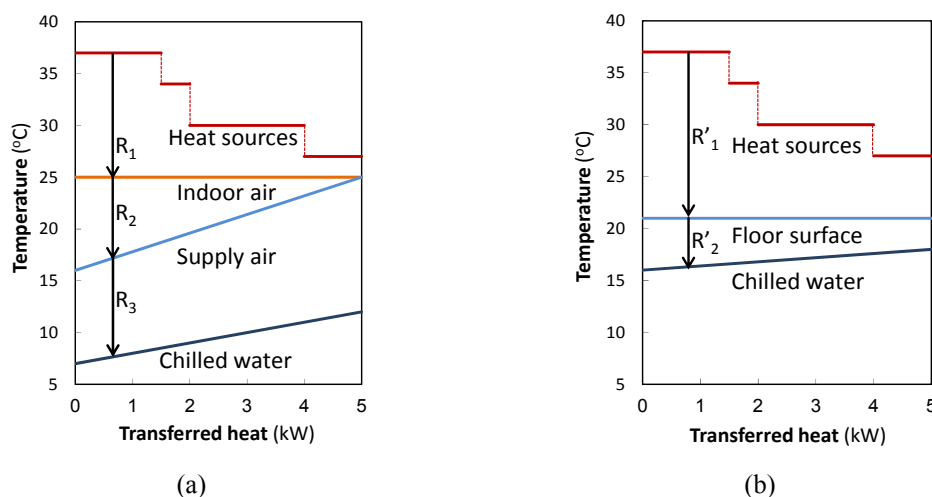


Fig. 3-24 T-Q diagram of (a) System I: jet ventilation; and (b) System II: radiant floor and displacement ventilation.

Direct solar radiation is common in large space buildings, since larger sections of the transparent building envelope are being used as ceilings or sidewalls, as shown in Fig. 3-25. Direct solar radiation can be considered as an entransy source to the system, which is determined by the temperature of the sun-exposed surface. In a jet ventilation system, heat brought in by direct solar radiation will be absorbed by the inner surface; it will go into the indoor air and then be removed by the supply air.



(a)



(b)

*Fig. 3-25 Direct solar radiation in a large space building: (a) ceiling; and (b) sidewall.*

The equivalent thermal resistance is still composed of  $R_1$ ,  $R_2$ , and  $R_3$ , which is the same as the other forms of heat sources. In a radiant floor system, the equivalent thermal resistance can be significantly reduced if the sunlight can reach the floor surface directly, as shown in Fig. 3-26. Solar heat will be absorbed by the floor surface and will transfer to the chilled water directly through the floor, so there is only one step from the heat source to the heat sink. In contrast, there are three steps of heat transfer in jet ventilation systems. The equivalent thermal resistances of System I (jet ventilation) and System II (radiant floor) are summarized in Fig. 3-27.

The minimum thermal resistance principle for the heat transfer process can be expressed as follows: for a given set of constraints, the heat transfer process is optimized (i.e., for a fixed temperature difference, the heat transfer rate is maximized; for a prescribed heat transfer rate, the temperature difference is minimized) when the thermal resistance is minimized. The minimum thermal resistance principle can be used to study indoor cooling systems in large space buildings. A smaller heat resistance means a larger cooling capacity in the condition of identical temperature difference, or a higher temperature of the chilled water in the condition of identical cooling capacity. In spaces where the sun shines directly on the floor (e.g., atriums, entrance halls, showrooms, etc.), the cooling capacity is significantly higher, and the temperature of the chilled water can also increase.

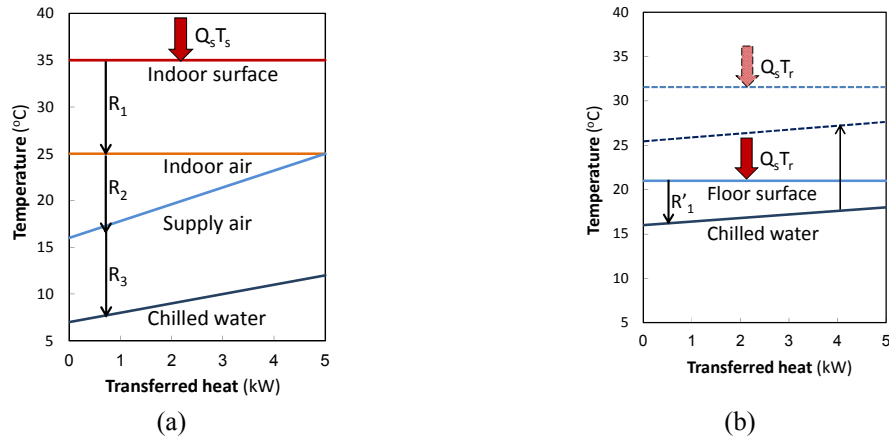


Fig. 3-26 T-Q diagram of direct solar radiation for: (a) System I: jet ventilation; and (b) System II: radiant floor and displacement ventilation.

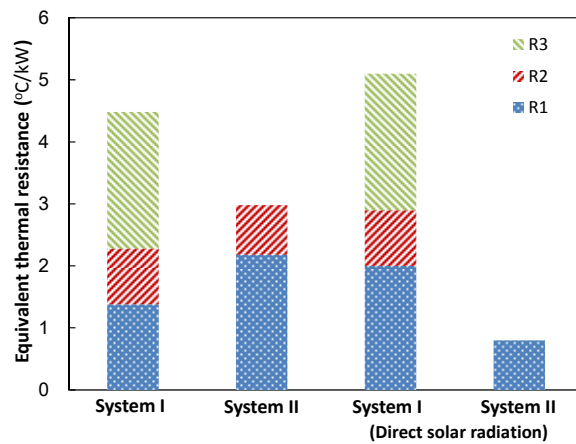


Fig. 3-27 Equivalent thermal resistance of System I and System II.

Based on this analysis, the core idea of indoor cooling systems in large space buildings is to reduce the equivalent thermal resistance from the heat sources to the heat sinks. The specific methods can be: (1) simplifying the heat transfer process from the heat sources to the chilled water; (2) reducing the mixture loss among heat sources with different temperatures, and minimizing the unnecessary mixing of hot and cold fluids; and (3) handling solar radiation directly.

## 4. Integration of HVAC System in Buildings

### 4.1. Reference building model

#### 4.1.1. Methodology for the reference building definition

The model described is developed based on the “Medium Office Commercial Reference Building Model”, retrieved from the U.S. Department of Energy (DOE) reference buildings collection (Department of Energy, 2012). The U.S. DOE developed a database of commercial reference buildings, formerly known as commercial benchmark building models, to be used for whole building energy analysis using building simulation software, such as EnergyPlus (Department of Energy, 2015). Overall 16 building types, representing approximately 70% of U.S. commercial buildings, are defined across 16 most typical climate locations. Some of the building data have been extracted from Excel files downloaded from (Department of Energy, 2012) for all 16 main U.S. climate zones.

Some adjustments were made to the DOE model to better fit the Annex 59 framework and objectives. In the original DOE version, the building model is composed of three main floors (Department of Energy, 2012): the ground floor, the mid floor and the top floor. In the proposed building model, a multiplier of ten is applied to the mid floor in order to obtain a 10-storey office building. Since the Annex 59 project aims at improving the HVAC system configurations, only the intermediate floors, called “reference floor”, were employed for simulation. The total building needs thus can be obtained by considering all of the 10 floors identical to the reference one. Due to the Annex 59 objectives, the original HVAC configuration of the DOE model was not taken into consideration, and thus the proposed model was defined by an ideal load calculation system for assessing the building space heating and cooling needs. Table 4-1 provides a picture of the main features of the Reference Building.

*Table 4-1 Building at a glance, main characteristics of the building*

Type of Reference Building	Theoretical
Location	Frankfurt, Germany
Main building activity	Office
Gross conditioned volume [m <sup>3</sup> ]	65804
Total conditioned floor area [m <sup>2</sup> ]	16607
Building length [m]	33.3
Building width [m]	49.9
Building height [m]	39.6
N° of Employees/Occupants	971
Mean Occupancy [person/ m <sup>2</sup> ]	0.058
Source	ASHRAE International Weather for Energy Calculations (IWEC)

The reference building is assumed to be located in Frankfurt, which is selected as representative location for the Northern and Center Europe climate with its moderately cold winters and warm summers. The corresponding reference weather file is thus used for running the simulation. The weather file used can be downloaded from the weather data section

arranged by the World Meteorological Organization region and Country, and available at the EnergyPlus website (Department of Energy, 2015), as a compressed folder containing three files, listed as follows:

- the EnergyPlus weather file (EPW);
- the weather summary report (STAT);
- the ASHRAE Design Conditions Design Day Data file (DDY).

All files can be converted into CSV format through the EnergyPlus Weather Converter.

*Table 4-2 Location data of Frankfurt, Germany*

Name weather file	Frankfurt am Main
Site Station	WMO=106370
Format Weather file	epw, EnergyPlus format
Latitude [deg]	50.05
Longitude [deg]	8.6
Elevation [m]	113
Time Zone	1 (GMT +1.0 Hours)
Source	ASHRAE International Weather for Energy Calculations (IWEC)

*Heating Degree Days = 3143 annual (standard) heating degree-days (18.3°C baseline)*

*Cooling Degree Days = 166 annual (standard) cooling degree-days (18.3°C baseline)*

#### **4.1.2. Description of the reference building model**

The model presented below can be used in the EnergyPlus and EES simulation software, and it can easily be translated into other languages/equation solver or simulation software. A general description of the building model is provided hereinafter. A more detailed description of the building model created by the EES software can be found in the Appendix. A brief summary of the building characterization is reported in Table 4-3. The building hereby presented is a ten-floor medium-sized office with a total gross area of approximately 16600m<sup>2</sup>, as pictured in Fig. 4-1. The number of floors is changed from the original DOE building model, from three to ten in order to represent a more typical medium-sized office building.

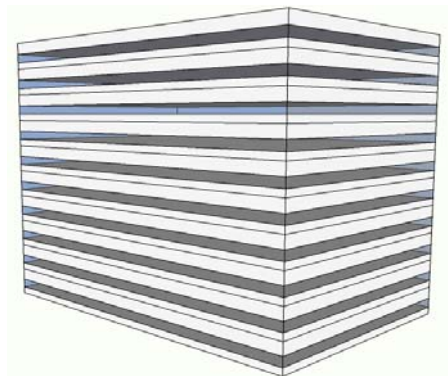


*Fig. 4-1 Axonometric view of the 10-floor medium-sized office building*

Table 4-3 Summary of the building

BUILDING TYPOLOGY	
Building Name	Annex59 Office Reference Building
Available Fuel Types	gas, electricity
Principal Building Activity	Office
FORM	
Total Floor Area [m <sup>2</sup> ]	16607
Building Shape	Rectangle
Aspect Ratio	1.5
Number of Floors	10
Window Fraction (Window to Wall Ratio)	
South	0.33
East	0.33
North	0.33
West	0.33
Total	0.33
Shading Geometry	None
Azimuth	0.0
Thermal Zoning	Core zone with four perimeter zones
Floor to Ceiling Height [m]	3.02 (inferior slab included)
Plenum Ceiling Height [m]	0.94
Floor to Floor Height [m]	3.96

BUILDING ENVELOPE	
Exterior walls	
Construction Type	Mass Non-residential Exterior Wall
Gross Dimensions - Total Area without external windows [m <sup>2</sup> ]	4415
Roof	
Construction Type	Flat roof, insulation entirely above deck
Gross Dimensions - Total Area [m <sup>2</sup> ]	1661
Window Dimensions [m <sup>2</sup> ]	
South	653
East	435
North	653
West	435
Total Area [m <sup>2</sup> ]	2176
Foundation	
Foundation Type	Slab Non-Residential with Insulation
Dimensions - Total Area [m <sup>2</sup> ]	1661
Interior Partitions	
Construction	2x4 steel-frame with gypsum board
Dimensions - Total Area [m <sup>2</sup> ]	426

Internal Mass	
Construction	15 cm wood
Dimensions - Total Area [m <sup>2</sup> ]	9964
Infiltration [ACH]	0.2

Fig. 4-2 represents the reference floor as defined in the model. As previously mentioned, only one floor is modeled. In order to simulate it as an intermediate floor, the lower and upper inferior and superior slabs are defined as adjacent to a zone with similar boundary conditions (adiabatic surfaces). In this regard, the bottom of the floor slab faces thus the top of the ceiling void. These assumptions are accurate enough since the building model is only used to feed the HVAC system under study.

The reference floor is divided into 6 zones: 5 occupancy zones, presented in a horizontal sectional view in Fig. 4-3, and 1 ceiling void (unique for the whole floor). The interior layout of the floor thus can be defined by four open offices located in the peripheral areas and one central core, which corresponds to a group of several meeting rooms, service areas and offices as well.

Table 4-4 and Table 4-5 report the main geometrical features of the six thermal zones of the reference floor.

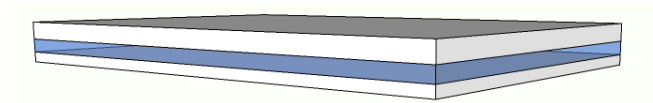


Fig. 4-2 Axonometric view of the Medium Office reference building floor

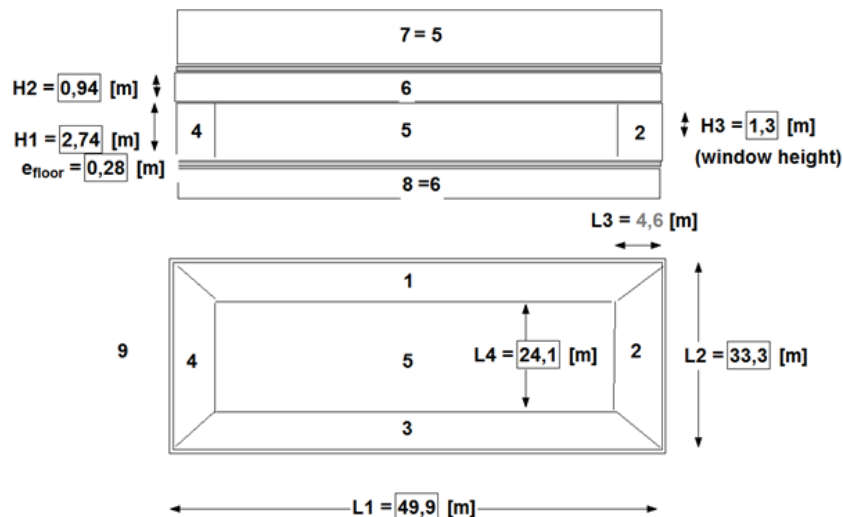


Fig. 4-3 Horizontal and vertical views of the reference floor.

Table 4-4 Building summary: geometrical data of each zone

Zone Name	Condit. [Y/N]	Area [m <sup>2</sup> ]	Volume [m <sup>3</sup> ]	Ceiling Height [m]	Gross Wall Area [m <sup>2</sup> ]	Window Glass Area [m <sup>2</sup> ]
Zone 1 (North)	Yes	207	569	2.74	151	65
Zone 2 (East)	Yes	131	360	2.74	101	44
Zone 3 (South)	Yes	207	569	2.74	151	65
Zone 4 (West)	Yes	131	360	2.74	101	44
Zone 5 (Core)	Yes	984	2698	2.74	0	0
Zone 6 (Plenum)	No	1661	2025	0.94	156	0
<b>Total Conditioned Zones</b>	-	<b>16607</b>	<b>51631</b>	-	<b>5173</b>	<b>2176</b>

Table 4-5 Building summary: adjacent area per zone

Zone Name	Adjacent area [m <sup>2</sup> ]					
	Zone 1	Zone 2	Zone 3	Zone 4	Zone 5	Zone 6
Zone 1 (North)	0	17	0	17	111	207
Zone 2 (East)	17	0	17	0	66	131
Zone 3 (South)	0	17	0	17	111	207
Zone 4 (West)	17	0	17	0	66	131
Zone 5 (Core)	111	66	111	66	0	983
Zone 6 (Plenum)	207	131	207	131	983	0

A schematic cross section of the reference floor is shown in Fig. 4-4

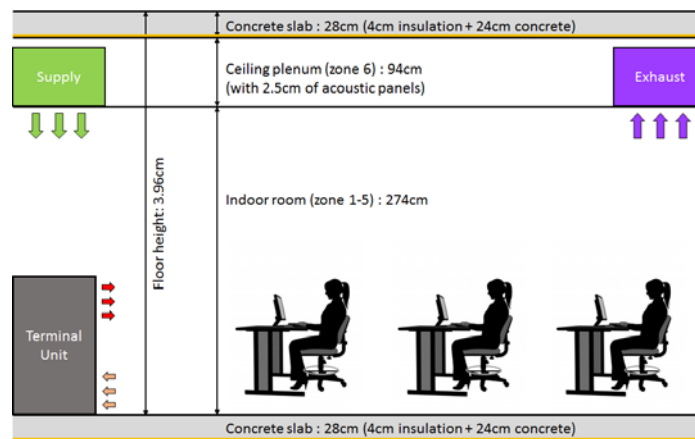


Fig. 4-4 Cross section of the reference floor

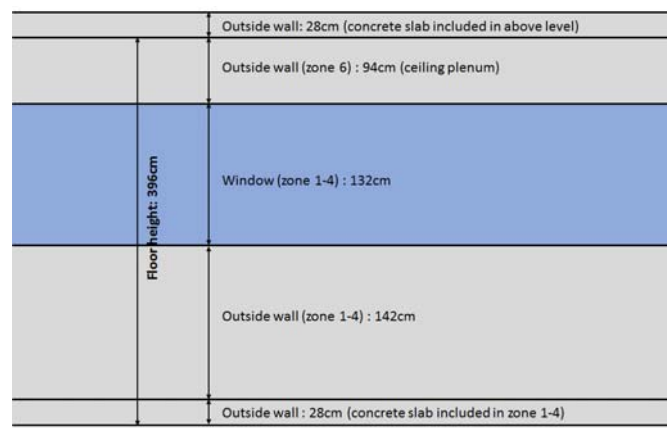
The thermo-physical features of the building envelope do not correspond to those of the DOE reference building; they are customized for the Annex 59 investigations. Table 4-6 lists the U-values of the main building envelope components.

Table 4-6 Building envelope summary

Construction type	Construction Name [idf file]	U-value [W/m <sup>2</sup> K]
Walls	Mass non-res ext wall	0.69

Roof	<i>IEAD Non-res Roof</i>	0.30
Ground Slab	<i>Slab</i>	1.00
Slab	<i>Int-Slab</i>	1.00
Windows	<i>Window non-res fixed</i>	1.60
Interior walls	<i>Int-walls</i>	3.00
Ceiling acoustic panels	<i>DropCeiling</i>	1.36

With regard to the transparent envelope component, the frame to window ratio is 0.25 with a window layer composition of 4/20/4 with 90%Argon. No solar shading device was modeled. The whole window solar gain factor is 0.52 and 0.7 for the glass solar factor. The wall in contact with the concrete slab is considered as included into the adjacent zone wall, as shown in Fig. 4-5.



*Fig. 4-5 Vertical view of the outside envelope of the reference floor*

*The internal partitions and furnishings of each zone are not geometrically modeled, but they are taken into account modelled as internal mass (Table 4-7).*

The construction associated to each internal mass corresponded to a 15 cm wood panel, called “InteriorFurnishings” within the EnergyPlus model (

Table 4-8). For the EES model, an empirical “indoor capacity factor” equal to 5 is used to increase the heat capacity of the room air to approximate energy storage in furniture and building constructions.

*Table 4-7 Internal mass summary*

Zone Name	Surface [m <sup>2</sup> ]
Zone 1	415
Zone 2	262
Zone 3	415
Zone 4	262
Zone 5	1976

Table 4-8 Internal mass, wood panel characteristics.

Construction type	Wood panel
Thickness [m]	0.15
Conductivity [W/mK]	0.12
Density [kg/m <sup>3</sup> ]	540
Specific heat [J/kg.K]	1210
Thermal absorptance [-]	0.9
Solar absorptance[-]	0.7
Visible absorptance [-]	0.7

With regard to the internal gains related to building operation, Table 4-9 reports the main assumptions of their definition in the building model. They are defined in compliance with the European Standard EN 15232 (European Committee for Standardization, 2007): the occupancy rate is defined as 13.3 m<sup>2</sup>/per person (integer number only); lighting and appliances power densities are set to 13W/m<sup>2</sup><sub>floor</sub> and 10 W/m<sup>2</sup><sub>floor</sub>, respectively.

Each occupant is supposed, due to his office working activity, to produce 70W of sensible heat. In particular, for the core zone, occupancy and appliances are defined as “active” only on 60% of the floor area, given the presence of services area (e.g. stairs, elevator and restrooms). The ventilation rate is set as reported in Table 4-9 by using the operation schedule drawn in Fig. 4-6.

Table 4-9 Building summary. Operational data per zone

Zone Name	People [per]	Lights [W]	Elec Plug and Process [W]	Ventilation [l/s*m <sup>2</sup> ]
Zone 1	16	2691	2073	0.386
Zone 2	10	1703	1313	0.382
Zone 3	16	2691	2073	0.386
Zone 4	10	1703	1313	0.382
Zone 5	45	12792	5904	0.228
Total (for the 10 floors)	971	215800	77760	0.291

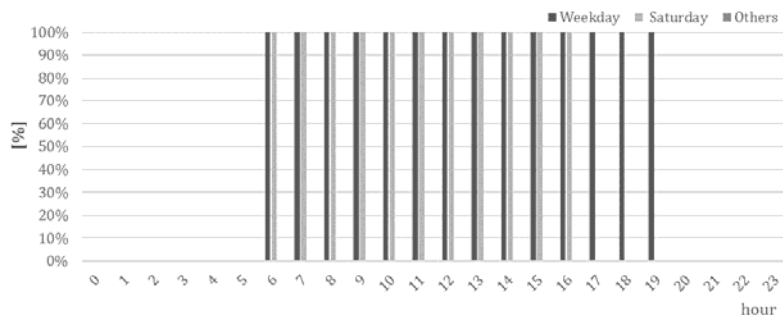


Fig. 4-6 Ventilation schedule of the Medium Office reference building model.

It is assumed that there is no transfer air between zones. Both supply and exhaust air flow rates are sized as identical, on the basis of 36m<sup>3</sup>/h per occupant.

The internal water production taken into account during modelling came only from the occupants, assumed to be a nominal value of 40 g/h per occupant. The occupancy schedule previously defined is also employed for this purpose. Moreover, a CO<sub>2</sub> balance per zone is also included in the model and is fixed similarly to the zone water balance model with a CO<sub>2</sub> production per occupant of 40 g/h.

The internal gains schedules are reported in Table 4-10 and in Fig. 4-7 to Fig. 4-9.

*Table 4-10 Internal gains schedules*

	Occupants			Lights			Appliances		
	Week	Sat.	Others	Week	Sat.	Others	Week	Sat.	Others
0	0	0	0	0.05	0.05	0.05	0.4	0.3	0.3
1	0	0	0	0.05	0.05	0.05	0.4	0.3	0.3
2	0	0	0	0.05	0.05	0.05	0.4	0.3	0.3
3	0	0	0	0.05	0.05	0.05	0.4	0.3	0.3
4	0	0	0	0.05	0.05	0.05	0.4	0.3	0.3
5	0	0	0	0.1	0.05	0.05	0.4	0.3	0.3
6	0	0.1	0	0.1	0.1	0.05	0.4	0.3	0.3
7	0.2	0.1	0	0.3	0.1	0.05	0.4	0.3	0.3
8	0.95	0.3	0	0.9	0.3	0.05	0.9	0.5	0.3
9	0.95	0.3	0	0.9	0.3	0.05	0.9	0.5	0.3
10	0.95	0.3	0	0.9	0.3	0.05	0.9	0.5	0.3
11	0.95	0.3	0	0.9	0.3	0.05	0.9	0.5	0.3
12	0.5	0.1	0	0.9	0.15	0.05	0.8	0.5	0.3
13	0.95	0.1	0	0.9	0.15	0.05	0.9	0.5	0.3
14	0.95	0.1	0	0.9	0.15	0.05	0.9	0.35	0.3
15	0.95	0.1	0	0.9	0.15	0.05	0.9	0.35	0.3
16	0.95	0.1	0	0.9	0.15	0.05	0.9	0.35	0.3
17	0.3	0	0	0.5	0.05	0.05	0.8	0.3	0.3
18	0.1	0	0	0.3	0.05	0.05	0.6	0.3	0.3
19	0.1	0	0	0.3	0.05	0.05	0.6	0.3	0.3
20	0.05	0	0	0.2	0.05	0.05	0.5	0.3	0.3
21	0.05	0	0	0.2	0.05	0.05	0.5	0.3	0.3
22	0.05	0	0	0.1	0.05	0.05	0.4	0.3	0.3
23	0.05	0	0	0.05	0.05	0.05	0.4	0.3	0.3

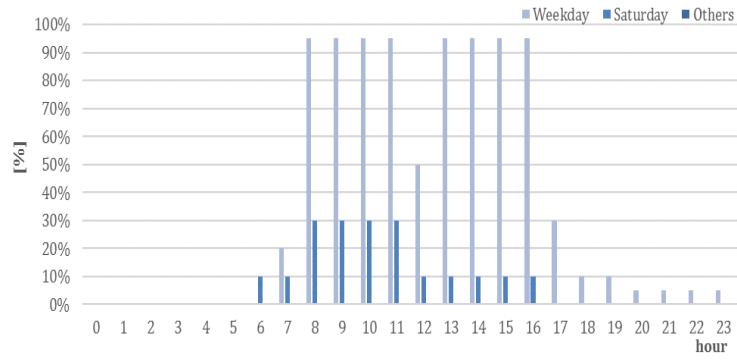


Fig. 4-7 Occupancy schedule of the Medium Office reference building model

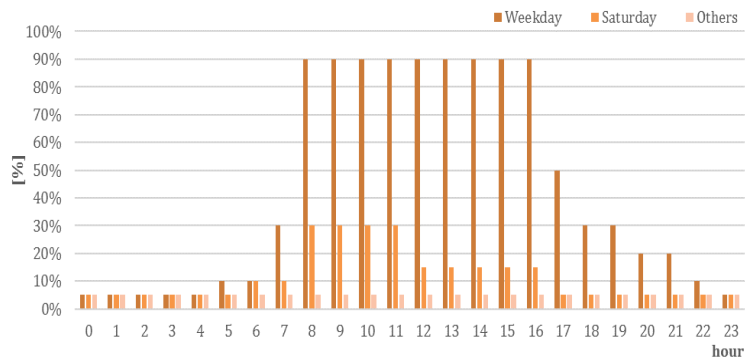


Fig. 4-8 Lighting schedule of the Medium Office reference building model

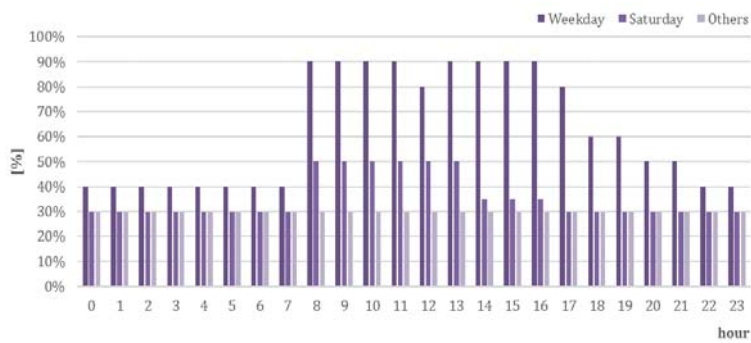


Fig. 4-9 Equipment schedule of the Medium Office reference building model

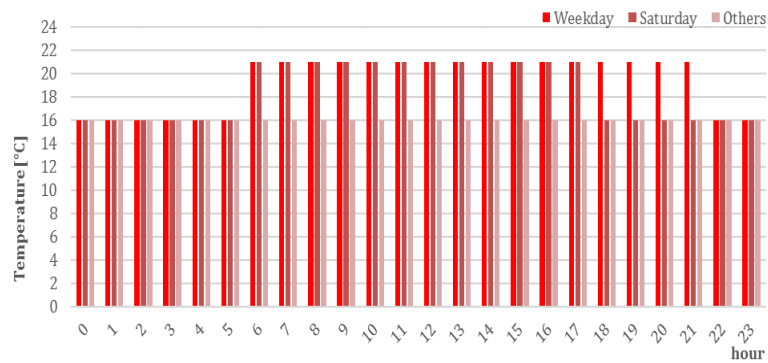


Fig. 4-10 Heating set point schedule of the Medium Office reference building model.

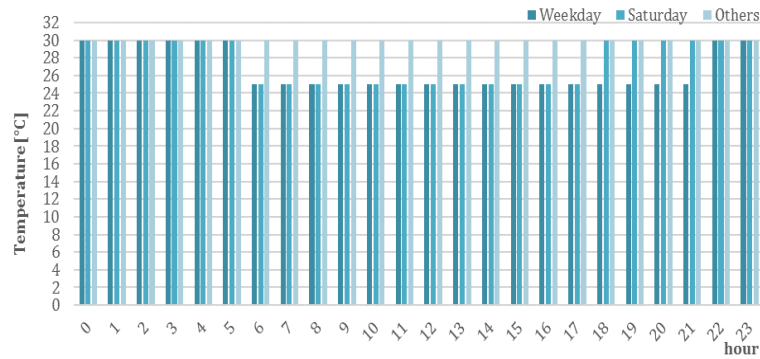


Fig. 4-11 Cooling set point schedule of the Medium Office reference building model.

The heating and cooling operation schedules are presented in Fig. 4-10 and Fig. 4-11. For heating, the temperature set point is set to 21°C during working hours, with a setback temperature of 16°C. For cooling, the temperature set point is set to 25°C during working hours, with a setback temperature of 30°C. In addition to the temperature set point, the humidity min/max set points are defined as RH = [40%; 60%].

To initialize the building model, the following assumptions are made:

- Indoor temperature of the air inside each zone: 20°C.
- Floor thermal mass temperatures: 20°C.
- Indoor air water content:  $\omega_{in} = 0.005$  [-].
- Indoor air CO<sub>2</sub> content: 400 ppm.

NB: Not all the software are allowed to modify initial conditions. In EnergyPlus these conditions cannot be altered.

### 4.1.3. Validation process

The validation process was carried out based on a 5-step simulation approach in order to compare the building models built within different simulation programs. The 5 steps performed in simulation are listed as follows:

0. Building model in quasi-steady condition with constant outdoor temperature;
1. Building model without internal gains and without solar radiation;
2. Building model without internal gains and with solar radiation;
3. Building model with solar radiation and internal gains;
4. Building model with solar radiation, internal gains and natural ventilation.

For each step, the following output data were checked:

- Mean ambient air temperature;
- Heating and cooling demand (only for step 4).

The Belgium partners (University of Liege) employed two different platforms for the Annex59 simulation: the EES program and the Modelica software. The modelling process of the reference building are defined, within both programs, based on the same assumptions.

#### 4.1.3.1. Step 0 – Envelope heat loss

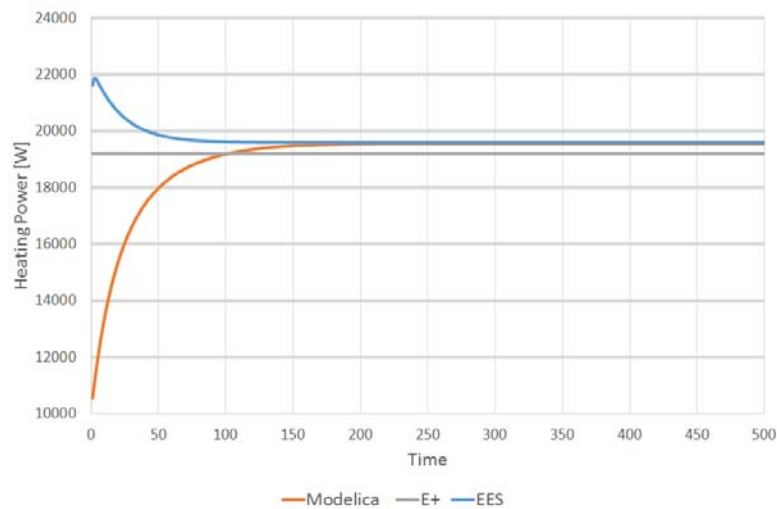


Fig. 4-12 Comparison of simulation results at Step 0

The EES and Modelica simulation results gave the same heating power demand of 19.5kW. The EnergyPlus results are close to the others with 19.2kW. The envelope dimension, the zones definition and the wall characteristics are well defined based on this comparison.

#### 4.1.3.2. Step 1 – Weather data effect

For step 1, simulation of the building model was performed only taking external temperature as thermal force, while solar radiation (global, diffuse and beam horizontal radiation), internal gains, ventilation and the ideal HVAC system (for temperature control) were assumed not in operation.

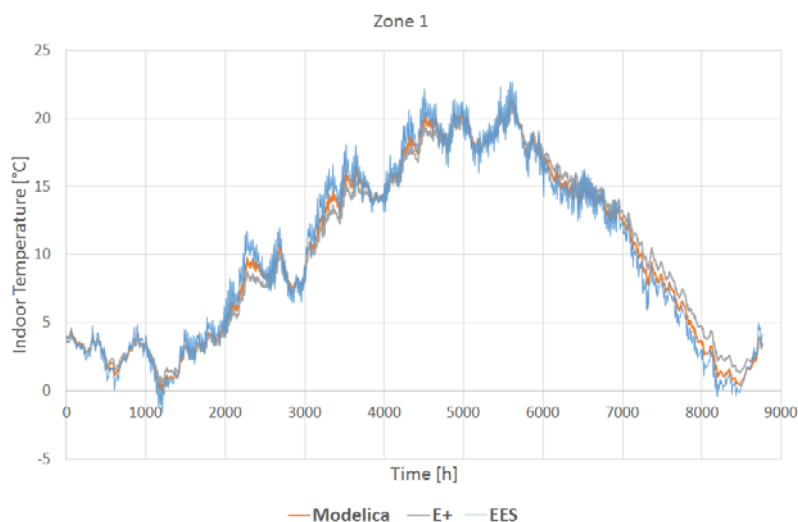


Fig. 4-13 Comparison of simulation results at Step 1

The simulation of indoor temperature in the reference building in one year under actual weather condition (outdoor temperature) on the basis of the three models shows coherence in the changing trend. Variation of indoor temperature simulated by the three models is within a

range of 3°C. The furniture and internal walls were modelled slightly differently, but this has no special impact on simulation results.

#### 4.1.3.3. Step 2 – Solar gains

In Step 2, the building model simulation was performed by activating the solar radiation, while internal gains, ventilation and the ideal HVAC system (for temperature control) were considered not in operation.

Simulation results show that the introduction of solar gains in the models brings larger variation in temperature between the EES and Modelica models, mostly due to their different internal partitions and furnishings models.

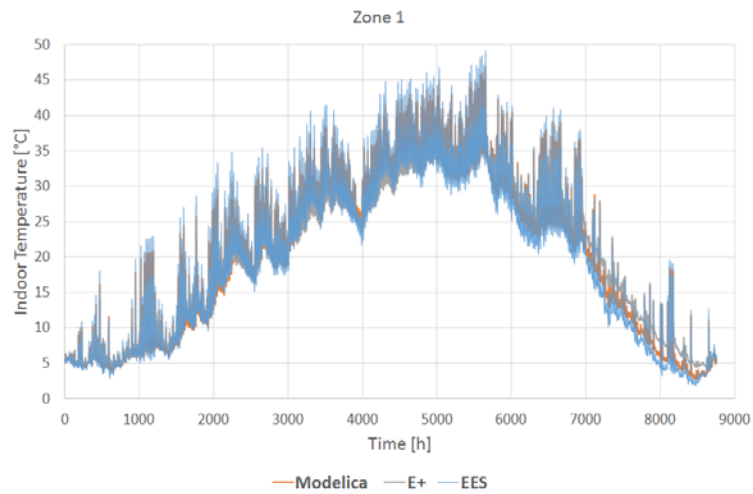
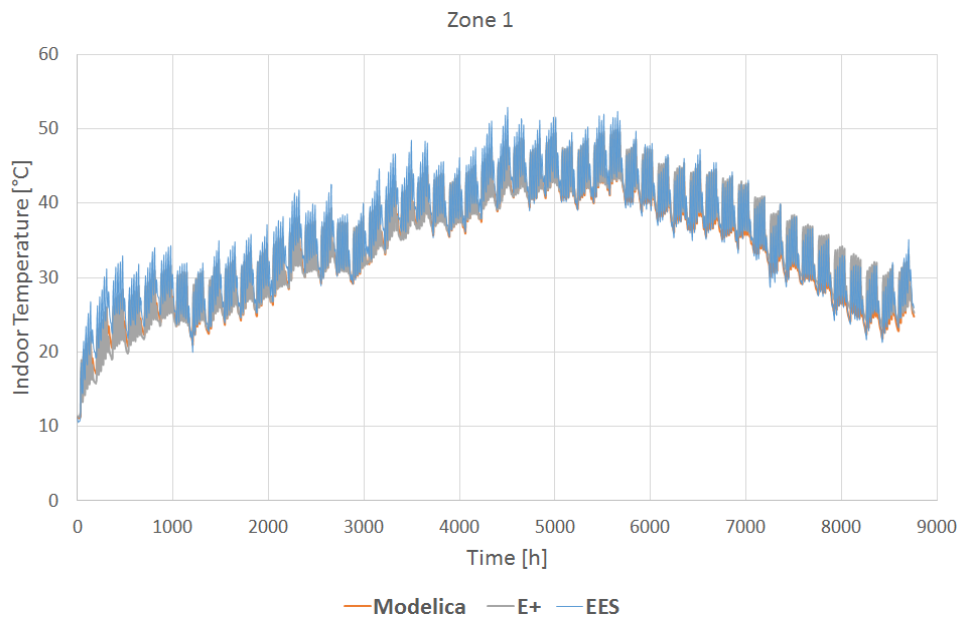


Fig. 4-14 Comparison of simulation results at Step 2

#### 4.1.3.4. Step 3a – Internal heat gains

In Step 3, the simulation was performed by activating the internal gains (lighting, equipment and occupancy), while ventilation and the ideal HVAC system (for temperature control) were assumed not in operation.



*Fig. 4-15 Comparison of simulation results at Step 3a*

**4.1.3.5. Step 3b – Internal heat gains and solar gains**

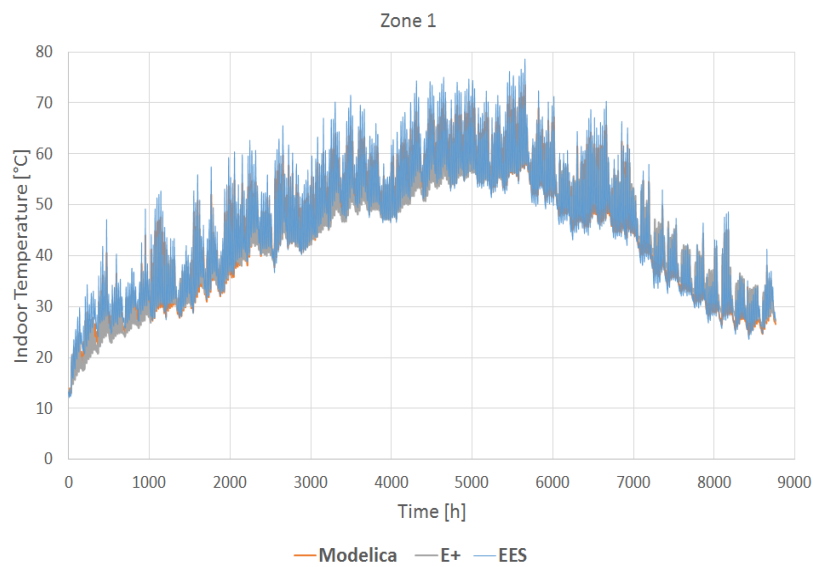


*Fig. 4-16 Comparison of simulation results at Step 3b*

The combined gains effect shows slightly different results with around 2°C difference on average temperature.

#### 4.1.3.6. Step 4 – Ventilation and infiltration

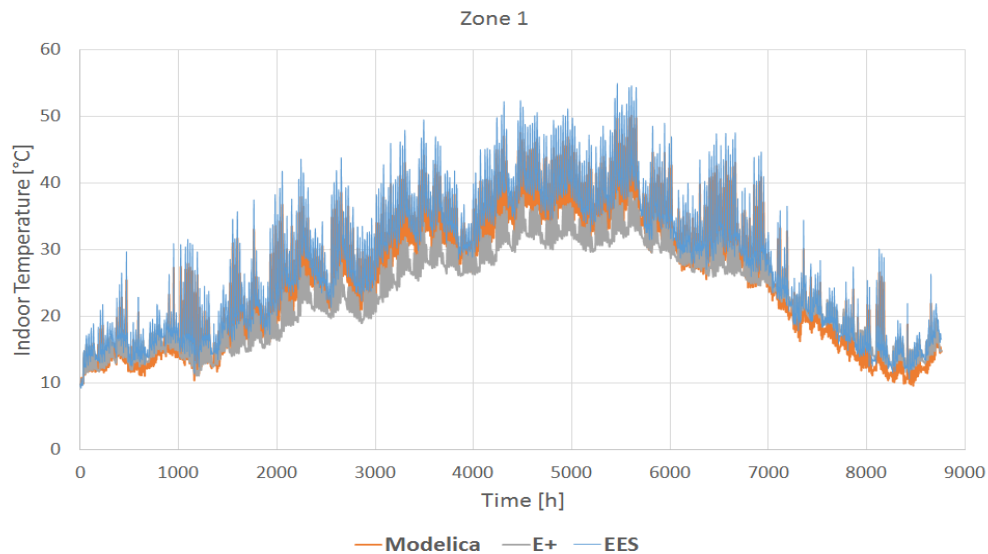


Fig. 4-17 Comparison of simulation results at Step 4

The combined gains effect shows slightly different results with around 2°C difference on average temperature.

#### 4.2. Description of the Reference Case of the HVAC system

The selected reference is a typical European HVAC system supposed to be installed in a medium-sized new office building. The system, whose whole scheme and hydraulic network are given in Fig. 4-18, is composed of the following components:

- one gas condensing boiler;
- two air-cooled chillers;
- one constant air volume air handling unit including filter, recovery heat exchanger, preheating coil, cooling coil, adiabatic humidifier, post heating coil, supply fan and exhaust fan;
- 4-tube fan coils used as terminal units (one equivalent unit per zone).

##### 4.2.1. Terminal Units

As mentioned in the description of the reference building, the cooling and heating set points for each building thermal zone were defined as follows:

- heating temperature set point was set to 21°C during working hours and the temperature setback is 16°C (see Fig. 4-19);
- cooling temperature set point was set to 25°C in working hours and the setback is 30°C (see Fig. 4-20).

Based on previous work done on the building reference floor, the terminal unit's sensible heating and cooling nominal loads in each zone of the building were evaluated. From these results, a component was selected for each occupancy zone. The characteristics of the fan

coils are obtained from manufacturer data (GEA, 2012) given in Appendix. The characteristics of the fan coils are presented in in Table 4-11.

*Table 4-11 Fan coil main characteristics*

	<b>Heating Capacity*</b> [kW]	<b>Cooling Capacity**</b> [kW]	<b>Fan consumption (Max/Min)</b> [kW]	
<b>Zone 1</b>	11.8	12.8	0.160	0.016
<b>Zone 2</b>	8.2	9.0	0.122	0.006
<b>Zone 3</b>	11.8	12.8	0.160	0.016
<b>Zone 4</b>	8.2	9.0	0.122	0.006
<b>Zone 5</b>	8.2	9.0	0.122	0.006
<b>Total</b>	<b>482.0</b>	<b>526.0</b>	<b>6.860</b>	<b>0.500</b>

\*HW 70/50°C –  $t_{a,su} = 20^{\circ}\text{C}$  at fan maximum speed and with the valve fully open

\*\*CW 6/12°C –  $t_{a,su} = 27^{\circ}\text{C}$  at fan maximum speed and with the valve fully open

The fan runs at maximal speed during occupancy hours and at minimal speed during the non-occupancy hours as first input of the fan coil is then control with an ideal control of the water flow rate in the coils (controlling the opening of the valve).



*Fig. 4-18 Scheme of the Reference Case of the HVAC System*

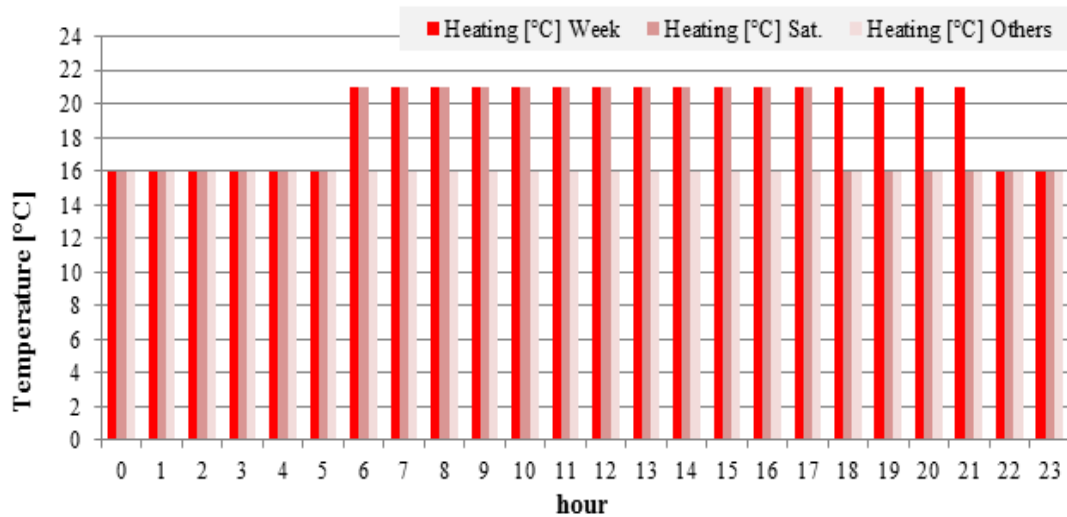


Fig. 4-19 Hourly schedule of heating set point

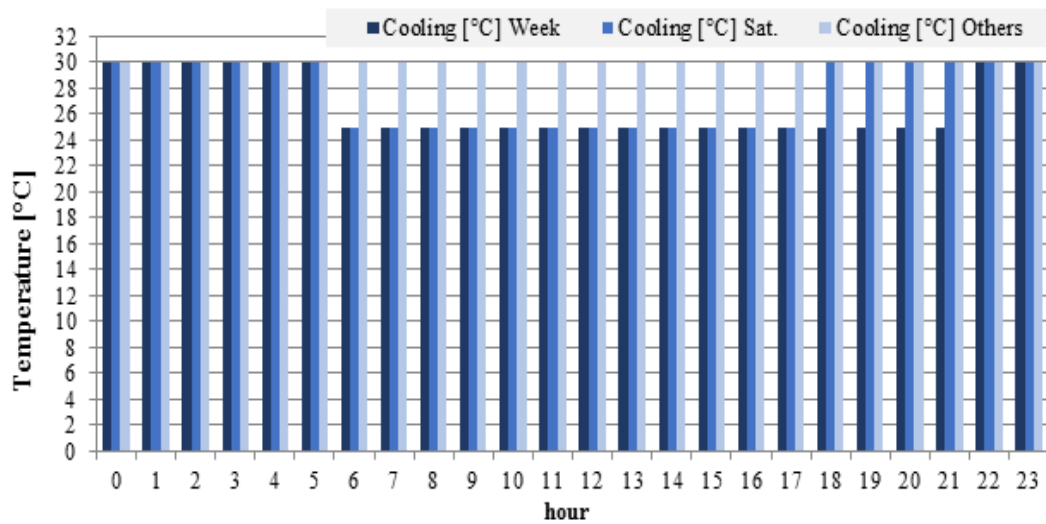


Fig. 4-20 Hourly schedule of cooling set point

#### 4.2.2. Air Handling Unit

In the reference building description, the ventilation flow rates are set as reported in Table 4-12 with the schedule shown in Fig. 4-21.

Table 4-12 Ventilation air flow rate per zone

	Units	Supply	Extraction
Zone 1	[m <sup>3</sup> /h]	576	576
Zone 2	[m <sup>3</sup> /h]	360	360
Zone 3	[m <sup>3</sup> /h]	576	576
Zone 4	[m <sup>3</sup> /h]	360	360
Zone 5	[m <sup>3</sup> /h]	1620	1620
Total	[m <sup>3</sup> /h]	34920	34920

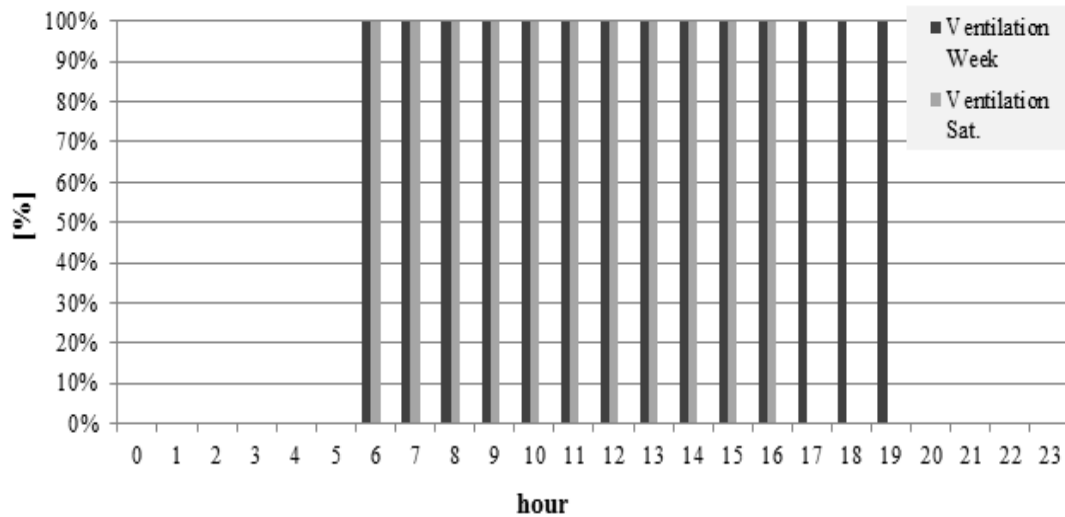


Fig. 4-21 Hourly schedule of ventilation

The AHU scheme is shown in Fig. 4-22. The air pressure drops in nominal conditions through components of the AHU and through the supply and return ducts are shown in Fig. 4-22 and summarized in

Table 4-13. These values are obtained from the European norm EN13779 (European Committee for Standardization, 2004).

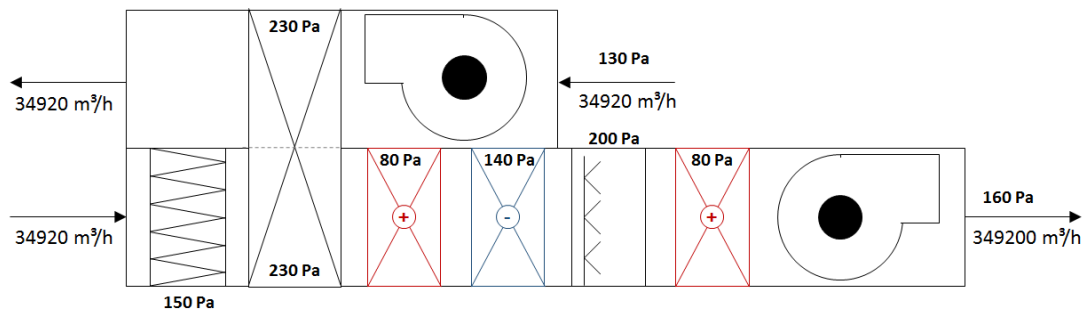


Fig. 4-22 Air handling unit scheme

Table 4-13 Reference air pressure drops inside the AHU

	Units	Value
Filter	[Pa]	150
Heat recovery	[Pa]	230
Preheating coil	[Pa]	80
Cooling coil	[Pa]	140
Adiabatic humidifier	[Pa]	200
Post heating coil	[Pa]	80

The components of the AHU are sized based on nominal conditions according to the set points defined in the following paragraphs.

#### 4.2.2.1. Exhaust fan

The nominal flow rate of exhaust fan is set to 34920 m<sup>3</sup>/h. The pressure drop associated to the fan is the sum of the pressure drops through the recovery heat exchanger (see section 4.2.2.2) and through the return duct. The return duct pressure drop is assumed, under nominal conditions, equal to 130 Pa (1Pa/m through a duct of 130m).

Fig. 4-23 shows characteristics of the selected fan and nominal operating point based on manufacturer data (FläktWoods). In this reference case, the air flow rate and the pressure drop stay constant. The characteristics of the fan are then only used in order to take the effect of temperature variation into account.

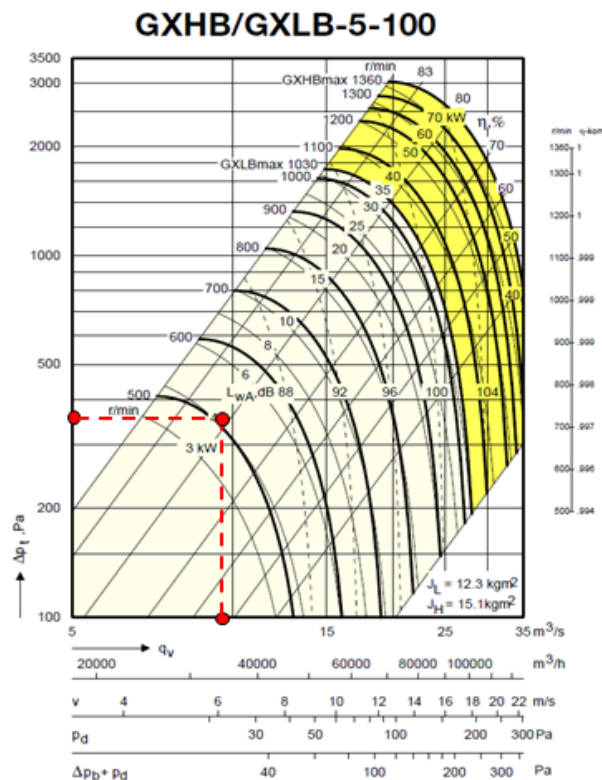


Fig. 4-23 Characteristics of exhaust fan

#### 4.2.2.2. Heat Recovery

The heat recovery device is supposed to be a static heat exchanger with a constant efficiency of 67% without auxiliary consumption. It works only when the outside temperature is lower than 16°C. The nominal pressure drops associated on both air side are equal to 230 Pa.

#### 4.2.2.3. Filter

A typical F7 filter with a nominal pressure drop of 150 Pa is considered for filtering fine dust.

#### 4.2.2.4. Preheating Coil

In the reference case, the preheating coil is sized and controlled to achieve a temperature of 12°C at the exhaust of the adiabatic humidifier (after humidification up to RH=95%). The sizing conditions and the preheating coil characteristics are presented in Table 4-14 and

Table 4-15, respectively. The water flow rate is kept constant in the preheating coil (to avoid frost in the coil), and the water supply temperature is controlled with a 3-way valve to achieve the exhaust air. The preheating coil only functions when the indoor temperature is lower than 12°C; its nominal air pressure drop is 80 Pa.

Table 4-14 Sizing conditions of the preheating coil

	Units	Value
$\dot{M}_{air,preheatcoil,n}$	[kg/s]	9.70
$t_{water,preheatingcoil,su,n}$	[°C]	70
$t_{water,preheatingcoil,ex,n}$	[°C]	50
$t_{air,preheatingcoil,su,n}$	[°C]	-10
$RH_{air,preheatingcoil,su,n}$	[-]	0.95
$t_{air,adiabhum,ex,n}$	[°C]	12
$RH_{air,adiabhum,ex,n}$	[-]	0.95

Table 4-15 –Characteristics of the preheating coil

	Units	Value
$\dot{Q}_{preheatcoil,n}$	[kW]	450.4
$\dot{M}_{water,preheatcoil,n}$	[kg/s]	5.38

#### 4.2.2.5. Cooling Coil

The cooling coil is sized to achieve a temperature of 12°C at its exhaust, leading to a maximum absolute humidity of 8.722 g<sub>water</sub>/kg<sub>air</sub> set at the exhaust of the coil. The sizing conditions and characteristics of the cooling coil are reported in Table 4-16 and

Table 4-17, respectively. The coil supplies at a constant water flow rate; its water supply temperature is controlled with the help of a by-pass and of a three-way valve. The cooling coil circuit only functions when the outdoor air temperature reaches or overpass 16°C.

Table 4-16 Sizing conditions of the cooling coil

	Units	Value
$\dot{M}_{air,preheatcoil,in}$	[kg/s]	9.70
$t_{water,coolingcoil,su,n}$	[°C]	6
$t_{water,coolingcoil,ex,n}$	[°C]	12
$t_{air,coolingcoil,su,n}$	[°C]	30
$t_{air,coolingcoil,ex,n}$	[°C]	12
$RH_{air,coolingcoil,su,n}$	[-]	0.7
$\epsilon_c,cooling,n$	[-]	0.9

Table 4-17 Characteristics of the cooling coil

	Units	Value
$\dot{Q}_{coolingcoil,n}$	[kW]	509.22
$\dot{M}_{water,coolingcoil,n}$	[kg/s]	20.27

#### 4.2.2.6. Humidifier

As mentioned above, the humidifier (air washer) is controlled together with the preheating coil to reach a temperature of 12°C and relative humidity of 95% at the exhaust of the component. The nominal pressure drop associated is 200 Pa.

#### 4.2.2.7. Post heating Coil

The post heating coil is sized to achieve a temperature of 16°C at exhaust. The sizing conditions and characteristics of the post heating coil are presented in Table 4-18 and

Table 4-19, respectively. The coil is ideally controlled with variable water flow rate and constant water supply temperature.

Table 4-18 Sizing conditions of the post heating coil

	Units	Value
$\dot{M}_{air,preheatcoil,in}$	[kg/s]	9.70
$t_{water,coolingcoil,su,n}$	[°C]	70
$t_{water,coolingcoil,ex,n}$	[°C]	50
$t_{air,coolingcoil,su,n}$	[°C]	12
$t_{air,coolingcoil,ex,n}$	[°C]	20

Table 4-19 Characteristics of the post heating coil

	Units	Value
$\dot{Q}_{coolingcoil,m}$	[kW]	47.014
$\dot{M}_{water,coolingcoil,m}$	[kg/s]	0.5614

#### 4.2.2.8. Supply fan

The nominal flow rate of the supply fan is set to 34920 m<sup>3</sup>/h. The pressure drop through the supply ducts is considered under the nominal condition equal to 160 Pa (1.3Pa/m for a duct of 122.8m). Fig. 4-24 shows characteristics of the selected fan and nominal operating point based on manufacturer data (FläktWoods). In the reference case, the air flow rate and the pressure drop stay constant.

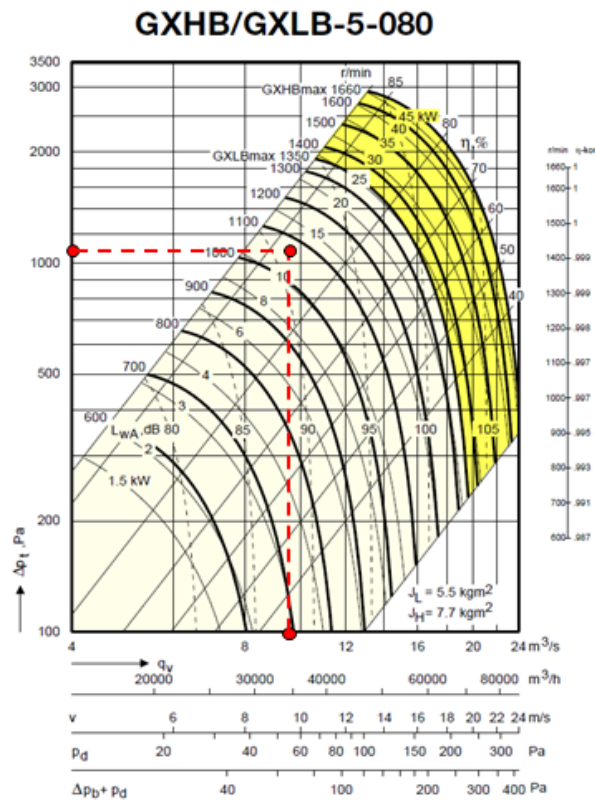


Fig. 4-24 Characteristic of the supply fan

#### 4.2.3. Hydraulic system

For the reference case, a hydraulic network was submitted to a typical design with the help of a Belgian partners working in the field.

#### 4.2.3.1. Hot water network

The primary distribution system of the hot water network is presented in Fig. 4-25. It connects the open header to the boiler at its primary side and to the supply and return hot water collector at its secondary side.

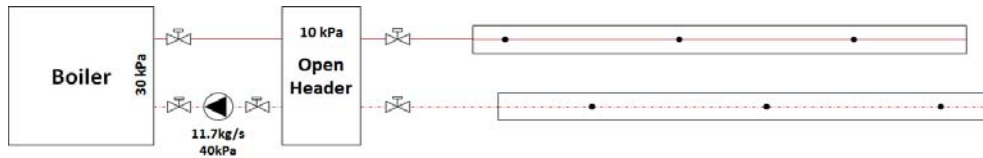


Fig. 4-25 Primary hot water distribution circuit

For the hot water collector and the primary distribution circuit between the collector and the open header, a simplified approach is employed to taken into account the ambient heat losses . The heat losses between the pipe and its environment are evaluated as follows (Vandenbulcke, 2013):

$$P_{loss} = \dot{M}_w * c_w * (T_{w,SM} - T_{amb}) * (1 - \exp(-NTU))$$

$$NTU = \frac{UA}{\dot{M}_w}$$

Where,  $T_{amb}$  is the ambient temperature and NTU is the Number of Transfer Units. The product heat transfer coefficient by area is calculated as a function of pipe dimensions and conductivity of insulating material. The values considered are given in Table 4-20.

Table 4-20 Assumed characteristics of the hot water collector and the primary distribution circuit

	Units	Value
Assumed pipe length	[m]	49.9
Assumed heat transfer coefficient	[W/m.K]	0.38
<b>Assumed UA-value</b>	<b>[W/K]</b>	<b>18.96</b>

The pipe section is considered based on a DN125 section and the assumed pipe length corresponds to 2.5 times of the width of the building. The heat transfer coefficient considered is assumed to be 4.2 cm of insulation with  $\lambda=0.04$  (European Committee for Standardization, 2012). Both systems are considered to be installed wholly in a technical room which is assumed to be at a constant temperature of 20°C. The heat is considered to be completely lost.

The water flow rate in the boiler and at the primary side of the open header is kept constant in the reference case. Characteristics of the associated pump are given in Table 4-21 and in Fig. 4-26.

Table 4-21 Characteristics of the boiler circuit pump

	Units	Value
Nominal pressure drop in the boiler circuit	[kPa]	40
Nominal water flow rate in the boiler circuit	[kg/s]	11.70

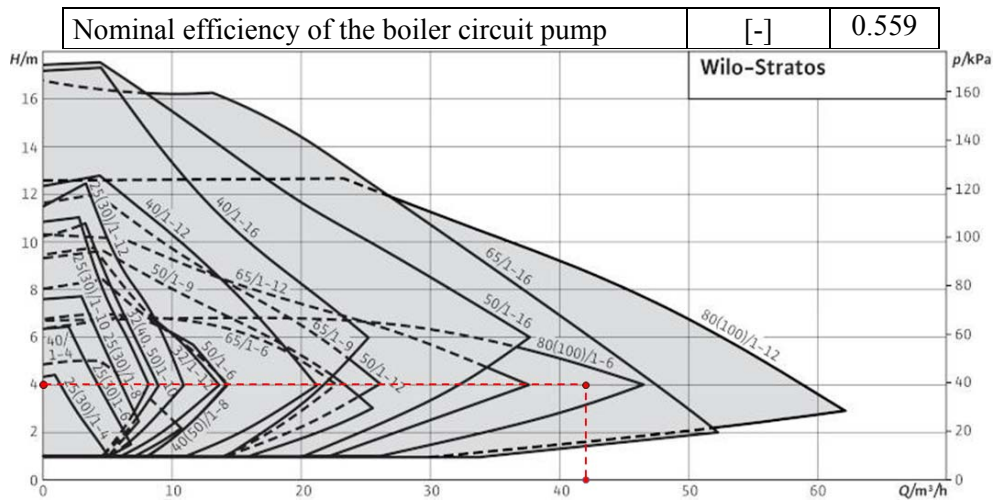


*Fig. 4-26 characteristics of the boiler circuit pump*

The schematic of the hot water collector and its secondary distribution circuit is presented in Fig. 4-27. It can be divided into 4 parts:

- the hot water collector itself,
- the distribution of the preheating and post heating coils,
- the risers that connect the hot water collector to the floor branches,
- the floor branches serving the fan coils.

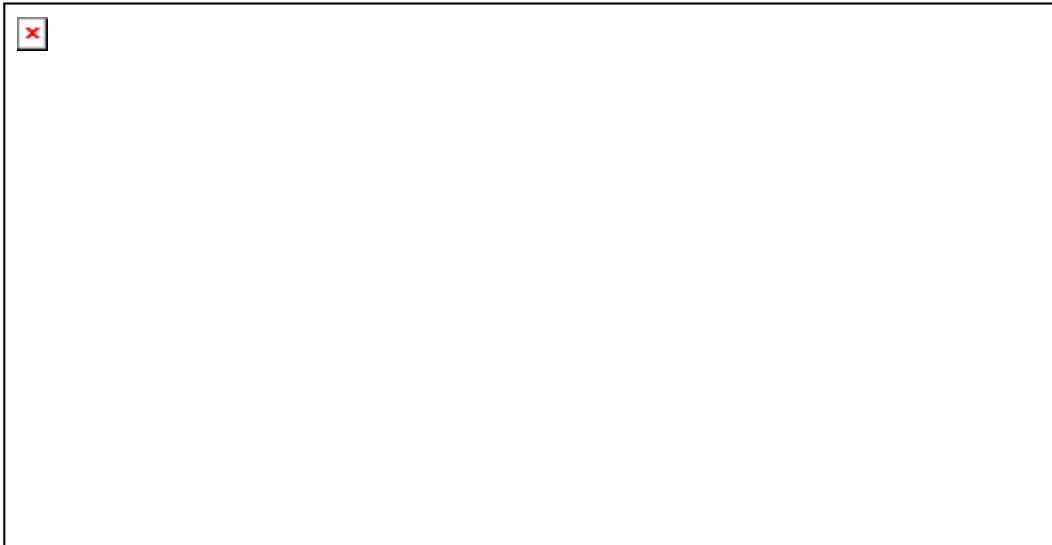


*Fig. 4-27 Hot water collector*

For heat losses, both distribution circuits are considered wholly inside the technical room, which is assumed to be at a constant temperature of 20°C, and the heat is considered to be completely lost. The assumed characteristics of the preheating and post heating coils distribution heat losses considered are presented in Table 4-22.

Table 4-22 Assumed characteristics of the preheating and post heating coils distribution heat losses

	Units	Value
Assumed pipe length	[m]	66.6
Assumed heat transfer coefficient	[W/m.K]	0.3
<b>Assumed UA-value</b>	<b>[W/K]</b>	<b>19.98</b>

The pipe section considered is based on a DN65 section and the assume pipe length corresponds to 4 times half the length of the building. The heat transfer coefficient is assumed considered 3.5 cm of insulation with  $\lambda=0.04$ .

The preheating and post heating circuit pumps characteristics are given in Table 4-23 and in both Fig. 4-28 and Fig. 4-29. In the preheating circuit, a constant flow rate pump is supply water to the coil and a 3-way valve is controlling the supply water temperature. For the post heating coil, the water flow rate is control based on exhaust air temperature.

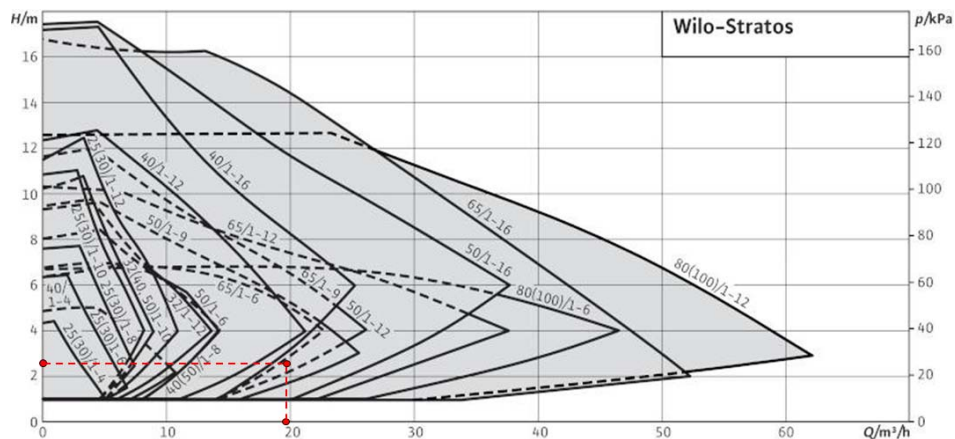


Fig. 4-28 Preheating circuit pump characteristics

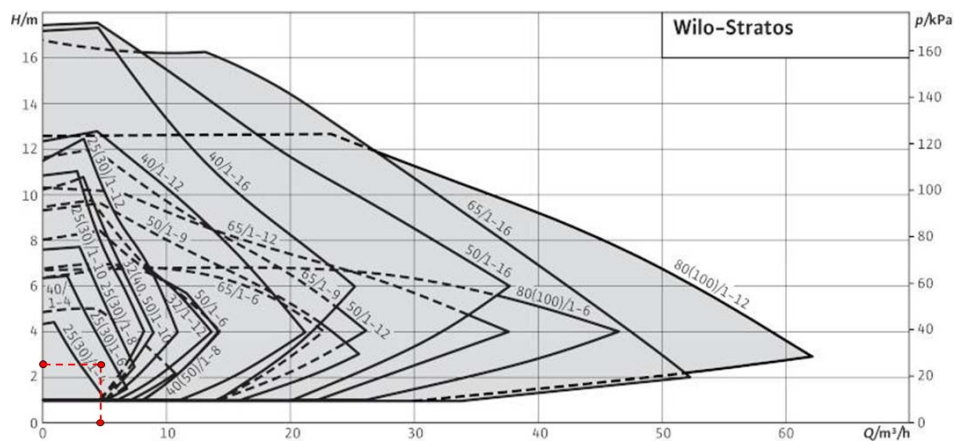


Fig. 4-29 Post heating circuit pump characteristics

*Table 4-23 Preheating and post heating circuit pump characteristics*

	<b>Units</b>	<b>Value</b>
Nominal pressure drop in the preheating circuit	[kPa]	25
Nominal water flow rate in the preheating circuit	[kg/s]	5.38
Nominal efficiency of the preheating circuit pump	[-]	0.490
Nominal pressure drop in the post heating circuit	[kPa]	25
Nominal water flow rate in the post heating circuit	[kg/s]	0.56
Nominal efficiency of the post heating circuit pump	[-]	0.485

All the hot water risers are considered fully inside the technical vein which is assumed to be at constant 20°C temperature. The heat is considered completely lost. The value considered are presented in

Table 4-24. The pipe section considered is based on a DN50 section and the assume pipe length corresponds to:

$$l_{\text{pipe}} = 2 * 5 * \left( \frac{l}{4} + \frac{w}{4} + h \right) = 604 \text{ m}$$

The heat transfer coefficient is assumed considered 2.8 cm of insulation with  $\lambda=0.04$ .

*Table 4-24 Assumed characteristics for the hot water risers heat losses*

	<b>Units</b>	<b>Value</b>
Assumed pipe length	[m]	604
Assumed heat transfer coefficient	[W/m.K]	0.26
<b>Assumed UA-value</b>	<b>[W/K]</b>	<b>157.04</b>

The heating terminal unit circuit pumps characteristics are given in Table 4-25 Fig. 4-25 and in Fig. 4-30.

*Table 4-25 – Heating terminal unit circuit pump characteristics*

	<b>Units</b>	<b>Value</b>
Nominal pressure drop in the heating terminal unit circuit	[kPa]	77.1
Nominal water flow rate in the heating terminal unit circuit	[kg/s]	5.51
Nominal efficiency of the heating terminal unit circuit pump	[-]	0.569

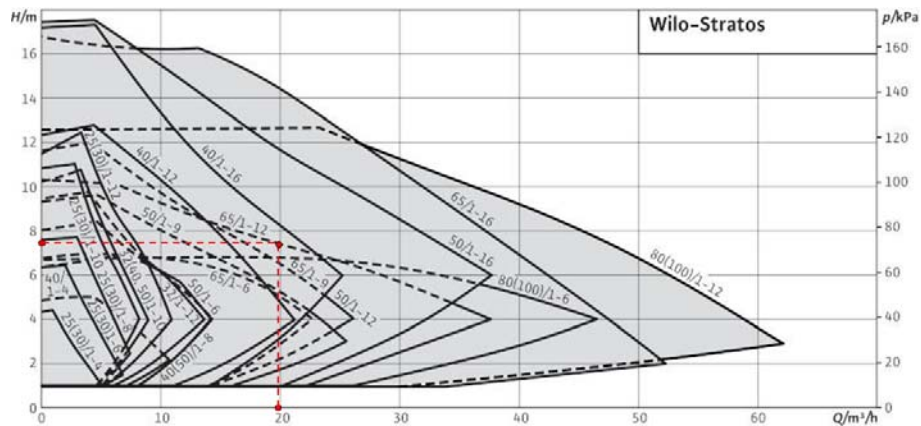


Fig. 4-30 Heating terminal unit circuit pump characteristics

The floor branches are considered fully inside the zones and the heat losses are considered completely injected into that zone. The value considered are presented in Table 4-26.

Table 4-26 Assumed characteristics for the 5 zones floor branches

	Units	Zone 1	Zone 2	Zone 3	Zone 4	Zone 5
Assumed pipe length	[m]	54.5	37.9	54.5	37.9	64.8
Assumed heat transfer coefficient	[W/m.K]	0.32	0.32	0.32	0.32	0.32
<b>Assumed UA-value</b>	<b>[W/K]</b>	<b>17.44</b>	<b>12.13</b>	<b>17.44</b>	<b>12.13</b>	<b>20.74</b>

The pipe section considered is based on a DN25 section and the assume pipe length corresponds to the length and the width of the zone. The heat transfer coefficient is assumed considered 0.7 cm of insulation with  $\lambda=0.04$ .

#### 4.2.3.2. Chilled water network

The primary distribution system is presented in Fig. 4-31. It connects the open header to the boiler on its primary side and to the supply and return hot water collector on its secondary side.

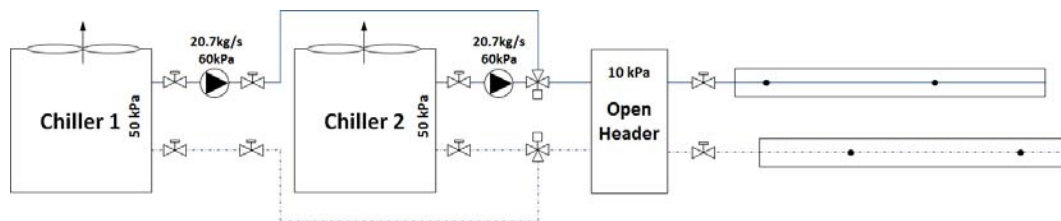


Fig. 4-31 Primary chilled water distribution circuit

Both systems are considered fully inside the technical room which is assumed to be at constant 20°C temperature. The heat is considered completely lost. The value considered are presented in Table 4-27.

Table 4-27 Assumed characteristics for the chilled water collector and the primary distribution circuit heat losses

	Units	Value
Assumed pipe length	[m]	49.9

Assumed heat transfer coefficient	[W/m.K]	0.32
<b>Assumed UA-value</b>	<b>[W/K]</b>	<b>15.97</b>

The pipe section considered is based on a DN150 section and the assume pipe length corresponds to 2 times half the width of the building. The heat transfer coefficient is assumed considered 4.2 cm of insulation with  $\lambda=0.03$  (Bureau for Standardisation, 1992).

The water flow rate in each evaporators is kept constant in the reference case when the chillers are in operation. The associated pumps characteristics are given in Table 4-21 and in Table 4-27.

Table 4-28 Characteristics of the evaporator 1-2 circuit pump

	Units	Value
Nominal pressure drop in the evaporator 1-2 circuit	[kPa]	60
Nominal water flow rate in the evaporator 1-2 circuit	[kg/s]	20.7
Nominal efficiency of the evaporator 1-2 circuit pump	[-]	0.589

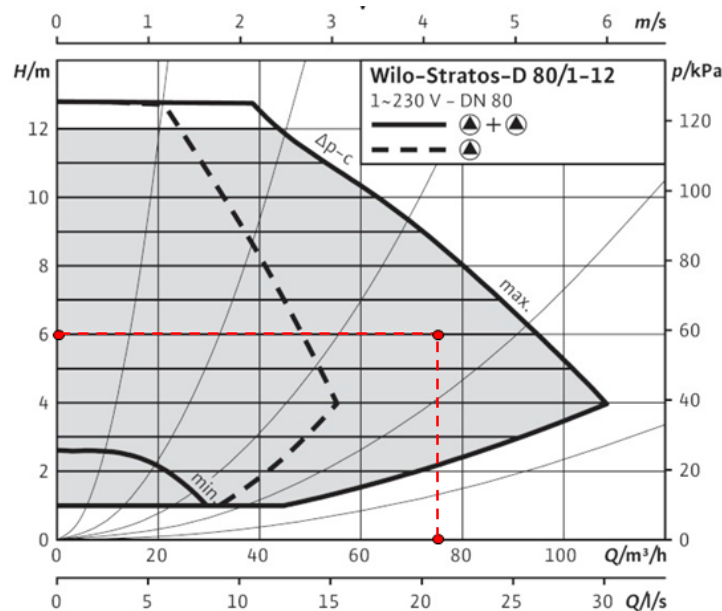


Fig. 4-32 Evaporator 1-2 circuit pump characteristics

The schematic of chilled water collector and its secondary distribution circuit is presented in Fig. 4-33. It can be divided into 4 parts:

- the chilled water collector and the primary distribution circuit connected to the open header and the chillers,
- the distribution to the AHU cooling coil,
- the risers that connects the chilled water collector to the floor branches,
- the floor branches serving the fan coils in each floor.

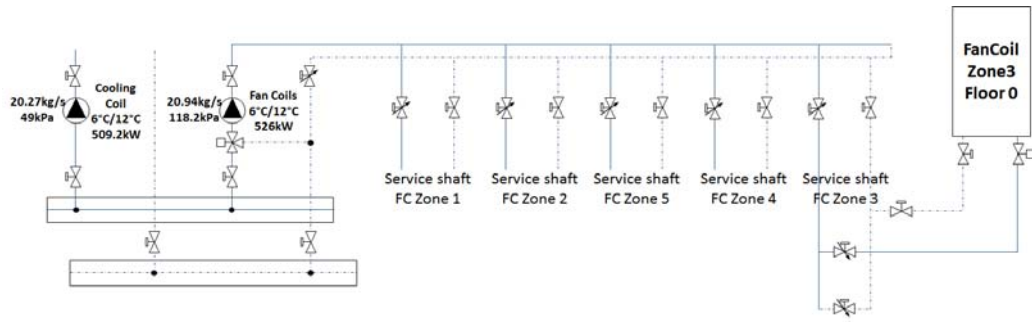


Fig. 4-33 Cold water collector

For the heat losses, the cooling coil circuit is considered wholly inside the technical room, which is assumed to be at a constant temperature of 20°C. The heat is considered completely lost. The values considered are presented in Table 4-29 and Table 4-22.

Table 4-29 Assumed characteristics for the cooling coil distribution heat losses

	Units	Value
Assumed pipe length	[m]	66.6
Assumed heat transfer coefficient	[W/m.K]	0.28
<b>Assumed UA-value</b>	<b>[W/K]</b>	<b>18.65</b>

The pipe section is considered based on a DN80 section and the assumed pipe length corresponds to 4.5 times of the length of the building. The heat transfer coefficient considered is assumed to be 3.8 cm of insulation with  $\lambda=0.03$ .

The characteristics of the cooling coil circuit pump are given in Table 4-30 and in Fig. 4-34.

Table 4-30 Characteristics of the cooling coil circuit pump

	Units	Value
Nominal pressure drop in the cooling coil circuit	[kPa]	49
Nominal water flow rate in the cooling coil circuit	[kg/s]	20.27
Nominal efficiency of the cooling coil circuit pump	[-]	0.571

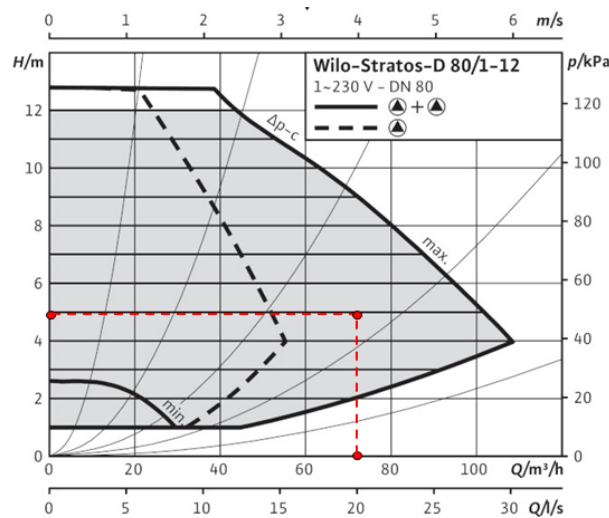


Fig. 4-34 Characteristics of the cooling coil circuit pump

For the cooling coil, the water flow rate is controlled based on the set value of exhaust air temperature.

All the chilled water risers are considered wholly inside the technical vein, which is assumed to be at a constant temperature of 20°C. The heat is considered completely lost. The values considered are presented in Table 4-31.

The pipe section is considered based on a DN80 section and the assumed pipe length corresponds to:

$$l_{\text{pipe,riser}} = 2 * 5 * \left( \frac{l}{4} + \frac{W}{4} + h \right) = 604 \text{ m}$$

The heat transfer coefficient considered is assumed to be 3.8 cm of insulation with  $\lambda=0.03$ .

Table 4-31 Assumed characteristics for heat losses of the chilled water risers

	Units	Value
Assumed pipe length	[m]	604
Assumed heat transfer coefficient	[W/m.K]	0.28
<b>Assumed UA-value</b>	<b>[W/K]</b>	<b>169.12</b>

The characteristics of circuit pumps of the cooling terminal unit are given in Table 4-32 and in Fig. 4-35 Characteristics of the circuit pump of the cooling terminal unit .

Table 4-32 Characteristics of the circuit pump of the cooling terminal unit

	Units	Value
Nominal pressure drop in the cooling terminal unit circuit	[kPa]	118.2
Nominal water flow rate in the cooling terminal unit circuit	[kg/s]	20.94
Nominal efficiency of the cooling terminal unit circuit pump	[-]	0.749

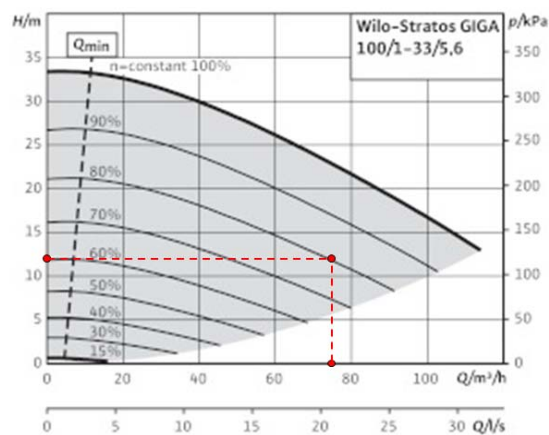


Fig. 4-35 Characteristics of the circuit pump of the cooling terminal unit

The floor branches are considered wholly inside the zones and the heat is considered to be completely injected into that zone. The values considered are presented in Table 4-33.

Table 4-33 Assumed characteristics for the 5 zones floor branches

	Units	Zone 1	Zone 2	Zone 3	Zone 4	Zone 5
Assumed pipe length	[m]	54.5	37.9	54.5	37.9	64.8
Assumed heat transfer coefficient	[W/m.K]	0.21	0.21	0.21	0.21	0.21
<b>Assumed UA-value</b>	<b>[W/K]</b>	<b>11.44</b>	<b>7.96</b>	<b>11.44</b>	<b>7.96</b>	<b>13.61</b>

The pipe section considered is based on a DN32 section and the assumed pipe length corresponds to the length and the width of the zone. The heat transfer coefficient considered is assumed having an insulation of 2.8 cm with  $\lambda=0.03$  (NBN D 30-041).

#### 4.2.4. Production

##### 4.2.4.1. Boiler

In the reference case, the hot water producer is a condensing boiler. In the simulation, the outside air temperature and humidity was set to  $-10^{\circ}\text{C}$  and 95%RH, respectively, and the nominal load in each zone and the recovery device were deactivated, under those conditions, the nominal power of the boiler was approximately equal to 980 kW ( $70^{\circ}\text{C}/50^{\circ}\text{C}$  – 11.7 kg/s water flow rate). The pressure drop associated to the boiler was 30 kPa and 10 kPa for the open header.

##### 4.2.4.2. Chiller

In the reference case, two air-cooled chillers were used as chilled water producers. In the simulation, the outside air temperature and humidity was set to  $30^{\circ}\text{C}$  and 70%RH, respectively, and the nominal load in each zone and the recovery device were deactivated, under those conditions, the nominal power of the boiler was approximately equal to 520kW ( $6^{\circ}\text{C}/12^{\circ}\text{C}$  – 20.7kg/s water flow rate). The pressure drop associated to the boiler was 50 kPa and 10 kPa for the open header.

#### 4.3. Performance assessment of the HVAC systems under typical conditions

This section presents a first assessment of the HVAC systems. This evaluation focuses on the impact on performance when increasing the cold water temperature level and lowering the hot water temperature level. To do so, it is essential to better understand the trade-off between energy use of the transportation system and performance of the primary systems. A steady state approach is used to study the total HVAC system by looking at different operation point of the system. This approach gives information on the actual operation system under both design conditions and off-design conditions.

### 4.3.1. Winter design conditions: impact of the chilled water temperature

The winter design conditions are defined in previous sections. The main simulation outputs of the model as defined in the reference case and in 70°C/50°C operation regime are presented in Table 4-34.

Table 4-34 Main simulation outputs of the model as defined in the reference case and in 70°C/50°C operation regime

Description		Units	Value	
Heating demand	Preheating coil	[kWh <sub>therm</sub> ]	186.73	
	Post heating coil		47.03	
	TU heating coils		277.62	
Cooling demand	Cooling coil		0.00	
	TU cooling coils		0.00	
	Evaporators		0.00	
Electricity consumption for HVAC	Preheating coil circuit pump		[kWh <sub>elec</sub> ]	0.12
	Cooling coil circuit pump			0.00
	Post heating coil circuit pump			0.56
	AHU fans	16.17		
	TU heating circuit pumps	0.34		
	TU cooling circuit pumps	0.00		
	TU fans	6.86		
	Boiler circuit pump	0.83		
	Evaporators circuit pumps	0.00		
Chillers	0.00			
Efficiency	Boiler efficiency	[%]	86.75%	
	Chiller 1 Energy Efficiency Ratio	[-]	-	
	Chiller 2 Energy Efficiency Ratio	[-]	-	
Gas consumption	Boiler	[kWh <sub>GAS,HHV</sub> ]	588.92	
Total	Electricity consumption for HVAC	[kWh <sub>elec</sub> ]	24.88	
	Primary energy consumption for HVAC	[kWh <sub>PE</sub> ]	651.12	

*One can observe that, under these conditions, boiler gas consumption is the main source of energy consumption. In order to improve the overall performance of the system, the boiler efficiency should be increase as much as possible. In section 2, the influence of the temperature at the exhaust and the return of the boiler, as well as the impact of the water flow rate, is presented. This analysis can now be extended to the entire system.*

Table 4-35 The impact of the temperature of the exhaust water boiler on the total system performance is presented in Table 4-35.

From these simulation results, the influence of the open header can be observed at high boiler return water temperature. For example, the mixing effect at the open header can be observed at a boiler exhaust water temperature of 90°C in Fig. 4-36.

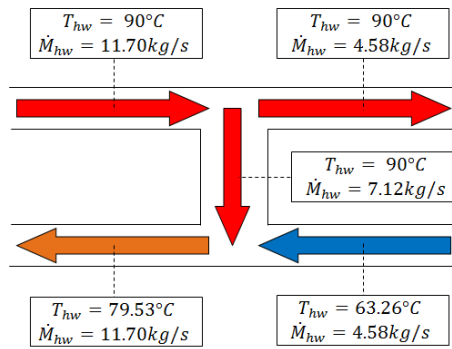


Fig. 4-36 Mixing effect in the hot water circuit open header

Table 4-35 Sensitivity of the performance of the overall system to the exhaust water temperature of the boiler

Boiler exhaust water T	Boiler return water T	Boiler efficiency	Gas consumption	Electricity consumption	Primary energy consumption	Primary energy improvement
°C	[°C]	[%]	[kWh <sub>GAS,HHV</sub> ]	[kWh <sub>elec</sub> ]	[kWh <sub>PE</sub> ]	%
90	79.5	85.24%	602.044	24.255	662.682	-1.98%
85	74.5	85.70%	598.350	24.275	659.038	-1.42%
80	69.6	86.14%	594.689	24.299	655.437	-0.86%
75	64.6	86.46%	591.776	24.329	652.599	-0.43%
70	59.6	86.75%	588.922	24.365	649.835	0.00%
65	54.6	87.01%	586.129	24.412	647.159	0.41%
60	49.6	90.07%	564.935	24.475	626.123	3.65%
55	44.7	92.20%	550.280	24.562	611.685	5.87%
50	39.7	94.29%	536.164	24.691	597.892	7.99%

\*Primary Energy factor:  $f_{PE,gas}=1$  and  $f_{PE,elec}=2.5$

The boiler return water temperature is increased because of the mixing inside the open header. This effect is due to the constant flow rate considered for the boiler circuit pump, leading to a lower boiler efficiency. Removing the constant speed pump and the open header can give a significant improvement to the total system efficiency, as presented in Table 4-36.

Table 4-36 Sensitivity of the overall system performance to the boiler exhaust water temperature when the open header and considering variable speed pump in the primary hot water circuit are removed

Boiler exhaust water T	Boiler return water T	Boiler efficiency	Gas consumption	Electricity consumption	Primary energy consumption	Primary energy improvement
[°C]	[°C]	[%]	[kWh <sub>GAS,HHV</sub> ]	[kWh <sub>elec</sub> ]	[kWh <sub>PE</sub> ]	%
90	63.3	86.54%	592.996	23.773	652.429	-0.40%
85	60.0	86.75%	591.062	23.806	650.577	-0.11%

<b>80</b>	56.9	86.75%	590.462	23.847	650.080	-0.04%
<b>75</b>	53.9	87.32%	585.863	23.900	645.613	0.65%
<b>70</b>	51.2	88.85%	574.996	23.971	634.924	2.29%
<b>65</b>	47.4	90.53%	563.273	24.043	623.381	4.07%
<b>60</b>	43.4	92.19%	551.903	24.128	612.223	5.79%
<b>55</b>	39.5	93.87%	540.448	24.245	601.061	7.51%
<b>50</b>	35.6	95.31%	530.371	24.414	591.406	8.99%

#### 4.3.2. Summer design conditions: impact of the chilled water temperature

The performances of the system designed for summer design conditions in the reference case in 6°C/12°C operation regime are presented in Table 4-37. Under these conditions, the chiller is the main energy consumer of the HVAC system, accounting for 85% of the total energy consumption.

To improve the efficiency of the total system, performance of the chiller is the most significant factor. As studied in the section 2, the performance of the air cooled chiller considered is mainly sensitive to the exhaust water temperature of the evaporator. The benefits of the higher chilled water temperature on the total system performance is presented in

Table 4-38.

Also, as for the hot water circuit, the open header in the primary chilled water circuit can be removed from the circuit and variable speed pump introduced for the evaporators pumps. Results of this change are presented in Table 4-39, showing less impact than that in the hot water circuit. This is mainly due to the low sensitivity of the air cooled chiller to the return water temperature of the evaporator.

*Table 4-37 Main simulation output of the model as defined in the reference case within 6°C/12°C operation regime*

Description		Units	Value	
Heating demand	Preheating coil	[kWh <sub>therm</sub> ]	0.00	
	Post heating coil		0.00	
	TU heating coils		0.00	
Cooling demand	Cooling coil		214.82	
	TU cooling coils		425.55	
	Evaporators		642.43	
Electricity consumption for HVAC	Preheating coil circuit pump		[kWh <sub>elec</sub> ]	0.00
	Cooling coil circuit pump			0.49
	Post heating coil circuit pump			0.00
	AHU fans	16.17		
	TU heating circuit pumps	0.00		

	TU cooling circuit pumps		2.59
	TU fans		6.86
	Boiler circuit pump		0.00
	Evaporators circuit pumps		4.51
	Chillers		173.39
Efficiency	Boiler efficiency	[%]	86.30%
	Chiller 1 Energy Efficiency Ratio	[-]	3.69
	Chiller 2 Energy Efficiency Ratio	[-]	3.69
Gas consumption	Boiler	[kWh <sub>GAS,HHV</sub> ]	0.00
Total	Electricity consumption for HVAC	[kWh <sub>elec</sub> ]	203.99
	Primary energy consumption for HVAC	[kWh <sub>PE</sub> ]	509.98

Table 4-38 Sensitivity of the performance of the overall system to the exhaust water temperature of the evaporator

Evaporator exhaust water T	Evaporator return water T	EER <sub>avg</sub>	Chiller consumption	Electricity consumption	Primary energy consumption	Primary energy improvement
°C	°C	[-]	[kWh <sub>elec</sub> ]	[kWh <sub>elec</sub> ]	[kWh <sub>PE</sub> ]	%
5	8.7	3.35	178.060	208.536	521.340	-2.23%
6	9.7	3.42	173.388	203.992	509.980	0.00%
7	10.7	3.49	168.874	199.626	499.065	2.14%
8	11.7	3.57	164.500	195.421	488.553	4.20%
9	12.7	3.64	160.264	191.382	478.455	6.18%
10	13.7	3.72	156.164	187.519	468.798	8.08%
11	14.7	3.79	151.486	183.111	457.778	10.24%
12	15.6	3.87	145.826	177.819	444.548	12.83%

Table 4-39 Sensitivity of the performance of the overall system to the exhaust water temperature of the evaporator when the open header and considering variable speed pump in the primary chilled water circuit are removed

Evaporator exhaust water T	Evaporator return water T	EER <sub>avg</sub>	Chiller consumption	Electricity consumption	Primary energy consumption	Primary energy improvement
°C	°C	[-]	[kWh <sub>elec</sub> ]	[kWh <sub>elec</sub> ]	[kWh <sub>PE</sub> ]	%
5	12.6	3.61	177.044	205.005	512.513	-2.14%
6	13.2	3.71	172.496	200.718	501.795	0.00%
7	13.7	3.80	168.096	196.629	491.573	2.04%
8	14.3	3.90	163.842	192.750	481.875	3.97%
9	14.8	4.00	159.728	189.102	472.755	5.79%
10	15.3	4.10	155.748	185.697	464.243	7.48%
11	15.8	4.20	151.196	181.691	454.228	9.48%

12	16.3	4.30	145.668	176.918	442.295	11.86%
----	------	------	---------	---------	---------	--------

In the summer design conditions, the building is considered to be at full occupancy. It is then important to keep tracking the comfort of the occupants in each case studied. To maintain similar comfort conditions in different building zones, the Predicted Percentage of Dissatisfied (PPD) variable during occupancy hours in each zone can be evaluated. In this case, the air temperature in the zone is taken into account to evaluate a simplified PPD index, with a constant PPD equal to 5% when the indoor temperature is beneath the heating and cooling temperature set point of [21°C;25°C], and progressively increasing when going outside of this range. The considered laws are presented in Fig. 4-37 and Fig. 4-38.

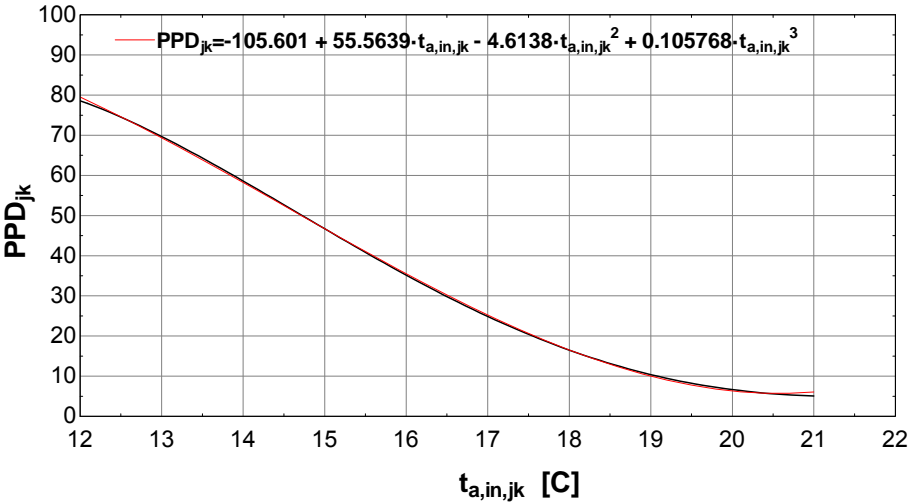


Fig. 4-37 Evolution of the PPD in the zone when the indoor temperature is below the heating set point

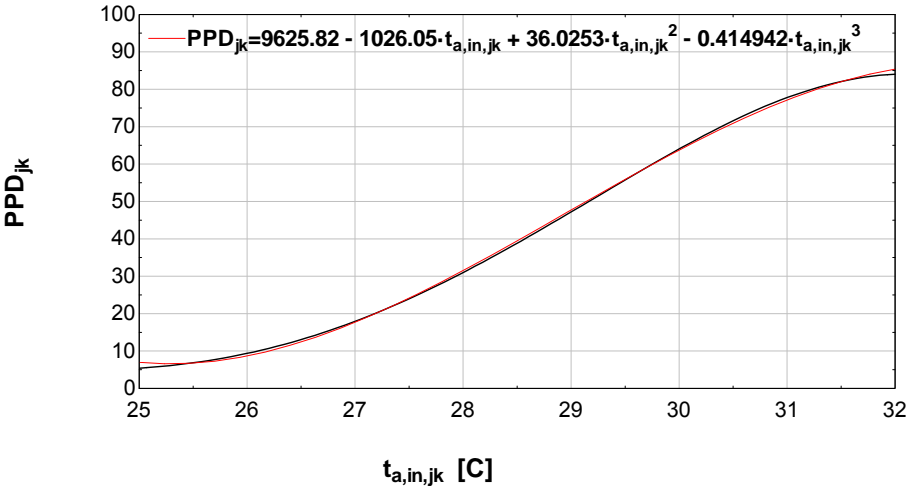


Fig. 4-38 Evolution of the PPD in the zone when the indoor temperature is above the cooling set point

In Table 4-40, it can be observed that the PPD increases quite significantly in each zone when increasing the chilled water temperature to 11°C or 12°C. To overcome this increase,

the terminal units cooling coils must be slightly oversized to keep the same level of comfort. The simulations are performed for fan coils units' power increased of respectively 10% and 25% for the 11°C and 12°C evaporator exhaust water temperature simulation (

Table 4-41 and

Table 4-42). This leads to a lower performance improvement under these conditions.

*Table 4-40 Evolution of the PPD of the 5 zones when the exhaust water temperature of the evaporator is changed, and the open header and considering variable speed pump in the primary chilled water circuit are removed*

Evaporator exhaust water T	Oversizing factor	PPD Zone 1	PPD Zone 2	PPD Zone 3	PPD Zone 4	PPD Zone 5
°C	-	%	%	%	%	%
5	1	7.51	7.36	7.51	7.36	7.17
6	1	7.66	7.49	7.66	7.49	7.27
7	1	7.83	7.64	7.83	7.64	7.38
8	1	8.03	7.82	8.03	7.82	7.52
9	1	8.26	8.03	8.26	8.03	7.68
10	1	8.54	8.28	8.54	8.28	7.87
11	1	9.85	8.61	9.85	8.61	8.17
12	1	12.87	10.84	12.87	10.84	8.84

*Table 4-41 Sensitivity of the performance of the overall system to the exhaust water temperature of the evaporator when oversizing the terminal unit to maintain similar PPD*

Evaporator exhaust water T	Evaporator return water T	EER <sub>avg</sub>	Chiller consumption	Electricity consumption	Primary energy consumption	Primary energy improvement
°C	°C	[-]	[kWh <sub>elec</sub> ]	[kWh <sub>elec</sub> ]	[kWh <sub>PE</sub> ]	%
5	12.6	3.61	177.046	205.007	512.518	-2.14%
6	13.2	3.71	172.494	200.716	501.790	0.00%
7	13.7	3.80	168.096	196.629	491.573	2.04%
8	14.3	3.90	163.842	192.750	481.875	3.97%
9	14.8	4.00	159.728	189.102	472.755	5.79%
10	15.3	4.10	155.748	185.697	464.243	7.48%
11	15.8	4.19	152.508	183.831	459.578	8.41%
12	16.2	4.29	149.624	183.043	457.608	8.81%

*Table 4-42 Evolution of the PPD of the 5 zones when changing the exhaust water temperature the evaporator, and removing the open header and considering variable speed pump in the primary chilled water circuit when oversizing the terminal unit*

Evaporator exhaust water T	Oversizing factor	PPD Zone 1	PPD Zone 2	PPD Zone 3	PPD Zone 4	PPD Zone 5
°C	-	%	%	%	%	%
5	1	7.51	7.36	7.51	7.36	7.17
6	1	7.66	7.49	7.66	7.49	7.27
7	1	7.83	7.64	7.83	7.64	7.38
8	1	8.03	7.82	8.03	7.82	7.52
9	1	8.26	8.03	8.26	8.03	7.68
10	1	8.54	8.28	8.54	8.28	7.87
11	1.1	8.40	8.16	8.40	8.16	7.78
12	1.25	8.16	7.94	8.16	7.94	7.62

#### 4.3.3. Off-design conditions: Impact of hot and chilled water temperature

In the winter and summer design conditions, the analysis was made for the system running in design or high load conditions. It can be interesting to extend the analysis to other conditions where the system is running in partial load conditions and eventually with simultaneous cooling and heating loads. The reference system is here directly considered without open header in both hot and chilled water circuits.

The selected conditions are defined in Table 4-43.

*Table 4-43 Selected off-design conditions*

ID	Outside Temp	Outside RH	I <sub>sun,vert</sub>	f <sub>appliances</sub>	f <sub>occupancy</sub>	f <sub>light</sub>	f <sub>ventilation</sub>	f <sub>TU</sub>
[-]	°C	%	W/m <sup>2</sup>	[-]	[-]	[-]	[-]	[-]
1	0	80	50	0.5	0.5	0.5	1	1
2	15	70	150	1	1	1	1	1
3	20	60	200	1	1	1	1	1
4	8	60	100	0.75	0.75	0.75	1	1

- Off-design condition 1: Heating load operation and no cooling

In the off-design condition 1, the actual heat demand is approximately 35% of the heat demand in winter design conditions while no cooling is needed.

Table 4-44 Summary of system loads and energy consumption in off-design condition 1 and in 6°C/12°C & 70°C/50°C operation regime

Description		Units	Off-design Condition 1	Winter Design
Heating demand	Preheating coil	[kWh <sub>therm</sub> ]	<b>109.08</b>	186.73
	Post heating coil		<b>47.03</b>	47.03
	TU heating coils		<b>40.28</b>	277.62
Cooling demand	Cooling coil		<b>0.00</b>	0.00
	TU cooling coils		<b>0.00</b>	0.00
	Evaporators		<b>0.00</b>	0.00
Electricity consumption for HVAC	Preheating coil circuit pump	[kWh <sub>elec</sub> ]	<b>0.12</b>	0.12
	Cooling coil circuit pump		<b>0.00</b>	0.00
	Post heating coil circuit pump		<b>0.06</b>	0.06
	AHU fans		<b>16.17</b>	16.17
	TU heating circuit pumps		<b>0.04</b>	0.33
	TU cooling circuit pumps		<b>0.00</b>	0.00
	TU fans		<b>6.86</b>	6.86
	Boiler circuit pump		<b>0.27</b>	0.83
	Evaporators circuit pumps		<b>0.00</b>	0.00
	Chillers		<b>0.00</b>	0.00
Efficiency	Boiler efficiency	[%]	<b>90.52%</b>	86.75%
	Chiller 1 Energy Efficiency Ratio	[-]	-	-
	Chiller 2 Energy Efficiency Ratio	[-]	-	-
Gas consumption	Boiler	[kWh <sub>GAS,HHV</sub> ]	<b>216.70</b>	588.92
Total	Electricity consumption for HVAC	[kWh <sub>elec</sub> ]	<b>23.51</b>	24.37
	Primary energy consumption for HVAC	[kWh <sub>PE</sub> ]	<b>275.46</b>	649.83

The first visible effect is the improvement in the boiler efficiency at a lower heating load. It is important to notice that this improvement is induced by the lower water flow rate in the boiler and reinforced by the lower pump consumption. This is made possible by the use of variable speed pump in the boiler water circuit, and thus the absence of open header in the hot water circuit. Table 4-45 presents the important impact of the presence of the open header on the boiler and the overall system performance in lower heating load operation.

Table 4-45 Impact of the open header on performance of the overall system

	Unit	Winter design with open header	Winter design without open header	Off-design condition 1 with open header	Off-design condition 1 without open header
<b>Boiler exhaust water T</b>	°C	70.0	70.0	70.0	70.0
<b>Boiler return water T</b>	°C	59.6	51.2	66.0	49.9
<b>Boiler Water Flow Rate</b>	kg/s	11.70	6.48	11.70	2.34
<b>Boiler efficiency</b>	%	86.75	88.85	86.58	90.52
<b>Gas consumption</b>	[kWh <sub>GAS,HHV</sub> ]	588.92	575.00	226.60	216.70
<b>Electricity consumption</b>	[kWh <sub>elec</sub> ]	24.37	23.97	24.07	23.51
<b>Primary energy consumption</b>	[kWh <sub>PE</sub> ]	649.83	634.92	286.77	275.46
<b>Primary energy improvement</b>	%	0.00%	2.29%	0.00%	3.94%

In Table 4-46, the influence of the exhaust water temperature of the boiler on the performance of the overall system can be observed, but smaller than that for the winter design operation. It is due to the proportion of the HVAC auxiliaries that have a relatively larger impact on energy consumption of the system.

Table 4-46 Sensitivity to the exhaust temperature of the evaporator in off-design condition 1

Evaporator exhaust water T	Boiler exhaust water T	Gas consumption	Chiller consumption	Electricity consumption	Primary energy consumption	Primary energy improvement
°C	°C	[kWh <sub>GAS,HHV</sub> ]	[kWh <sub>elec</sub> ]	[kWh <sub>elec</sub> ]	[kWh <sub>PE</sub> ]	%
<b>6</b>	<b>80</b>	225.62	0.00	23.494	284.353	-3.23%
<b>6</b>	<b>75</b>	223.41	0.00	23.500	282.164	-2.43%
<b>6</b>	<b>70</b>	216.70	0.00	23.506	275.464	0.00%
<b>6</b>	<b>65</b>	213.39	0.00	23.515	272.180	1.19%
<b>6</b>	<b>60</b>	210.36	0.00	23.526	269.177	2.28%
<b>6</b>	<b>55</b>	207.35	0.00	23.543	266.212	3.36%
<b>6</b>	<b>50</b>	204.19	0.00	23.570	263.110	4.48%

- Off-design conditions 2 and 3: Cooling load operation and no heating

The two conditions considered here present a lower cooling load than in the summer design conditions (approximately 40% and 50% for conditions 2 and 3, respectively). The influence of the partial load of the chiller is quite clear, with the chiller EER raising to 5.21 and 4.67 compared with the 3.69 in design conditions. Working with variable speed pump in both conditions allows a better performance of the system with lower pumping consumption.

Table 4-47 Summary of the system loads and energy consumption in off-design conditions 2/3 and in 6°C/12°C & 70°C/50°C operation regime

Description		Units	Off-design Condit. 2	Off-design Condit. 3	Winter Design	
Heating demand	Preheating coil	[kWh <sub>therm</sub> ]	0.00	0.00	0.00	
	Post heating coil		0.00	0.00	0.00	
	TU heating coils		0.00	0.00	0.00	
Cooling demand	Cooling coil		0.00	97.87	214.82	
	TU cooling coils		253.85	212.96	425.55	
	Evaporators		255.57	312.77	642.43	
Electricity consumption for HVAC	Preheating coil circuit pump		[kWh <sub>elec</sub> ]	0.00	0.00	0.00
	Cooling coil circuit pump			0.00	0.39	0.49
	Post heating coil circuit pump			0.00	0.00	0.00
	AHU fans	16.17		16.17	16.17	
	TU heating circuit pumps	0.00		0.00	0.00	
	TU cooling circuit pumps	1.73		1.57	2.59	
	TU fans	6.86		6.86	6.86	
	Boiler circuit pump	0.00		0.00	0.00	
	Evaporators circuit pumps	0.97		1.07	4.51	
Chillers	48.50	66.70	173.39			
Efficiency	Boiler efficiency	[%]	-	-	-	
	Chiller 1 Energy Efficiency Ratio	[-]	5.21	4.67	3.69	
	Chiller 2 Energy Efficiency Ratio	[-]	-	-	3.69	
Gas consumption	Boiler	[kWh <sub>GAS,HHV</sub> ]	0.00	0.00	0.00	
Total	Electricity consumption for HVAC	[kWh <sub>elec</sub> ]	74.22	92.75	203.99	
	Primary energy consumption for HVAC	[kWh <sub>PE</sub> ]	185.55	231.87	509.98	

The influence of the exhaust water temperature of the evaporator on performance of the overall system is as important as it is under the summer design conditions. Under the off-design conditions, the cooling is only working for the sensible load of the terminal units. The water temperature could then be, in principle, higher. However, when doing so, the PPD in some of the zones is increasing. To allow a higher chilled water temperature, the terminal units should be sized differently (oversized). The effect and optimization of the oversizing will be investigated on the full year simulation.

Table 4-48 Sensitivity to the exhaust temperature of the evaporator in off-design condition 2

Evaporator exhaust water T	Boiler exhaust water T	Gas consumption	Chiller consumption	Electricity consumption	Primary energy consumption	Primary energy improvement
°C	°C	[kWh <sub>GAS,HHV</sub> ]	[kWh <sub>elec</sub> ]	[kWh <sub>elec</sub> ]	[kWh <sub>PE</sub> ]	%

		l				
5	70	0.00	49.71	75.336	188.340	-1.51%
6	70	0.00	48.50	74.219	185.548	0.00%
7	70	0.00	47.32	73.147	182.868	1.44%
8	70	0.00	46.17	72.122	180.305	2.83%
9	70	0.00	45.05	71.146	177.865	4.14%
10	70	0.00	43.95	70.214	175.535	5.40%
11	70	0.00	42.68	69.129	172.823	6.86%
12	70	0.00	41.29	67.979	169.948	8.41%

Table 4-49 – Sensitivity to the exhaust temperature of the evaporator in off-design condition 3

Evaporator exhaust water T	Boiler exhaust water T	Gas consumption	Chiller consumption	Electricity consumption	Primary energy consumption	Primary energy improvement
°C	°C	[kWh <sub>GAS,HHV</sub> ]	[kWh <sub>elec</sub> ]	[kWh <sub>elec</sub> ]	[kWh <sub>PE</sub> ]	%
5	70	0.00	68.42	94.348	235.870	-1.73%
6	70	0.00	66.70	92.748	231.870	0.00%
7	70	0.00	65.04	91.222	228.055	1.65%
8	70	0.00	63.43	89.775	224.438	3.21%
9	70	0.00	61.87	88.418	221.045	4.67%
10	70	0.00	60.35	87.150	217.875	6.04%
11	70	0.00	58.88	85.936	214.840	7.34%
12	70	0.00	57.45	84.887	212.218	8.48%

- Off-design condition 4: Simultaneous cooling and heating load operation

The observation made previously for only heating or cooling load operation, can be extended to the simultaneous cooling and heating load operation. The influence on the reference system of such operation point are presented first under nominal conditions specified in Table 4-50. The impact of the higher evaporator exhaust water temperature and lower boiler exhaust water temperature can be combined to improve the overall system performance as presented in Table 4-51.

Table 4-50 Summary of the system loads and energy consumption under off-design condition 4 and in 6°C/12°C & 70°C/50°C operation regime

Description		Units	Value
Heating demand	Preheating coil	[kWh <sub>therm</sub> ]	19.95
	Post heating coil		47.03
	TU heating coils		0.00
Cooling demand	Cooling coil		0.00

	TU cooling coils		98.10
	Evaporators		99.28
Electricity consumption for HVAC	Preheating coil circuit pump	[kWh <sub>elec</sub> ]	0.12
	Cooling coil circuit pump		0.00
	Post heating coil circuit pump		0.06
	AHU fans		16.17
	TU heating circuit pumps		0.00
	TU cooling circuit pumps		1.18
	TU fans		6.86
	Boiler circuit pump		0.24
	Evaporators circuit pumps		0.53
	Chillers		19.46
	Efficiency		Boiler efficiency
Chiller 1 Energy Efficiency Ratio		[-]	5.03
Chiller 2 Energy Efficiency Ratio		[-]	-
Gas consumption	Boiler	[kWh <sub>GAS,HHV</sub> ]	76.78
Total	Electricity consumption for HVAC	[kWh <sub>elec</sub> ]	44.60
	Primary energy consumption for HVAC	[kWh <sub>PE</sub> ]	188.28

Table 4-51 Sensitivity to exhaust temperature of the evaporator under off-design condition 4

Evaporator exhaust water T	Boiler exhaust water T	Gas consumption	Chiller consumption	Electricity consumption	Primary energy consumption	Primary energy improvement
°C	°C	[kWh <sub>GAS,HHV</sub> ]	[kWh <sub>elec</sub> ]	[kWh <sub>elec</sub> ]	[kWh <sub>PE</sub> ]	%
6	80	77.19	19.45	44.600	188.688	-0.17%
6	75	76.87	19.45	44.601	188.373	0.00%
6	70	76.78	19.45	44.601	188.279	0.05%
6	65	74.59	19.45	44.593	186.072	1.22%
6	60	72.80	19.44	44.581	184.256	2.19%
6	55	71.34	19.43	44.569	182.767	2.98%
6	50	70.08	19.42	44.554	181.463	3.67%
8	80	76.96	18.59	43.792	186.435	1.03%
8	75	76.64	18.60	43.793	186.121	1.20%
8	70	76.54	18.60	43.792	186.022	1.25%
8	65	74.38	18.59	43.784	183.837	2.41%
8	60	72.59	18.58	43.773	182.022	3.37%
8	55	71.13	18.57	43.761	180.536	4.16%
8	50	69.87	18.56	43.747	179.238	4.85%
10	80	76.68	17.71	42.976	184.115	2.26%
10	75	76.36	17.71	42.976	183.799	2.43%
10	70	76.26	17.72	42.976	183.701	2.48%
10	65	74.12	17.71	42.968	181.542	3.63%
10	60	72.33	17.70	42.956	179.721	4.59%
10	55	70.88	17.69	42.945	178.242	5.38%
10	50	69.62	17.68	42.931	176.947	6.07%
12	80	76.33	16.60	41.944	181.190	3.81%
12	75	76.02	16.60	41.944	180.875	3.98%
12	70	75.92	16.60	41.943	180.774	4.03%
12	65	73.81	16.59	41.935	178.647	5.16%
12	60	72.02	16.58	41.923	176.823	6.13%
12	55	70.57	16.58	41.912	175.348	6.91%
12	50	69.31	16.57	41.899	174.059	7.60%

#### 4.4. Investigation on performance of the total system

##### 4.4.1. Analysis of the equivalent thermal resistance of heating systems

Blending of heat and cooling fluid, especially in the open header, three-way valves and the post-heating in the AHU, causes a decrease in the thermal efficiency of the condensing boiler. On the basis of entransy dissipation, an equivalent thermal resistance ( $R_H$ ) between

temperature of hot water supplied from the boiler and the indoor environment is proposed to evaluate the temperature level loss from plant to terminals. The original heating system is depicted in Fig. 4-39. It could be found that the constant supply water temperature in the primary network and the constant flow rate in the secondary circuit, the blending in the open header, the three-way valve in the terminal unit all contribute to the increase of the return water temperature, resulting in decrease in thermal efficiency of the condensing boiler. Fig. 4-40 illustrates the fresh air handling process in the psychrometric chart. The outdoor fresh air is preheated first and then humidified adiabatically with a spray chamber, and finally postheated. The postheating process wastes a large amount of energy.

*Fig. 4-39 Schematic of the original heating system*

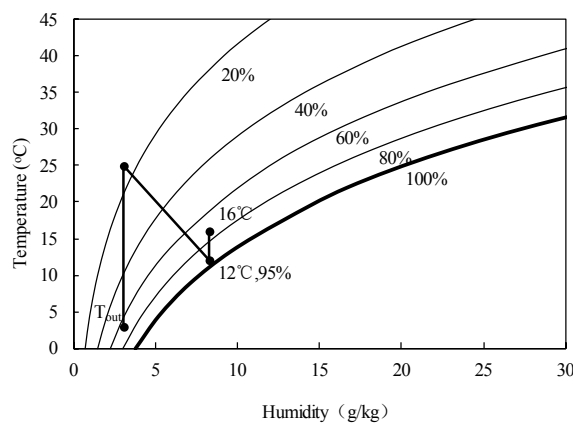


*Fig. 4-40 Fresh air handling process in psychrometric chart*

Based on the disadvantages of the original heating system described above, improvements of the heating system configuration were made step by step. Five systems are denoted as follows. System 1 acting as a reference sample represents the original heating system. Variable flow rate control is applied in the second hot water circuit in System 2 named as Variable speed. In System 3 named as No open header, the open header is canceled

and the variable flow rate control is applied. Compared with System 3, System 4 named as no postheating further cancels the postheating process in the AHU. And in System 5 named as heating curve, except for other improvement described above, a weather compensation based on outdoor temperature is added to control the supply hot water temperature.

Table 4-52 shows the energy consumption and thermal efficiency of boiler of different systems. Compared with the reference system, the System 2 named as variable speed system uses 23% less energy by the pump in the secondary hot water circuits. With the open header canceled, the thermal efficiency of condensing boiler increases from 0.87 to 0.92 due to the decrease of return water temperature. With the postheating canceled, the heat load could be decreased by 20%. Furthermore, with the help of weather compensation control on the supply water temperature, the thermal efficiency increases sharply to 0.93.

Table 4-52 Comparison of energy consumption and efficiency of different systems

Heating season-		Reference building	No open header	No postheating	Heat curve
Q <sub>gas</sub>	MWh	395.5	374.1	334.5	325.7
Q <sub>boiler</sub>	MWh	342.9	344.4	301.3	304.2
$\eta_{boiler}$	-	0.87	0.92	0.90	0.93
Q <sub>preheating</sub>	MWh	268.7	268.7	268.7	268.7
Q <sub>postheating</sub>	MWh	55.4	55.4	0	0
Q <sub>TUheating</sub>	MWh	20.7	20.7	33.0	35.9

From the perspective of the equivalent thermal resistance ( $R_H$ ), it can be found in Fig. 4-41 that the  $R_H$  decreases with rising partial load rate in the four different systems. The size of the boiler and AHU equipment were determined based on design conditions, and the supply hot water temperature is relatively high for a low part load rate. These factors all contribute to a high value of equivalent thermal resistance in part load. The equivalent thermal resistance of the reference heating system is the smallest at different part load, that of System 2 named as no open header comes second, that of the System 4 named as heating curve is the smallest. The larger the equivalent thermal resistance is, the lower the thermal efficiency of the boiler. Thus the variance of the  $R_H$  explains the difference in energy consumption and boiler efficiency.

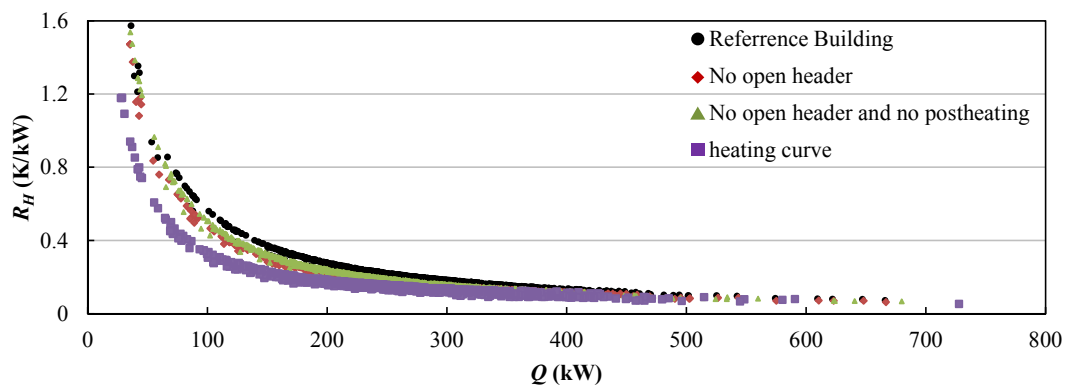


Fig. 4-41 Comparison of equivalent thermal resistances of different systems

In detail, the equivalent thermal resistance from heat plant to indoor environment consists of three parts, including the equivalent thermal resistance of mixing loss (RH\_mix\_sys), equivalent thermal resistance of heat transfer resulting from limited heat exchange area (RH\_UA\_sys), and the equivalent thermal resistance of unmatching loss in the heat transfer processes (RH\_unmatch\_sys). Fig. 4-42 shows the constituents of equivalent thermal resistance of different systems at various outdoor temperatures. In part load, i.e., at a relatively high outdoor temperature, the contribution of RH\_unmatch\_sys to the whole thermal resistance could be ignored, while the RH\_mix\_sys, which plays a crucial role on the whole resistance, varies a lot among different systems. Minimizing the thermal resistance of mixing loss significantly decreases the energy use and increases the thermal efficiency of the condensing boiler.

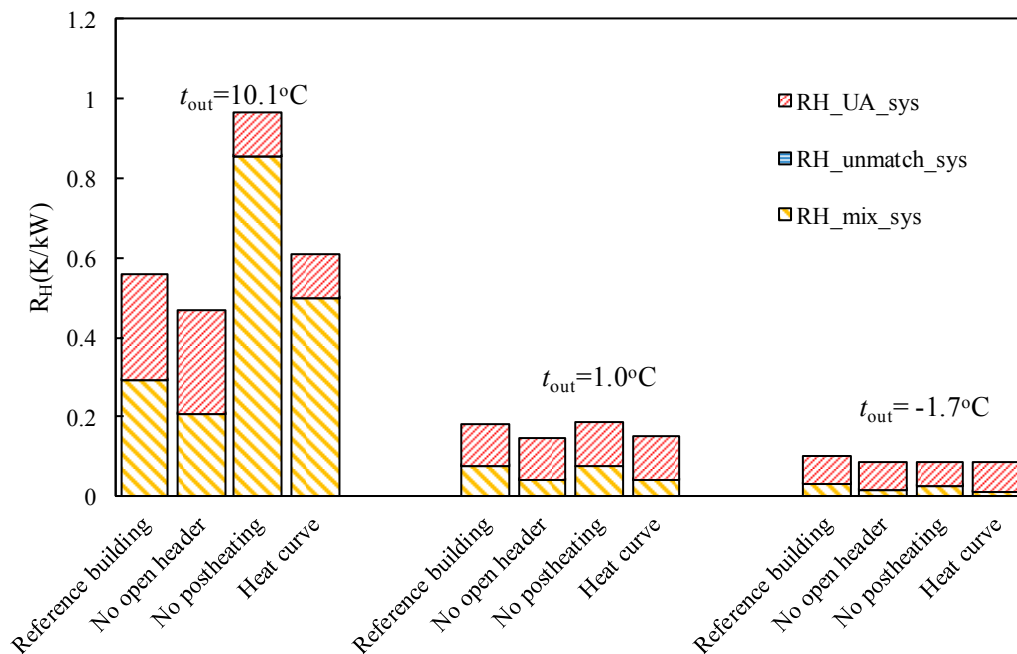


Fig. 4-42 Constituent parts of equivalent thermal resistance in different systems

Table 4-53 illustrates the energy consumption of different systems at typical outdoor temperatures in detail. With the open header and the three-way valve being canceled and weather compensation control, the System 5 named as heat curve achieves energy saving and lowering the temperature level of the heat source under different part load rate. In addition, the energy saving rate of System 5 increases with the decrease of the part load rate. The consumption of the auxiliaries, in this case tested here, shows no significant influence on the system performance if properly designed and controlled. The use of variable speed pumps allows to draw these conclusions. The impact of non-optimal hydraulic configurations allowing mixing (with open header in our example) and associated constant pumps showed on another side the important losses in system efficiency as well as on electricity consumption.

Table 4-53 Comparison of energy consumption of different systems at typical outdoor temperatures

t_out	10.1°C					1°C					-1.7°C				
	Boiler /kW	$\eta$	Gas /kW	Fans /Kw	Pumps /kW	Boiler /kW	$\eta$	Gas /kW	Fans /Kw	Pumps /kW	Boiler /kW	$\eta$	Gas /kW	Fans /Kw	Pumps /kW
Reference building	101.2	0.86	117.1	40.8	1.55	302.1	0.87	348.3	40.8	1.55	494.0	0.87	569.5	40.8	1.55
No open header	102.4	0.89	114.6	40.8	0.29	303.3	0.93	327.9	40.8	0.30	495.1	0.91	544.4	40.8	0.39
No postheating	55.5	0.87	63.8	40.8	0.25	256.4	0.91	282.8	40.8	0.26	514.1	0.90	571.1	40.8	0.50
Heat curve	55.5	0.93	59.4	40.8	0.25	256.3	0.94	272.9	40.8	0.27	451.4	0.91	494.5	40.8	0.42

#### 4.4.2. Analysis of annual energy consumption of the total system

The performance of the system is evaluated on a full year basis by looking at the impact of the temperatures under various operating conditions. The heating, cooling needs, as well as the energy consumption of the building considering the reference case system (in 6°C/12°C & 70°C/50°C operation regime) are presented in Fig. 4-43, Fig. 4-44 and Table 4-54.

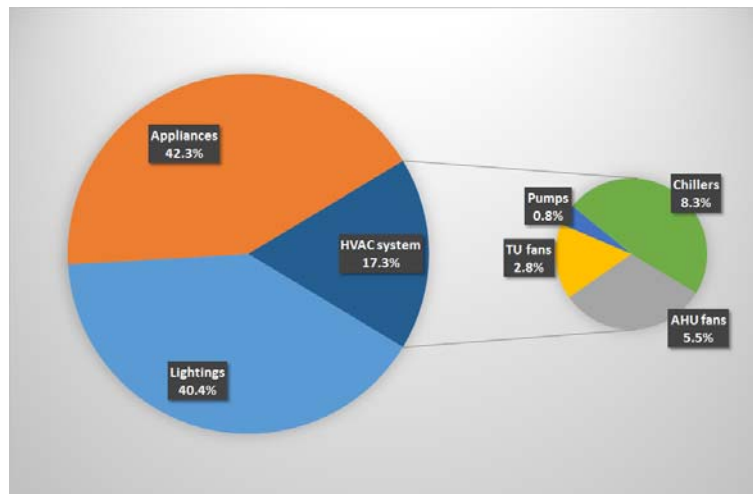


Fig. 4-43 Annual electricity consumption split between main consumers

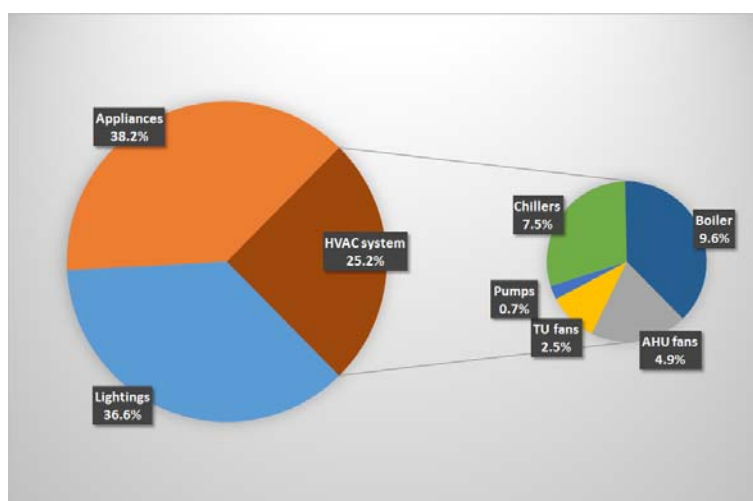


Fig. 4-44 Annual primary energy consumption split between main consumers

Table 4-54 Summary of the system loads and energy consumption

Description		Units	Value
Heating demand	Preheating coil	[MWh <sub>therm</sub> ]	52.33
	Post heating coil	[MWh <sub>therm</sub> ]	60.77
	TU heating coils	[MWh <sub>therm</sub> ]	80.66
Cooling demand	Cooling coil	[MWh <sub>therm</sub> ]	81.15
	TU cooling coils	[MWh <sub>therm</sub> ]	197.05
Electricity consumption	Light	[MWh <sub>elec</sub> ]	341.99
	Appliances	[MWh <sub>elec</sub> ]	357.73
	AHU fans	[MWh <sub>elec</sub> ]	46.23
	TU fans	[MWh <sub>elec</sub> ]	23.67
	Pumps	[MWh <sub>elec</sub> ]	6.56
	Chillers	[MWh <sub>elec</sub> ]	69.81
Gas consumption	Boiler	[MWh <sub>GAS,HHV</sub> ]	223.46
Total	Electricity consumption	[MWh <sub>elec</sub> ]	845.99
	Primary energy consumption	[MWh <sub>PE</sub> ]	2338.43

One can observe the hypothesis related to the appliances and lighting installed power and schedule of operation are giving high electricity consumption (82%) compared to HVAC (only 18%). It has an impact on the indoor terminal unit with much higher cooling loads (197.05 MWh) compared with that with heating loads (80.66 MWh). However, the aim of present analysis is to improve the performance of the overall system almost independently to the type of load profile. In this case, the targeted are than the 18% (corresponding to 854.99 MWh per year) of electricity consumption related to the HVAC.

In Table 4-55 to Table 4-58, the influence of the hot and chilled water temperature set points on annual boiler consumption, electricity consumption and primary energy consumption is presented. The reference case with both open headers is considered in this simulation and both set points are maintained constant.

Table 4-55 Sensitivity of annual electricity consumption of the HVAC system to exhaust temperature of evaporator and exhaust water temperature of boiler

Electricity consumption for HVAC			Evaporator exhaust water temperature			
			[°C]			
			6	8	10	12
Boiler exhaust water temperature	[°C]	80	146.31	143.21	140.35	137.84
		70	146.27	143.18	140.31	137.79
		60	146.27	143.19	140.30	137.81

	50	146.27	143.20	140.30	137.81
--	----	--------	--------	--------	--------

Table 4-58

Table 4-56 Sensitivity of annual boiler consumption to exhaust temperature of evaporator and exhaust water temperature of boiler

Boiler consumption			Evaporator exhaust water temperature			
			[°C]			
			6	8	10	12
Boiler exhaust water temperature	[°C]	80	228.07	228.04	228.00	227.95
		70	223.46	223.43	223.40	223.35
		60	218.19	218.14	218.11	218.07
		50	201.84	201.82	201.79	201.73

Table 4-57 Sensitivity of annual electricity consumption to exhaust temperature of evaporator and exhaust water temperature of boiler

Electricity consumption for HVAC			Evaporator exhaust water temperature			
			[°C]			
			6	8	10	12
Boiler exhaust water temperature	[°C]	80	146.31	143.21	140.35	137.84
		70	146.27	143.18	140.31	137.79
		60	146.27	143.19	140.30	137.81
		50	146.27	143.20	140.30	137.81

Table 4-58 Sensitivity of annual primary energy consumption to exhaust temperature of evaporator and exhaust water temperature of boiler

Primary energy consumption for HVAC			Evaporator exhaust water temperature			
			[°C]			
			6	8	10	12
Boiler exhaust water temperature	[°C]	80	593.83	586.07	578.86	572.54
		70	589.14	581.38	574.18	567.84
		60	583.87	576.12	568.87	562.59
		50	567.52	559.82	552.52	546.26

Table 4-59 Number of hours per year and per zone with a PPD above 10% under the different set point conditions considered

	Number of hours per year with PPD above 10%				
	Zone 1	Zone 2	Zone 3	Zone 4	Zone 5
	[h]	[h]	[h]	[h]	[h]
80°C/6°C	0	0	0	0	0

70°C/6°C	0	0	0	0	1
60°C/6°C	0	0	0	0	6
50°C/6°C	1	1	1	1	10
80°C/8°C	0	0	0	0	0
70°C/8°C	0	0	0	0	1
60°C/8°C	0	0	0	0	6
50°C/8°C	1	1	1	1	10
80°C/10°C	0	0	0	0	1
70°C/10°C	0	0	0	0	2
60°C/10°C	0	0	0	0	7
50°C/10°C	1	1	1	1	11
80°C/12°C	0	3	1	0	5
70°C/12°C	0	3	1	0	6
60°C/12°C	0	3	1	0	11
50°C/12°C	1	4	2	1	15

In these conditions, the influence on the electricity consumption of the HVAC system gives a 5.8% improvement from 80°C/6°C conditions to 50°C/12°C conditions while the impact on the boiler is quite high with an improvement of 11.55%. In the overall, the primary energy consumption can be reduced by 8% between this conditions.

As presented before, the PPD is also evaluated hourly in each building zone. For an interior space, the recommended acceptable PPD range for thermal comfort from the ASHRAE 55 is that less than 10% people will feel uncomfortable. The number of hours by year and by zone with PPD above 10% is quite small, with zone 5, only 15 hours, is the worst case (50°C/12°C).

The impact of removing both open headers is presented from Table 4-60 to

Table 4-62. This influence on boiler consumption is significant, with a 14% improvement from 80°C/6°C conditions to 50°C/12°C conditions.

When comparing the 50°C/12°C conditions with and without open header, the boiler consumption is reduced by 4% just by avoiding the mixing effect. Same trend can be observed in the electricity and primary energy consumption of the HVAC, reduced by 1.5% and 2.4%, respectively.

The study, focusing on a few steady state point including design and off design operating conditions, can be used to analyze the impact of temperature on system performance. Following this, the annual simulation has given a confirmation of these findings with similar order of magnitude for the system performance improvement.

Table 4-60 Sensitivity of annual boiler consumption to exhaust temperature of evaporator and exhaust water temperature of boiler

Boiler consumption			Evaporator exhaust water temperature			
			[°C]			
			6	8	10	12
Boiler exhaust water temperature	[°C]	80	225.19	225.16	225.12	225.07
		70	206.57	206.54	206.50	206.46
		60	200.88	200.84	200.81	200.77
		50	193.70	193.67	193.64	193.59

Table 4-61 Sensitivity of annual electricity consumption to exhaust temperature of evaporator and exhaust water temperature of boiler

Electricity consumption for HVAC			Evaporator exhaust water temperature			
			[°C]			
			6	8	10	12
Boiler exhaust water temperature	[°C]	80	143.68	140.71	138.03	135.79
		70	143.58	140.62	137.94	135.69
		60	143.59	140.64	137.94	135.71
		50	143.61	140.67	137.96	135.74

Table 4-62 Sensitivity of annual primary energy consumption to exhaust temperature of evaporator and exhaust water temperature of boiler

Primary energy consumption for HVAC			Evaporator exhaust water temperature			
			[°C]			
			6	8	10	12
Boiler exhaust water temperature	[°C]	80	584.38	576.94	570.20	564.55
		70	565.52	558.08	551.35	545.68
		60	559.86	552.43	545.66	540.04
		50	552.73	545.35	538.54	532.93

## 5. Principles for achieving HTC&LTH systems

### 5.1. Reducing dissipations of internal processes in the system

The task of active heating and air-conditioning system is to realize the heat or moisture transfer process between indoor sources and outdoor appropriate sinks with certain driving forces. And the driving forces are consumed in intermediate processes. Proportions of temperature differences consumed in intermediate processes should be investigated from the perspective of reducing the entire requirement for driving forces and improving system performance. Then the most efficient link could be determined for reducing the consumed driving forces. Then effective approaches could be proposed for performance optimization.

It's also an important issue to choose appropriate outdoor sources or sinks for thermal built environment. Temperature levels and corresponding characteristics have been introduced in section 2.4. As for cooling in buildings, a heat sink with a relatively low temperature is recommended to be selected according to the building function and climate region. It will be beneficial to reduce the driving temperature difference in active air-conditioning system. For example, outdoor air temperature could be as high as 35°C in summer but the humidity ratio may be relatively low in dry regions such as Xinjiang Province, China. Then the heat sink with a relatively low temperature could be achieved by utilizing direct evaporative cooling (corresponding to outdoor wet bulb temperature) or indirect evaporative cooling (corresponding to outdoor dew point temperature) method. Outdoor design parameters are 34.1°C and 8.5g/kg in Urumchi, with corresponding wet bulb and dew point temperatures of 18.5°C and 7.5°C respectively. Chilled water with a temperature of about 12~16°C could be obtained through indirect evaporative cooling device. Then there will be a driving temperature difference of 9~13°C between indoor and chilled water. It will be sufficient for covering the temperature differences consumed for cooling in buildings. And there is no need to utilize mechanical chiller for producing chilled water and remarkable energy saving results could be achieved.

As there are fixed indoor requirements and outdoor heating source/sink, most of the intermediate links in thermal built environment are heat or mass transfer processes. Then the driving forces are temperature difference and humidity ratio difference. Entransy dissipation is precisely the parameter to depict losses existing in these processes quantitatively. In Subtasks A~C, entransy dissipation is adopted to depict the losses in heat and moisture collection of terminal handling process, sensible heat transfer process, coupled heat and mass transfer processes, periodic heat transfer process successively. Equivalent thermal resistance is also derived based on entransy dissipation analysis, and the intermediate link with a relatively high thermal resistance could then be determined. Then it could be clarified whether the key factor restricting performance is limited transfer ability or unmatched properties (including unmatched flow rates, unmatched inlet parameters and etc.). It's helpful to make the direction for performance improvement clear.

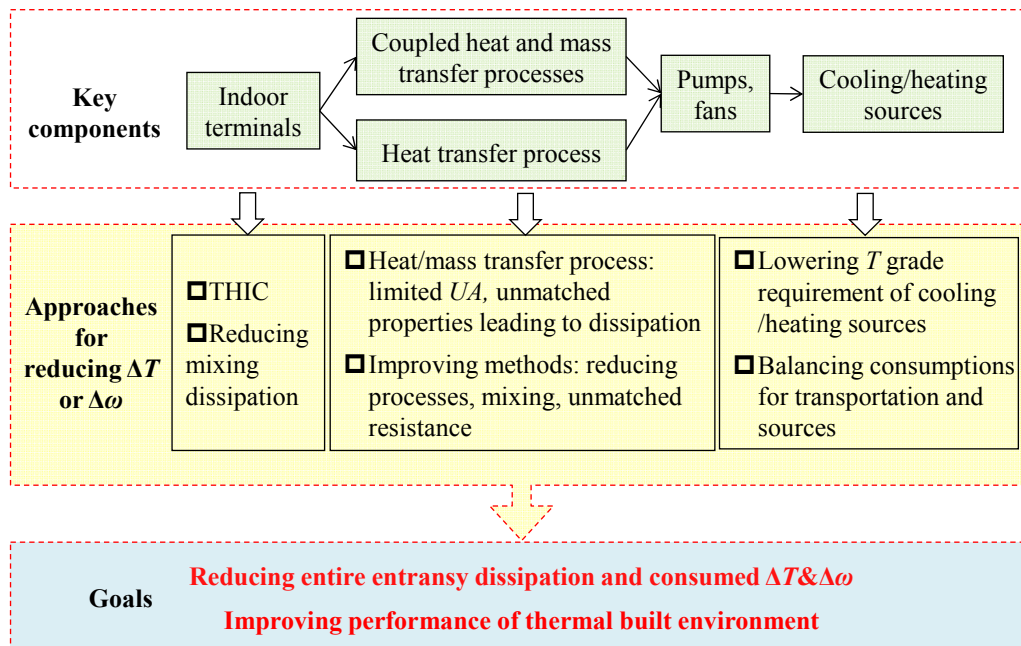


Fig. 5-1 Key approaches to improve performances of main links

The starting point of thermological analysis in thermal built environment is to focus on dissipations in intermediate processes and depict them quantitatively. Then system improvement could be achieved according to optimizing each intermediate process. The research ideas of above chapters could be illustrated as Fig. 5-1. The present thermological analysis method is quite different from the conventional method for process design and system analysis. It's to find solutions for reducing temperature difference consumptions with a clear understanding on reasons leading to temperature difference. The approaches to reduce temperature difference will be beneficial to improve system performance and save energy in thermal built environment. Thus thermological analysis is not to propose a new calculation method. **It's indeed to investigate the system from a novel perspective and develop a new understanding systematically. It will help to inspire new ideas and propose novel solutions for thermal built environment.**

## 5.2. Principles for reducing dissipations of key processes

As indicated by the characteristics of each link in the system, reducing dissipation in each transfer process contributes to improve performance of the single link. This is a kind of partial performance optimization with emphasis on single link. While the goal for system optimization is to improve the overall performance. Performance improvement of the system should be based on performance of each link, comprehensively considering indoor collecting, intermediate transportation, cooling/heating sources and so on. Therefore it's not contradictory between partial optimization and global optimization. They can supplement each other and promote each other, as shown in Fig. 5-2.

Evaluation indexes of system performance mainly contain total entransy dissipation  $\Delta E_{n,sys}$ , total driving temperature difference consumed  $\Delta T_{sys}$ , system energy efficiency  $COP_{sys}$ , etc. Requirements suggested for these indexes to improve system performance could be

summarized as reducing transfer dissipation, reducing total driving force consumed, lowering the temperature grade requirements of cooling/heating sources and so on. While parameters for each link of the system mainly contain temperature difference  $\Delta T$  for transfer process, entransy dissipation  $\Delta E_n$ , equivalent thermal resistance  $R$ , unmatched thermal resistance, etc. And effective approaches could be proposed from analyses on these parameters for improving performances of intermediate processes.

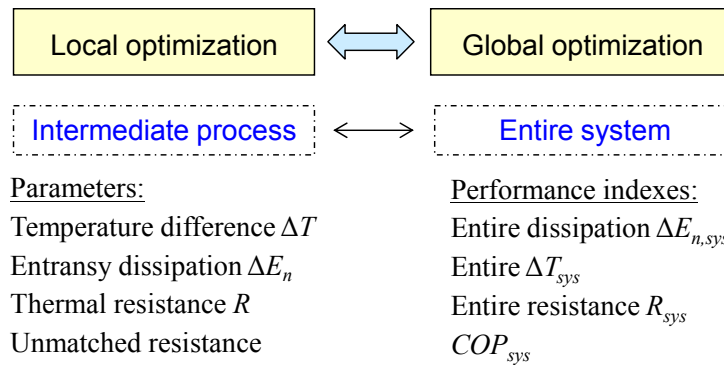


Fig. 5-2 Relation between local optimization and global system optimization

Optimization of each link such as indoor collection, heat transfer, coupled heat and mass handling processes is in accordance with decreasing the overall system dissipation. And reducing temperature difference consumed by each link also contributes to decreasing the total requirement of driving force in heat and moisture removing processes. What calls for special attention is that influence of transportation on system performance should be fully considered, and energy consumption for transportation and cooling source energy should be balanced in system performance analysis. Driving force requirement of the entire system could be lowered through reducing driving forces  $\Delta T$  and  $\Delta\omega$  consumed in intermediate processes, which also contributes to decreasing the temperature grade requirement of system cooling/heating source. “High temperature cooling and low temperature heating” could be achieved and energy efficiency could then be improved in thermal built environment.

Activated air-conditioning system should be constructed and optimized on the basis of designing appropriate buildings and building envelopes. There are some common characteristics of intermediate links including indoor heat and moisture collection, sensible heat transfer, coupled heat and mass transfer processes as mentioned above. General principles are then summarized as following for constructing optimized processes and system design in active air-conditioning system.

**a) Principle 1: reducing heat and cold offset (humid and dry offset)**

Various links are involved in thermal built environment to meet the requirements for removing indoor extra heat and moisture. As the transferred target i.e. heat capacity  $Q$  or moisture removal  $m_w$  is fixed, the first is to avoid any unnecessary increase of heat/moisture transferred rate. It’s to say that unnecessary heat-cold offset and dry-wet offset should be avoided.

**b) Principle 2: reducing transfer links**

Certain driving forces, i.e. entransy dissipation are required for heat and moisture removing processes in thermal built environment. And the driving forces are consumed by the

various internal links. As indicated by the characteristic of driving force in a single transfer process, temperature difference  $\Delta T$  is the driving force in sensible heat transfer process, and humidity ratio difference  $\Delta \omega$  is the driving force in moisture transfer process. A certain driving force is required in each transfer link to meet the transfer requirement. The less the transfer links, the lower the driving force (temperature difference) consumed possibly. It contributes to the reduction of total driving force or entransy dissipation required in the system.

**c) Principle 3: reducing mixing dissipation**

Although there is no heat or mass loss brought by mixing processes, there occurs heat or mass transfer process due to mixing of different fluids. Transfer dissipation of the entire system is then increased. Dissipations could be arisen from the mixing processes in different links of the air-conditioning system, such as mixing process between two flows of chilled water with different temperatures, between supply air and indoor air. Mixing dissipations in indoor collecting process and intermediate transfer process result in the increase of driving forces provided by cooling/heating sources. Decreasing unnecessary mixing processes can contribute to reducing the transfer dissipations of the entire air-conditioning system, which will also be beneficial for performance improvement.

**d) Principle 4: improving match properties**

The active air-conditioning system is composed of various heat exchangers, coupled heat and mass transfer processes and etc. In addition to limited transfer ability  $UA$ , unmatched properties are the main reasons leading to dissipations in transfer processes, which could be depicted by the unmatched thermal resistance. The unmatched properties mainly include unmatched flow patterns, unmatched flow rates, unmatched inlet parameters in coupled heat and mass transfer processes, etc. It's an important issue to reduce unmatched dissipation and improve match properties in constructing a handling process in thermal built environment.

### **5.3. Balance between consumptions of “sources” and “transportation”**

Energy consumptions of an active air-conditioning system mainly consist of the consumption consumed by heating/cooling sources and transportation devices (i.e. fans and pumps). Heating/cooling capacity is provided by the heating/cooling sources with the help of heat-work conversion (heat pump cycle) or combustion of fossil fuel. And the transportation devices are responsible for delivering the heating/cooling capacity from sources to the terminal users. Thus both consumption of heating/cooling sources and transportation consumption should be taken into account comprehensively for energy saving in the HV&AC system. As for the “high temperature cooling and low temperature heating” system, it's natural for the researchers to recommend utilizing the natural cooling sources or free heating sources as much as possible, which do good to improve the energy efficiencies of sources. Increasing the circulating flow rates helps to realize “high temperature cooling and low temperature heating” in thermal built environment, but the corresponding transportation consumption may be also increased. Then how to make an overall consideration and a comprehensive analysis on consumptions of heating/cooling sources and transportation devices?

The common intermediate medium for transportation system is water or air in the thermal built environment. There are significant discrepancies in the physical properties such as density and specific heat capacity between air and water. With a same heating/cooling capacity to be transported, the energy consumed by water pumps is significantly lower than that by fans, and the former is only about 1/5~1/10 of the latter. And water pipes account for less spaces than air duct. With an perspective of reducing transportation consumption, water is recommended as the intermediate media for transportation rather than air. Besides, there is usually a minimum fresh air flow rate to satisfy the indoor air quality in buildings. This outdoor air flow rate could be regarded as the lower limiting value (or upper limit) for adopting air as the media. There are various kinds of air-conditioning systems with the help of developments up to today. For example, there are all air system with either double air ducts or single duct firstly developed in the US, the fan coil unit (FCU) and outdoor air system widely used in China at the present stage, the emerging radiant terminal and outdoor air system in Europe in recent years, the variable refrigerant flow (VRF) and outdoor air system firstly developed in Japan and so on. Transportation consumptions for these air-conditioning systems above are decreased successively. As for the all air system, air is chosen as the intermediate media for heating/cooling transportation and the air flow rate is fairly high. In the FCU and outdoor air system, the intermediate medias include both air and water, thus the air flow rate is far less than that in the all air system. In the radiant terminal and outdoor air system, indoor fan's consumption is reduced due to a lower circulating air flow rate. In the VRF and outdoor air system, refrigerant is chosen as the intermediate media.

As the intermediate media is determined, power consumed by fans or pumps of the transportation system could be calculated according to Eq. (5-1).

$$W_A = \frac{G_a \Delta p_a}{\eta_a}, W_P = \frac{G_w \Delta p_w}{\eta_w} \quad (5-1)$$

where  $W_A$  and  $W_P$  are power consumptions of fan and water pump, W;  $G_a$  and  $G_w$  are volume flow rates of air and water respectively,  $m^3/s$ ;  $\Delta p_a$  and  $\Delta p_w$  are pressure heads of fan and water pump respectively, Pa;  $\eta_a$  and  $\eta_w$  are efficiencies of fan and pump respectively.

It can be concluded that transportation consumption is just in direct proportion to the circulating flow rate  $G$  and the pressure drop  $\Delta p$ .  $G$  is determined by the required heating/cooling capacity of indoor space and the temperature difference  $\Delta T$  of supply and return air (or water). And  $\Delta p$  is closely related to the system structures. For instance the centralized air handling units are utilized in airport terminals and commercial markets. The corresponding  $\Delta p$  of fans could be as high as hundreds of Pascal, or even higher than 1000Pa. While if the air handling units could be set decentralized in different regions or floors,  $\Delta p$  could be significantly reduced. Even if circulating flow rate  $G$  is increased,  $\Delta p$  is possible to be reduced through a reasonable setup and system optimization. The transportation consumption is not only determined by the flow rate. Increasing circulating flow rate is not meaning to increase the transportation consumption. With an optimized system setup,  $\Delta p$  is variable and the transportation consumption could also be unchanged or even reduced with an increased flow rate.

To reduce the energy consumption of pumps and fans in the transportation system, there are more and more transportation systems adopting large temperature difference mode. As in the low temperature air supply system or the large temperature difference chilled water system, the circulating air or water flow rate  $G$  is significantly reduced. However the corresponding temperature grade requirement of cooling/heating sources will be increased in this kind of large temperature difference mode, to the disadvantage of improving energy performances of cooling/heating sources. Then whether the “high flow rate and low temperature difference” mode or the “low flow rate and high temperature difference” mode is recommended in the system design? Just as mentioned in the introduction chapter, there are different starting points for the low temperature air supply system and the THIC system. Advocators of the former insist that a lower supply air temperature helps to increase the temperature difference between supply air and return air, beneficial to reduce air flow rate and fan consumption. While supporters of THIC system emphasize that a high temperature cooling source contributes to increase the evaporating temperature, with advantage in improving chiller’s  $COP$  and reducing the corresponding power consumption. Thus these two kinds of proposals show emphasis on different aspects for reducing energy consumptions. In an actual HV&AC system, the dominant factor or the focus of attention might be different in terms of the building functions or climate influences. A comprehensive analysis should be investigated with consideration in both heating/cooling sources and transportation devices.

Operating temperatures of chilled water in a central air-conditioning system are usually about 7/12°C, with a temperature difference of about 5°C. There are more and more large commercial complexes and super high-rise buildings in recent years. Transportation consumptions in the centralized air-conditioning systems of these buildings account for a considerable proportion of the entire consumption. To reduce the energy consumption of the transportation system for chilled water, a large temperature difference of chilled water is adopted in this kind of large temperature difference air-conditioning system. The design temperature difference of chilled water could be as high as 8°C~10°C, significantly higher than that (~5°C) in conventional system. A large temperature difference of chilled water is adopted in this kind of large temperature difference air-conditioning system. With a certain heating/cooling capacity to be delivered, the corresponding water flow rate and pump consumption will be reduced compared to that of the conventional system with a water temperature difference of 5°C. However evaporating temperature will be lowered in this circumstance and chiller’s  $COP$  will also be brought down. As the transportation consumption accounts for a relatively low proportion in the consumption of the entire system, the key issue becomes to improve the energy efficiency of the sources. It’s recommended to adopt the “high flow rate and low temperature difference” mode, which will be beneficial to achieve a higher evaporating temperature and improve the efficiency. If the transportation consumption accounts for a great proportion in the entire consumption, the basis for performance optimization changes to reduce the transportation consumption. The “low flow rate and high temperature difference” mode is more meaningful, and it’s suggested to optimize the performance of the cooling source as well. Then for this kind of system with a large  $\Delta T$ , the unmatched properties in heat transfer process will be prominent if a cooling source with a single temperature is adopted. Under this circumstance, adopting a multi-stage evaporator is

supposed to be an approach for improving the match properties. It will be beneficial to achieve a more energy-efficient process for the water chiller.

In the district heating system, the distance for transportation system is usually about several kilometers or even dozens of kilometers. In normal circumstances, a large temperature difference of hot water in the primary network is chosen to reduce energy consumed by the transportation system. Another consideration is to avoid an overhigh pipe diameter buried underground. The typical supply and return temperatures of hot water are 130°C and 70°C respectively, with a corresponding temperature difference of about 60°C. The secondary network is usually a water circulation system directly connecting with the terminal devices such as radiators and FCUs of users. Its distance is significantly shorter than that of the primary network. Operating water temperature difference of the secondary network is usually about 15~25°C, significantly lower than that of the primary network. Then in the transportation system, a “lower flow rate and larger temperature difference” mode is adopted for the primary network while a “higher flow rate and lower temperature difference” mode is selected for the secondary network and terminal users.

Thus there is no conflict between the “lower flow rate and larger temperature difference” mode and the “higher flow rate and lower temperature difference” mode. The former focuses on reducing the circulating flow rate to reduce the transportation consumption, while the latter puts emphasis in the terminal devices, aiming to improve the performances of heating/cooling sources. A global performance optimization of the HV&AC system should be carried out on basis of the building functions and service conditions.

To sum up, input heat or mass transfer ability, power consumption for transportation and power consumption of heating/cooling sources are three kinds of parameters indicating the input of an active air-conditioning system. Input heat or mass transfer ability is related to the initial cost, while transportation power and cooling/heating sources' power represent the operating consumption. The relationship among these three kinds of input consumptions is changing with the development of times and technical progress. In the design and operation of an actual air-conditioning system currently, temperature levels of main links and match properties should be taken into account. The restriction for system performance could be obtained based on a comprehensive analysis of temperature levels and match properties. Then effective approaches for performance improvement are desired to be proposed.

## **6. Brief summary of this report**

In this study, the influence of the temperature of hot water and chilled water on system performance has been clearly identified. It has been established that increasing the chilled water temperature and lowering the hot water temperature have significantly impact on performance of the overall system if properly designed. The design guide for the high temperature cooling and low temperature heating could be summarized as following:

- (1) Decrease heat transfer processes could reduce heat transfer loss directly.

- (2) Minimize the mixing loss of fluids with different temperatures contributes to the increase/decrease the temperature of the cooling/heating source.
- (3) Decrease the unmatched loss of the heat and mass transfer processes with limited heat exchanger area.
- (4) T-Q diagram and entransy dissipation as well as equivalent thermal resistance could be used for better design of the whole system.

## • References

- [1] ASHRAE. (2008). S01. HVAC System Analysis and Selection. Dans *ASHRAE Handbook - HVAC Systems and Equipment*. SI Edition.
- [2] Beausoleil-Morrison, I. (2007). *Experimental Investigation of Residential Cogeneration Devices and Calibration of Annex 42 Models*. IEA/ECBCS Annex 42 Report.
- [3] BERG. (2015). *Annual Report on China Building Energy Efficiency*. Building Energy Research Center Tsinghua University, Beijing Chinese Architectural and Industrial Press.
- [4] Bertagnolio, S., Stabat, P., Soccia, B., Gendebien, S., & Andre, P. (2010). Simulation Based Assessment of Heat Pumping Potential in Non-Residential - Part 1: Modeling. *Proceedings of the 10th REHVA World Congress - Clima 2010*. Antalya.
- [5] Bourdouxhe, J.-P., Godent, M., Lebrun, J., & Saavedran, C. (1999). *ASHRAE HVACI Toolkit: A Toolkit for Primary System Energy Calculation*. Atlanta: American Society of Heating, Refrigerating and Air-Conditioning Engineers, Inc.
- [6] Brelih, N., & Seppänen, O. (2012). Preface. Dans N. Brelih, O. Seppänen, T. Bertilsson, M.-L. Maripuu, H. Lamy, & A. Vanden Borre, *Design of Energy Efficient Ventilation and Air-Conditioning Systems*. REHVA Guidebook.
- [7] Bureau for Standardisation. (1992). *Central heating, ventilation and air conditioning - Common requirements for all systems - Thermal insulation*.
- [8] CIBSE CHP Group. (2012). *Spark-ignition gas-engine CHP, Datasheet 02*. Récupéré sur <http://www.cibse.org/getmedia/33137fd2-fd03-492d-8358-58f92d2b37cb/Datasheet-2-Spark-Ignition-Engines.pdf.aspx>
- [9] Department of Energy. (2012, November 13). *New Construction - Commercial Reference Buildings*. Récupéré sur <http://energy.gov/eere/buildings/new-construction-commercial-reference-buildings>
- [10] Department of Energy. (2015, September 1). *EnergyPlus Energy Simulation Software*. Récupéré sur <http://energy.gov/eere/buildings/energyplus-energy-simulation-software>

- [11] European Committee for Standardization. (2004). *Ventilation for non-residential buildings - Performance requirements for ventilation and room-conditioning systems*. European Standard.
- [12] European Committee for Standardization. (2007). *Energy Efficiency in buildings – Influence of Building Automation and Control and Building Management*. European standard.
- [13] European Committee for Standardization. (2012). *Heating systems in building. Design for water-based heating systems*.
- [14] FläktWoods. (s.d.). *Centrimaster GX - Technical Data*.
- [15] GEA. (2012, December). GEA Fan coil Units - Comfort Edition. *GEA Flex-Geko*.
- [16] Knight, I., & Ugursal, I. (2005). *Residential Cogeneration Systems: A Review of the Current Technologies*. IEA/ECBCS Annex 42 Report.
- [17] Lemort, V., & Bertagnolio, S. (2010). A generalized simulation model of chillers and heat pumps to be calibrated on published manufacturer's data. *International symposium on refrigeration technology*. Zhuhai, China.
- [18] Lemort, V., & Bertagnolio, S. (2010). The use of semi-empirical modeling to extrapolate chiller performance maps. *ASHRAE Annual Meeting - Seminar 26*. Albuquerque.
- [19] Perez-Lombard, L., Ortiz, J., & R., M. I. (2011). The map of energy flow in HVAC system. *Applied Energy*, 88, 5020-5031.
- [20] Rosato, A., & Sibilio, S. (2012). Calibration and validation of a model for simulating thermal and electric performance of an internal combustion engine-based microgeneration device. *Applied Thermal Engineering* 45-46, pp. 79-98.
- [21] Stabat, P., & Marchio, D. (2004). Simplified model for indirect-contact evaporative cooling-tower behaviour. *Applied Energy*, 78, 433-451.
- [22] Vandenbulcke, R. (2013). *Hydronic Simulation and Optimization - A simulation based study on the energy efficiency and controllability of hydronic heating systems*. PhD Thesis, University of Antwerp.
- [23] Zhao, X., Fu, L., Zhang, S., Jiang, Y., & Li, H. (2010). Performance of a 70kWe natural gas colbined heat and power (CHP) system. *Energy* 35, pp. 1848-1853.
- [24] Zhu, K. (2014). *Analysis and Study of Reducing Energy Quality Loss in District Heating System*. Master Thesis, Tsinghua University.

## PART 2

# 1 Application in an office building (humid region of China)

## 1.1 Description of the THIC System in an office building

### 1.1.1 Basic information

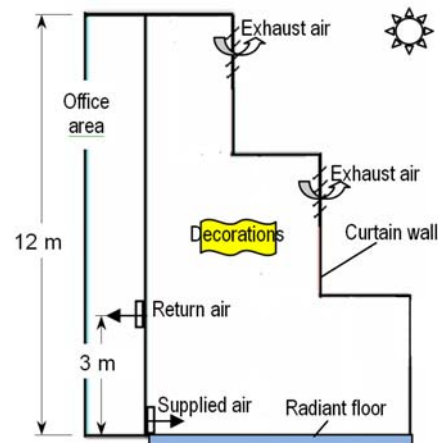
A 5-story office building, as shown in Fig. 0-1, is located in Shenzhen, China, with total building area of 21,960m<sup>2</sup> and the areas of 5940m<sup>2</sup>, 5045m<sup>2</sup>, 3876m<sup>2</sup>, 3908m<sup>2</sup>, 3191m<sup>2</sup> for the 1<sup>st</sup> to 5<sup>th</sup> floor, respectively. The main functions of the 1<sup>st</sup> floor are mess hall, archive and carport, while the 2<sup>nd</sup> to 4<sup>th</sup> floors are the office rooms, with the 5<sup>th</sup> floor as the meeting room. And there is a vestibule vertically through up the 2<sup>nd</sup> to 4<sup>th</sup> floors in the north of this building. As to the vestibule, curtain wall with ventilation shutters on the top is applied on its north facade, as shown in Fig. 0-2.



Fig. 0-1 The tested office building in Shenzhen.



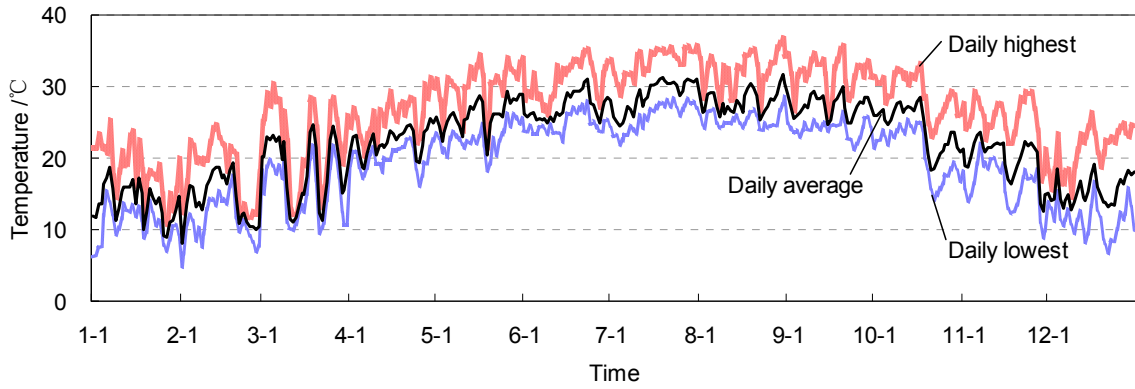
(a)



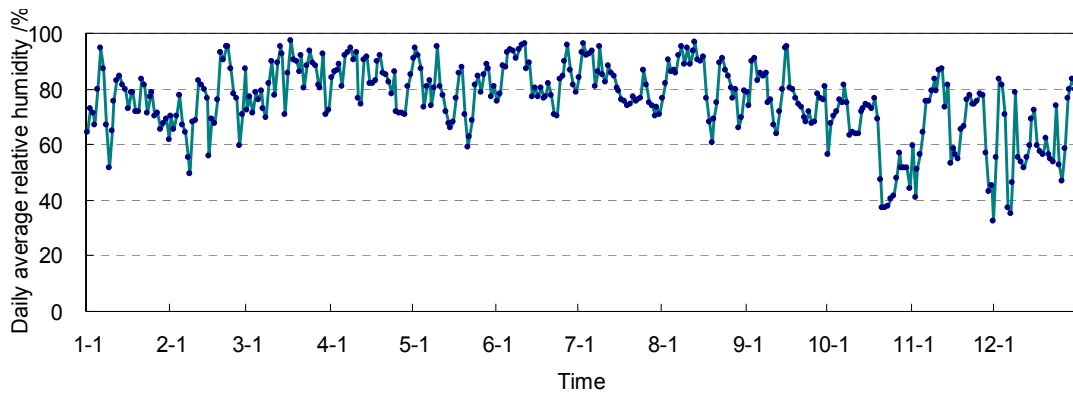
(b)

Fig. 0-2 Vestibule in the office building: (a) photo; (b) schematic figure.

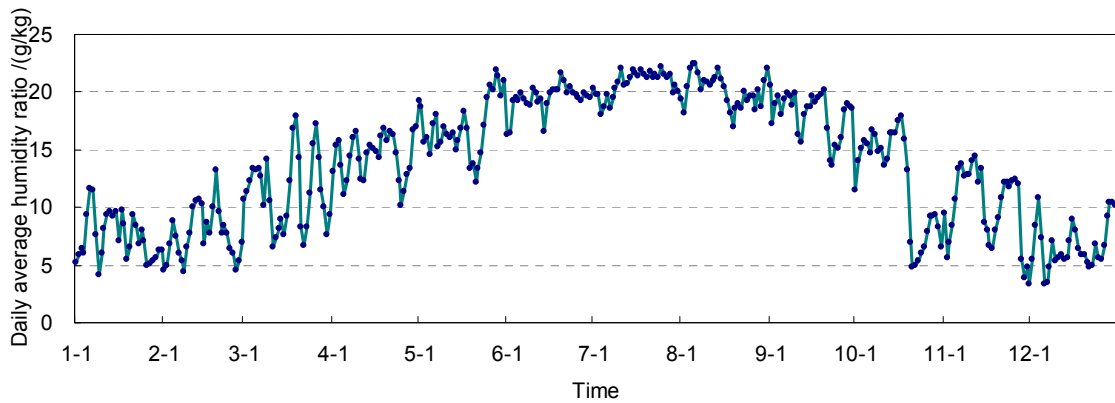
The outdoor condition in Shenzhen is rather hot and humid all through the year as shown in Fig. 0-3. The annual outdoor air relative humidity is about 80% and humidity ratio in summer is as high as 20g/(kg dry air). The building requires both cooling and dehumidification in a long period of time, and no heating and humidification requirement in winter. Therefore, how to handle the moisture efficiently is the key issue in such a subtropical area.



(a)



(b)



(c)

Fig. 0-3 Annual weather data of Shenzhen: (a) daily highest, average and lowest temperatures; (b) daily average relative humidity; (c) daily average humidity ratio.

### 1.1.2 THIC air-conditioning system

The THIC system serves from 1<sup>st</sup> to 4<sup>th</sup> floor with the net air-conditioning area of 13,180m<sup>2</sup> (the total area of 18,769m<sup>2</sup>), and the 5<sup>th</sup> floor is served by several stand-alone air-conditioners and is not within the scope of our discussion. The schematic of the THIC system is represented in Fig. 0-4 with the main devices' parameters listed in Table 0-1.

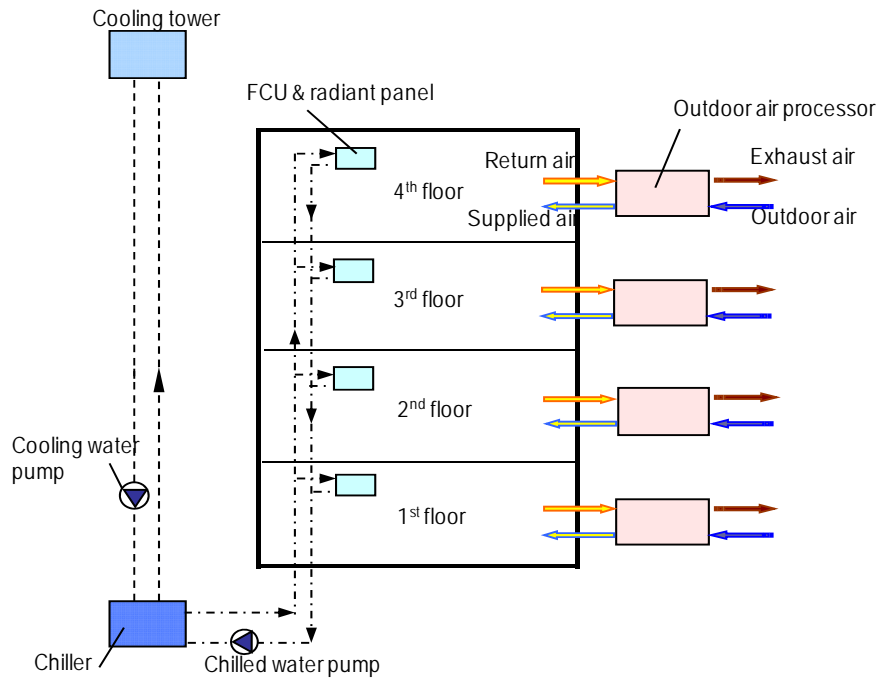


Fig. 0-4 Schematic of the THIC air-conditioning system.

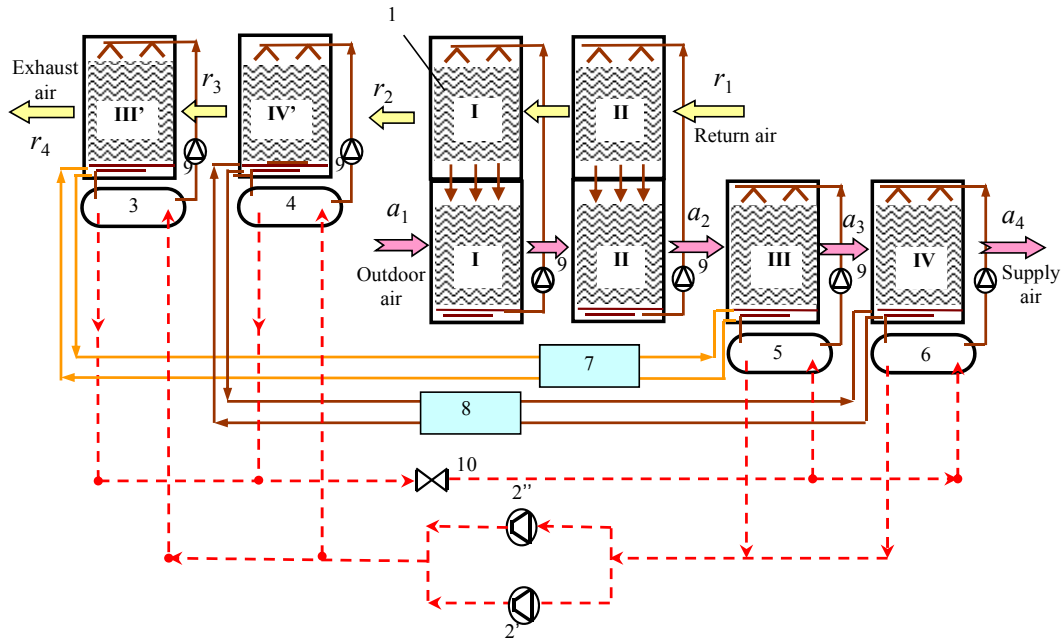
Table 0-1 Main devices of the THIC system in the office building

Subsystem	Device	Quantity	Rated parameters
Temperature control subsystem	Chiller	1	Cooling capacity: 893 kW; Power consumption: 107 kW; rated COP=8.3
	Cooling tower	1	Flow rate: 200 m <sup>3</sup> /h; Power consumption: 7.5kW
	Cooling water pump	1	Flow rate: 180 m <sup>3</sup> /h; Head: 29 m; Power consumption: 22 kW
	Chilled water pump	1	Flow rate: 262 m <sup>3</sup> /h; Head: 32 m; Power consumption: 37 kW
	Indoor terminal devices	-	Radiant panels and dry FCUs, serving 19% and 81% of the entire sensible cooling respectively
Humidity control subsystem	Outdoor air handling units	1	Fresh air flow rate 2000 m <sup>3</sup> /h, Cooling capacity 39 kW, Power consumption* 10 kW; for offices in the 4 <sup>th</sup> floor
		2	Fresh air flow rate 4000 m <sup>3</sup> /h, Cooling capacity 83 kW, Power consumption* 25 kW; for offices in the 4 <sup>th</sup> floor
		4	Fresh air flow rate 5000 m <sup>3</sup> /h, Cooling capacity 103 kW, Power consumption* 28 kW; 2 units for the 2 <sup>nd</sup> floor, and 2 units for the 3 <sup>rd</sup> floor
		1	Fresh air flow rate 8000 m <sup>3</sup> /h, Cooling capacity 166 kW, Power consumption* 45 kW, for vestibule in the 2 <sup>nd</sup> floor
		1	Fresh air flow rate 10000 m <sup>3</sup> /h, Cooling capacity 196 kW, Power consumption* 45 kW, for restaurant in the 1 <sup>st</sup> floor

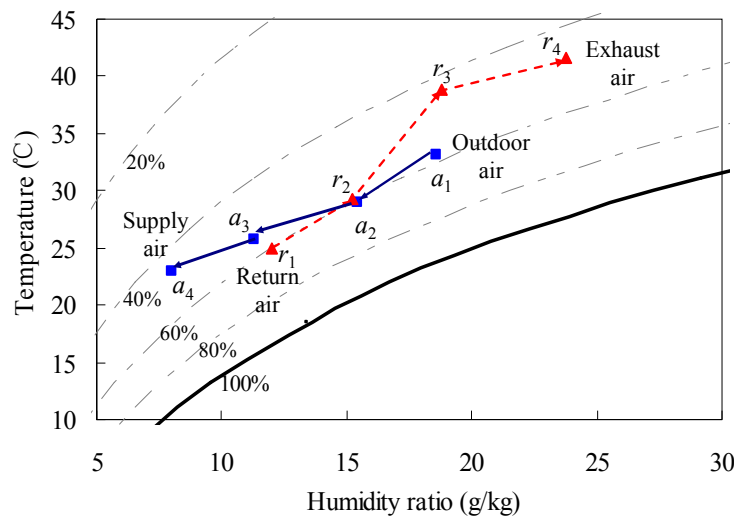
\*Including power consumption of compressors, solution pumps, and fans inside the outdoor air units

The right side of Fig. 0-4 is the humidity control subsystem, including 9 liquid desiccant outdoor air handling units that supply adequate dry outdoor air into the occupied spaces. As the flow rate of the supplied outdoor air is proportional to the number of people, the pollutants, CO<sub>2</sub> and latent heat produced by human bodies can be removed by outdoor air. The schematic of the heat pump driven outdoor air processors using liquid desiccant is illustrated in Fig. 0-5, which is composed of a two-stage enthalpy recovery device and a two-stage air handling device coupled with refrigeration cycles. LiBr aqueous solution is employed as liquid desiccant in these air processors. The enthalpy recovery device is used to recover the energy from indoor exhaust air to decrease the energy consumption of the outdoor air handling

process. And in the heat pump driven air handling device, the diluted solution from the dehumidification modules is heated by the exhaust heat from the condenser and concentrated in the regeneration modules. Then the hot concentrated solution is cooled by passing through the heat exchanger and evaporator before it enters the dehumidification modules, and lastly used to remove moisture from the outdoor air.



1-heat recovery module; 2-compressor; 3-condenser I; 4-condenser II; 5-evaporator I; 6-evaporator II; 7-plate heat exchanger I; 8-plate heat exchanger II; 9-solution pump; 10-expansion valve  
(a)



(b)

Fig. 0-5 Summer operation principle of the two-stage liquid desiccant outdoor air processor with enthalpy recovery: (a) operating schematic; and (b) air handling process shown in psychrometric chart.

The left side of Fig. 0-4 is the temperature control subsystem that undertakes the rest sensible load to control indoor temperature, including a high-temperature chiller, a cooling tower, a cooling water pump, a chilled water pump, and indoor terminal devices (radiant panels and dry fan coil units). The high-temperature chiller is a centrifugal chiller with the

rated COP of 8.3 (designed condition: the inlet and outlet temperature of the chilled water and cooling water are 20.5°C/17.5°C and 30.0°C/35.0°C, respectively), which is much higher than the conventional chiller operating at the chilled water temperature of 12°C/7°C. As for indoor terminal devices, as shown in Fig. 0-6, FCUs operating in ‘dry condition’ are set up in the restaurant, archive and office regions which serve about 81% of the entire cooling load of the temperature control subsystem, while radiant floor and radiant ceiling panels are applied in vestibule and some office rooms which serve the rest 19%.

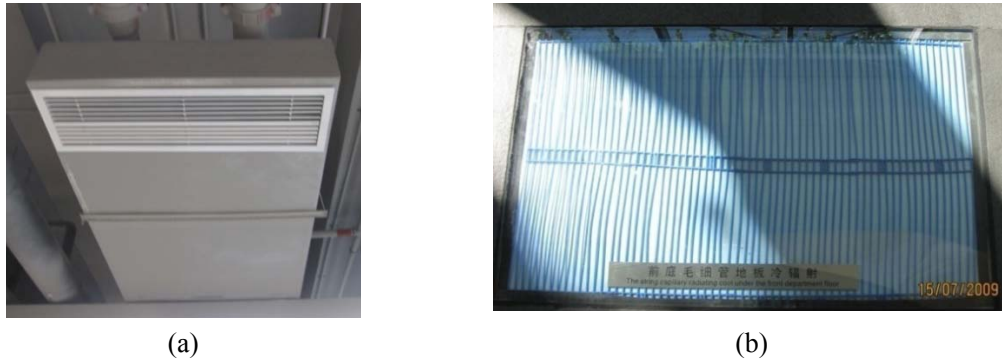


Fig. 0-6 Indoor terminal devices: (a) dry fan coil unit; (b) capillary radiant panel.

The whole THIC system layout has been introduced briefly as analyzed above. Particularly, stratified air conditioning, a key design principle of large space, is selected in the air-conditioning design of the vestibule as shown in Fig. 0-2(b). Specifically, in the occupied zone (indicating the area with a height within 2 m), chilled water with a temperature of 17.5°C is pumped and distributed into radiant floor for cooling, and the handled dry outdoor air is supplied in the bottom with indoor exhaust air expelled in the middle of the space, as shown in Fig. 0-7(a). This configuration forms a "dry air layer" to protect the cold floor surface from condensation. Solar radiation that enters through glass curtain wall is absorbed by the ornamental decorations in the higher space above occupied zone, and the heat is then carried away by natural ventilation through the shutters (shown in Fig. 0-7(b)) directly.

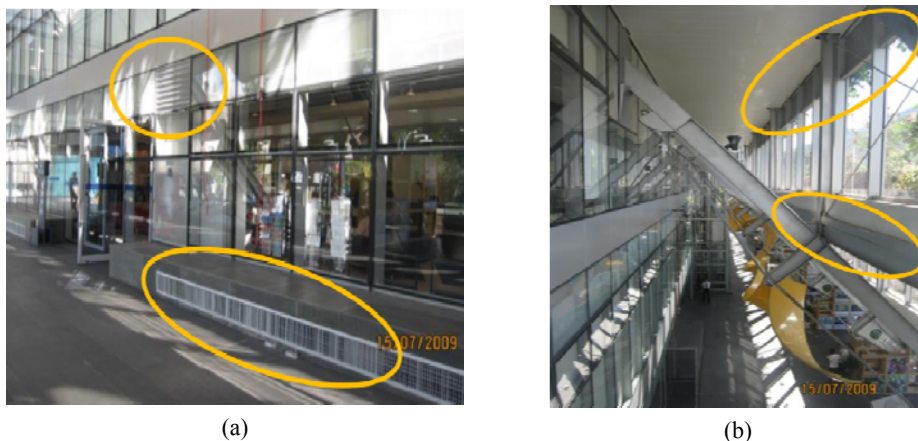


Fig. 0-7 Supply, return air vents and top shutter: (a) supply and return air vents; (b) top shutter.

The temperature control subsystem and humidity control subsystem can be operated separately according to ambient condition and indoor requirement.

- The two subsystems operate together at hot and humid outdoor climate;
- Only the humidity control subsystem operates at cold but humid ambient condition;
- Outdoor air is directly introduced into occupied spaces after filter when outdoor air is dry

enough, such as with a humidity ratio of 11g/kg.

## 1.2 Performance test of the THIC system

The field test of the energy efficiency of the THIC system was conducted under both the partial load condition and design condition. The former one was with ambient temperature of 29.3°C and relative humidity of 79%, and the latter one was with ambient temperature of 34.9°C and relative humidity of 61%. The measurement was divided into two parts: humidity control subsystem and temperature control subsystem.

### 1.2.1 Indoor thermal environment

#### 1) Outdoor condition

The outdoor condition in Shenzhen is rather hot and humid, as shown in Fig. 0-8. The peak air temperature was 35°C and the humidity ratio was as high as 20g/kg. The solar radiation was measured by a portable solar pyranometer. The peak solar radiation was as high as about 1000W/m<sup>2</sup> at noon, as indicated by Fig. 0-9.

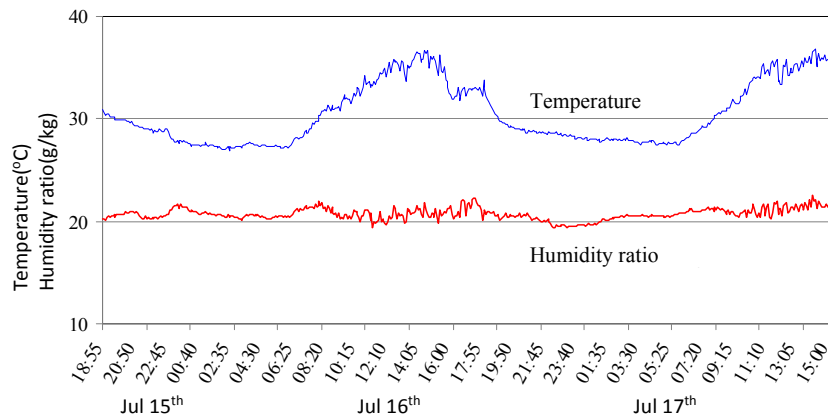


Fig. 0-8 Ambient temperature and humidity ratio during the test.

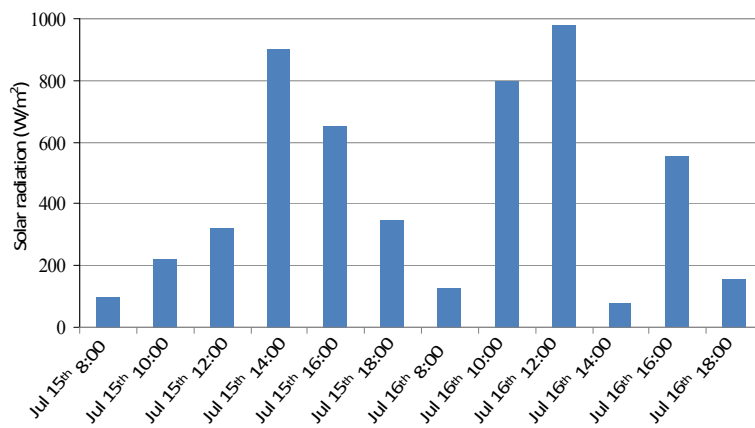
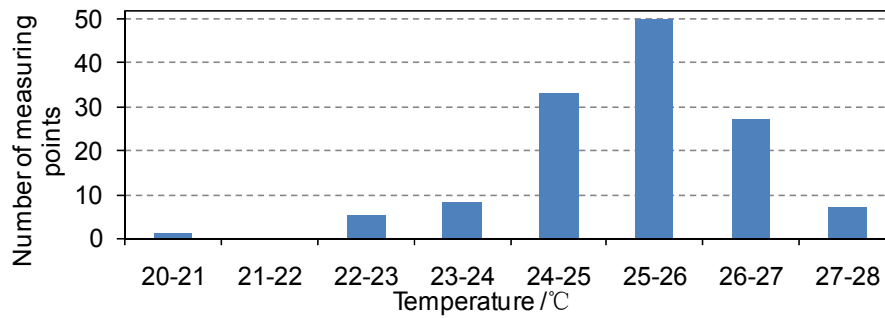


Fig. 0-9 Solar intensity during the test.

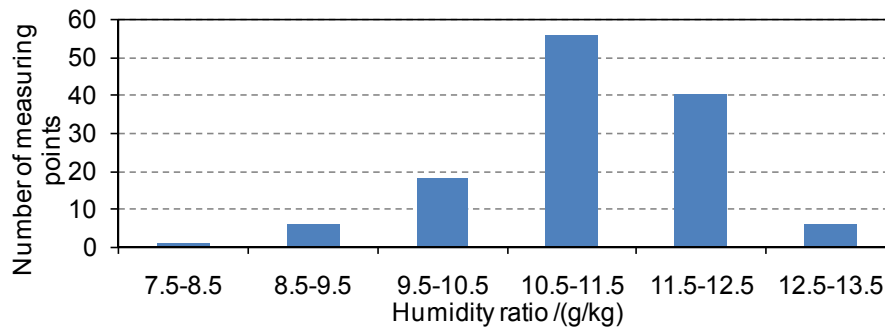
#### 2) Indoor thermal environment

This system has been brought into operation since July 2008. Fig. 0-10 shows the tested results of indoor temperatures, humidity ratios and CO<sub>2</sub> concentrations with the outdoor temperature and relative humidity of 34.9°C and 61%, respectively. As indicated by the figure, the THIC system could provide a comfortable indoor environment with suitable thermal

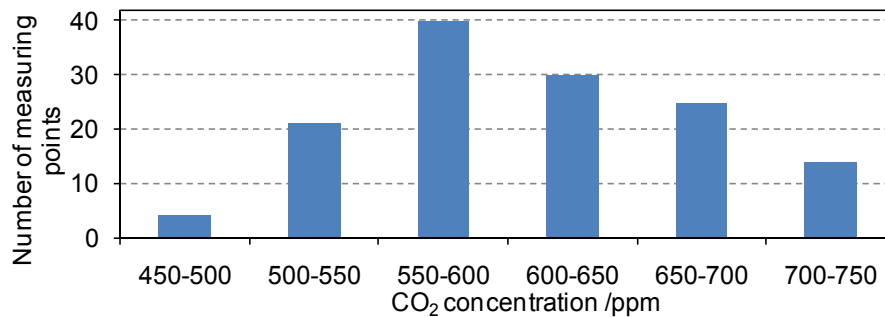
condition and good indoor air quality.



(a)



(b)



(c)

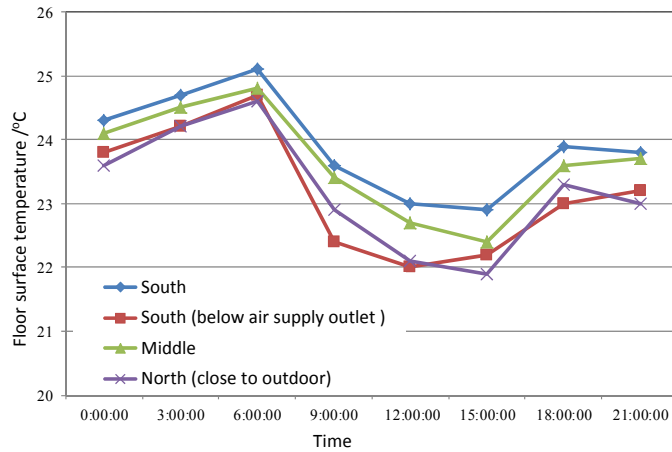
Fig. 0-10 Indoor air parameters of the office building: (a) temperature; (b) humidity ratio; (c) CO<sub>2</sub> concentration.

### 3) Radiant floor surface temperature distribution

The radiant floor surface temperature distribution is shown in Fig. 0-11. The air-conditioning system was switched on at 6:30 in the morning and the radiant floor surface temperature reached steady at 9:30. During the afternoon (16:00~17:00), the radiant floor surface temperature rose when direct solar radiation reached the floor surface.



(a)



(b)

Fig. 0-11 Radiant floor surface temperature profile: (a) field test points; (b) radiant floor surface temperature profile.

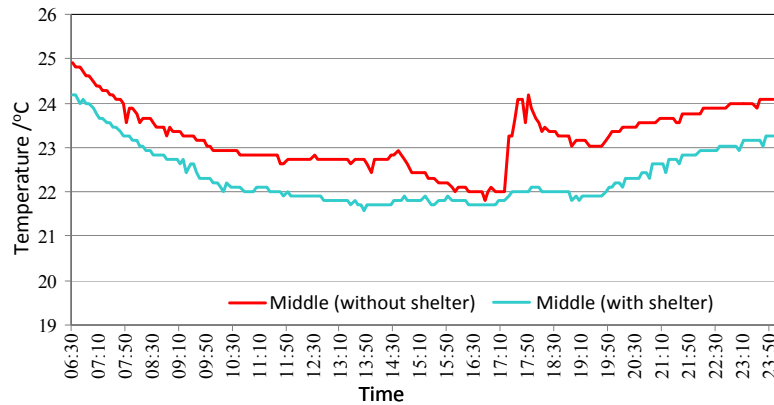


Fig. 0-12 Effect of the indoor furniture shelter on the radiant floor surface temperature.

The effect of the indoor furniture shelter on the surface temperature of the radiant floor is shown in Fig. 0-12. As the radiation heat transfer with the surrounding environment of the sheltered radiant floor is weakened by the furniture shelter, the floor surface temperature is about 1°C lower than the unsheltered radiant floor. Hence, the surface of the sheltered radiant floor could have a risk of condensation. The temperature and humidity parameters of the air near the floor were measured, as shown in Fig. 0-13. It can be seen that the dew point temperature of the surrounding air was about 15°C, lower than the lowest temperature of the radiant floor surface. Therefore, there was no risk of condensation during the test.

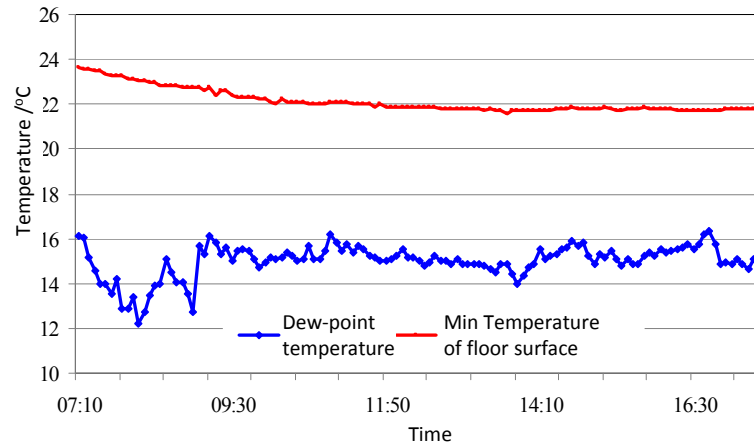


Fig. 0-13 Test results of radiant floor minimum temperature and surrounding air dew point temperature.

#### 4) Air temperature and humidity ratio distribution in the vertical direction

Fig. 0-14 depicts the tested temperatures and humidity ratios along the vertical direction in the vestibule. In the occupied zone (the height within 2m), the temperature and humidity ratio were about 26°C and 12g/kg, respectively. The results meet human thermal comfort well.

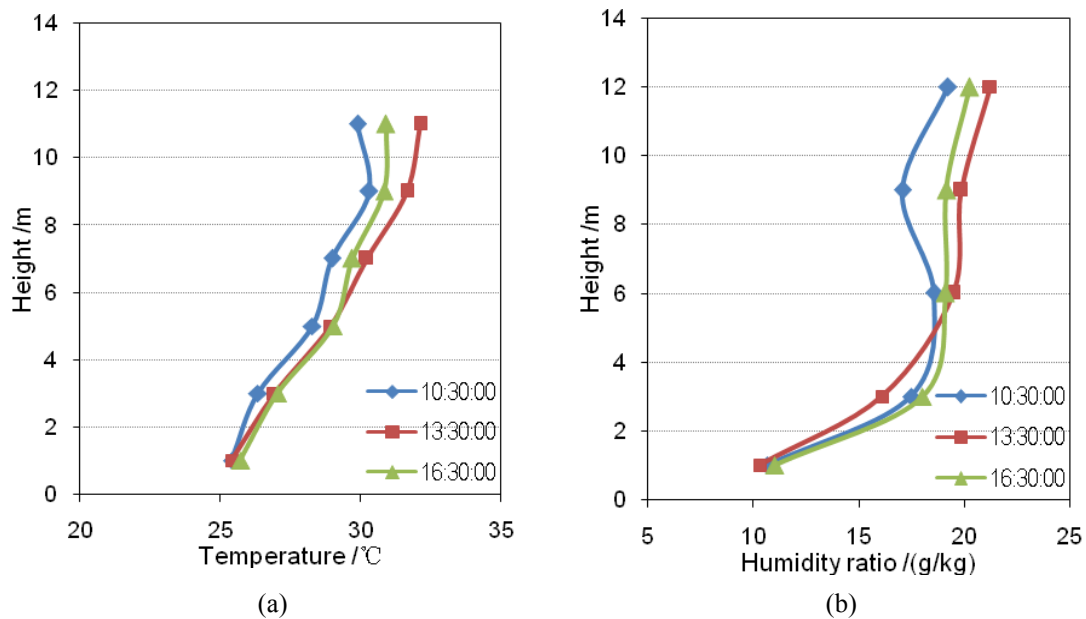


Fig. 0-14 Temperature and humidity ratio distribution in the vertical direction of the vestibule: (a) temperature; (b) humidity ratio.

Both the temperature and humidity ratio increased fast along the vertical direction, which reached about 30°C and 20g/kg at the height of 10m. And the peak temperature at top space (above 7 m) occurred at noon, due to the strong solar radiation and high ambient temperature. According to the test results, the THIC system applied in large space is effective on energy-saving, which only keeps the occupied zone in comfort condition and forms apparent stratification of indoor temperature and humidity ratio along the vertical direction. Moreover, the natural ventilation from the shutters contributed to removal of the absorbed heat from decorations to outdoor environment.

### 1.2.2 Energy efficiency of humidity control subsystem

The performances of the liquid desiccant outdoor air units were tested one by one according to the measured flow rates, air inlet and outlet parameters through the processor and input power of compressors, solution pumps and fans. The tested results of seven outdoor air units are summarized in Table 0-2; the other two processors are neglected due to the difficulty of installing the sensors.

Table 0-2 Performance of the outdoor air handling units (outdoor condition: 29.3°C and 20.3g/kg)

Location	Supply outdoor air			Cooling capacity /kW	Power consumption /kW		$COP_{air}$	$TC_{fan}$	$COP_{hum}$
	Flow rate /( $m^3/h$ )	Temperature /°C	Humidity ratio /(g/kg)		Compressors and solution pumps	Fans			
East side of 2 <sup>nd</sup> floor	5059	17.1	6.2	82.6	17.8	2.2	4.7	37.5	4.2
West side of 2 <sup>nd</sup> floor	5195	16.7	6.1	86.0	17.6	2.3	4.9	37.4	4.3
East side of 3 <sup>rd</sup> floor	4972	16.8	6.5	80.4	18.2	2.2	4.4	36.5	4.0
West side of 3 <sup>rd</sup> floor	5215	16.6	6.2	86.4	17.6	2.2	4.9	39.3	4.4
East side of 4 <sup>th</sup> floor	4261	16.7	6.4	69.5	15.0	1.7	4.6	40.9	4.2
Middle side of 4 <sup>th</sup> floor	1940	16.5	6.2	32.1	7.1	0.9	4.5	35.7	4.0
West side of 4 <sup>th</sup> floor	4307	16.3	6.1	72.0	15.3	1.8	4.7	40.0	4.2

The east side processor of the 2<sup>nd</sup> floor is a typical example for the outdoor air unit, and its specific operation information is shown in Table 0-3. The outdoor air flow rate was 5059m<sup>3</sup>/h, the outdoor air parameters were 29.3°C and 20.3g/kg, and the supply air parameters were 17.1°C and 6.2g/kg. So the cooling capacity ( $Q_{air}$ ), calculated by energy balance equation, was 82.6kW. The power consumption of compressors together with solution pumps ( $P_{air}$ ) inside the processor was 17.8kW, and the power consumption of the supply air and exhaust air fans ( $P_{fan}$ ) was 2.2kW. Therefore, the performance of the outdoor air unit ( $COP_{air}$ ), the transport coefficient of fans ( $TC_{fan}$ ) and the performance of the entire humidity handling process ( $COP_{hum}$ ), as shown in Eqs. (0-1)~ (0-3), are 4.7, 37.5 and 4.2, respectively.

**Error! Objects cannot be created from editing field codes.** (0-1)

**Error! Objects cannot be created from editing field codes.** (0-2)

**Error! Objects cannot be created from editing field codes.** (0-3)

Table 0-3 Operation condition of a typical outdoor air handling unit (east side of 2nd floor)

Outdoor condition	Supplied outdoor air	Stage	Evaporating temperature /°C	Condensing temperature /°C	Solution parameter (temperature & concentration)	
Temperature: 29.3°C Humidity ratio: 20.3g/kg	Temperature: 17.1°C Humidity ratio: 6.2g/kg Flow rate: 5059m <sup>3</sup> /h	I	11.0	50.8	Dehumidification module	Inlet: 15.8°C, 34.6% Outlet: 20.5°C, 34.4%
					Regeneration module	Inlet: 44.2°C, 34.9% Outlet: 38.3°C, 35.2%
		II	4.4	51.3	Dehumidification module	Inlet: 9.0°C, 44.1% Outlet: 14.0°C, 43.9%

As shown in Table 0-2, the  $COP_{air}$  of the tested seven outdoor air units were in the range of 4.4~4.9, the  $TC_{fan}$  of the fans are 35~40, and the  $COP_{hum}$  of the entire humidity handling processes were 4.0~4.4.

According to the tested data and rated parameters of the outdoor air units and fans, the calculated cooling capacity of the entire humidity control subsystem was 773.0kW with total inside compressors and solution pumps input power of 166.9kW and total fans input power of 20.0kW, so the coefficient of performance of the humidity control subsystem ( $COP_{HUM}$ ), shown in Eq. (0-4), is 4.1.

**Error! Objects cannot be created from editing field codes.** (0-4)

Similarly, on the basis of the tested data, the  $COP_{HUM}$  under the design condition was 4.1, with the calculated cooling capacity of 915.0kW, total inside compressors and solution pumps input power of 194.4kW and total fans input power of 25.1kW.

### 1.2.3 Energy efficiency of temperature control subsystem

The performances of the chiller, cooling tower, cooling & chilled water pumps and indoor dry FCUs were measured, based on the measured flow rates, water inlet and outlet parameters through the chiller and input powers of above facilities. The tested results of each device, under both partial load condition and design condition, are listed in Table 0-4.

Table 0-4 Performance of the temperature control subsystem

	Cooling capacity	Device	Power consumption	Tested performance	Comments
Partial load condition	$Q_{CH}=446.1$ kW	Chiller	$P_{CH}=52.5$ kW	$COP_{CH} = \frac{Q_{CH}}{P_{CH}} = 8.5$	Outdoor: 29.3°C, 20.3 g/kg Chilled water flow rate: 239 m <sup>3</sup> /h Cooling water flow rate: 180 m <sup>3</sup> /h Chilled water temperatures: 17.5°C /19.1°C Cooling water temperatures: 31.0°C /33.3°C
		Cooling tower	$P_{CT}=3.7$ kW	$TC_{CT} = \frac{Q_{CH} + P_{CH}}{P_{CT}} = 134.8$	
		Cooling water pump	$P_{CTP}=14.6$ kW	$TC_{CTP} = \frac{Q_{CH} + P_{CH}}{P_{CTP}} = 34.2$	
		Chilled water pump	$P_{CWP}=30.6$ kW	$TC_{CWP} = \frac{Q_{CH}}{P_{CWP}} = 14.6$	
		Fan coil units (serve 81% of the $Q_{CH}$ )	$P_{FCU}=19.4$ kW	$TC_{FCU} = \frac{0.81 \times Q_{CH}}{P_{FCU}} = 18.6$	
Very hot and humid condition	$Q_{CH}=543.4$ kW	Chiller	$P_{CH}=63.8$ kW	$COP_{CH} = \frac{Q_{CH}}{P_{CH}} = 8.5$	Outdoor: 34.9°C, 21.6 g/kg Chilled water flow rate: 260 m <sup>3</sup> /h Cooling water flow rate: 180 m <sup>3</sup> /h Chilled water temperatures: 17.5°C /19.3°C Cooling water temperatures: 32.9°C /35.7°C
		Cooling tower	$P_{CT}=3.7$ kW	$TC_{CT} = \frac{Q_{CH} + P_{CH}}{P_{CT}} = 147.0$	
		Cooling water pump	$P_{CTP}=14.4$ kW	$TC_{CTP} = \frac{Q_{CH} + P_{CH}}{P_{CTP}} = 37.7$	
		Chilled water pump	$P_{CWP}=29.4$ kW	$TC_{CWP} = \frac{Q_{CH}}{P_{CWP}} = 18.5$	
		Fan coil units (serve 81% of the $Q_{CH}$ )	$P_{FCU}=22.3$ kW	$TC_{FCU} = \frac{0.81 \times Q_{CH}}{P_{FCU}} = 24.4$	

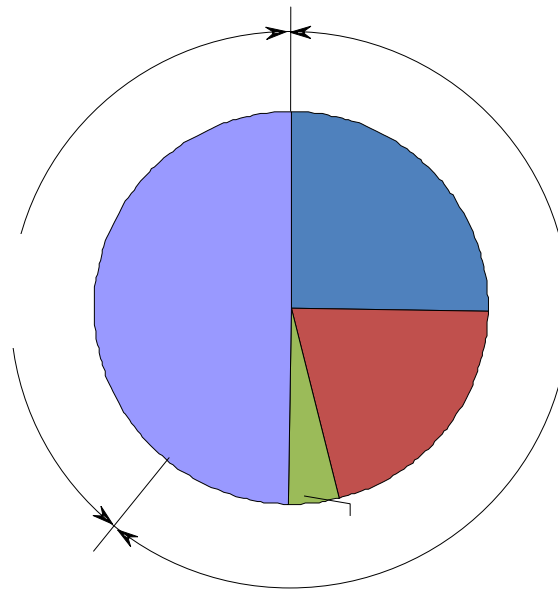
According to the tested data under the partial load condition, the calculated cooling

capacity of the temperature control subsystem ( $Q_{CH}$ ) was 446.1kW with total input power of 120.8kW. So the  $COP$  of the temperature control subsystem ( $COP_{TEMP}$ ), as shown in Eq. (0-5), was 3.7. The  $COP_{TEMP}$  under the design condition was 4.1, with the calculated cooling capacity of 543.4kW and overall power consumption of 133.6kW.

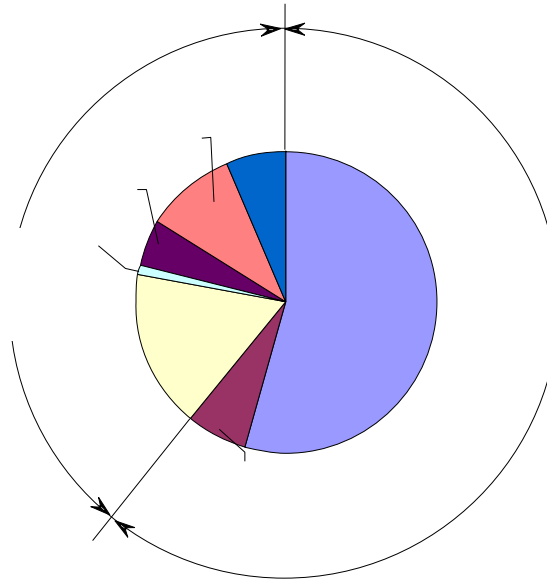
**Error! Objects cannot be created from editing field codes.** (0-5)

#### 1.2.4 Energy efficiency of the entire THIC system

The entire load of the building is composed of the latent load and sensible load. The former consists of both the moisture introduced by outdoor air and produced from occupants, and the latter is caused by the ventilation, heat transfer, solar radiation, heat dissipation of devices and activity of occupants etc, as illustrated in Fig. 0-15. In the THIC system, processed outdoor air is used to remove the entire latent load and part of the sensible load, while cooling plant provides high temperature chilled water to remove the rest sensible load. By calculation, under the partial load condition, the humidity control subsystem removed 63% of entire cooling load with 61% environmental control energy consumption, and the temperature control subsystem removed the rest 37% load with the rest 39% energy consumption. The same conclusion also can emerge from the test of design point.



(a)



(b)

Fig. 0-15 Cooling load and power consumption of the THIC system: (a) cooling load proportion; (b) power consumption proportion.

Calculated from the above tested data, the overall COP of the THIC system ( $COP_{SYS}$ ) under partial load condition and design condition were 4.0 and 4.1, respectively, as shown in Eq. (0-6).

**Error! Objects cannot be created from editing field codes.** (0-6)

Based on the tested results of these two typical operating conditions, it is convinced that the THIC system in this office building has achieved a high efficiency with its total COP over 4.0. By comparison, the measured average coefficient of performance of whole system in traditional fan-coil systems is usually around 3.0. Therefore, there is a remarkable energy efficiency improvement of the THIC system comparing with the conventional system.

### 1.3 Energy consumption of the THIC system

Energy consumption of the THIC system was measured by the power metering monitoring system. Fig. 0-16 shows the monthly power consumption of the system from 15<sup>th</sup> April to 15<sup>th</sup> October (apart from weekends and statutory holidays). The total energy consumption was 425,000kWh during the cooling season, and the humidity control subsystem occupied 61% of the total power consumption which was proportional to the ratio of cooling load that the humidity control subsystem undertook.

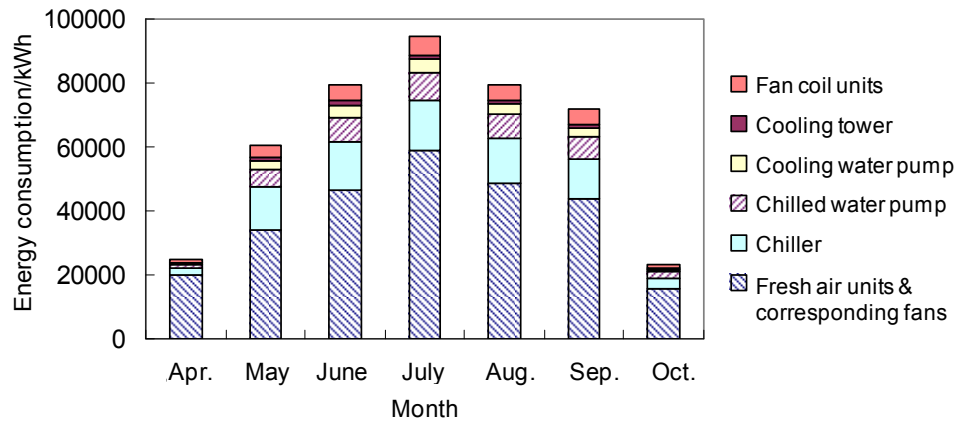


Fig. 0-16 Monthly power consumption of the THIC system.

The annual energy consumption in unit building area and unit net air-conditioning area of the tested THIC system were  $22.6\text{kWh}/(\text{m}^2\cdot\text{yr})$  and  $32.2\text{kWh}/(\text{m}^2\cdot\text{yr})$ , respectively. However, the average energy consumption levels of office building of the similar building envelope and occupant density during the same time in Shenzhen were around  $42\sim 49\text{kWh}/(\text{m}^2\cdot\text{yr})$  according to the investigated results. Therefore, the THIC system in this office building achieved noticeable energy saving in operation compared with the conventional air-conditioning system, and the added cost can be recalled within two years.

## 1.4 Discussions

According to our knowledge, cooling air can be realized more easily than dehumidification by condensation, since the latter one requires lower temperature of cooling source than the former. However, the COP of the tested temperature control subsystem is lower than that of the humidity control subsystem in present THIC system. Thus, this section focuses on how to improve the performance of the temperature control subsystem.

According to the performance of each component in the temperature control subsystem shown in Table 0-4, three main improvements of the temperature control subsystem are recommended: (1) reducing the frequency of the chilled water pump; (2) improving the cooling tower performance by tightening the strap of the fan's belt; and (3) improving the performance of FCUs under dry working condition. The first two methods can be easily achieved in the building, while the third one depends on the improvement of new FCU products.

### 1.4.1 Improve the performance of chilled water pump

As indicated in Fig. 0-15(b) and Table 0-4, the power consumption of the chilled water pump was near 60% of the chiller. It was because the variable-speed pump has operated at 50Hz in the past that the chilled water temperature difference between the inlet and outlet of chiller was only  $1.6\sim 1.8^\circ\text{C}$ , while the designed value was  $3.0^\circ\text{C}$ . Therefore, the power consumption of the chilled water pump can be considerably cut down after reducing the chilled water flow rate by frequency regulation. For instance, the energy savings of the chilled water pump could be up to 42%, if the transport coefficient of chilled water pump ( $TC_{\text{CWP}}$ ) is increased from the current 14.6 to an empirical value of 25.

### 1.4.2 Improve the performance of cooling tower

According to Table 0-4, the transport efficient of cooling tower ( $TC_{CT}$ ) was near 140, which was lower than the empirical index of 200. Detailed performance test was then launched. For the cooling tower, the mass flow rate ratio of air to water was 0.55, with air flow rate of 99,620kg/h and water flow rate of 180,000kg/h, and the temperatures of inlet water, outlet water and outdoor air wet bulb were 35.6°C, 32.9°C and 28.3°C, respectively. Hence, the efficiency of the cooling tower (the temperature variance of the cooling water divided by the possible maximal temperature variance) was  $(35.6-32.9)/(35.6-28.3)=37\%$ . By field survey, the low air flow rate, which led to low efficiency of the cooling tower, was caused by the loose strap of fan.

The energy consumption of the cooling tower in the entire air-conditioning system is relatively small, but it seriously influences the chiller performance by affecting the condensing temperature. The expected efficiency of the cooling tower can be higher than 55% if the air flow rate increases to about 180,000 kg/h, and thus the condensing temperature can decrease at least 2°C. As a result, the COP of the chiller ( $COP_{CH}$ ) can be increased from current 8.5 to 9.3.

### 1.4.3 Improve the performance of FCU

As the chilled water inlet temperature is higher than the indoor dew point temperature in this THIC system, fan coil units that operate under dry working condition are put into use in this building to remove large part of the sensible load of the building. At present, the configuration of the adopted dry FCUs is similar to the originally wet FCUs (with standard chilled water inlet temperature of 7°C and transport coefficient of 50). However, the tested transport coefficient of the dry FCUs ( $TC_{FCU}$ ) was around 20, as shown in Table 0-4. Factually, the configuration of dry FCUs should be rather different from wet FCUs, since condensing water no longer exists in dry FCUs, and some dry FCUs with new configuration have appeared with  $TC_{FCU}$  close to 50. So there is a huge potential to improve the performance of dry FCU with the transport coefficient increased to around 40.

The contribution of the above three improvements to the temperature control subsystem is summarized in Table 0-5. And the expected  $COP_{TEMP}$  and  $COP_{SYS}$  can be increased to 4.8 and 4.4 after these alterations, respectively. Therefore, the energy consumption of the altered temperature control subsystem can save 23% compared to present situation, and the entire THIC system can save 9% compared to its performance at present.

Table 0-5 Improvement of the temperature control subsystem

		Chiller	Cooling tower	Cooling water pump	Chilled water pump	Fan coil units
Partial load condition	Present power consumption /kW	52.5	3.7	14.6	30.6	19.4
	Expected power consumption /kW	47.7 ( $COP_{CH}$ increases from 8.5 to 9.3)	3.7	14.6	17.8 ( $TC_{CWP}$ increases from 14.6 to 25)	9.0 ( $TC_{FCU}$ increases from 18.6 to 40)
Very hot and humid condition	Present power consumption /kW	63.8	3.7	14.4	29.4	22.3
	Expected power consumption /kW	58.4 ( $COP_{CH}$ increases from 8.5 to 9.3)	3.7	14.4	21.7 ( $TC_{CWP}$ increases from 18.5 to 25)	13.6 ( $TC_{FCU}$ increases from 24.4 to 40)

## 1.5 Conclusion

The operating performance of the THIC system in an office building in Shenzhen is presented in this section. Liquid desiccant outdoor air units are used to supply dry outdoor air to control indoor humidity, and chilled water with the temperature of 17.5°C is pumped and distributed into radiant panels and dry fan coil units to control indoor temperature. The followings are the conclusions based on the tested results:

- 1) The THIC system can provide a comfortable indoor environment that indoor temperatures, humidity ratios as well as CO<sub>2</sub> concentrations were all within the comfortable ranges.
- 2) The *COP* of the entire THIC system can reach 4.0, with the *COP* of the temperature control subsystem and humidity control subsystem of 3.7~4.1 and 4.1 respectively. The energy consumption of the THIC system in the tested office building was 32.2kWh/(m<sup>2</sup>·yr) (net air-conditioning area), that was, the energy efficiency was much higher than that of the conventional air-conditioning system available in literature.
- 3) Possible improvements of the temperature control subsystem are provided, including modification on the chilled water pump, cooling tower and FCUs. Thus, the expected system *COP* can be further increased to 4.4, which can save 9% compared to present air-conditioning system.

## 2 Application in an office building (China)

### 2.1 Description of the system

#### 2.1.1 Basic information



Fig. 0-17 Outlook of Antaeus low energy building

Antaeus low energy building is an office building, located in Jinan, Shangdong Province. The building has a total building area of 5,450 m<sup>2</sup>, 4,583 m<sup>2</sup> above ground and the air conditioning area is 3,815 m<sup>2</sup>. It has six floors: one underground floor and five that are above ground. As a typical office building, it includes five meeting rooms, others are office rooms. Fig. 0-17 shows the outlook of the office building. Table 0-6 gives some detailed information

of different floors.

Table 0-6 Detailed information of different floors

Floor	Area(m <sup>2</sup> )	Person	Lighting(W/m <sup>2</sup> )	Equipment(kW)	Working time
F1	892.16	2	10		8:30-17:30
F2	819.05	15	10	1	8:30-17:30
F3	919.21	55	10	5	8:30-17:30
F4	918.42	38	10	5	8:30-17:30
F5	918.42	10	10	5	8:30-17:30
B1	Equipment room for HVAC system				

### 2.1.2 Air-conditioning system

During cooling season (May 15<sup>th</sup> to September 15<sup>th</sup>), THIC air-conditioning system is employed in this building. In this THIC system, outdoor air is dehumidified by a fresh air handling unit and then the dry fresh air is supplied into the indoor environment for humidity control. Radiant floors are used for temperature control in the THIC system. The 7°C chilled water in fresh air handling system is made by heat pumps and the 18°C supply water in radiant floors is from made by the ground heat exchangers and buried tubes. Fig. 0-18 shows operating schematic of air conditioning system in summer.

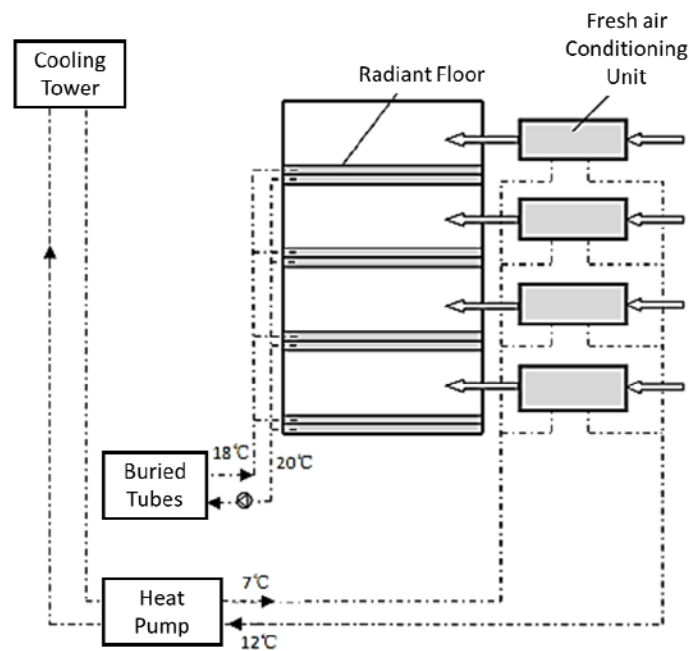


Fig. 0-18 Schematic of air conditioning system in summer

During heating season (November 15<sup>th</sup> to March 15<sup>th</sup>), air-conditioning is operated as Fig. 0-19. Heat pump evaporator absorbs low temperature heat from the underground buried tubes and then condenser supplies 40°C warm water to the radiant floor and fresh air handling unit.

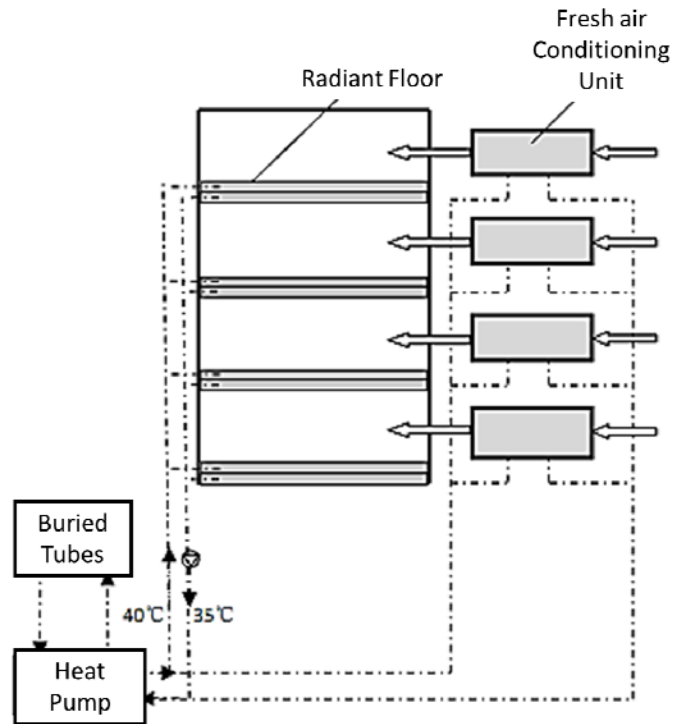


Fig. 0-19 Schematic of air conditioning system in winter

## 2.2 Performance in summer

This air-conditioning system consists of 2 parts, the buried tubes direct supply system and the fresh air system. In the buried tubes direct supply system, water pump is the only energy consuming device and the fresh air system consists of heat pumps, chilled water pump, AHU fan, cooling water pump and cooling tower.

Table 0-7 shows the annual cooling capacity and energy consumption of buried tubes system and fresh air system.

Table 0-7 Detailed information of different floors

	Buried tubes system	Fresh air system	Total
Cooling capacity per unit area $\text{kWh}_c/(\text{m}^2 \cdot \text{a})$	25.4	8.9	34.3
Power consumption per unit area $\text{kWh}/(\text{m}^2 \cdot \text{a})$	1.3	4.3	5.6
EER	19.3	2.1	6.1

Fig. 0-20 gives detailed power consumption distribution of different devices in the fresh air system.

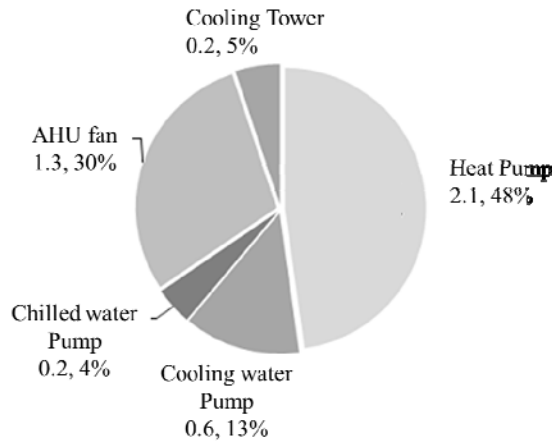


Fig. 0-20 Schematic of air conditioning system in winter

### 2.2.1 Cooling capacity measurement data of buried tube system

Buried tube system consists of 56 drill holes and the total length is 5600m. It is separated into 2 loops: South loop (36 drill holes) and North loop (20 drill holes). Water pump in buried tube system keeps operating day and night, and during the nighttime it operates to store cooling capacity for daytime. Fig. 0-21 to Fig. 0-23 gives continuous measurement data of water flow rate, supply water temperature and return water temperature in above 2 loops respectively. It could be seen that the supply temperature only raise in a small amount along summer and keeps around 18°C during the whole cooling season. And the cooling capacity during summer of 2013 is shown in Fig. 0-24, total cooling capacity of buried tube system is 96.8Mwh, namely 25.4kWh/m<sup>2</sup>.

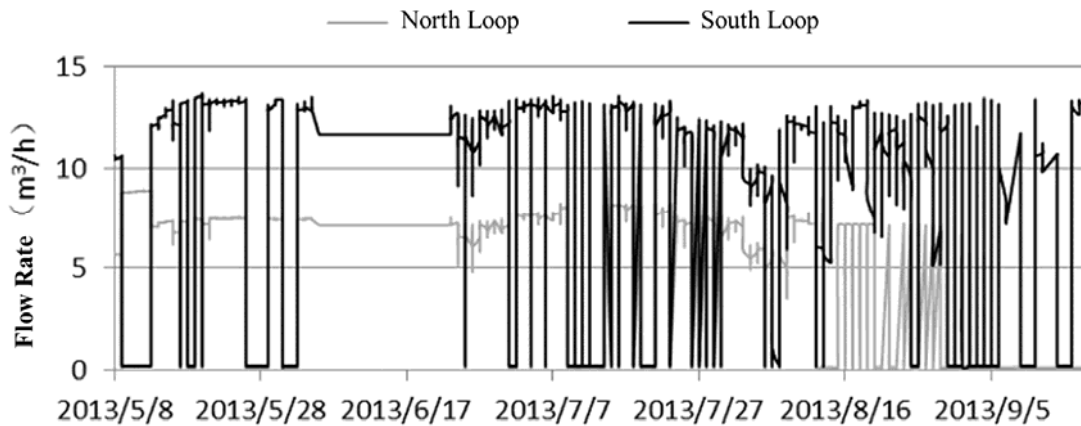


Fig. 0-21 Flow rate data in 2013

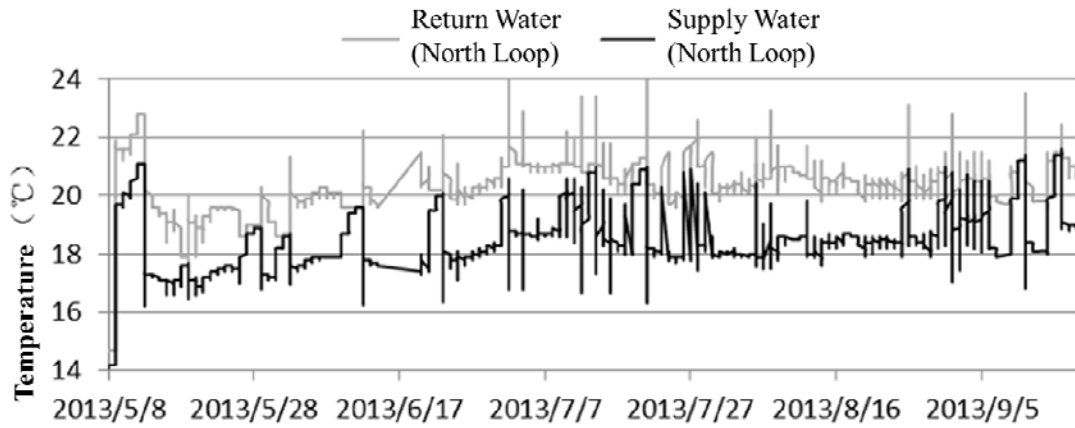


Fig. 0-22 Return and supply water temperature of north loop in 2013

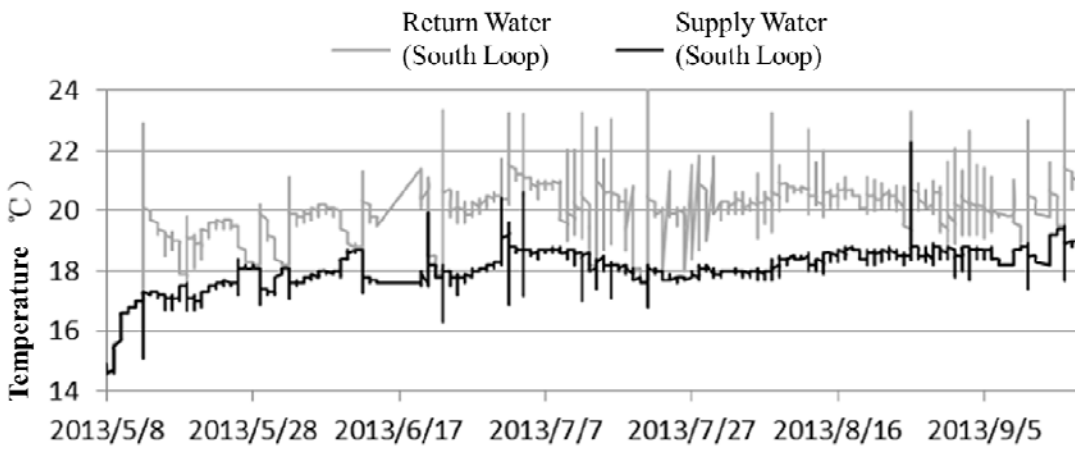


Fig. 0-23 Return and supply water temperature of south loop in 2013

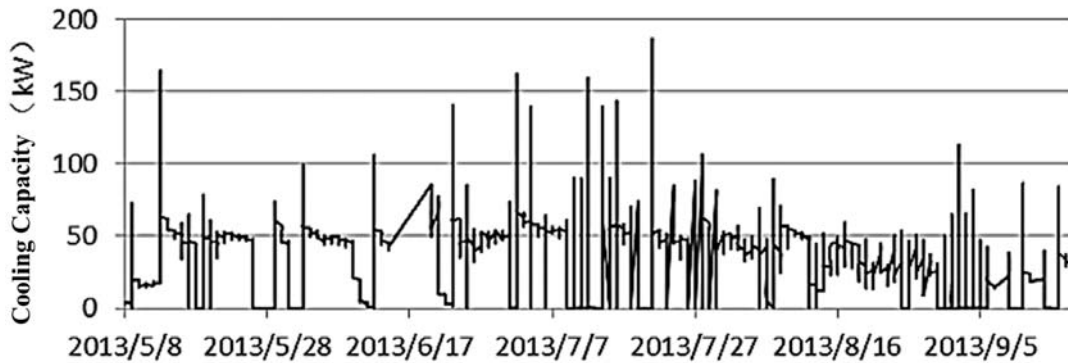


Fig. 0-24 Cooling capacity of buried tube system in 2013

### 2.2.2 Cooling capacity measurement data of fresh air system

Cooling capacity in summer of 2013 is given in Fig. 0-25. In Jinan, the humidity ratio of fresh air is relatively low in May, June and August, so the fresh air system is not employed during these three months. Thus cooling capacity during whole cooling season in 2013 amounts to 34.1MWh, namely 8.9kWh/m<sup>2</sup>.

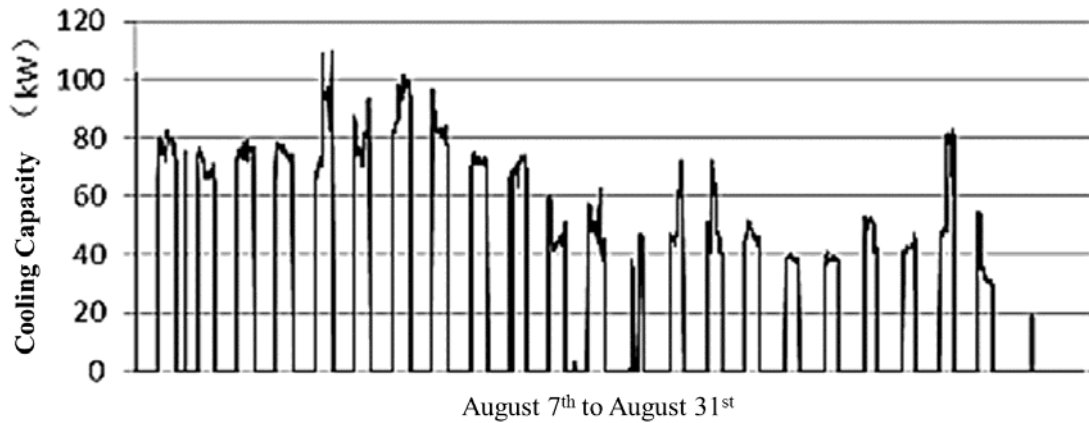


Fig. 0-25 Cooling capacity of fresh air system in 2013

### 2.3 Performance in winter

Fig. 0-26 has shown heating capacity of the heat pump and heat absorbed from buried tubes from December 22<sup>nd</sup>, 2012 to March 15<sup>th</sup>, 2013. Thus, heating capacity of the whole heating season is 35.8kWh/m<sup>2</sup>, electricity consumption is 10.9kWh/m<sup>2</sup> and the average heating COP is 3.28.

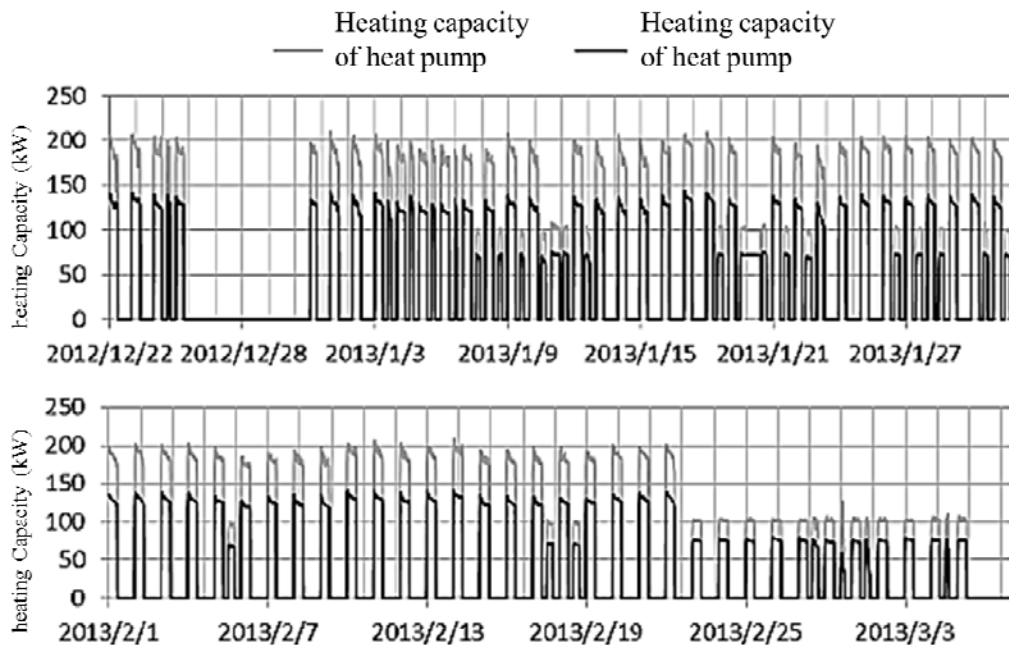


Fig. 0-26 heating capacity of heat pump and buried tubes in 2013

### 2.4 Conclusion

The air-conditioning system in Antaeus office building has been used since December 2011, and an advanced THIC system is employed in this building. Performances of this system both in summer and in winter are investigated in this section and the main conclusions can be summarized as follows:

1) In summer, ground water (18°C) serves as the high temperature cooling source through heat exchanger directly for radiant floor, thus that only water pump consuming power, ground water offers over 70% of the cooling load with a COP as high as 20. Besides the humidity control is guaranteed by fresh air handling unit. In winter, this system utilizes heat

pump to absorb heat from ground buried tubes and supplies low temperature heating water (40°C) to radiant floor.

2) Total energy consumption of this building is much smaller than regular office building. Cooling capacity during whole cooling season in 2013 amounts to 34.1MWh, namely 8.9kWh/m<sup>2</sup> and the average COP of whole air-conditioning system is 6.1. Heating capacity of the whole heating season is 35.8kWh/m<sup>2</sup>, electricity consumption is 10.9kWh/m<sup>2</sup> and the average heating COP is 3.28.

3) Compared with conventional system, system in this building shows advantages in two aspects. On one hand, low-cost utility of geothermal energy to produce high temperature cooling water (18°C) to radiant floor largely cuts down the electricity consumption in summer. And on the other hand, ground source heat pump has higher energy efficiency than common air source heat pump because of the high evaporation temperature.

### **3 Application in a building (Japan)**

#### **3.1 Introduction**

The “Temperature and Humidity Individual Control (THIC) system” is developed to reduce the energy consumption for air conditioning. THIC system is consisted of the sensible capacity enhanced VRF (multi-split type air-conditioning system) and HP desiccant (humidity controllable outdoor air processing unit). It can control sensible and latent heat individually.

THIC system is realized by the new technologies as below:

/ Improvement of efficiency of multi-split type air-conditioning system at partial load condition

/ Improvement of efficiency of humidity controllable outdoor air processing unit

/ Development of controller for the optimized operation of VRF and HP desiccant

The demonstration test is carried out in the office of Nagoya University in Japan by installing the THIC system and the conventional air-conditioning system (which is consisted of the conventional VRF and the heat recovery ventilator with humidification function) in the adjacent rooms and performance is compared each other.

As a result, THIC system reduced the energy consumption by 47% and provided more comfortable indoor condition by controlling the humidity appropriately in summer. And also THIC system reduced the energy consumption by 26% in winter.

#### **3.2 Composition of the THIC system**

In this section, the THIC system consisted of the humidity controllable outdoor air processing unit (HP desiccant) which mainly treats the latent heat load and the sensible capacity enhanced VRF which mainly treats the sensible heat load. These two mechanisms are appropriately operated by the controller to simultaneously maintain the comfort of the room and save energy. The system composition is shown in Fig. 0-27.

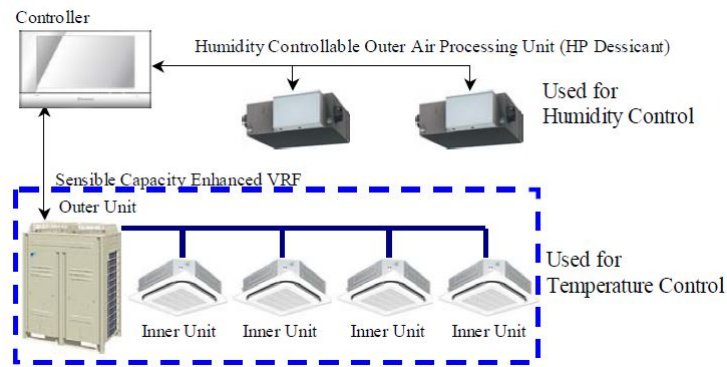


Fig. 0-27 Composition of Temperature and Humidity Individual Control System

### 3.3 Demonstration test

The demonstration test was carried out to assure the effectiveness of the developed THIC system. The test was conducted in cooperative with Nagoya University and Nikken Sekkei Research Institute, under the subsidy of NEDO (New Energy and Industrial Technology Development Organization).

The test site was the office in Nagoya University. We divided one room into two for the comparison of the conventional system and the THIC system as shown in Fig. 0-28.

For the eastern area of the office (right hand area), a combined system of conventional VRF and HRV with humidifier was installed as a conventional system. For the western area (left hand side), a combined system of HP desiccant and sensible capacity enhanced VRF was installed as a THIC system. The area of two rooms isn't equal, therefore energy performance of system was discussed by using the value per area.

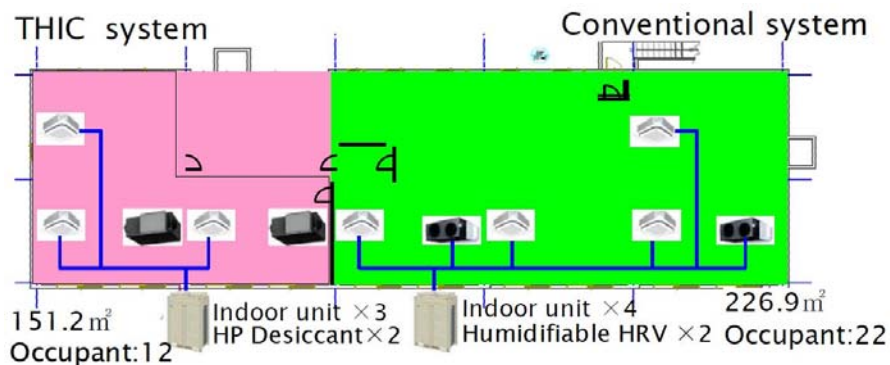


Fig. 0-28 Outline of Field Test Site

#### 3.3.1 Results of test in summer

##### a) Indoor Condition

Fig. 0-29 and Fig. 0-30 show the comparison of the indoor conditions of conventional and THIC systems, respectively. In the case of the set point temperature is 28°C, the conventional system cannot provide adequate dehumidification capacity. And with the set temperature of 26°C, the conventional system over-dehumidifies the room air and consumes

too much electricity. On the contrary, the THIC system can control the indoor condition around the edge of the target conditions region on both set temperatures.

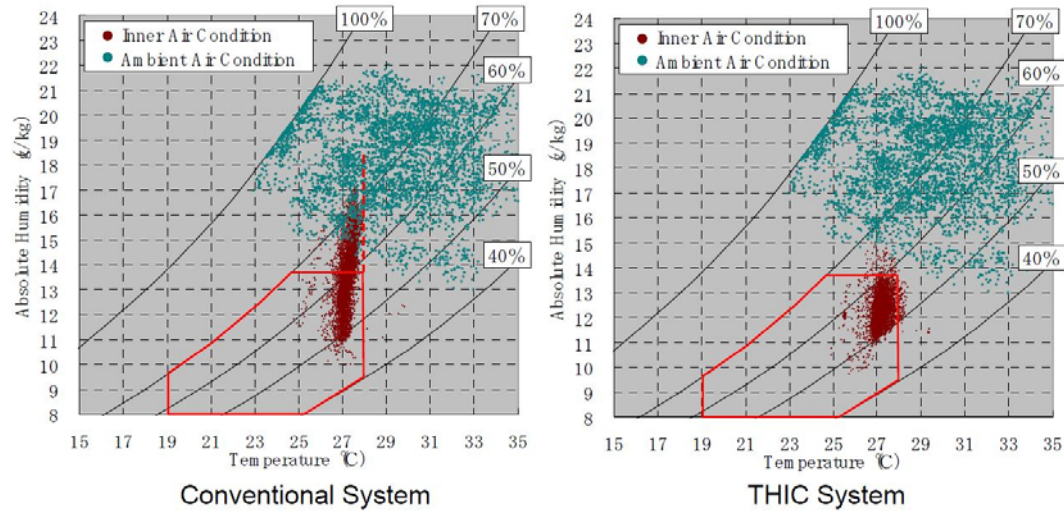


Fig. 0-29 Indoor Condition (Set Temperature is 28°C)

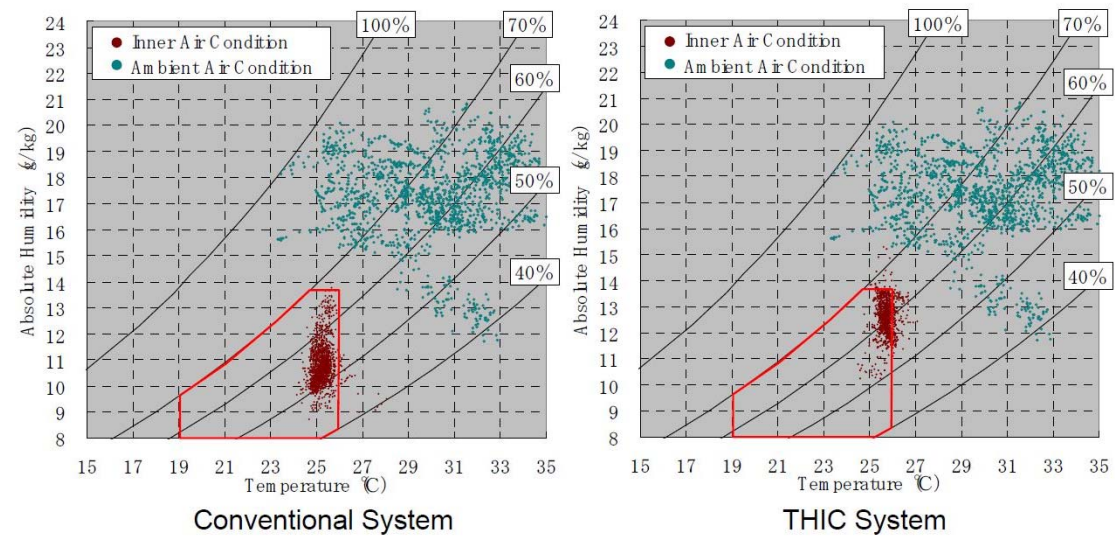


Fig. 0-30 Indoor Condition (Set Temperature is 26°C)

In Japan, it was common to set the target temperature to 26°C. However after the 3.11 disaster, it became common to set it to 28°C to correspond with the lack of electricity. The result shows that the conventional air conditioning system, without humidity control function, cannot maintain a comfortable air condition in a humid summer like in Japan, when the set temperature is 28°C.

b) Energy Consumption

Fig. 0-31 shows the comparison of the integrated energy consumption of the test period. The energy consumption can be reduced by approximately 50% with the THIC system during summer test.

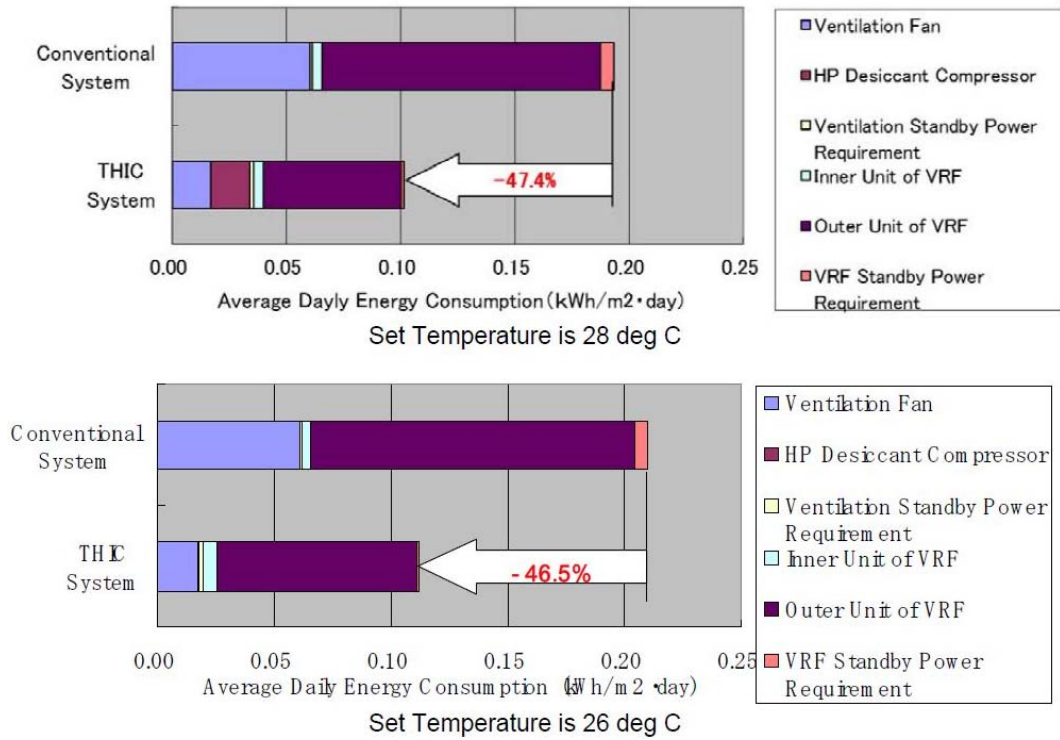


Fig. 0-31 Daily Energy Consumption

### 3.3.2 Results of test in winter

The winter test is carried out from December to February, also by measuring the temperature and the humidity of the room and energy consumption.

#### a) Indoor Condition

Fig. 0-32 shows the comparison of the indoor room conditions of the conventional and THIC systems, respectively. Different from the results of the summer test, by using the HRV with the function of humidify both the conventional and THIC system can control the indoor air to the target condition.

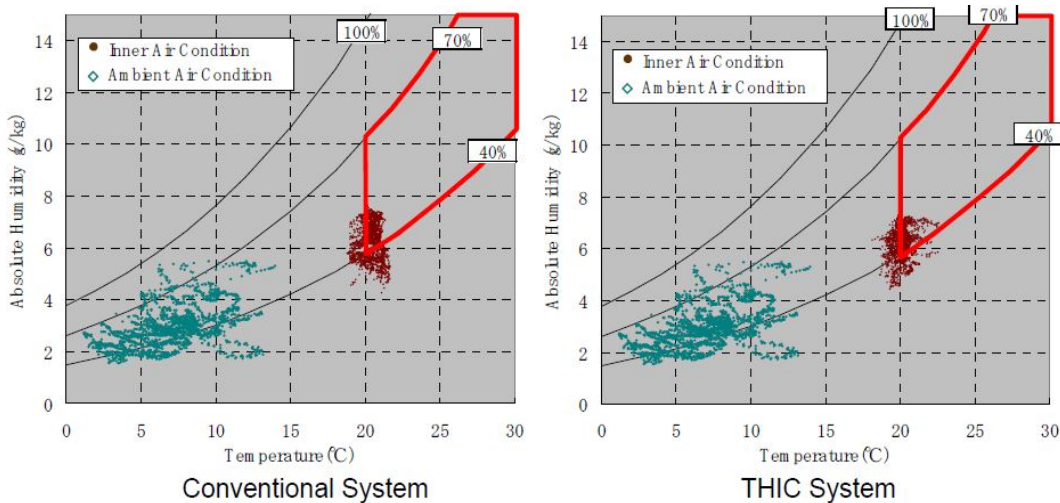


Fig. 0-32 Indoor Air Condition (Set Temperature is 20°C)

## b) Energy Consumption

Fig. 0-33 shows the comparison of the total energy consumption of the test period. The energy consumption can be reduced by approximately 30% with the THIC system during winter test.

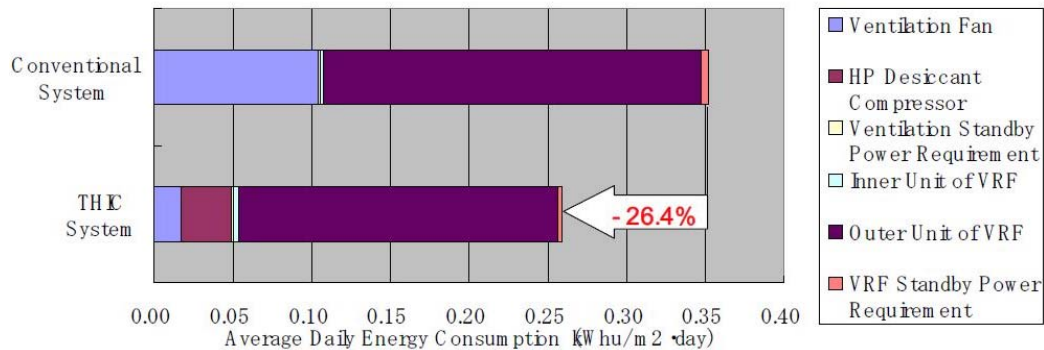


Fig. 0-33 Daily Energy Consumption

## 3.4 Conclusion

The developed THIC system can maintain a comfortable inner air condition and drastically reduce the energy consumption at the same time.

## 4 Application of solar thermal system application (Italy)

### HIGH TEMPERATURE COOLING AND LOW TEMPERATURE HEATING SYSTEMS

#### 4.1 SYSTEM TYPE

*Type:*

Solar thermal system with storage tank for exploitation of renewable energy.

Low temperature heating from renewable sources.

*Application:*

This system is at the prototypal phase.

After a conceptual/design phase, a full scale prototype was built in the laboratories of the Department of Energy at the Politecnico di Torino.

The system is intended for space heating only. It provides control over the air temperature (sensible loads). It does not provide any control over the relative humidity (latent heat loads). To control RH, coupling with another system is required (separate control of T and RH).

#### 4.2 BRIEF DESCRIPTION

Solar thermal collector are the most common device for converting solar energy into thermal energy. The proposed system is suitable for the application of a solar thermal system coupled with low temperature radiant heating panels for space heating.

Phase change materials (PCMs) have long been used for thermal energy storage due to the large amount of heat they absorb or release during their phase transition. They can be chosen to select the most suitable phase change temperature range for a specific application. PCMs can be organic materials (paraffin or non-paraffin) as well as inorganic materials. In recent years, PCMs have been developed into an always liquid form to increase the heat transfer rate by rising the surface to volume ratio. This binary system is called micro-encapsulated phase change slurry (mPCS).

The application of PCMs and PCSs in solar thermal systems was studied and developed just in the storage tank. Generally, they were coupled with traditional HTFs (water or water-glycol) in the primary loop of the solar collector. Nevertheless, this strategy implies exchanges with finite temperature differences between the HTF flowing inside the solar collector loop and the PCM storage as well as between the storage and the carrier fluid flowing to the terminal units. These heat exchanges introduce irreversibilities and energy-exergy losses. To avoid these inefficiencies and reduce the overall temperature difference, a thermal solar system based only on mPCS is proposed. The mPCS can be directly used as a heat transfer fluid in the various loops of the system.

The whole slurry-PCM based system that has been conceived includes a PCM-based heat storage unit coupled with the solar collector, and a secondary, water-based circuit to supply heat to the indoor environment.

### 4.3 WORKING PRINCIPLE AND STRATEGIES

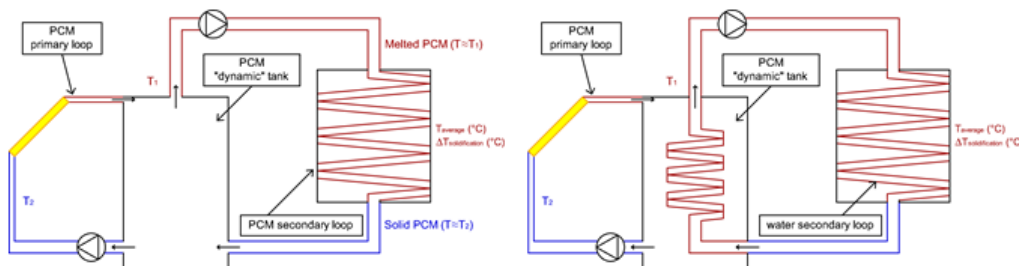


Fig. 1. (a) a two open-loops circuit; (b) an open-loop circuit with PCS and a closed-loop circuit with water

Figures 1(a) and 1(b) show two possible system configurations that can be adopted. The option described in figure 1(a) is a two open-loops circuit filled with mPCS. This option guarantees the maximum theoretical thermal efficiency due to the complete absence of finite temperature differences in the heat exchange between the primary and the secondary loops of the system. However, it is more challenging from a technological point of view than the option in figure 1(b).

In figure 1(b), an open primary loop circuit with mPCS coupled with a closed secondary loop circuit with water is shown. This configuration is less efficient from the heat transfer point of view, due to the temperature difference between storage tank and secondary HTF loop. However, the storage tank contains mPCS as well as the previous solution and it guarantees an easier technological implementation, since a water glycol solution is used inside the radiant panels. For these reasons, this last solution was adopted in the first development of the prototype.

The system works in a similar way to a traditional solar thermal collector circuit. The main difference is represented by a different HTF flowing in the pipes and in the storage tank. This requires special care, since the mPCS could be affected by problems of creaming/sedimentation, capsule rupture or increasing of the pressure drops. Moreover, in order to ensure the complete exploitation of latent heat benefits, the flow rate of HTF have to be suitably controlled. To overcome these possible drawbacks that can affect the system, some specific design solutions and control strategies were adopted.

The following figure is a conceptual scheme of the solar thermal system, the monitoring apparatus and the devices to simulate the energy demand:

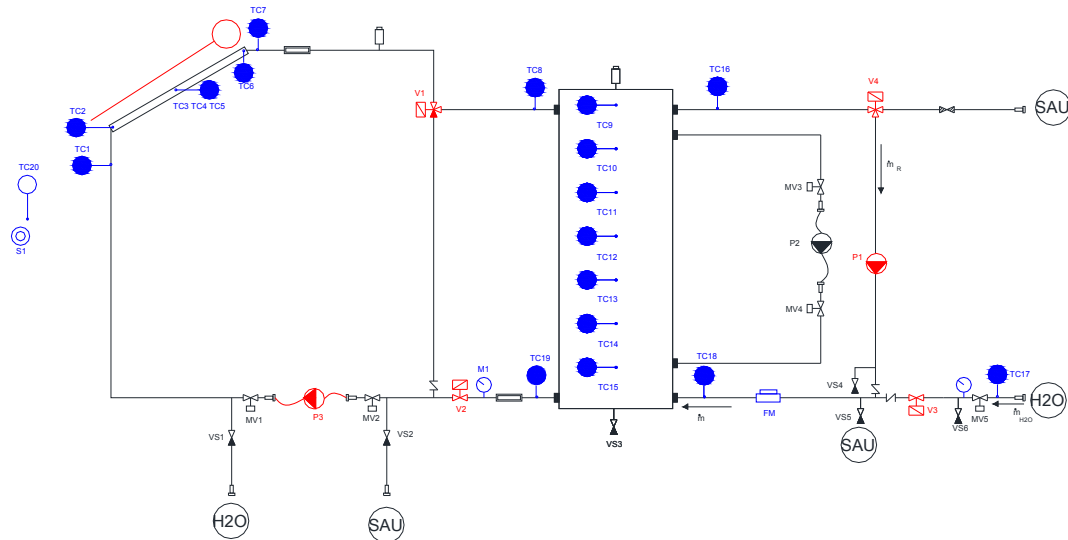


Figure 2 - Scheme of the solar thermal system.

Pumps P1 and P3 are programmable peristaltic pumps (whose flow rate can be controlled). They were adopted for further certainty of no broken microcapsules due to the pump action. These pumps have the advantage of not touching the fluid flowing inside the pipe and of stressing the capsules less than other kinds of pumps.

When the PCS is not in motion – such as in the storage tank – the problem of creaming occurs. For this reason in the design process of the prototype, the HTF was chosen to be continuously maintained in motion also in the storage tank. This was made possible by the use of partitions in the storage tank and of a bypass circuit with two controlling valves (V1 and V2) a second peristaltic pump P3, which is switched on when the main pump of the primary loop is stopped. This process implies an increase of the energy consumption, compared to the amount strictly required for the theoretical operation of the system, and a more complex pumping system.

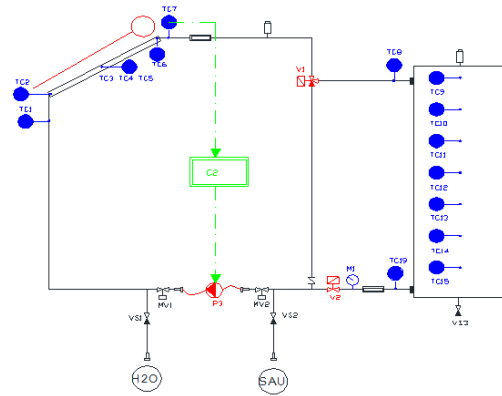


Figure 3 - The pump speed is regulated on the outlet temperature of the panel. The upper melting range temperature was chosen as optimal.

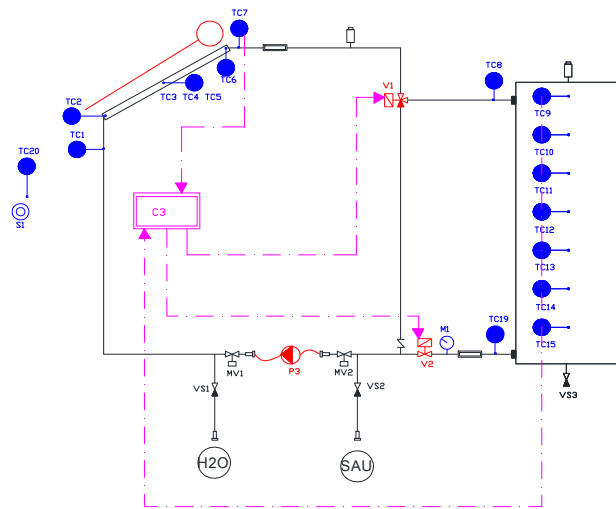


Figure 4 - Control scheme of opening/closing of the bypass circuit.

Besides, natural convection within the tank usually causes a thermal stratification in the HTF. This phenomenon is generally used to improve the heat transfer with the secondary closed loop. By maintaining the PCS in motion, this stratification of HTF in the storage tank cannot be exploited. However, the adoption of a bypass circuit was chosen because it was easiest way to overcome the creaming phenomenon. Finding a chemical solution for the creaming problem was beyond the scope of this work and it can be a proposal for the future. Furthermore, since the system is designed to exploit, as much as possible, the latent heat at constant temperature, the fact that the stratification is disrupted inside the tank does not represent a significant problems as far as the energy efficiency is concerned.

The right part of the scheme – with the controlling valves V3 and V4 and the flow meter FM – is a device adopted to simulate the time profile of the energy demand of the occupants of traditional buildings.

The schemes represented in the following figure summarize the control strategies of the system. The flow rate of the circuit is controlled by regulating the pump speed, according to solar irradiation availability. Furthermore, the controlling valves V1 and V2 close/open themselves.

#### 4.3.1 Heat sources and sinks

The heat source is the solar radiation, collected by a proper solar collector.

#### 4.3.2 Heat carrier fluid

*Type of fluid:*

Slurry PCM (PCS) is used as heat transfer fluid in the primary loop of the prototype (PCS could also be used inside the secondary loop for a different configuration, as shown in figure 1a).

The PCS is a suspension of two component: a carrier fluid and a suspended material. The carrier fluid is a mixture of water and glycol. Generally the mass percentage of glycol is related to the climate conditions of the installation location. In this paper a 40% concentration of glycol was adopted for all the simulations. This is the typical average concentration adopted for traditional panels installed in Europe (such as 2500-3000 HDD). Table shows the main properties of the heat transfer fluid.

Table 1. Specifications of the water and glycol mixture of the HTF.

Specification	Symbol	Value	M.u.
Water density	$\rho_w$	1000	kg m <sup>-3</sup>
Glycol density	$\rho_g$	1110	kg m <sup>-3</sup>
Mass percentage of glycol	$a_{gl}$	40.0	%
Mixture (water+glycol) density	$\rho_{w+gl}$	1044	kg m <sup>-3</sup>
Mixture (water+glycol) specific heat	$c_{p_{w+gl}}$	3600	J kg <sup>-1</sup> K <sup>-1</sup>
Mixture (water+glycol) conductivity	$\lambda_{w+gl}$	0.369	W m <sup>-1</sup> K <sup>-1</sup>

The suspended material in the suspension is the mPCM. It was chosen on the basis of its melting temperature. Generally, the lower HTF temperature the better system efficiency. Nevertheless, in order to allow the heat exchange with the other loops of the heating system (e.g. the radiant floor panels), the mPCS in the storage tank should remain always at a temperature slightly higher than the temperature required for the application. For example in low temperature radiant panel systems that work at 30-35°C, the minimum temperature in the thermal storage for allowing the heat exchange has to be about 38°C-40°C. To match this requirement a micro-encapsulated n-eicosane was chosen in Table 2. The n-eicosane phase-change temperature range is 36°-38°C. Several data on this material were available in literature and others were provided by the manufacturer. However, sometimes in different literature sources different values for the same property are reported. In such case the average value of the available data was adopted. Table describes the main thermo-physical properties of the n-eicosane adopted for the preliminary calculations.

Table 2. Thermo-physical properties of the chosen mPCM: n-eicosane

Specification	Symbol	Value	M.u.
Core density (solid/liquid)	$\rho_{mPCM\_core}$	815/780	kg m <sup>-3</sup>
Mean core density adopted	$\rho_{mPCM\_core}$	797.5	kg m <sup>-3</sup>
Shell density	$\rho_{mPCM\_shell}$	1190	kg m <sup>-3</sup>
Average particle diameter	$D_{mPCM}$	17-20·10 <sup>-6</sup>	m
Mass percentage of the core	$a_{core}$	87.5	%
Conductivity (solid/liquid)	$\lambda_{mPCM}$	0.23/0.15	W m <sup>-1</sup> K <sup>-1</sup>
Mean conductivity adopted	$\lambda_{mPCM}$	0.19	W m <sup>-1</sup> K <sup>-1</sup>

Specific heat (solid/liquid)	$c_{p,mPCM}$	$1.92/2.46 \cdot 10^3$	$\text{kJ kg}^{-1} \text{K}^{-1}$
Mean specific heat adopted	$c_{p,mPCM}$	$2.19 \cdot 10^3$	$\text{kJ kg}^{-1} \text{K}^{-1}$
Latent heat	$r_{mPCM}$	$1.95 \text{ or } 2.47 \cdot 10^5$	$\text{kJ kg}^{-1}$
Mean latent heat adopted	$r_{mPCM}$	$2.21 \cdot 10^5$	$\text{kJ kg}^{-1}$
Nominal phase change temperature	$T_{mPCM}$	36.4	$^{\circ}\text{C}$
		37	$^{\circ}\text{C}$
Phase change range	$T_{inf,mPCM} - T_{sup,mPCM}$	36-38	$^{\circ}\text{C}$

*Typical energy consumption for fans and pumps:*

The main features of the pumps used in the prototype are as follows:

Table 3. Specifications of the Verderflex Scientific AU UV 3000 HD pump.

Specification	Value	M.u.
Power consumption	100	VA
Protection rating	IP66	-
Speed control	4-20	mA
	0-10	V
Speed range	10-250	RPM
Standard tube material	Verderprene	-
Standard tube inner diameter size	0.0080	M
Standard tube inner diameter thickness	0.0032	M
Nominal flow rates	5,82-145,50	l/h

Table 4. Specifications of the Verderflex OEM M3000 pump.

Specification	Value	M.u.
Power consumption	100	W
Protection rating	IP66	-
Speed control	Setted	-
Speed possibilities	55 or 125 or 240	RPM
Standard tube material	Verderprene	-
Standard tube inner diameter size	0.0096	M
Standard tube inner diameter thickness	0.0032	M
Nominal flow rates	46,9 or 106,5 or 204,5	l/h

*Typical fans and pumps head:*

Depends on the circuit configuration and on the type of application. Figures of general validity cannot be supplied.

#### 4.3.3 Terminals

Heating system with low temperature radiant floor panels.

## 4.4 FEATURES AND POTENTIALITIES

*Size (installed power):* Solar thermal panel of  $2,31 \text{ m}^2$

*Temperature levels of the fluids:*

Solar thermal collector loop:

Optimal maximum return:  $38-40^{\circ}\text{C}$

Allowable maximum:  $60^{\circ}\text{C}$

Optimal minimum supply:  $28-30^{\circ}\text{C}$

Allowable minimum:  $-22^{\circ}\text{C}$

Radiant panel loop:

Supply temperature: 30-35°C

Return temperature: 23-28°C

*Best suited application:*

Heating system with low temperature radiant floor panels

*Limitations:*

Nowadays not suitable for system/devices requiring high temperature thermal levels (such as DHW production). However, several types of application are possible, simply choosing different PCS with different phase change temperatures.

## 4.5 EXAMPLE (theoretical and/or actual case studies)

After a conceptual/design phase, a full scale prototype was built in the laboratories of the Department of Energy at the Politecnico di Torino.

The system is based on the configuration shown in figure 1b. Picture in figure 5 shows the prototype located in the flat roof of the Department of Energy.



Figure 5 - The real-scale prototype: general view and details of the storage tank and the electronic control unit.

### 4.5.1 Results from experimental monitoring

At the present, the experimental monitoring activities are starting and data are not yet available. Performance and behaviour of the system has been simulated by means of a purposely developed numerical model.

### 4.5.2 Results from numerical simulations

On the basis of the well-known Hottler-Willer (HW) model for traditional flat plate solar collectors, a theoretical model describing the behaviour of the PCS filled solar collector was developed. In this model, the panel is divided in sections whose size/number depend on the type of the heat exchange mechanism – sensible or latent – occurring in the HTF (see e.g. figure 6). The panel can be divided at most in three parts. The first part (whose length is  $\Delta y_1$ ) represents the segment of panel between the inlet and the point where the HTF reaches the lower limit of the mPCM melting temperature range (sensible heat exploitation). The second part (whose length is  $\Delta y_2$ ) is located between the end of section 1 and the point where the whole amount of mPCM completes the phase change (e.g. where the HTF temperature starts rising from the lower limit to the upper limit of the mPCM melting temperature range).

Latent heat exploitation). In the last segment (whose length is  $\Delta y_3$ ) sensible heat exploitation occurs again and the HTF reaches the outlet temperature. The length of any part changes according with any variation in the boundary conditions. By integrating the HW equations, using melting temperature limits and enthalpy of fusion of n-eicosane mPCM as constant terms, the length of each segment can be determined.

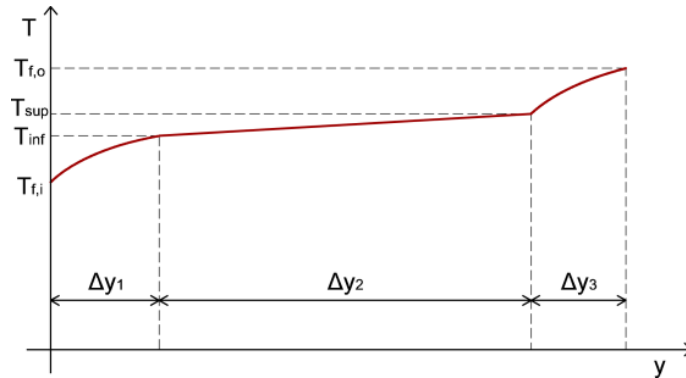


Figure 6 - Theoretical temperature distribution of the HTF through a slurry PCM filled solar panel

A set of simulations were run to compare the performance of a water based flat plate solar collector against the performance of a slurry PCM filled one. From the thermal point of view, results showed that the slurry PCM filled solar collector was more efficient than the traditional one. The mean seasonal efficiency increases of about 5% to 9% depending on the boundary conditions. Further benefits due to the storage tank were not studied yet for this particular type of system. However, many literature sources on thermal energy storage with PCMs are available that provide information of better energy performances of a LHTS (Latent Heat Thermal Storage) compared to SHTS (Sensible Heat Thermal Storage).

In Figure 7 the instantaneous efficiency of the slurry PCM-based and of the water based solar collector are plotted, for different outdoor air temperature and different solar irradiance. The results show that the conversion efficiency of the slurry PCM-based solar collector is always higher than the reference technology. The difference between the efficiencies of the two systems is in the range 6 to 8% , regardless of the boundary conditions. This means that the useful heat converted by the slurry PCM system is always higher than that of the reference. As expected, following the behavior of a conventional system, the slurry PCM-based collector (transition temperature of mPCM = 37 °C) shows an increase in the efficiency when the outdoor air temperature rises. Moreover, the improvement with respect to the water based system grows as the outdoor temperature rises too.

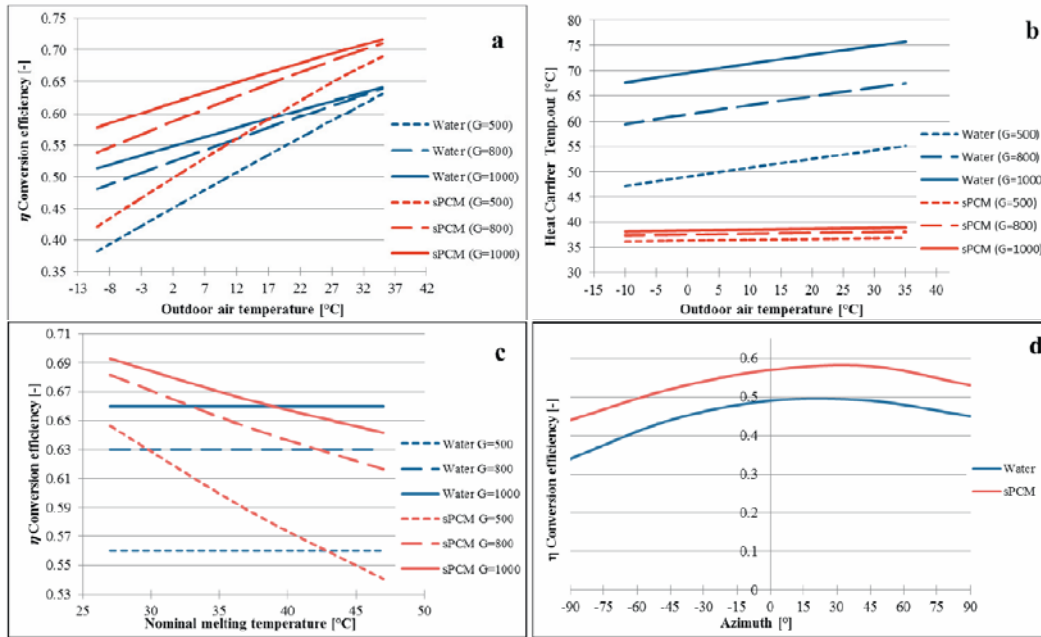


Figure 7 - (a) conversion efficiency ; (b) outlet temperature of the heat carrier fluid; (c) conversion efficiency with different mPCM nominal melting.

Annual and seasonal conversion efficiency was also calculated for different locations (Table 5). It is remarkable that, while the annual efficiency increase of approx. 7 % regardless of the climates, the heating season efficiency always shows a higher increase + 14%, + 8% and + 10%, in Palermo, Torino and Frankfurt, respectively. This nonlinear behaviour can be due to the combination of nominal melting temperature of the mPCM and of boundary conditions. In Figure 8 the useful converted heat during the heating season is plotted, for the innovative and the reference technology. The increase in the extracted heat spans in the range +20% ÷ +40%, with the highest increase in the coldest climate (Frankfurt). This reveals that the technology is particularly promising in cold climates, where even if the seasonal efficiency is still lower than in other, warmer location, the highest percentage increase in the converted heat is achieved.

Table 5. Annual and seasonal conversion efficiency in different location

City	Climate [12]	$\eta_{annual}$		$\eta_{heating\ season}$	
		water	sPCM	water	sPCM
Palermo	CSA	0.46	0.53	0.67	0.81
Torino	CFA	0.45	0.52	0.35	0.43
Frankfurt	CFB	0.38	0.45	0.25	0.35

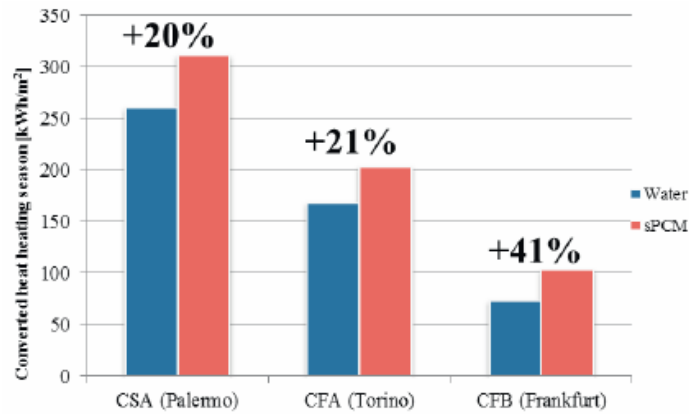


Figure 8 - Converted heat during the heating season for different climates.

#### 4.5.3 Entransy analysis

A preliminary entransy analysis of the solar thermal collector was done, based on the results of the simplified Simulink model. In particular, the (Q,T) diagrams were plotted for both a traditional (water based) collector and for the collector working with the mPCS fluids. Figure 8, 9 and 10 show the entransy losses due to the heat exchange between the absorber plate and the fluid for different concentration of the microencapsulated PCM (25 % and 50 % w.t.) and for a water based collector. Data shown in these charts refer to a incident solar radiation of  $800 \text{ W/m}^2$  and an outdoor air temperature of  $20 \text{ }^\circ\text{C}$ . Due to the simplified model the entransy losses were assessed on the base of the average absorber plate temperature.

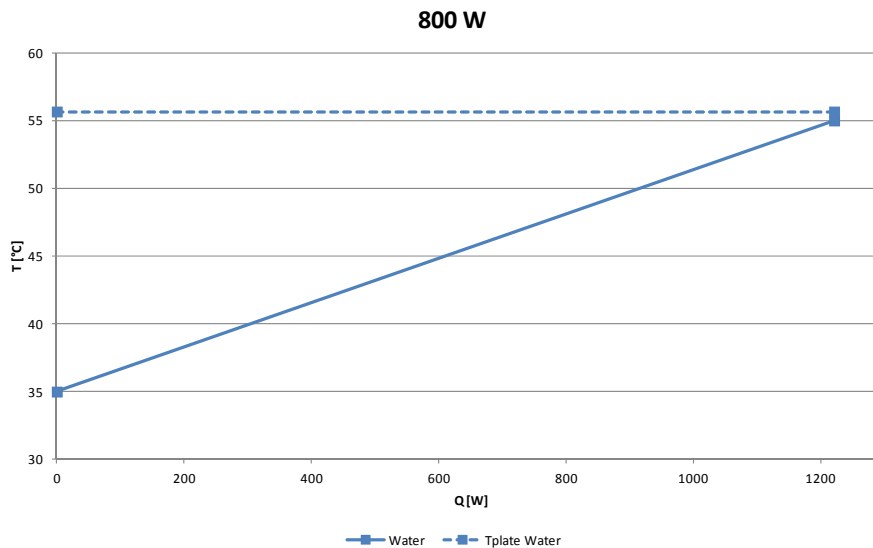


Figure 8 – (Q, T) diagram – Water glycol solution.

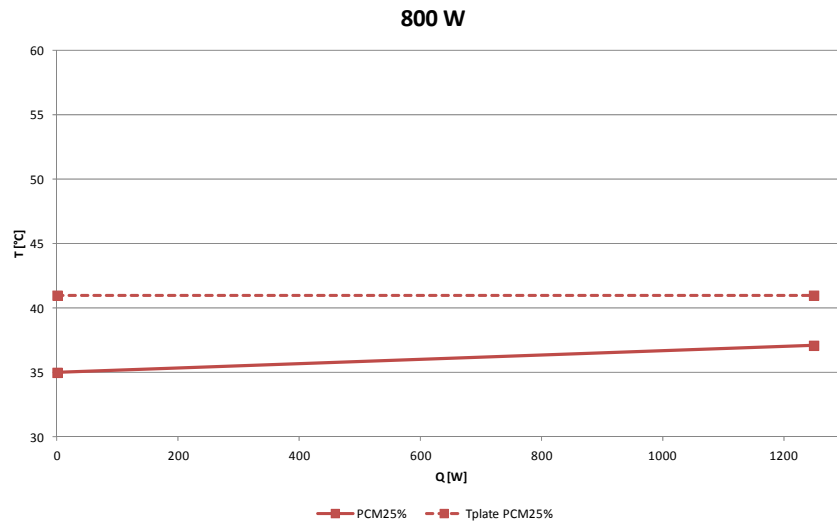


Figure 9 – (Q, T) diagram – mPCS concentration 25% (weight).

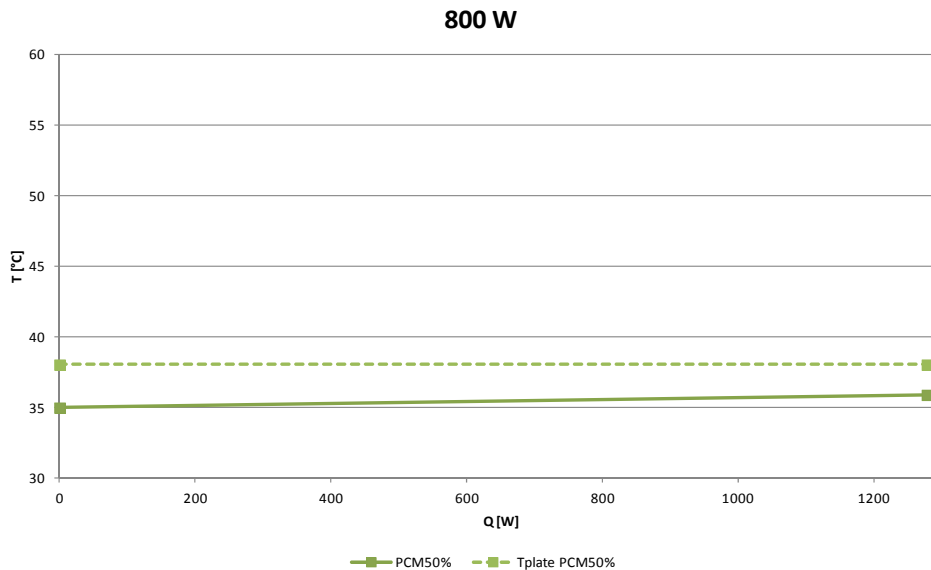


Figure 9 – (Q, T) diagram – mPCS concentration 50 % (weight).

#### 4.5.4 Conclusions & “Lessons learnt”

Flat-plate solar thermal collectors are the most common devices to convert solar energy into heat. Water-based fluids are commonly adopted as heat carrier for this technology, although their efficiency is limited by some thermodynamic and heat storage constraints. To overcome some of these limitations, an innovative approach based on the use of latent heat, which can be exploited by means of micro-encapsulated slurry PCMs (mixtures of micro-encapsulated PCMs, water and surfactants), has been proposed.

A prototypal system based on n-eicosane PCS was developed, built and tested. Some of the thermo-physical and rheological properties of the slurry PCM were analysed. To overcome the possible problems related to the use of PCSs as HTF – such as high pressure drops, clogging in the pipes, sedimentation in the storage tank and capsule rupture due to the pumping work – specific design solutions were adopted.

Though the system is still at the prototypal phase, the simulated performance has shown

the promising potentialities of the innovative systems compared to traditional hot water solar thermal installations.

Improvements of the flat plate solar collector efficiency in the order of magnitude of 10% can be expected and increases of the heat collection as high as 40% have been estimated.



Figure 9 - The monitoring system: thermocouples



Figure 10 - The monitoring system: pyrometer



Figure 11 - The controlling system: peristaltic pump

## 5 Application in a building in Denmark

### 5.1 Radiant heating and cooling systems in plus-energy houses

The houses considered in this part of the report were designed as plus-energy houses, by the students of Technical University of Denmark, to compete in an international competition Solar Decathlon Europe 2012 and 2014.

#### 5.1.1 Description of the house, *Fold*

The first house, *Fold*, competed in Solar Decathlon Europe 2012 in Madrid, Spain. After the competition, the house was used as an experimental facility where different heating and cooling strategies were tested. The house was located in Denmark. Year-round measurements of indoor thermal environment, energy performance and physical parameters in the HVAC system were taken from October 2013 to October 2014.

The name of the house, *Fold*, stems from the structural shape of the house. The idea behind the shape of the house was to take a piece of paper and fold it in such a way, around the occupants, that will give the optimum inclination and orientation for the photovoltaic/thermal panels on the roof and at the same time it will minimize the heat losses and heat gains from the ambient (i.e. solar gains). The folding strategy (inclination of the walls, inclination and angle of the roof, length of the overhangs, orientation and so forth) is a function of the geographical location. An example of the folding procedure is shown in Fig. 0-34.

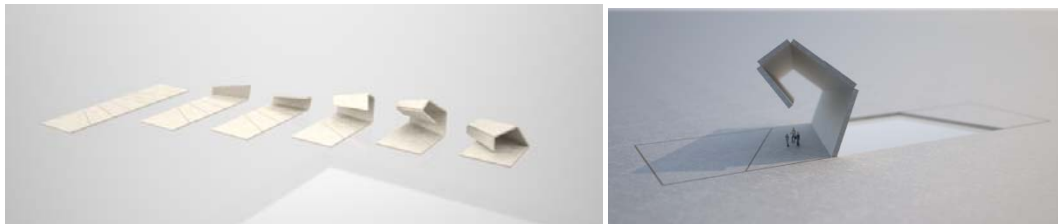


Fig. 0-34 An example of the folding strategy

*Fold* was a single-family, detached, one-story house with a floor area of 66.2 m<sup>2</sup> and a conditioned volume of 213 m<sup>3</sup>. The house was constructed from wooden elements. The house was insulated with a combination of 20 cm of conventional mineral wool and 8 cm of compressed stone wool fibers and Aerogel, Aerowool.

Inside the house, there was a single space combining kitchen, living room and bedroom areas. The glazing façades in the South and North sides of the house were partly shaded by the overhangs. No solar shading was installed in the house except for the skylight window. The largest glazing façade was oriented to the North with a 19° turn towards the West. Fig. 0-35 and Fig. 0-36 show the exterior and the interior of the house.



Fig. 0-35 Outside views of the house, seen from North-West (left) and South-West (right)



Fig. 0-36 Inside views of the house, competition (left) and measurement (right) configurations

The surface areas and corresponding thermal properties of the structural parts of the house are given in Table 0-8:

Table 0-8. *Thermal properties of the walls*

<i>External walls</i>	<i>South</i>	<i>North</i>	<i>East</i>	<i>West</i>	<i>Floor</i>	<i>Ceiling</i>
Area [m <sup>2</sup> ]	-	-	37.2	19.3	66.2	53
U-value [W/m <sup>2</sup> K]	-	-	0.09	0.09	0.09	0.09
<i>Windows</i>	<i>South</i>	<i>North</i>	<i>East</i>	<i>West</i>	<i>Floor</i>	<i>Ceiling</i>
Area [m <sup>2</sup> ]	21.8	36.7	-	-	-	0.74
U-value [W/m <sup>2</sup> K]	1.04	1.04	-	-	-	1.04
Solar transmission	0.3	0.3	-	-	-	0.3

### 5.1.2 Descriptions and operation principles of the heating, cooling, and ventilation systems of Fold

The design of the house's HVAC system exploited the advantages of well-known and proven technologies combined with those of less mature technologies in order to achieve an innovative, efficient and sustainable solution.

Fold's HVAC system consisted of these main parts: embedded pipes in the floor and in the ceiling (dry radiant system), photovoltaic/thermal panels (PV/T), domestic hot water (DHW) tank, mechanical and natural ventilation, ground heat exchanger and ground coupled heat pump (GHEX and GCHP).

The main heat source and heat sink of the house was designed to be the ground, realized by means of a borehole (single U-tube ground heat exchanger). During the heating season, the ground was used as a heat source, if space heating was needed then the heat pump was activated. In the cooling season, when the ground was acting as a heat sink, the heat pump

was by-passed and free cooling was obtained by a circulation pump.

The main sensible heating and cooling strategy of the house relied on the low temperature heating and high temperature cooling principle by the hydronic radiant system. There were pipes embedded in the floor and in the ceiling. The embedded pipes in the ceiling were designed to be used for cooling purposes only while the embedded pipes in the floor could be used for heating as well as cooling during the peak loads.

The floor heating and cooling system was a dry radiant system, consisting of a piping grid installed in the wooden layer, with aluminum profiles on the pipes for better thermal conductance. The details of the floor system were: chipboard system, with aluminum heat conducting profiles (thickness was 0.3 mm and length was 0.17 m), PE-X pipe, 17x2.0 mm. Pipe spacing was 0.2 m. In total there were four loops in the floor. The details of the ceiling system were: foam-board system, with aluminum heat conducting profiles (thickness was 0.3 mm and length was 0.12 m), PE-X pipe, 12x1.7 mm. Pipe spacing was 0.125 m. In total there were six loops in the ceiling.

A mixing station (and a controller), that links the indoor terminal unit with the heat source and sink, was installed in the system to control the flow to the individual loops, flow rate, and the supply temperature to the embedded pipes. The operation of the radiant system was based on the operative temperature set-point that was adjusted from a room thermostat and on the relative humidity inside the house (to avoid condensation).

PV/T part (67.8 m<sup>2</sup>) was intended to produce electricity (by photovoltaic cells), and produce heat for the domestic hot water (DHW) and domestic appliances' use (dishwasher, washing machine and tumble dryer). Extraction of heat from the PV/T panels also cools the panels, which helps keeping the electrical efficiency close to the maximum. Based on this approach, the PV/T area was divided into two parts; Part A (45.4 m<sup>2</sup>) and Part B (22.4 m<sup>2</sup>). It was possible for the Part B to interact with the ground.

Part A was only intended to charge DHW tank when there was a need (no interaction with the ground). Part B served two purposes; charging the DHW tank and cooling the PV/T panels. When there was a DHW need, Part B contributed to the charging of the DHW tank. There was a drain-back tank between the PV/T loops and the DHW tank which made it possible to drain all the water from the PV/T loops, when necessary, in order to avoid boiling or freezing of the water in the circuits.

The DHW tank, 180 liters, was equipped with two spiral heat exchangers and an electric heater. One of the spiral heat exchangers was connected to the PV/T panels via the drain-back tank and the other one to the active heat recovery system of the air handling unit. The top part of the tank (54 liters) was heated by the electric heater, when necessary.

It was possible to ventilate the house mechanically (by means of an air handling unit, AHU) and naturally (by window openings in the façades). Mechanical ventilation gives a higher degree of control over indoor environmental quality but at the expense of energy consumption. This energy consumption can be eliminated with the use of natural ventilation. It was intended that the natural ventilation will overrule the mechanical ventilation system when the outside conditions are suitable, to take advantage of the passive means. The mechanical ventilation was only used to provide fresh air to the house since the main sensible heating and cooling terminal of the house was the radiant system. This also enables to have lower ventilation rates compared to a case where space heating and cooling is mainly obtained

by mechanical ventilation.

Fresh air was provided into the house by an AHU which had passive and active heat recovery possibilities. The passive heat recovery was obtained by means of a cross-flow heat exchanger and it had an efficiency of 85% (sensible heat). The active heat recovery was obtained by means of a reversible air-to-water heat pump that was coupled to the AHU and the DHW tank. The AHU could supply fresh air at a flow rate up to 320 m<sup>3</sup>/h at 100 Pa. The design ventilation rate was determined to be 0.5 ach. Humidification of the supply air was not possible due to the limitations of the AHU.

Fig. 0-37 shows the mechanical installations in the house and Fig. 0-38 shows the hydronic scheme.

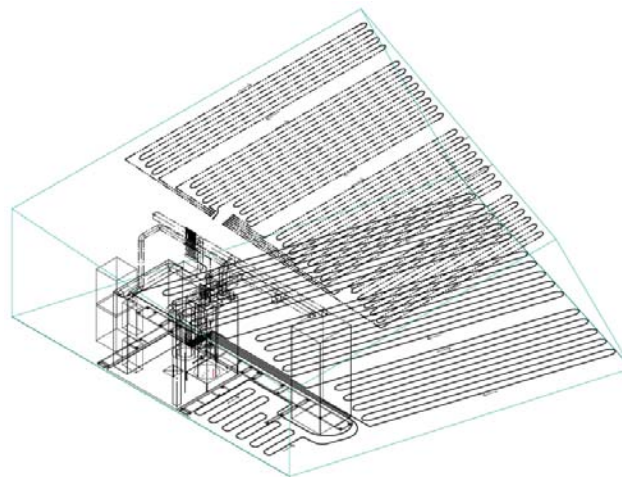


Fig. 0-37 Mechanical installations in the house

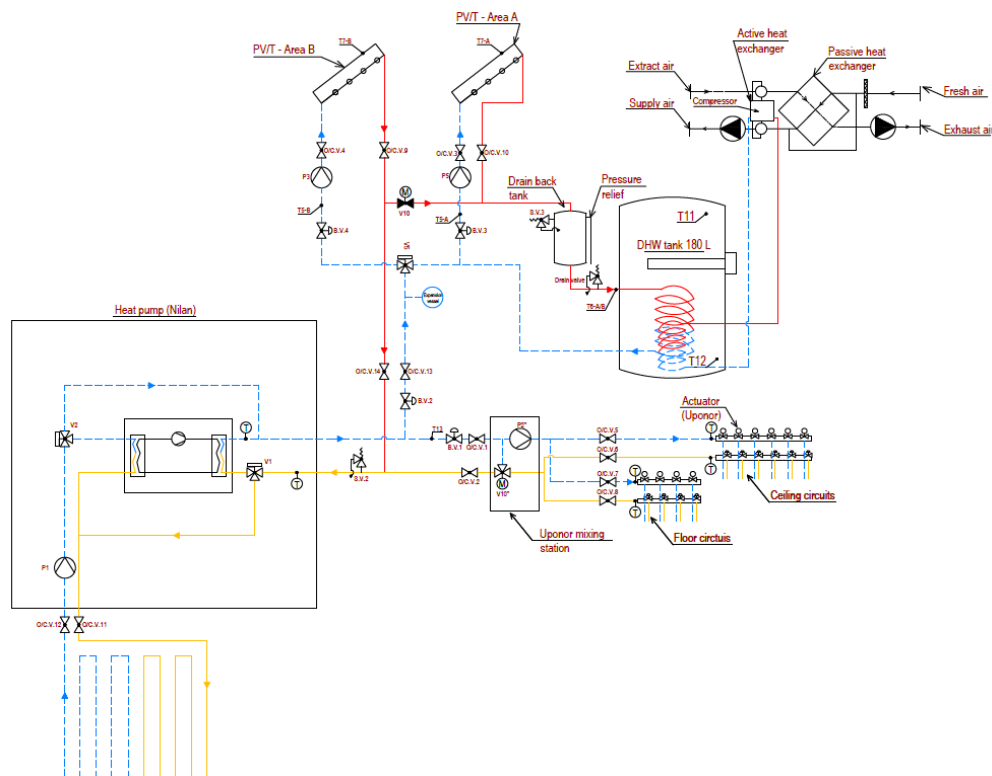


Fig. 0-38 Hydronic scheme

Due to the limitations in the practical implementation and chosen experimental

conditions, some differences occurred compared to the initially designed system. These differences were:

- It was not possible to install a ground heat exchanger during the competition, due to the competition regulations. Therefore the ground heat exchanger (GHEX) was simulated by a reversible air-to-water heat pump that was coupled to a 500 L buffer tank.
- Before the experiments in Denmark, the buffer tank was taken out of the system. A flat-plate heat exchanger was installed between the house’s space heating and cooling system and the air-to-water heat pump. This heat pump became the main heat source and sink of the house for space heating and cooling.

### 5.1.3 Energy performance and thermal indoor environment of Fold

The results presented here are obtained during the design phase, during the competition period in Madrid (September 2012), from simulations and from the year-round measurements [1-3]:

- Calculations, simulations, and experiments were performed in order to evaluate the applicability of phase change materials (PCM) in the house. The simulations showed that a combination of embedded pipes and PCM enables energy savings up to 30% in the early and late cooling season and 20% in the peak month, in Madrid. The results of the experiments showed a better performance than the calculations and it was possible to discharge the PCM panels in 5 hours, but further development and testing were needed (due to corrosion, unexpected behavior of melting and solidifying, etc.) in order to fully employ the tested PCM panels, therefore PCM was not used in the final design of the house.
- Free cooling concept with the GHEX enables the same cooling output to be obtained with 8% of the energy consumption of a chiller (air-to-water heat pump).
- The simulations showed that the PV/T panels produced more electricity than the house consumed, on a yearly basis, for both of the locations (Madrid and Copenhagen), enabling the house to be a plus-energy house. The thermal part of the PV/T panels helped to keep the electrical efficiency of the PV cells close to the maximum, and the thermal part of the PV/T panels yielded a solar fraction of 63% and 31% in Madrid and Copenhagen, respectively.

Energy performance of the house during the competition period is given in Table 0-9 .

*Table 0-9. Energy values during the competition*

Production [kWh]	275.6
Use [kWh]	196.9
Use without chiller [kWh]*	129.4
Balance with chiller [kWh]	78.7
Balance without chiller [kWh]*	146.2

\*Chiller consumption was 67.5 kWh

The results show that the house produced more energy than it used during the competition. The results indicate that the energy use of the chiller corresponded to 34% of the

total consumption. At this point it should be noted that this chiller was used to simulate the ground heat exchanger and it was not a part of the initial system design.

Fig. 0-39 and Fig. 0-40 show the overall thermal indoor environment results during the heating and cooling seasons, respectively.

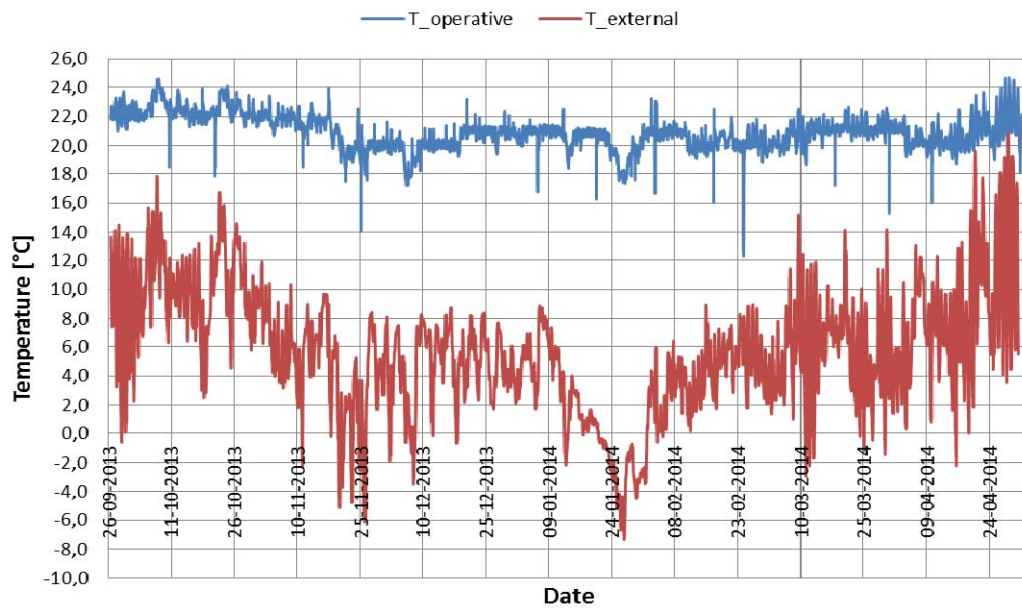


Fig. 0-39 Operative temperature and external air temperature during the heating season

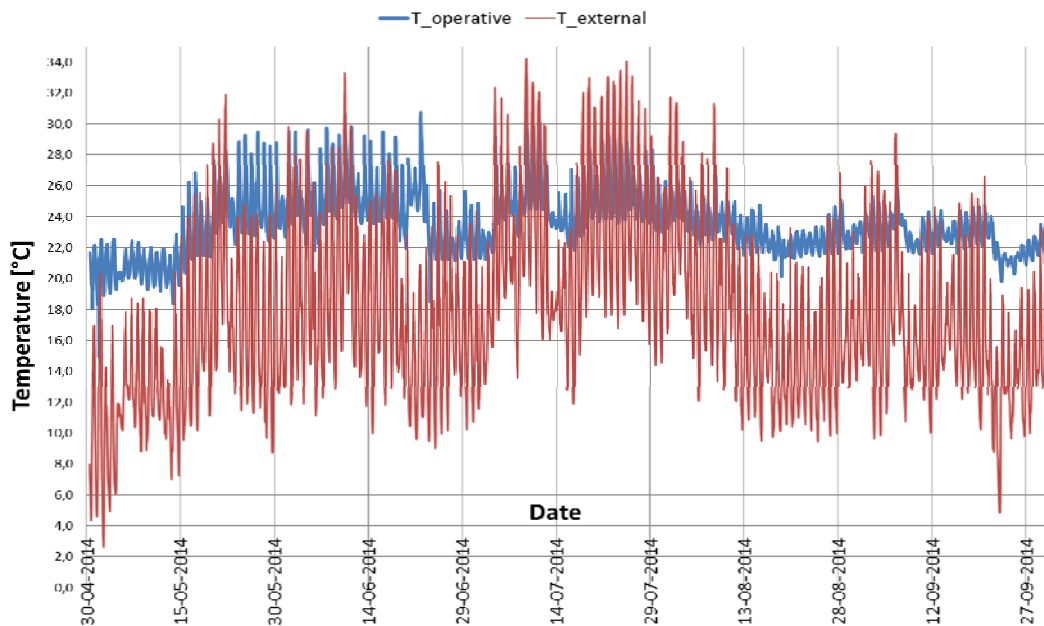


Fig. 0-40 Operative temperature and external air temperature during the cooling season

Different heating strategies were tested during the measurement period. For the heating season, the overall performance regarding the indoor environment was satisfactory, i.e. 80% of the time in Category 2 of EN 15251 (2007). Among the investigated cases, floor heating with heat recovery on the ventilation was the optimal heating strategy concerning occupant thermal comfort, and thermal stratification (heat loss, hence energy efficiency).

The house performed worse in the cooling season than the heating season; 57% of the

time in Category 2 of EN 15251 (2007). Overheating was a significant problem and the total hours above 26°C and 27°C exceeded the values recommended in DS 469 (2013). The most significant problems of the house were the large glazing façades (including the lack of solar shading) and the lack of thermal mass in order to buffer the sudden thermal loads.

Despite the large glazing façades, the radiant floor enabled to have a uniform temperature distribution in the space [4].

The annual electricity production from the PV/T panels (4043.9 kWh) was lower compared to the simulation results from TRNSYS (for Copenhagen), 7434.3 kWh. Several factors caused this difference, lower peak power values obtained compared to the simulations, different climatic conditions, damaged PV/T panels, shadows on the PV/T panels.

#### 5.1.4 Description of the house, Embrace

The second house, Embrace, competed in Solar Decathlon Europe 2014 in Versailles, France. After the competition, the house was transported back to Denmark, where it is currently being used as a test facility (as of October 2015), and it is going through a measurement campaign from April 2015 to April 2016. The results presented in this report are simulation results and measurement results obtained during the two-week competition period in Versailles, France.

Embrace was designed as a single-family house for two people, with a net floor area of 59 m<sup>2</sup>. Passive architectural solutions were combined with active (mechanical) solutions. The building envelope consists of two parts: the thermal envelope and the weather shield. The space between the weather shield and the thermal envelope creates a sheltered garden which is a semi-outdoor space. The Embrace's concept is to install it on rooftops of existing buildings to densify urban areas.

Fig. 0-41 shows the exterior view of the house and Fig. 0-42 shows the interior view of the house.

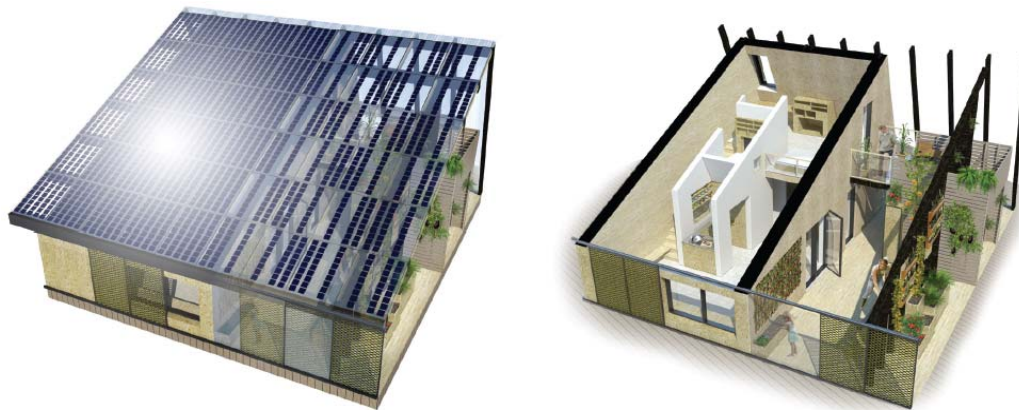




Fig. 0-41 Renderings of the house [5], and the house in Versailles (© Solar Decathlon Europe)



Fig. 0-42 Photo of the interior of the house [5]

The thermal properties of the envelope are given in *Table 0-10*.

*Table 0-10. Thermal properties of the envelope*

Component	U-value [W/m <sup>2</sup> K]
External wall	0.08
Roof	0.085
External floor	0.1
Internal walls	0.38
Internal floor	0.25
Glazing, Type 1	0.83
Glazing, Type 2	0.79

### 5.1.5 Descriptions and operation principles of the heating, cooling, and ventilation systems of Embrace

The theoretical design of the systems is presented in this report, which differs slightly from the realized system. The systems are designed to create heating and cooling locally for

the house, using the solar resource. The additional needs are provided by active (mechanical) systems.

For heating production, solar collectors are mounted on the weather shield: they produce hot water that is used for domestic hot water (DHW). Due to the transient nature of the sun as a resource, other systems had to be implemented: necessary heat for DHW can also be provided by a compressor that is included in the ventilation system, which acts as active heat recovery and extracts heat from the ventilation air of the house. The space heating needs require another system: an air-to-water heat pump that is placed outside the house for this purpose, and linked to the storage tank (750 liters) in the technical room.

For cooling, the main concept is to exploit nighttime radiative cooling opportunity. This is done through the installation of unglazed solar collectors on the ground next to the house, where water is circulated at night and the water is cooled by radiation towards the nocturnal sky. The cooled water is stored in the storage tank to be used during the next day. In case this free cooling is insufficient, the reversible air-to-water heat pump is used as well.

Only one storage tank is installed, therefore it is used to store cold water in the cooling season and hot water during the heating season.

The heating and cooling is provided to the indoor space through a radiant floor composed of six loops distributed over the two floors of the house.

A mechanical ventilation system with heat recovery (Nilan Compact P) provides air change in the conditioned space. The air flow rate is kept to a minimum because the aim of the ventilation system is only to improve the air quality and not to condition the space. Fig. 0-43 summarizes the different sources and their usage.

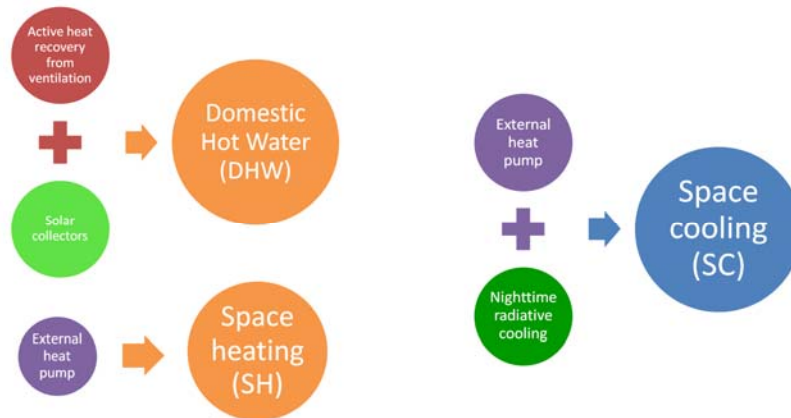


Fig. 0-43 Schematic drawing of the heating and cooling production

Fig. 0-44 shows the overall hydronic scheme, which has been split into different loops to explain the operation loop by loop (collectors loop, Nilan Compact P, radiant floor loop).

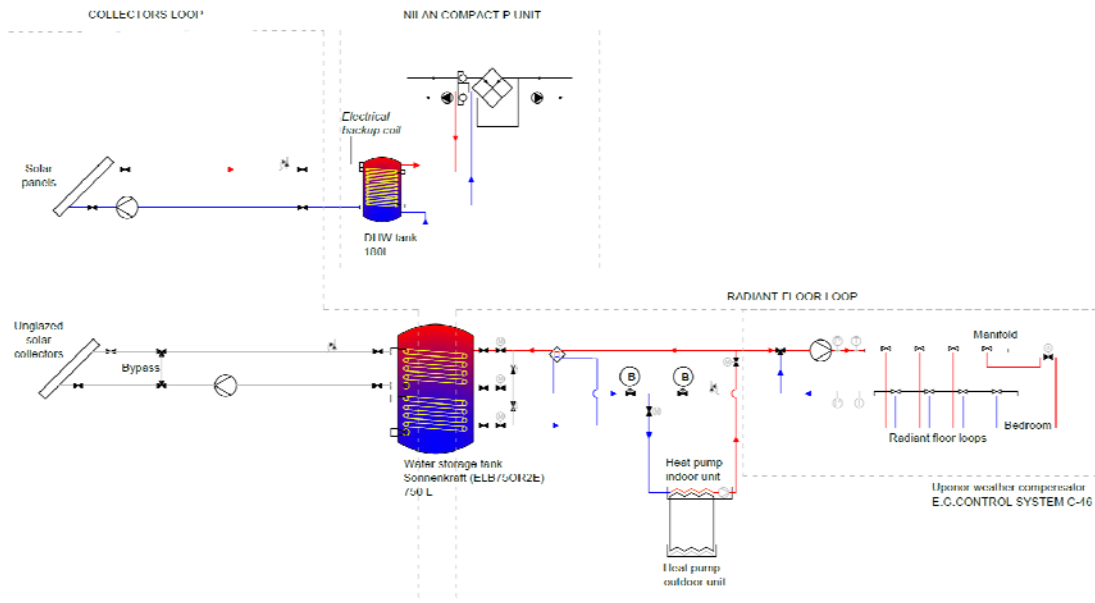


Fig. 0-44 Overall hydronic scheme

DHW production: DHW production does not depend on whether the system operates in heating or cooling mode. Priority is given to the solar thermal collectors to produce the DHW. In case of poor solar production, the active heat recovery included in the mechanical ventilation system can cover the remaining DHW needs. Fig. 0-45 shows the DHW connections in the system.

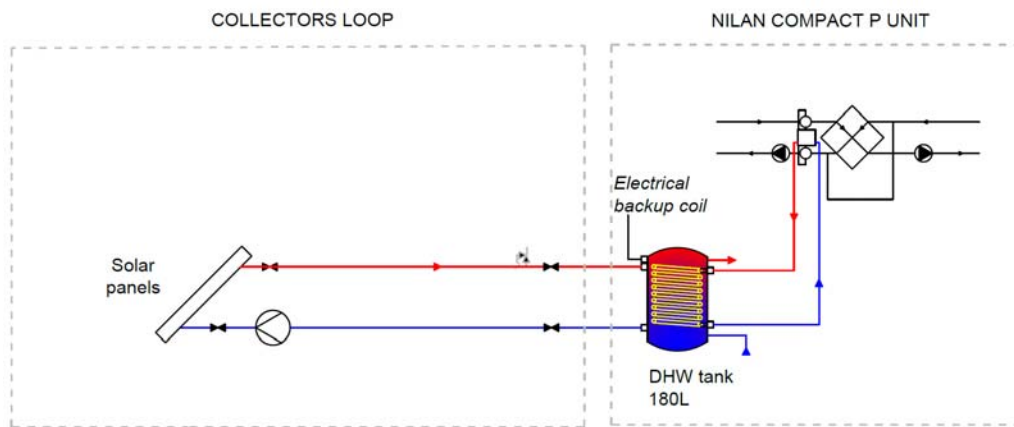


Fig. 0-45 DHW production scheme

Heating mode: In the radiant floor loop, the external heat pump is activated when needed. In the first operation mode (Fig. 0-46), the water in the tank is warm enough to supply directly to the radiant floor, therefore the heat pump is not activated. If the temperature in the tank drops, the heat pump is activated (Fig. 0-47). In this case, part of the hot water is directly supplied to the radiant floor and the rest is stored in the storage tank. When the hot water tank is warm enough, the system goes back to the first operation mode. This operation is made so that the heat pump can work at full-load, where its efficiency is the highest.

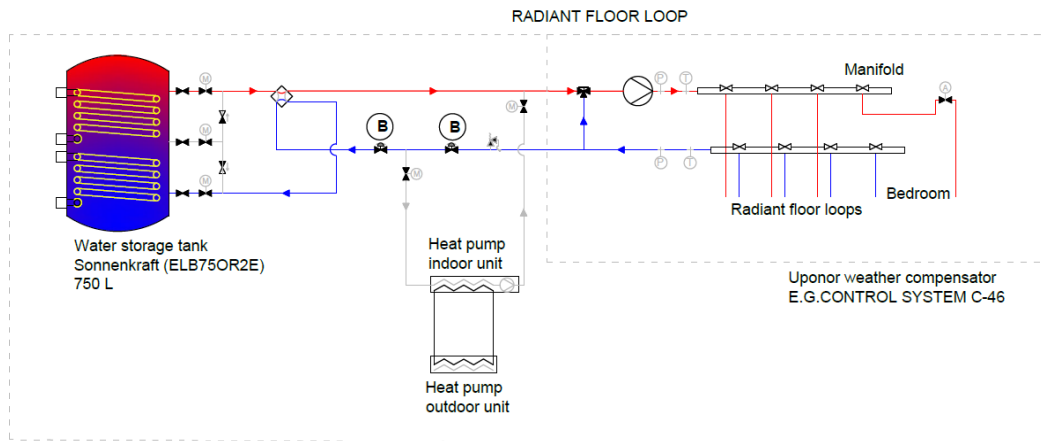


Fig. 0-46 Radiant floor loop in heating – First operation mode, without the heat pump

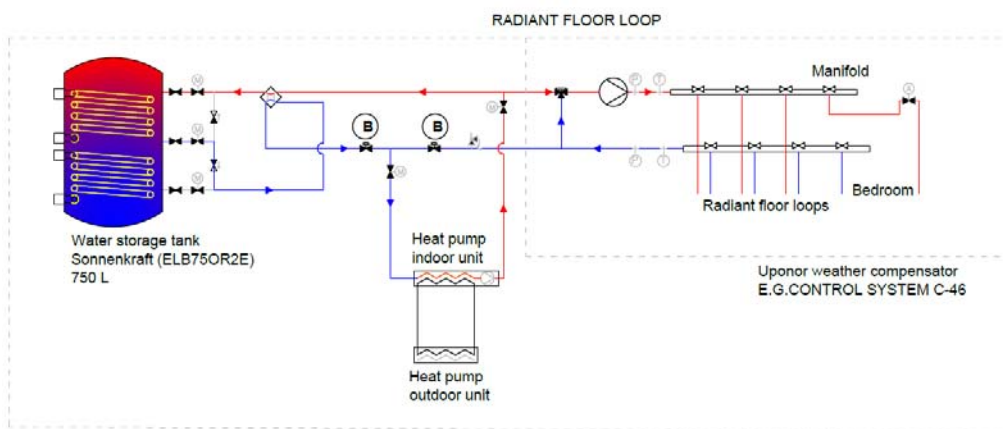


Fig. 0-47 Radiant floor loop in heating – Second operation mode, with heat pump activated

Cooling mode: In cooling mode, the unglazed collectors loop is activated at night: water is circulated through the panels which are facing the sky (Fig. 0-48 and Fig. 0-49). This process enables to cool the water in the tank during the night, and it can then be used during the day for space cooling through the radiant floor.

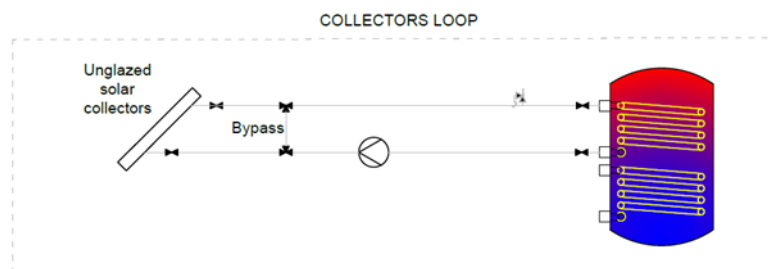


Fig. 0-48 Collectors loop in cooling – Day operation

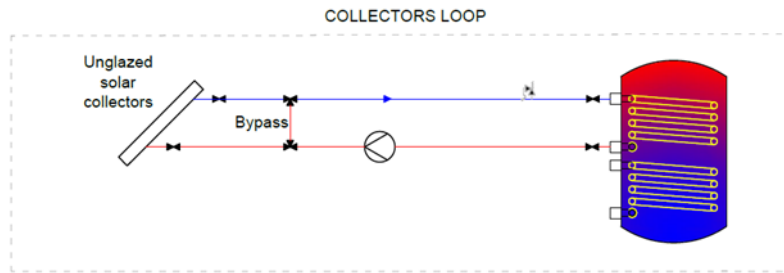


Fig. 0-49 Collectors loop in cooling – Night operation

The functioning of the radiant loop for cooling (Fig. 0-50 and Fig. 0-51) is similar to the heating mode. The tank is primarily used to supply directly to the radiant floor. The heat pump is activated when the storage tank is not cold enough, and it supplies both the radiant floor and the storage tank. The only notable difference is that the cold water is taken from the bottom of the tank, and the warm water is taken from the top of the tank (this difference between heating and cooling mode is made possible by a 4-way valve).

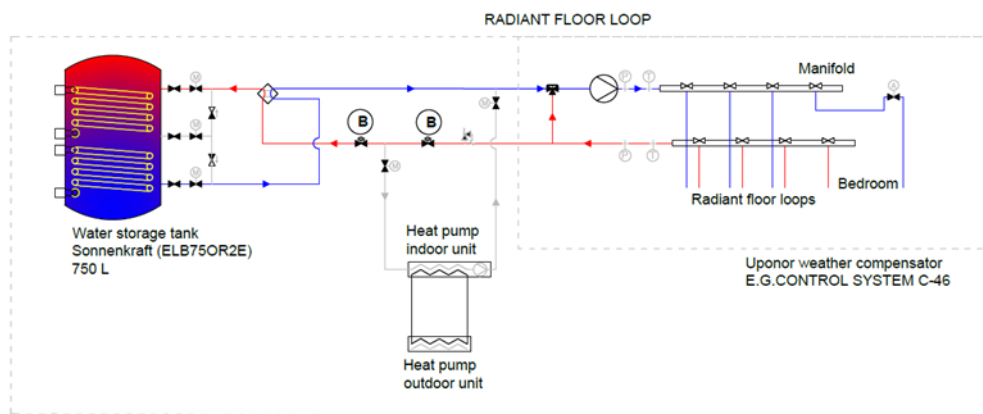


Fig. 0-50 Radiant floor loop in cooling – First operation mode, without the heat pump

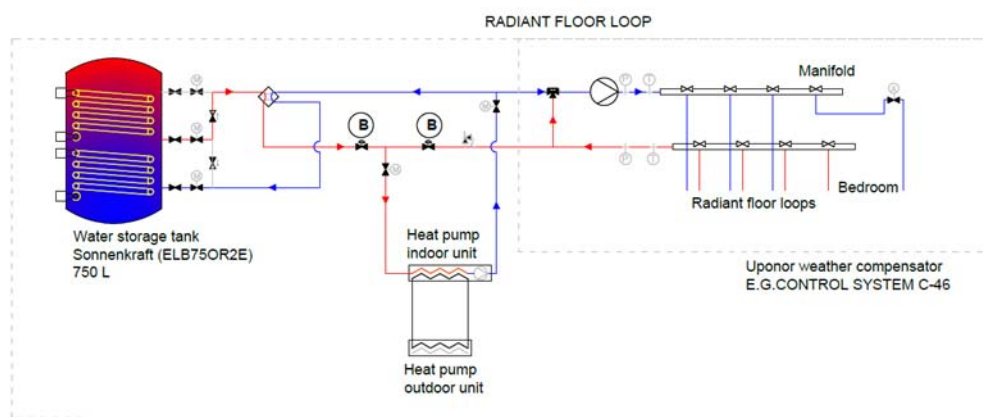


Fig. 0-51 Radiant floor loop in cooling – Second operation mode, with the heat pump activated

The primary energy converter for space heating and cooling is an air-to-water heat pump, model Altherma from Daikin. It is composed of an outdoor and an indoor unit, which includes also a pump and an additional electrical heater. The annualized values of SCOP and EER have been calculated for the climate of Copenhagen: seasonal COP is 3.8 and EER is 4.5.

The indoor terminal unit is a dry radiant floor, made of chipboard plates on which are

installed aluminum plates (Fig. 0-52). The PEX pipes are inserted into the aluminum plates, with a pipe spacing of 20 cm. Six loops are installed in the house; two on the first floor and four on the ground floor.

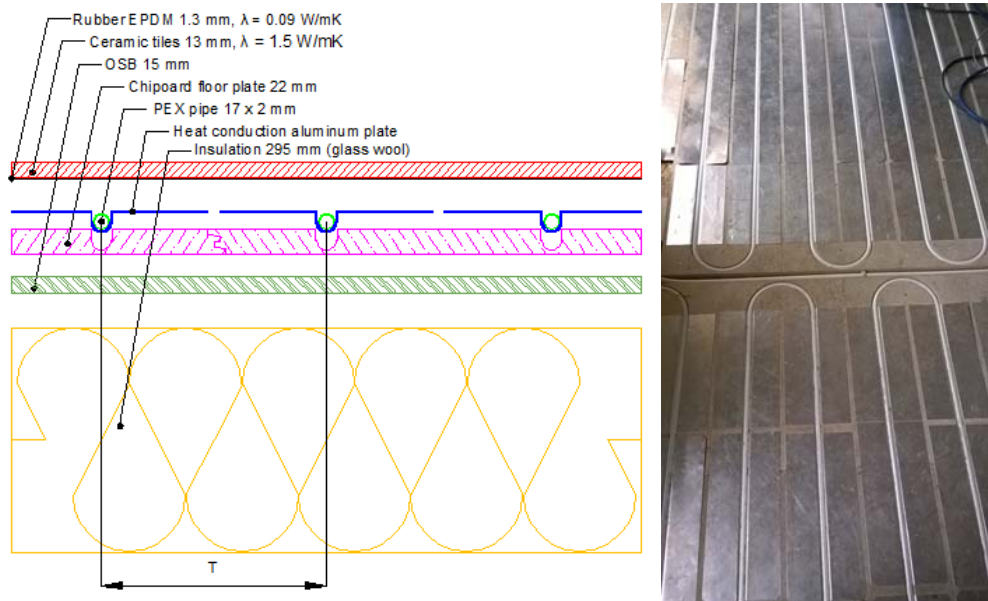


Fig. 0-52 Section and layout of the radiant floor system

#### 5.1.6 Energy performance and thermal indoor environment of Embrace

The house and its mechanical systems were assembled in Versailles, France for the Solar Decathlon Europe 2014, where it was monitored for two weeks (July 2014). In the assembly in Versailles, the major difference was the position of the heat pump: it was directly connected to the storage tank.

The results from simulations regarding the energy performance of the house are given in Table 0-11.

Table 0-11. Annual electricity consumption and production values for Embrace [5]

Energy (kWh/year)	Paris	Copenhagen
Electricity consumed	1891 kWh, (32 kWh/m <sup>2</sup> )	2236 kWh, (38 kWh/m <sup>2</sup> )
Electricity consumed per person	1260 kWh/person	1490 kWh/person
Electricity consumed no light, no appliances	960 kWh, (16 kWh/m <sup>2</sup> )	1090 kWh, (18 kWh/m <sup>2</sup> )
Electricity produced	4506 kWh	5357 kWh

For both of the locations, Paris and Copenhagen, the electricity consumed is less than the produced. Using less energy than the production, the house reaches the requirements for a plus-energy house. The electricity production is higher in Copenhagen, because of the low tilt of the photovoltaic panels (22°), combined with the higher latitude of Copenhagen.

The results from experimental monitoring are given in Fig. 0-53, which shows the indoor temperature in the house, in relation to the boundaries imposed by the competition organizers, and in Fig. 0-54, which shows the energy use of the different HVAC system components during the competition period.

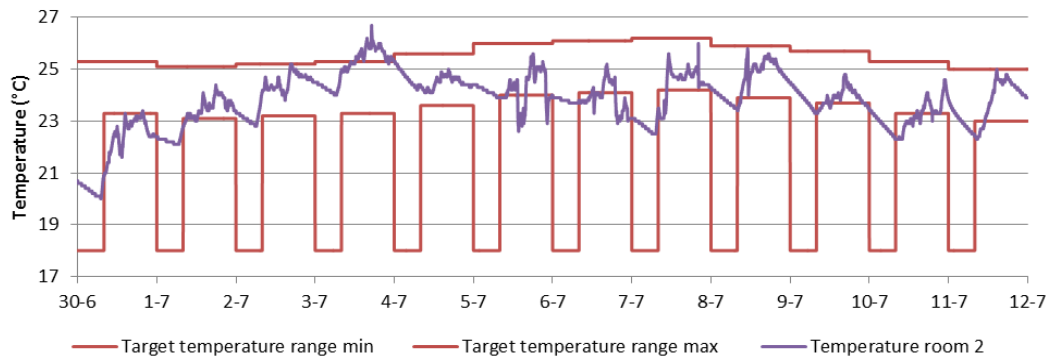


Fig. 0-53 Operative temperature in the ground floor of EMBRACE in Versailles, July 2014

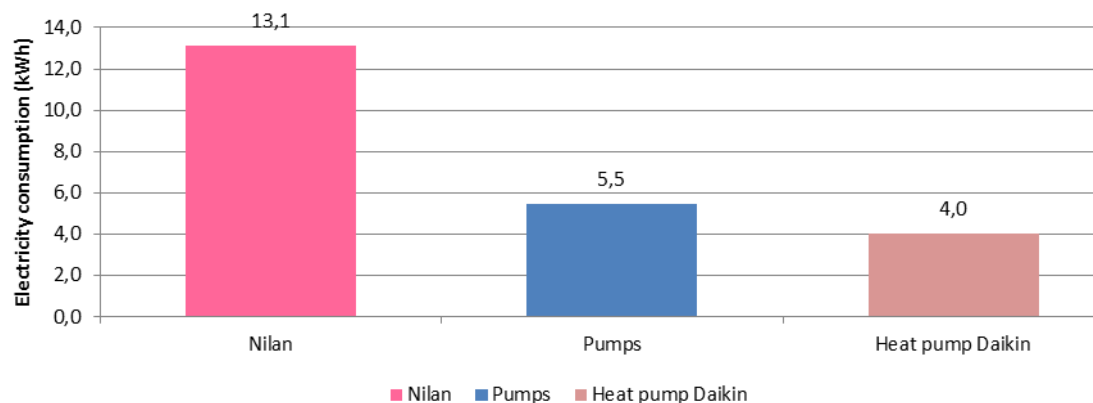


Fig. 0-54 Division of the HVAC electricity consumption in Versailles, July 2014

It should be noted that the weather was exceptionally cold during this period, and it resulted in low cooling needs and solar production. This explains the low consumption of the Daikin heat pump and the high consumption of the Nilan Compact P, which had to cover the remaining DHW needs not covered by the solar production. The indoor environment was satisfactory during the measurement period.

The energy performance of Embrace is close for Paris and Copenhagen climates. The house achieved the plus-energy targets both in the computer simulations and during the competition period, producing more than double energy than its total use.

### 5.1.7 Discussion and conclusion

Radiant heating and cooling systems have been used in both of the presented plus-energy houses. The results show that:

- The initial and a crucial step is to minimize the heating and cooling demands of the building, then the most energy-efficient heating and cooling systems should be employed to meet these demands.
- Low temperature heating and high temperature cooling operating principle enables the integration of natural and sustainable energy resources (ground and night radiative cooling in this context) into the heating and cooling systems. This principle also enables the heat pumps to operate at high efficiency conditions due to an increase in the required evaporation temperatures and due to a decrease in the required

condensation temperatures.

- Using a water-based system for heating and cooling is more energy efficient than using an air-based system (smaller pipe diameters than ducts, lower electricity use of pumps compared to fans, less air movement which reduces the risk of draught, etc.)
- Radiant systems enable to use the space freely and requires no cleaning
- Radiant systems create uniform temperature distribution in indoor spaces and operate with no noise in indoor spaces

These characteristics were proven in the design, simulation, and operation phases of the two plus-energy houses, confirming that radiant heating and cooling systems are a crucial means of achieving low energy and even plus-energy levels in buildings while providing optimal thermal indoor environment for building occupants.

### 5.1.8 References

- [1] O. B. Kazanci, M. Skrupskelis, P. Sevela, G. K. Pavlov and B. W. Olesen, "Sustainable heating, cooling and ventilation of a plus-energy house via photovoltaic/thermal panels," *Energy and Buildings* 83, pp. 122-129, 2014.
- [2] M. Skrupskelis and O. B. Kazanci, "Solar sustainable heating, cooling and ventilation of a net zero energy house," Technical University of Denmark, Kgs. Lyngby, 2012.
- [3] O. B. Kazanci and B. W. Olesen, "Sustainable Plus-energy Houses: Final Report," Technical University of Denmark, Department of Civil Engineering, Kgs. Lyngby, 2014.
- [4] O. B. Kazanci and B. W. Olesen, "Horizontal Temperature Distribution in a Plus-Energy House: Cooling Season Measurements," in *Proceedings of 2015 ASHRAE Annual Conference*, Atlanta, 2015.
- [5] L. Gennari and T. Pean, "Conditioning of a plus-energy house using solar systems for both production of heating and nighttime radiative cooling," Technical University of Denmark, Kgs. Lyngby, 2014.

## 5.2 A novel system: TABS with diffuse ceiling ventilation

### 5.2.1 Introduction and system description

The increasing insulation levels, air-tightness requirements in building codes, and the increase of electronic equipment used in buildings, and particularly in offices, increase the cooling loads and even in cold climates as in Denmark, office buildings started to require cooling throughout the whole year.

The cooling of office spaces should be done with occupant thermal comfort and energy-efficiency in focus. Based on this context, a new system solution has been proposed based on natural ventilation, building thermal mass activation (using thermally active building systems, TABS) and diffuse ceiling ventilation principles for cooling and ventilation in office buildings [1]. This concept has been studied by means of simulations and experiments at Aalborg University in Denmark. Fig. 0-55 shows the schematic view of this new system solution.

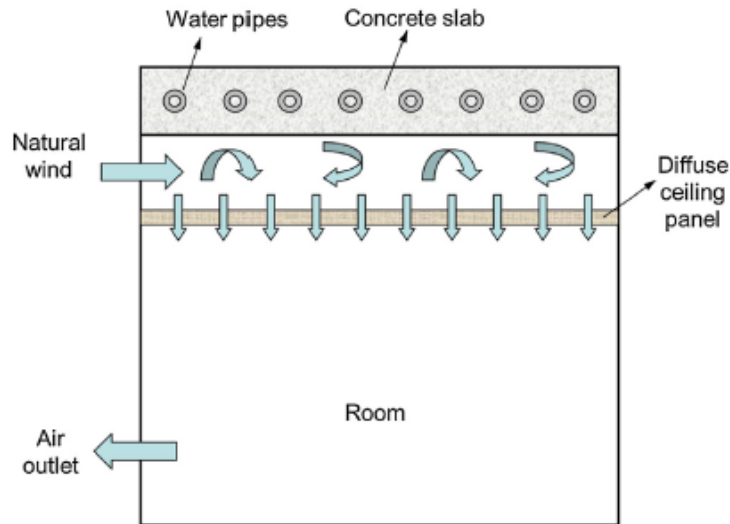


Fig. 0-55 Schematic view of the system combining TABS and diffuse ceiling ventilation [1]

In this system solution, the outdoor air is taken through controlled vents into the plenum (between the diffuse ceiling panels and the concrete slab), and it is supplied to the room through the small openings in the diffuse ceiling panel. The concrete slab is activated only if there is a peak heating or cooling demand. The air is exhausted through the air outlet placed in the room and under the diffuse ceiling. This system allows the use of natural means (outdoor air) to be used during all seasons of the year.

### 5.2.2 Simulations

In order to study the performance of the proposed system, Yu et al. [1] carried out a simulation study, by means of commercially available building simulation software, BSim. A typical office room (external dimensions of 8.0 m x 3.6 m x 4.8 m) with a net floor area of 26.0 m<sup>2</sup> was used in the simulations. A heavy-weight building construction was used. Fig. 0-56 shows the studied office room.

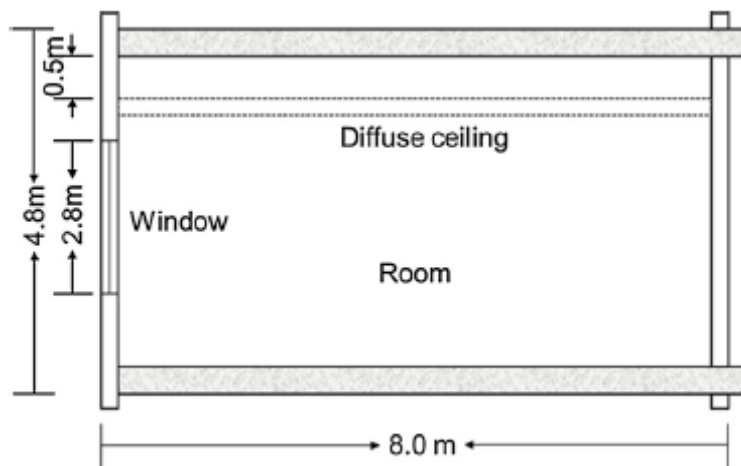


Fig. 0-56 Geometry of the simulated office room [1]

The energy performance of the proposed system was compared to other heating and cooling systems; air-based heating and cooling system without the ceiling panel, TABS without the ceiling panel and with separate ventilation air supply, air-based heating and

cooling system with the ceiling panel (ventilation air supplied through the diffuse ceiling), and an air-based system where the heated/cooled air and the ventilation air are both supplied into the room directly. For air-based systems, cases with and without heat recovery (75%) were considered. The office building was considered to be in Copenhagen, Denmark [1].

The simulation results show that among the investigated cases, the proposed system has less primary energy use when the internal loads were higher than  $30 \text{ W/m}^2$ , and the energy saving potential increases with the increasing internal heat load. The energy saving potential is as high as 50% for an internal load of  $30\text{-}40 \text{ W/m}^2$ .

While in winter, the minimum natural ventilation rate is sufficient for cooling, in peak cooling load conditions TABS should be activated to provide the necessary extra cooling effect.

### 5.2.3 Experiments

In order to extend the study of Yu et al [1], Zhang et al. [2] carried out experiments on TABS and diffuse ceiling in a hot box where the authors studied the effects of different weather, internal loads, TABS activation mode, and the inclusion of a diffuse ceiling on energy performance and thermal indoor environment. A total of 12 cases were studied. Fig. 0-57 shows the vertical cross-section of the used hot box [2].

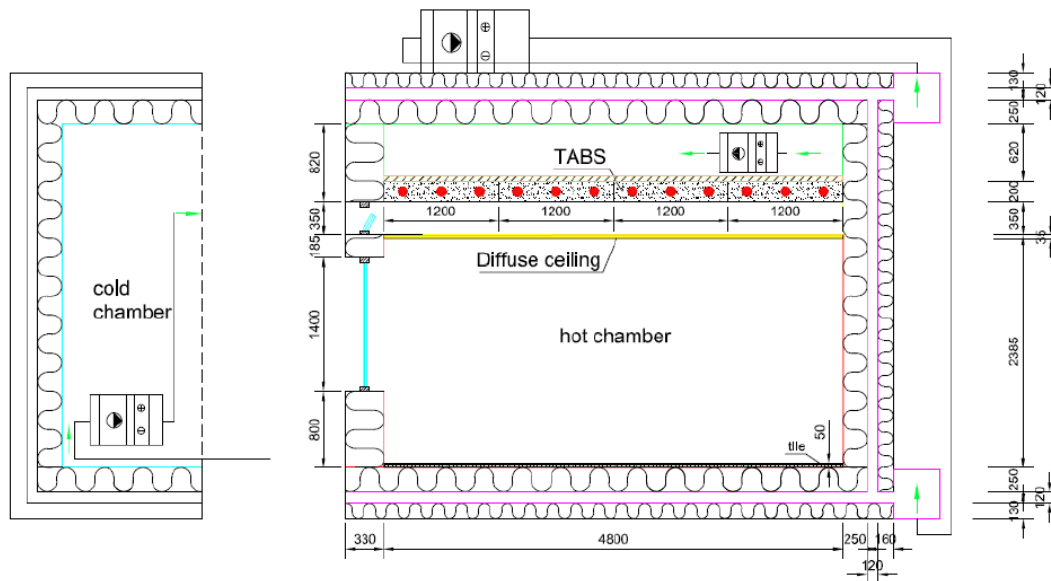


Fig. 0-57 Vertical cross-section of the hot box apparatus chamber [2]

Zhang et al. [2] showed that this system combining TABS and diffuse ceiling ventilation improves the overall thermal comfort, as well as the certain parameters of local thermal comfort; it was shown to reduce the draught risk, and to reduce the risk of warm ceiling that could result in radiant temperature asymmetry.

In terms of energy performance, the diffuse ceiling had different effects on TABS for heating and cooling operation. The heat transfer coefficients of TABS for heating and cooling modes were increased and decreased, with the inclusion of diffuse ceiling, respectively. This means that lower water supply temperatures than usually are needed for cooling operation and this will limit the use of natural energy resources, increase the condensation risk and limit the high temperature cooling opportunity.

Based on the investigations on thermal indoor environment and energy performance, the

authors concluded that this system enables to use the outdoor air directly for ventilation throughout whole year without creating thermal discomfort for the occupants [2].

In addition to the 12 conditions studied by Zhang et al. [2], Yu et al. [3] continued the experimental work and compared 20 conditions, for the same proposed system. The work of Yu et al. focused on the effects of diffuse ceiling on the heat transfer from the TABS and the ventilation inside the plenum [3].

The authors used the same hot box configuration given in Fig. 0-57, and considered two types of cases; TABS operation with and without a diffuse ceiling panel. Fig. 0-58 shows the studied cases [3].

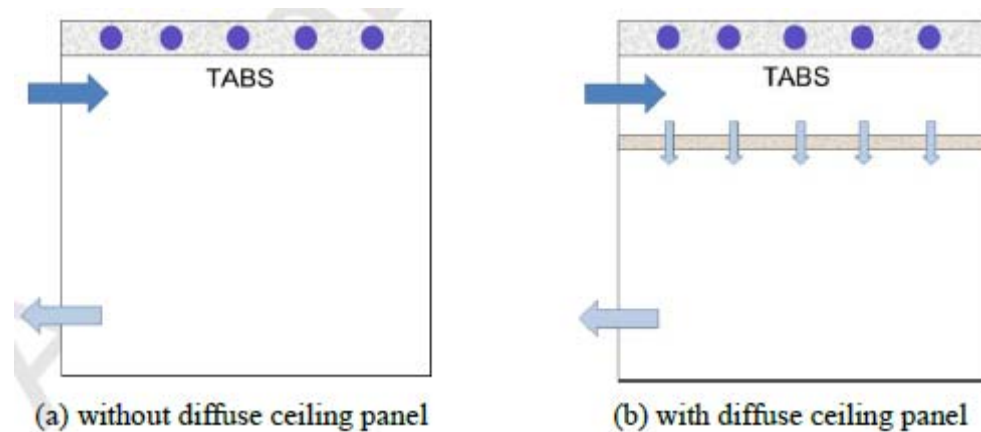


Fig. 0-58 Studied configurations [3]

Five climate conditions (extreme winter, winter, transition season, summer, and extreme summer) and two internal load levels ( $28.4 \text{ W/m}^2$  and  $57.7 \text{ W/m}^2$ ) were studied [3].

The results show that the inclusion of a diffuse ceiling decreases the cooling energy delivered to the room, compared to a case without a diffuse ceiling. In the heating conditions, the inclusion of a diffuse ceiling proved to be beneficial; more than 90% of the heating energy was transferred to the test room.

When there was a diffuse ceiling, the radiative heat transfer coefficient decreased to  $4.3 \text{ W/m}^2\text{K}$  from  $5.4 \text{ W/m}^2\text{K}$ . It was found that the convective heat transfer coefficient increased with the increasing ventilation rate and the inlet air temperature. The authors also found that the cooling from the diffuse ceiling to the room depended on the conductivity of the diffuse ceiling material and on the ventilation rate, with increasing proportion of the cooling through ventilation with the increasing ventilation rate. The authors concluded that further studies on this system should consider the dynamic effects and the effects of control system on the energy performance, since TABS operation in practice relies on the thermal mass and the steady-state studies might not be enough to fully grasp the effects on the energy performance [3].

#### 5.2.4 Summary

A novel heating, cooling and ventilation system benefiting from natural ventilation and using the diffuse ceiling ventilation and thermally active building system principles has been studied by means of simulations and experiments, in terms of thermal indoor environment and energy performance.

The results show that this system has significant energy savings potential compared to the conventional systems: up to 50% energy saving potential for an internal load of 30-40 W/m<sup>2</sup>, and the energy saving potential increases with the increasing internal heat load. This system also enables to use the outdoor air directly for ventilation throughout whole year without creating thermal discomfort for the occupants.

Experimental results show that the proposed system improves the overall thermal comfort, and decreases the risk of draught, radiant temperature asymmetry, and the vertical air temperature gradient.

The heating and cooling capacities of TABS increased and decreased after installing the diffuse ceiling, respectively. In connection to this effect, the low supply water temperature and resulting low surface temperature of the TABS poses a condensation risk.

The studies so far have been carried out under steady-state conditions and future studies will consider the dynamic behavior of TABS and the control system.

### 5.2.5 References

- [1] T. Yu, P. Heiselberg, B. Lei, M. Pomianowski and C. Zhang, "A novel system solution for cooling and ventilation in office buildings: A review of applied technologies and a case study," *Energy and Buildings*, vol. 90, p. 142–155, 2015.
- [2] C. Zhang, P. K. Heiselberg, M. Pomianowski, T. Yu and R. L. Jensen, "Experimental study of diffuse ceiling ventilation coupled with a thermally activated building construction in an office room," *Energy and Buildings*, vol. 105, pp. 60-70, 2015.
- [3] T. Yu, P. Heiselberg, B. Lei, M. Pomianowski, C. Zhang and R. Jensen, "Experimental investigation of cooling performance of a novel HVAC system combining natural ventilation with diffuse ceiling inlet and TABS," *Energy and Buildings*, vol. 105, pp. 165-177, 2015.